Innovative routes to develop multi-functional sustainable active films for food packaging

Annalisa Apicella

UNIVERSITY OF SALERNO

DEPARTMENT OF INDUSTRIAL ENGINEERING
Ph.D. Course in Industrial Engineering
Curriculum in Chemical Engineering - XXXII Cycle

Innovative routes to develop multi-functional sustainable active films for food packaging

Supervisor
Prof. Loredana Incarnato

Ph.D. student
Annalisa Apicella

Scientific Referees
Prof. Paola Scarfato
Dr. Astrid F. Pant

Ph.D. Course Coordinator
Prof. Francesco Donsì

To my Mother, the strongest, bravest, best person I have ever met.
For teaching me to never give up,
for always being close to me on this long climb.
If I am here today, it is thanks to you.

A PhD is so much more than a degree.
It can break you down into your most vulnerable form,
but has the potential to build you back together to become a resilient,
determined, ambitious and knowledgeable researcher.
This process takes time and patience.
Please don't give up on yourself. It's just not about getting the degree.
It's about becoming who you are meant to be.

Acknowledgements

First of all, I would like to thank my scientific supervisor, Prof. Loredana Incarnato. She has been much more than a supervisor for me, she was a mentor, and in difficult moments her advice helped me to go straight and not lose sight of the goal. Thanks to her I enjoyed some of the best experiences of my life.

My gratitude also goes to Prof. Luciano Di Maio and to Prof. Paola Scarfato, thanks to her precious teachings and her wide knowledge today I am a better researcher.

A big thank you to my colleagues and Friends, for having been with me since the very beginning of this journey, and for sharing the best and worst moments of it. Thanks to Lucia and Emilia, my pillars, to Arianna, for her precious smile, and to Bartolomeo, a brother for me.

A special thank you also goes to Pina, for her sincere advice, her great patience, her truthful friendship.

Thank you so much to my colleagues of the Fraunhofer Institute, for welcoming me so warmly and for being my second family there in Munich. A sincere thank you to Astrid, Marius, Norbert and Zusana, with you I had some of the happiest moments of my life.

A special thanks also to Lucia, Francesco P., Matteo, Pierpaolo, Francesco A. and Mario, for sharing the big ADI adventure and for the great moments spent together.

Thanks to all the people I have not mentioned here, but who have been by my side over the years.

To conclude, the biggest thank you is for Antonio, for his infinite love and patience, and for my parents, for their constant, irreplaceable support they have never denied me.

List of publications

Journal articles:

Di Maio L., Marra F., Apicella A., Incarnato L., (2017). *Evaluation and Modeling of Scavenging Performances of Active Multilayer PET Based Films for Food Preservation*, Chemical Engineering Transactions, Vol.57 pp.1879-1884. Doi:10.3303/CET1757314

Apicella A., Scarfato P., Di Maio L., Hayouka Z., Incarnato L. (2017*). Antimicrobial biodegradable food packaging films based on LAE*, Journal of Applied Biomaterials and Functional Materials. 30;15(4). Doi:10.5301/jabfm.5000369

Apicella A., Scarfato P., Di Maio L., Incarnato L., (2018)a. *Transport properties of multilayer active PET films with different layers configuration*, Reactive and Functional Polymers, Vol.127 pp. 29-37. Doi: 10.1016/j.reactfunctpolym.2018.03.015

A. Apicella, P. Scarfato, L. Di Maio, L. Incarnato, (2018)b. *Oxygen absorption data of multilayer oxygen scavenger-polyester films with different layouts*, Data in Brief, Vol.19, pp. 1530-1536, ISSN 2352-3409. Doi: 10.1016/j.dib.2018.06.024

Apicella, A., Scarfato, P.; Di Maio, L.; Garofalo, E.; and Incarnato, L. (2018)c. *Preparation and performance analysis of active packaging PET films combining oxygen scavenging with barrier properties for shelf life extension of sensitive foods*, Journal of Applied Packaging Research: Vol. 10 : No. 2 , Article 2 (ISSN: 1557-7224)

A. Apicella, P. Scarfato, L. Di Maio, E. Garofalo, L. Incarnato, (2018)d. *Evaluation of performance of PET packaging films based on different copolyester O2-scavengers.* AIP Conference Proceedings 1981, 020130 Doi: 10.1063/1.5045992

A. Apicella, P. Scarfato, L. D'Arienzo, L. Di Maio, E. Garofalo, L. Incarnato, (2018)e. *Antimicrobial biodegradable coatings based on LAE for food packaging applications*, AIP Conference Proceedings 1981, 020010 (2018). Doi: 10.1063/1.5045872

Apicella, A., Adiletta, G., Di Matteo, M., Incarnato, L. (2019)a. Valorization of olive industry waste products for development of new eco-sustainable, multilayer antioxidant packaging for food preservation. Chem. Eng. Trans. 75, 85-90. Doi: 10.3303/CET1975015

Apicella A., Scarfato P., Di Maio L., Incarnato L. (2019)b. *Sustainable active PET films by functionalization with antimicrobial bio-coatings*, Frontiers in Materials. Vol. 6, art.243. Doi: 10.3389/fmats.2019.00243

Apicella A., Scarfato P., Di Maio L., Incarnato L. (2019)c. *Antioxidant Activity Of Bio-Coatings For Food Packaging*. Italian Journal of Food Science, suppl. SLIM 2019: Shelf-life International Meeting: IJFS; 198-203.

Leneveu-Jenvrin C., Apicella A., Bradley K., Meile J.C., Chillet M., Scarfato P., Incarnato L., Remize F. (2019). *Limitation of quality loss of minimally-processed mangoes (Mangifera indica) over refrigerated storage*. LWT-Food Science and Technology. (Submitted).

Book chapters:

A. Apicella, L. Incarnato (2019). *Oxygen Scavengers in Food Packaging*. Book Chapter in: Reference Module in Food Science. ISBN 9780081005965. Doi: 10.1016/B978-0-08-100596-5.22942-9

(On invitation letter of Prof. Gordon L. Robertson, Editor of the Food Packaging section for Elsevier Reference Module in Food Science).

Contents

List of Figures

List of Tables

Glossary of Terms, Acronyms, Abbreviations and Symbols

°C	degrees Celsius
A	area
AA	antioxidant activity
Ag	silver
Ag^{+}	silver ions
Ag^{0}	metallic silver
Ag NPs	silver nanoparticles
AMS_DFC4020	Amosorb DFC 4020 (oxygen scavenger)
AMS_SOLO	Amosorb SolO2 (oxygen scavenger)
atm	atmosphere
ATP	adenosine triphosphate
ATR-FTIR	attenuated total reflectance Fourier transform infrared spectroscopy
a_w	water activity
BHA	butylated hydroxyanisole
BHT	butylated hydroxytoluene
BO	biaxially oriented
BOPET	biaxially oriented poly(ethylene terephthalate)
BOPP	biaxially oriented polypropylene
C^*_{ab}	color saturation value
C_b	oxygen concentration in the bulk of the test cell
C_{ox}	oxygen concentration
C_{ox_cell}	oxygen concentration in the test cell
C_s	oxygen concentration at the film interface
C_{sc}	scavenger concentration
ca.	approximately
CA_w	static water contact angle
CA_{EG}	static ethylene glycol contact angle

$CaCl_3$	calcium carbonate
CAGR	Compound Annual Growth Rate
$Ca(OH)_2$	calcium hydroxide
$CaSO_3$	calcium sulphite
cfu	colony-forming unit
CNF	cellulose nanofibril
CO	carbon monoxide
CO2	carbon dioxide
$Co(NO_3)_2$	cobalt nitrate
$Co(SCN)_4^{2-}$	cobalt(II) thiocyanate ion
CPA	Circular Plastics Alliance
CRP	Controlled Release Packaging
$CuSO_4$	copper (II) sulfate
d_S	expected shelf life duration of the product
D	diffusion coefficient
D_i, D_a	oxygen diffusion coefficient in the film inert and active layers, respectively
DM	dry matter
dMbNO	nitrosomyoglobin
DPPH	2,2-difenil-1-picrylhydrazyl
DSC	Differential Scanning Calorimeter
DTGmax	temperature at the maximum rate of weight loss
E	elastic modulus
ΔE^*_{ab}	CieLab colour variation
EDTA	ethylenediaminetetraacetic acid
EFSA	European Food Safety Authority
EO	essential oil
EU	European Union
EVOH	ethylene-vinyl alcohol copolymer
FDA	Food and Drug Administration
GAE	Gallic Acid Equivalent
GRAS	Generally Recognized As Safe
GTE	green tea extract
h_{ab}	hue angle

h_{ox}	oxygen convective mass transfer coefficient
HDPE	high density polyethylene
ΔH_{cc}	cold crystallization enthalpy
ΔH_m	melting enthalpy
ΔH_∞	melting enthalpy of purely crystalline polymer
HLB	Hydrophilic-Lipophilic Balance
HPLC	High Performance Liquid Chromatography
HPMC	hydroxypropyl-methylcellulose
HyTy	hydroxytyrosol, hydroxytyrosol content
J	oxygen molar flux in the polymer
k	reaction rate constant; initial oxygen scavenging rate
k_R	bulk reaction rate constant for reactive layer
K	Kelvin
KCl	potassium chloride
K_2CO_3	potassium carbonate
$KNaC_4H_4O_6$	potassium sodium tartrate
KOH	potassium hydroxide
L_1, L_2, L	thickness of the inert layer, of the active layer and of the total film, respectively
LAE	Ethyl-Nα-dodecanoyl-L-arginate or Ethyl Lauroyl Arginate
LDPE	low density polyethylene
LLDPE	linear low density polyethylene
Log(CFU)	logarithm of colony forming units
LRV	log reduction value
M_t	concentration (or amount) of substance diffused at time t
M_∞	concentration (or amount) of substance diffused at equilibrium
MAP	modified atmosphere packaging
MBC	minimum bactericidal concentration
mg	milligram (1×10^{-3} gram)
MgO	magnesium oxide
MIC	minimum inhibitory concentration
MIG	multi-stage pulse counter-current

MIR	mid-infrared spectroscopy
MJ	megaJoule
mL	milliliter (1×10^{-3} liters) = cc = cm^3
MMb	metymioglobin
MMT	montmorillonite;
MPa	megaPascal
MSE_{exp}	experimental mean square deviation
MXD6	meta-xylylene diamine/adipic acid nylon
n	concentration of reactive sites; absorption capacity
n_0	initial concentration of reactive sites
N	total number of observations
n_{ox}	amount of substance of O_2
NaCl	sodium chloride
NaOH	sodium hydroxide
$Na_2S_2O_4$	sodium dithionite
NH_4SCN	ammonium thiocyanate
nm	nanometer (1×10^{-9} meter)
O2Mb	oxymyoglobin
OEO	oregano essential oil
OP	olive pomace
OPE	olive pomace extract
OPE_liq	liquid olive pomace extract
OPE_liq	powder olive pomace extract
OS	oxygen scavenger
OTR	oxygen transmission rate
OW	olive milling wastewaters
OWE	olive wastewaters extract
P	packaging permeability
p_{ox}	oxygen partial pressure
p_{ox_dow}	oxygen partial pressure on the downstream side of the film
p_{ox_ups}	oxygen partial pressure on the upstream side of the film
ΔP	partial water vapor pressure difference
P_{O2}	oxygen permeability coefficient

P_{WV}	water vapor permeability coefficient
PBAT	polybutylene adipate terephthalate
PCL	polycaprolactone
PE	poly(ethylene)
PET	poly(ethylene terephthalate) = polyester
PETG	poly(ethylene glycol-co-1,4-cyclohexanedimethanol terephthalate)
PHB	polyhydroxybutyrate
PLA	polylactic acid or polylactate or polylactide
PP	polypropylene
ppb	parts per billion (1×10^{-9})
ppm	parts per million (1×10^{-6})
PS	polystyrene
PUFA	polyunsaturated fatty acid
PVA	poly(vinyl alcohol)
PVdC	poly(vinylidene chloride)
Q	oxygen permeate per unit area
R	ideal gas constant (= 8.314 J K^{-1} mol^{-1})
RH	relative humidity; allylic carbon-hydrogen bond
RMSE	root mean square error
RS	reducing sugars
s	solubility coefficient of permeant in polymer
S	surface of the film
SE	surface energy
SEM	Scanning Electron Microscopy
SeNP	Selenium nanoparticle
SiO2	silicon dioxide
SiOx	oxides of silicon
SO2	sulfur dioxide
SOLO2_V	violet component of the oxygen scavenger Amosorb SolO2
SOLO2_W	white component of the oxygen scavenger Amosorb SolO2
SPI	soy protein isolate

SSQ	sum of squared residuals
T_{550}	transmittance at 550 nm
TBHQ	tert-butylhydroquinone
Tcc	cold crystallization temperature
Tc	crystallization temperature
t_E	exhaustion time
Tg	glass transition temperature
TGA	thermogravimetric analysis
TiO_2	titanium dioxide
Tm	crystalline melting temperature
Toc	α-tocopherol
TP	total polyphenols
TSA	Tryptic Soy Agar
TSB	Tryptic Soy Broth
USD	United States Dollar
UV	ultraviolet
V_{cell}	volume of the cell
V_{HS}	head space volume
V_{IN}	volume of oxygen which permeates through the packaging during the shelf life period
V_{O2}	total volume of oxygen absorbed
V_{O2}'	total volume of oxygen absorbed, normalized over percentage of active phase in the scavenger
V_{Ox}	total volume of oxygen absorbed, normalized over surface area
V_P	volume of the finished pack
V_{SC}	total volume of O_2 that must be scavenged over time
W_P	weight of the finished pack
WPI	Whey Protein Isolate
WPI_COAT	Whey Protein Isolate coating layer
WVTR	water vapor transmission rate
x	thickness of polymeric material; position in the film
Xc	crystallinity degree
YE	yeast extract

ZnO	zinc oxide

Greek letters

γ_s^d	dispersion component of the surface energy
γ_s^p	polar component of the surface energy
ε_b	strain at break
μ	scavenging capacity
μg	microgram (1×10^{-6} gram)
μm	micrometer (1×10^{-6} meter)
ν	stoichiometric factor
σ_b	stress at break
Φ	fraction of active film
ω	content of oxygen scavenger phase

Abstract

Active packaging solutions are among the latest and the most attractive innovations in the food packaging field: this technology plays a dynamic role in food preservation, directly interacting with the food and/or the surrounding packaging atmosphere, by releasing protective substances or absorbing others that accelerate the decay.
Among all, oxygen scavengers, antioxidants and antimicrobials are the most interesting and promising active systems, since they deeply affect the quality preservation and the extension of the shelf-life of foodstuff.

Oxygen scavengers and antioxidants interfere with oxidation mechanisms responsible of qualitative decay of many sensitive foods, while antimicrobials are able to kill or inhibit the growth of pathogenic microorganisms that may contaminate packaged food products

The main challenges in developing active films for food packaging involve the realization of effective systems, with satisfactory functional properties, easy-to-produce by conventional technologies and, last but not least, with high eco-compatibility.

Indeed, the recent concerns toward waste-management issues and shortage of resources, have increasingly shifted the research focus towards the development of highly eco-compatible and sustainable packaging solutions, by means of biomass-derived biodegradable or completely recyclable polymers, or a combination of both.

At the same time, the selection of the proper active agent, as well as the choice of the optimal packaging layout, is an important and not an easy task in the design and application of active packaging.

In particular, the premature exhaustion of the oxygen scavenging films, due to the reduced thicknesses involved, must be avoided, while for antimicrobial and antioxidant structures a tunable release must be achieved.

In order to face these requests, the appropriate design and sizing of the active packaging is essential, by tailoring the performances of the package to the shelf-life requirements of the specific food products.

These considerations inspired the scope of this PhD work, which aimed at investigating innovative routes for the development of sustainable, multi-

functional active packaging films, to be successfully applied to extend the shelf-life of sensitive foods.

The first part of the PhD work involved the realization of mono-material, active films based on polyethylene-terephthalate (PET) and co-polyester oxygen scavengers (OS), with prolonged effectiveness over time.

Multilayer structures were realized by cast co-extrusion, inserting the active layer, at an optimized concentration (10% w/w) of a single-phase OS, between two PET inert layers. Four different configurations were designed, and the scavenging properties were extensively investigated, exploring the influence of the multilayer layout on absorption kinetic and parameters.

As further upgrade, the potential of an innovative formulation of the same OS, enhanced by a second, high-oxygen barrier phase, was investigated. Single-layer active PET structures were produced by cast extrusion, and the concentration of the 2-phases OS was optimized. The absorption performances have been thoroughly analyzed and compared with those of the multilayer films, highlighting the similarities, the application potentialities and the advantages of each.

A mathematical model was also developed and appropriately validated, evaluating the potential of the virtualization tool to extrapolate predictive data for evaluating, comparing, and optimizing the scavenging performance of active films, significantly reducing the experimental matrix to explore.

Moreover, shelf life tests were carried out, to assess effectiveness of both multilayer and single-layer films in preserving sensitive food matrices during medium-long storage term.

In the second part of the work, the possibility of functionalizing PET substrates through active biodegradable coatings, easy soluble to be removed, was investigated. An innovative, non-harmful antimicrobial named LAE (Ethyl-Nα-dodecanoyl-L-arginate) was incorporated (from 0 to 20% w/w) into a Poly-lactic acid (PLA) coating layer. The produced films combined the structural and barrier performance of PET with the PLA sealing capacity and the LAE antimicrobial activity, while the coating technology ensured to avoid thermal stresses to the heat-sensitive active compound.

The antimicrobial activity of the multilayer films was tested *in vitro* against *E.Coli* CECT 434 strain as pathogenic agent in liquid culture media, and tunable release kinetics were obtained. Moreover, the LAE chemical interaction with the PLA matrix was investigated, as well as its effect on the adhesion, wetting, optical and barrier properties of the films.

The third part of the PhD studies aimed at exploring new possibilities to develop eco-compatible active films, through the valorization of natural bioactive compounds deriving from food industry wastes.

The first part of the research, carried out at the Fraunhofer Institute for Process Engineering and Packaging IVV (Germany), involved the extraction of polyphenolic antioxidants from olive pomace. The olive pomace extract (OPE) was thoroughly characterized, to evaluate chemical-physical properties, antioxidant and O2-scavenging potential, which provided basic knowledge for tailor-made packaging design. A second-order mathematical model was also applied to describe the oxidation-kinetics of the extract, underlining the potential of the model to predict quite accurately the O2-scavenging performance of a variety of polyphenols.

Then, the OPE (at 5% and 10% w/w) was used to realize active bio-coatings based on Whey Protein Isolate (WPI), spread on a PET substrate film. The produced films combined the environmental advantages deriving from the revaluation of food industry by-products, with the high technical performance offered by the PET film and the protein coating.

The antioxidant activity of the films was evaluated by release tests in fatty foods simulant, and the diffusion kinetic was investigated, suggesting a suitable application of the films for long storage greasy foods. The films compliance to the migration limits established by the European Union Legislation was assessed by overall migration tests. Moreover, the OPE chemical interaction with the WPI matrix was investigated, as well as its effect on the adhesion, wetting, optical and barrier properties of the films.

Finally, as further step forward, 100% biodegradable antioxidant films were also developed, all based on biopolymers and natural extracts derived from olive milling wastewaters (OWE). The antioxidant activity of three different extracts was analyzed. Then, the most performing one was added to a PLA coating layer (from 5 to 20% w/w), spread on a biodegradable substrate made of PLA and PBAT (Polybutylene adipate terephthalate).

The produced multilayer structures were then characterized in order to evaluate the interaction of the antioxidant phase with the polymer matrix, and its effect on the physical and functional performance of the active systems. Lastly, the release kinetics and antioxidant activity in fatty foods simulant endorsed the promising perspectives of the films to be used as 100% eco-compatible alternative for the preservation of oxidative-sensitive food products with high respiration rates.

Introduction

Objectives of the PhD work and dissertation outline

Nowadays, the increasing demand for safe food products with prolonged shelf life, as well as functional, low cost, environmental friendly packaging, represent the driving forces that have prompted the food packaging industry towards innovations in materials and technologies.

Among all these innovations, active packaging solutions are certainly the most challenging: this technology allows the packaging to interact directly with food or food surfaces by releasing or absorbing specific substances, to prolong the shelf life of sensitive foods and to guarantee their safety and freshness, through a continuous modification of the environment inside the packaging. Food and packaging are no more seen as two separate entities, and the old, traditional role of generic containment of the packaging is overcome.

The wide diversity of active packaging systems comprise additives with a multitude of active functions, as shown in Figure 1: absorbing/scavenging properties (e.g., oxygen, carbon dioxide, ethylene, moisture, flavours, taints and UV light); releasing/emitting properties (e.g., ethanol, carbon dioxide, antioxidants, preservatives, sulphur dioxide and flavours); removing properties (catalysing food component removal: lactose, cholesterol); and temperature, microbial and quality control (Yildirim et al., 2018).

Unlike the huge popularity enjoyed since the 1970s in some countries, such as Japan, the use of active packaging in Europe is only now beginning to increase, as the high cost, low consumer acceptance and stringent legislation have been the key points hindering its diffusion in the EU market.

As a matter of fact, active packaging systems should comply with the requirements of regulatory agencies, such as the Food and Drug Administration (USA), the European Food Safety Authority (European Union), or others, that set the legal basis for their accurate use, safety and marketing (Restuccia et al., 2010).

Figure 1 Active food packaging: categories and agents (Vilela et al., 2018).

Nevertheless, the recent impressive surge of interest in the concept of active packaging is testified by the increasing research and development (R&D) and growing dissemination approaches for communicating the outcomes, as shown by the expanding publication trends in the field of active packaging and active food packaging in the last 30 years (Figure 2). Indeed, over the last 10 years, an increase in the number of publications equal to 94% and to 48% was observed in the active packaging and active food packaging fields, respectively.

The attention is motivated by the growing market demand: the last year (2019) the global active and intelligent packaging market was valued at USD 17.5 billion, and is expected to reach a value of USD 25.16 billion by 2025, registering a CAGR of 6.78% during the forecast period of 2020-2025 (Anonymous, 2019a) .

A considerable portion of this market is occupied by oxygen scavengers (OS), antioxidants and antimicrobials, which are the most interesting and promising active systems, since they deeply affect the quality preservation and the extension of the shelf-life of foodstuff.

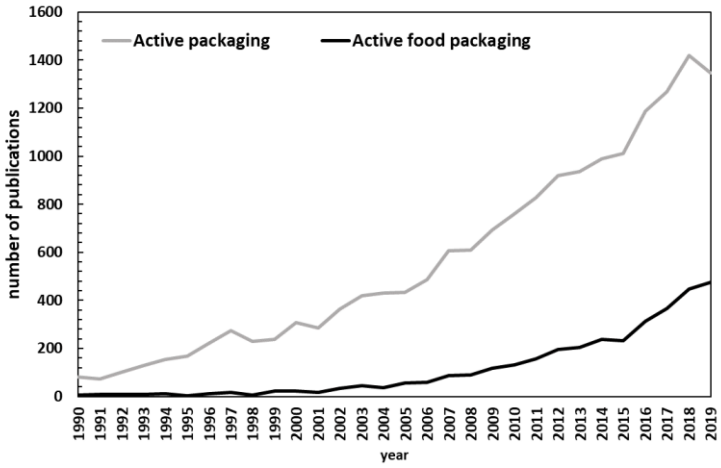

Figure 2 Publication trends of active packaging and active food packaging from 1990 to 2019. Data collected from Web of Science using the keywords "active packaging" and "active food packaging". (https://www.webofknowledge.com)

The in-depth bibliographic research carried out within this PhD thesis revealed that an extensive study has been performed so far on different oxygen scavengers, antimicrobials and antioxidant formulations, incorporated within synthetic or biodegradable polymer matrices using several methods, such as melt compounding, coating deposition, adhesives blending or covalent bonding on a substrate.

The main issues with the current approaches are related to the following critical factors:

- the realization of efficient active films, with multiple functional properties;
- the use of conventional processes, scalable at industrial level;
- the effective control of the films activity and exhaustion time, in order to be suitable for industrial applications;
- the assessment of active films stability and their compliance to the current European Legislation for food contact;
- the realization of packages with the least number of materials or mono-material, to be easy recyclable/degradable and with reduced environmental impact;

- the development of mathematical models to describe the reaction phenomena and to predict the scavenging performance, reducing the experimental matrix to explore.

The PhD research, focused on the development of multi-functional active films, aimed at:

- ✓ extend the shelf life of sensitive foods;
- ✓ satisfy primary functionalities of food packaging (barrier, mechanical, optical, adhesion, sealability properties):
- ✓ obtain prolonged effectiveness of active films, by controlling the absorbing/releasing kinetics;
- ✓ obtain tailor-made performance, based on food preservation requirements.

Among the production goals, were emphasized the aspects of:

- ✓ sustainability, keeping in mind the principles of circular economy: mono-material, 100% recyclable PET multilayer films were realized, and PET was also selected as substrate for the realization of biodegradable coatings, easy to be removed by non-toxic solvents at disposal, ensuring the complete recovery of the recyclable substrate. Moreover, 100% biodegradable films were also realized.
- ✓ industrial feasibility, using conventional technologies such as extrusion and coating, easy to be implemented in existing packaging/converting lines;
- ✓ suitability for food applications, using non-harmful natural active agents, or approved by FDA and EFSA for food contact, and verifying the compliance with EU Regulation requirements on plastic materials and articles intended to come into contact with food (EU No 10/2011).

Moreover, mathematical models were developed and applied to the data sets, aimed at:

- ✓ describing the scavenging performance of the films and of the active agents, identifying the parameters which most affect their activity;
- ✓ using them as predicting tools, in order to confidently extrapolate predictive data on films performance by varying the layout, with no need of further experimentals.

The dissertation is organized as follows:

In **Chapter I** the **State of the Art** about Active Packaging technologies is extensively investigated. Challenges and issues with different antimicrobial, antioxidant and oxygen scavenging agents are presented, the mechanisms of reaction and incorporation techniques are explored, and the development of integrated polymeric flexible systems is outlined. Then, hands-on approaches to improve food packaging sustainability are discussed, as well as strategies for the proper design, manufacturing and performance optimization of oxygen scavenging and controlled release films. Design equations to describe the transport phenomena occurring during the oxygen scavenging and controlled release mechanisms are also examined, and the possibilities to predict the scavenging performance of different film layouts through mathematical modelling are shown.

In **Chapter II, III, IV, V and VI** the results of the PhD research are presented. As reported above, this thesis work was focused on several factors and, in order to achieve the proposed objectives, it was structured on 3 different sections:

- **Section I – "Mono-material, active films based on polyethylene-terephthalate (PET) and co-polyester oxygen scavengers (OS) with extended effectiveness" (Chapters II and III):** in this section, mono-material oxygen scavenging PET films were developed by extrusion process. Two different strategies were studied to avoid the rapid exhaustion of the scavenger, by controlling the O_2 diffusive mechanism through the active films.
  In particular, in **Chapter II** multilayer structures were realized by cast co-extrusion, inserting the active layer, at an optimized concentration (10% w/w) of a single-phase OS, between two PET inert layers. Four different configurations were designed, and the scavenging properties were extensively investigated, exploring the influence of the multilayer layout on absorption kinetic and parameters. A mathematical model was also developed and appropriately validated, evaluating the potential of the virtualization tool to extrapolate predictive data for evaluating, comparing, and optimizing the scavenging performance of active films, significantly reducing the experimental matrix to explore.
  In **Chapter III**, the potential of an innovative formulation of the same OS, enhanced by a second, high-oxygen barrier phase, was investigated. Single-layer active PET structures were produced by cast extrusion, and the concentration of the 2-phases OS was optimized. The absorption performances have been thoroughly

analyzed and compared with those of the multilayer films, highlighting the similarities, the application potentialities and the advantages of each one.
Shelf life tests were also carried out, to assess effectiveness of both multilayer and single-layer films in preserving sensitive food matrices during medium-long storage term.
These outcomes of the research were disclosed in the published studies: Di Maio, Apicella et al. 2017, Apicella et al. 2018a, Apicella et al. 2018b, Apicella et al. 2018c and Apicella et al. 2018d.

- **Section II – "Sustainable active films based on PET functionalized by Antimicrobial Bio-coatings" (Chapter IV):** in this chapter, the possibility of functionalizing PET films through antimicrobial biodegradable coatings, easy soluble to be removed, was investigated. An innovative, non-harmful antimicrobial named LAE (Ethyl-Nα-dodecanoyl-L-arginate) was incorporated (from 0 to 20% w/w) into a Poly-lactic acid (PLA) coating layer. The produced films combined the structural and barrier performance of PET with the PLA sealing capacity and the LAE antimicrobial activity, while the coating technology ensured to avoid thermal stresses to the heat-sensitive active compound. The antimicrobial activity of the multilayer films was tested *in vitro* against *E.Coli* CECT 434 strain as pathogenic agent in liquid culture media, and tunable release kinetics were obtained. Moreover, the LAE chemical interaction with the PLA matrix was investigated, as well as its effect on the adhesion, wetting, optical and barrier properties of the films.
  These results are part of the published studies: Apicella et al. 2017, Apicella et al. 2018e, and Apicella et al. 2019b.

- **Section III – "Antioxidant films with natural extracts from valorization of olive industry wastes: PET functionalization by high performance bio-coatings and development of 100% biodegradable structures" (Chapter V and VI):** in this section, new possibilities to develop eco-compatible active films, through the valorization of natural bioactive compounds deriving from food industry wastes, were explored.
  In **Chapter V**, PET was functionalized by high barrier Whey Protein Isolate (WPI) coatings, loaded with an olive pomace extract. Firstly, the extraction of polyphenolic antioxidants from olive pomace, the chemical-physical characterization and the evaluation and modelling of the oxygen scavenging properties were carried out, during a six-months internship at the

Fraunhofer Institute for Processing Engineering and Packaging (IVV) in Munich. The activities were also part of the EU Horizon2020 Project AgriMax- "Agri & food waste valorization co-ops based on flexible multi-feedstocks biorefinery processing technologies for new high added value applications".

The olive pomace extract (OPE) was thoroughly characterized, to evaluate the antioxidant and O_2-scavenging potential, which provided basic knowledge for tailor-made packaging design. A second-order mathematical model was also applied to describe the oxidation-kinetics of the extract, underlining the potential of the model to predict quite accurately the O_2-scavenging performance of a variety of polyphenols.

Then, the OPE (at 5% and 10% w/w) was used to realize active bio-coatings based on Whey Protein Isolate (WPI), spread on a PET substrate film. The produced films combined the environmental advantages deriving from the revaluation of food industry by-products, with the high technical performance offered by the PET film and the protein coating.

The antioxidant activity of the films was evaluated by release tests in fatty foods simulant, and the diffusion kinetic was investigated, suggesting a suitable application of the films for long storage greasy foods. The films compliance to the migration limits established by the European Union Legislation was assessed by overall migration tests. Moreover, the OPE chemical interaction with the WPI matrix was investigated, as well as its effect on the adhesion, wetting, optical and barrier properties of the films.

The promising outcomes were presented at the 2nd International Meeting on the Horizon2020 EU Project Agrimax (York, 3-4 October 2018) and the 3rd Innovations in Food Packaging, Shelf Life and Food Safety Conference (Munich, 8-10 October 2019), and are going to be part of upcoming publications.

In **Chapter VI**, 100% biodegradable antioxidant films were developed, all based on biopolymers and natural extracts derived from olive milling wastewaters (OWE). The antioxidant activity of three different extracts was analyzed. The best performing one was added to a PLA coating layer (from 5 to 20% w/w), spread on a biodegradable substrate made of PLA and PBAT (Polybutylene adipate terephthalate). The produced multilayer structures were then characterized in order to evaluate the interaction of the antioxidant phase with the polymer matrix, and its effect on the physical and functional performance of the active systems. Lastly, the release kinetics and antioxidant activity in fatty foods simulant endorsed the promising perspectives of the

films to be used as 100% eco-compatible alternative for the preservation of oxidative-sensitive food products with high respiration rates.
Some of these outcomes were published in the studies: Apicella et al., 2019a and Apicella et a., 2019c.

Finally, in **Chapter VII** the **Concluding remarks** regarding the active films developed are discussed, and recommendations for future work are presented.

Chapter I

State of the Art

I.1 Active packaging based on antimicrobials

Antimicrobial agents are one of the most studied active components, since microbial contamination after processing is one of the major causes of foodborne diseases, representing both a public concern and an economic issue (Higueras et al., 2013; Coronel-Leon et al., 2016). At the same time, consumers demand is increasingly addressed towards the consumption of safe food products with fewer chemicals addition.

Therefore, antimicrobial agents are one of the active agent classes with the higher number of commercial products, in the form of emitting sachets or absorbent pads (Biomaster®, AgIon®, Irgaguard®, Surfacine®, IonPure®, Bactiblock®, Biomaster®, Food-touch®, Sanic Films, SANICO® and Wasaouro®) (Vilela et al., 2018).

In recent years, great attention has been paid to the development of antimicrobial controlled release systems, through the incorporation of the active molecules into a bulk matrix. This avoids the direct addition, by dipping or spraying, of large antimicrobial amounts onto the food surface, where a large portion of spoilage and contamination occurs. As a matter of fact, the rapid diffusion of the antimicrobial into the food matrix results in an immediate reduction of bacterial populations, but does not allow controlling the metabolism growth of surviving biomass after depletion of antimicrobial residues (Chi-Zhang et al., 2004). The use of carriers such as polymers, instead, allows the gradual delivery of the active agent during the storage and distribution of food packaging, with less antimicrobial concentration, tunable release and tailor-made applications. (Lagaron, 2011).

The list of scientific papers, reviews and books on the topic is extensively growing in the last years, with an increase in the number of publications equal to 118% in the last five years, and equal to 300% in the last ten years (Figure 3).

A multitude of antimicrobial agents have been investigated in polymer matrices, such as metal ions (e.g., silver, copper, gold and platinum), metal oxides (e.g., TiO_2, ZnO and MgO), essential oils (e.g., thyme, oregano, pimento, clove, citron, lemon verbena, lemon balm and cypress leaf), plant extracts (e.g., grape seed, green tea, pomegranate peel/rind, acerola, pine bark, bearberry, cinnamon bark, rosemary, garlic, oregano, ginger and sage), polysaccharides (e.g. chitosan), pure bioactive components (e.g., thymol and carvacrol), peptides (e.g., nisin and lactoferrin), enzymes (e.g., peroxidase and lysozyme) and synthetic antimicrobial agents (e.g., quaternary ammonium salts, ethylenediaminetetraacetic acid (EDTA), and propionic, benzoic and sorbic acids) (Vilela et al., 2018).

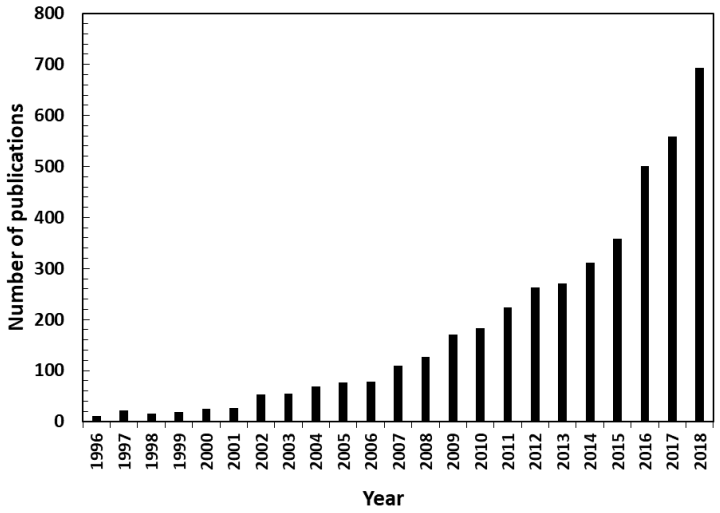

Figure 3 Publication trends of antimicrobial packaging and antimicrobial food packaging from 1996 to 2019. Data collected from Web of Science using the keywords "antimicrobial packaging" and "antimicrobial food packaging". (https://www.webofknowledge.com)

Classification of antimicrobials, inhibition mechanisms and applications

Antimicrobial agents used in active packaging can be organic acids, metals, antibiotics, bacteriocins, enzymes, chelating agents, spices etc.. The classification proposed in Table 1 tabulates the antimicrobial agents on the basis of their nature and antimicrobial mechanisms.

Table 1 Classification of antimicrobial agents depending on their nature and antimicrobial mechanism.

Classification	Antimicrobial agents	Antimicrobial mechanisms
Metals	Silver, silver-zinc, silver-titanium dioxide	Electrostatic interaction of metal ions with the microorganism cell membrane, with enzymes inactivation in cytoplasm.
Organic Acids	Potassium sorbate, sorbic acid, sodium benzoate, citric acid, lactic acid	Effect on enzymes such as dehydrogenases, inhibiting their activity in the microorganism cell
Bacteriocin	Nisin, pediocin, sakacin-A	Pores formation onto the cytoplasmic membrane of microorganism cell wall, resulting in degradation of proton motive force and loss cellular ions, amino acids and ATP.
Essential oils	Carvacrol, linalool, eugenol, cinnamaldehyde, thymol, clove, ginger, fingerroot, plai, allyl iso-thiocyanate, rosemary, cinnamon, coriander	The mechanism of antimicrobial action of essential oils is still unclear
Polysaccharide	Chitosan	The positive charge of chitosan affects microorganisms electrostatically: promotes changes in the properties of membrane wall permeability and leads to the leakage of intracellular electrolytes
Enzymes	Lysozyme, glucose oxidase, lactoperoxidase	N-acetylmuramoyl hydrolase

	enzymic activity, resulting in peptidoglycan hydrolysis and cell lysis.

Metals are still among the most widely used antimicrobial agents. In particular, silver and silver compounds, metallic silver (Ag^0), silver ions (Ag^+) or silver nanoparticles (Ag NPs), are able to exert the most effective antimicrobial action against a broad range of microorganisms at exceptionally low concentrations and present very little systemic toxicity toward humans. Substituted zeolites with silver ions are incorporated into polymers like polyethylene, polypropylene, nylon and butadiene styrene at levels of 1-3% (Brody, 2001). Commercial examples of silver substituted zeolites include Zeomic®, Apacider®, AgIon, Bactekiller and Novaron.

Among other metals, a recent study of Li et al. (2017) showed that the incorporation of ZnO nanoparticles into the poly(lacticacid) (PLA) matrix originated films with remarkable inhibition of microbial growth. In fact, ZnO nanoparticles were responsible for the reduction of the microbiological levels of bacterial, yeast and fungi counts in fresh-cut apple (Li et al., 2017).

Organic acids such as sorbic acid, acetic acid, lactic acid and benzoic acids have long usage history in food industry and they are recognized as safe (GRAS). Sorbic acid and its potassium, calcium or sodium salts are called as sorbates. The mechanism of sorbic acids against microbial growth lethally is partly due to the effects on enzymes such as dehydrogenases. Sorbate can turn the enzymes into the more stable forms such as thiohexenoic acid derivate and inhibit the enzyme activity in microorganism cell. The efficiency of sorbic acid is dependent on pH of the environment, with increasing pH the efficiency is decreased and after pH 6.5, sorbic acid loses its antimicrobial properties. Sorbic acid and its derivatives can be incorporated into any type of packaging materials (biodegradable or petroleum polymer). Hauser and Wunderlich (2011) proposed using sorbic acid incorporated packaging films (PVA) to inhibit the growth of contaminated microorganism as *E. Coli, L. monocytogenes, S.cerevisiae* on the surfaces of Gouda cheese and pork loin, and they had suggested that antimicrobial film containing sorbic acid is able to prevent and reduce the growing of pathogens on food surfaces.

Biomacromolecules such as peptides and proteins (e.g., nisin and lactoferrin), enzymes (e.g., lysozyme) and polysaccharides (chitosan), are also being studied as active agents due to their well-recognized antimicrobial

activity. Lysozyme, for example, is known as a natural antimicrobial agent with activity against numerous pathogens (Aziz & Karboune, 2018). Lysozyme has been incorporated into cellulose ester films by solvent

compounding in order to prevent heat denaturation of the enzyme (Appendini et al., 1997). Recently, the incorporation of lysozyme nanofibers into pullulan films endowed the multifunctional materials with antimicrobial activity against *S. aureus* (Silva et al., 2018).

Although bacteriocins and peptides are relatively heat-resistant, their antimicrobial activity may be higher when heat is not used in the process. Studies on nisin, the only bacteriocin peptide approved for food applications, showed that the activity of the bacteriocin in cast films was three times greater than that of heat-pressed films. The films were made from methylcellulose, hydroxypropylmethylcellulose , carrageenan and chitosan (Cha et al., 2003). Recently, nisin activated poly(hydroxybutyrate) /poly(caprolactone) (PHB/PCL) nanocomposite films were tested against *Lactobacillus plantarum* (used as processed meat spoilage bacterium model) inoculated on ham and the results confirmed the effectiveness of these films as shelf-life extender for vacuum-packed sliced cooked ham (Correa et al., 2017).

Chitosan, a cationic polysaccharide prepared via N-deacetylation of chitin, is by far the most studied polysaccharide in the context of food packaging due to its antimicrobial activity against a plethora of Grampositive (e.g., S. aureus, Listeria innocua and lactic acid bacteria) and Gram-negative (e.g., E. coli, Pseudomonas spp. and Salmonella spp.) bacteria, and fungus (e.g., Candida albicans and Aspergillus niger) (Wang et al., 2018). This polysaccharide was already combined with various agents, particularly with antioxidant additives, including quercetin (Souza et al., 2015), ellagic acid (Vilela et al., 2017), essential oils (Hafsa et al., 2016;), among others. The antimicrobial activity of chitosan is generally associated with the amino group, but the mechanism of action is different in Gram-positive and in Gram-negative bacteria.

Essential oils (EOs) are volatile aromatic mixtures composed of low molecular weight compounds (e.g. phenolic compounds, such as monoterpenes, flavonoids and phenolic acids) derived by plants (e.g., rosemary, clove, oregano, coriander, tea tree, lemongrass, basil, grape seed extract and fennel), or their isolated components (e.g., carvacrol, eugenol, thymol and cinnamaldehyde). They have shown high efficacy, and have been used as antimicrobial additives in active food packaging of cheese, fish, meat, fruits and vegetables (Maisanaba et al., 2017).

Although the mechanism of antimicrobial action of EOs is still unclear (Aziz & Karboune, 2018), different combinations of polymer matrices and active compounds are possible (Ribeiro-Santos et al., 2017; Severino et al., 2015; Yuan et al., 2016). Among bio-based composites, gelatin films incorporated with clove essential oil and zinc oxide nanorods were recently investigated (Ejaz et al., 2018), as well as nanocomposite films based on soy

protein isolate (SPI) montmorillonite (MMT) and clove essential oil for the preservation of muscle fillets of bluefin tuna (Echeverría et al., 2018). Javidi et al. (2016) also evaluated the potential use of *Origanum vulgare L*. essential oil (OEO) in PLA-based matrices to obtain developed bio-based films with enhanced mechanical properties as well as antimicrobial performance. The antimicrobial activity of incorporated essential oil was more effective with a direct food/package contact, than in vapor phase. The films also showed shelf life extension of packaged rainbow trout during chilled storage.

However, the main drawback of EOs (and their components) is the need for high concentrations to achieve the same effectiveness in the real food, which could affect the organoleptic features of the food products.

I.2 Active packaging based on antioxidants and oxygen scavengers

Considerable interest has also been placed on antioxidant agents: after microbial growth, the main cause of food and beverage deterioration is the presence of oxygen inside the package of sensitive foods. Oxygen causes acceleration in fruits and vegetables metabolism, changes in texture, flavors, color, oxidative rancidity of unsaturated fats, degradation of vitamins and nutrients, enzymatic and nonenzymatic browning, as well as encourages aerobic microbial growth and spoilage (Vermerein et al., 1999; Brody et al., 2001).

Antioxidant compounds can be classified according to the mechanism of action as primary (or chain-breaking) antioxidants, namely free-radical scavengers, and secondary (or preventive) antioxidants, including metal chelators, UV absorbers, singlet oxygen ($^1O_2$) quenchers and oxygen scavengers (Vilela et al., 2018).

The advantage of secondary antioxidants lies in their capacity to reduce or prevent the occurrence of oxidation reactions, whereas the primary antioxidants react with free radicals to convert them into (fairly) stable products that do not engage in further initiation or propagation reactions. Worth noting is the fact that some active agents exhibit both mechanisms of action (Tian et al., 2013).

Free-radical scavengers are among the most studied class of antioxidants, commonly incorporated in controlled-release packages such as films and trays. They can donate hydrogen to reactive free radicals and form stable free radicals unable to perpetrate initiation or propagation reactions (Tian et al., 2013).

Examples of free-radical scavengers comprise synthetic agents, namely butylated hydroxytoluene (BHT), butylated hydroxyanisole (BHA) and tert-butylhydroquinone (TBHQ), which are now suspected to be potentially harmful to human health, as well as natural antioxidants, such as natural compounds (e.g., tocopherol, caffeic acid, carvacrol, quercetin, catechin,

thymol, ferulic acid, carnosic acid and ascorbic acid), plant and fruit extracts (e.g., rosemary, grape seed, green tea, oregano, murta, mint, and pomegranate peel), and essential oils from herbs and spices (e.g., cinnamon, lemongrass, clove, thyme, ginger, oregano, pimento and bergamot) (Amorati et al., 2013; Ganiari et al., 2017; Sanches-Silva et al., 2014).

Recently, the preparation and study of selenium nanoparticles (SeNPs) as novel, synthetic free radical scavenger has gained growing interest, thanks to the high antioxidant performance, low toxicity and excellent bioavailability. Vera et al. (2016) developed active PET/PE multilayer films by incorporating SeNPs at different concentrations in a water-based polyurethane adhesive. The antioxidant capacity of the packaging material was demonstrated through a non-disruptive analytical method, previously described by Pezo et al. (2008), by exposing the laminates to an atmosphere enriched in free radicals without sample extraction. It was confirmed that SeNPs were effective in trapping the primary free radicals derived from oxygen, with no migration of the nanoparticles, and the new multilayer material recently received a positive opinion from EFSA (European Food Safety Authority) (Vera et al., 2018).

Other antioxidant compounds were successfully incorporated into adhesive formulations as vehicle for the active agent, and the radical scavenging activity was demonstrated through the in situ gas-phase hydroxyl radical generation method mentioned above.

Carrizo et al. (2016) realized flexible bags of multilayer OPP25µm + OPP25µm containing green tea extract, and the performance of the antioxidant packaging was studied over 16 months on dark chocolate peanuts and milk chocolate cereals, yielding to a significant reduction of food rancidity and extending the shelf life of the packaged foods.

Wrona et al. (2019) incorporated an extract of *Arctostaphylos uva-ursi* leaves into a water-based adhesive, used to laminate active films made of PET12µm + LDPE40µm, obtaining a stronger antioxidant capacity by increasing the percentage of active agent.

The same approach was also applied to produce active films containing olive leaf and cake extracts, incorporated at different concentrations in the adhesive formula used for laminating multilayer materials consisting of polyethylene/polyethylene (PE/PE) films (extract concentration 1% and 2% m/m) and polyethylene/paper (PE/P) (extract concentration from 1% to 10%) (Moudache et al., 2016; Moudache et al., 2017).

The effectiveness of these configurations, in all the cases, has been validated by the demonstration that neither the release nor the direct contact between the packaging and the food are necessary to obtain free radical scavenging activity (Nerín, 2010).

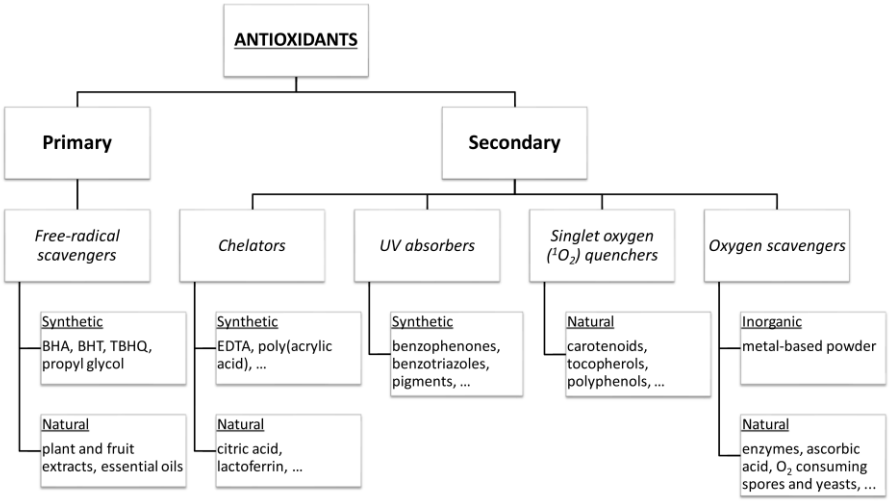

Figure 4 Classification of antioxidants and oxygen scavengers based on their mechanism of action (from: Vilela et al., 2018).

Oxygen scavengers, on their side, have revolutionized and simplified the process of gas reduction in packages, thanks to their ability to reduce the residual oxygen concentration to less than 0.01%, and to actively control the headspace composition over time, preventing all the oxidative damages described before and extending the shelf life of fresh foods from 3–4 to 14 days or more (Gaikwad & Lee, 2017a).

In fact, traditional attempts to remove oxygen from the package headspace, such as vacuum packaging, inert gas flushing or modified atmosphere packaging (MAP), in combination with passive barriers such as multilayer structures containing EVOH or aluminum foils, or polymer blends or nanocomposites (Di Maio et al., 2017; Li et al., 2012) never resulted in complete removal of oxygen from the package headspace. Typically, residual oxygen concentrations of 0.1-2% are obtained, due to the oxygen dissolved into the food or trapped inside the packaging material after sealing.

Furthermore, an internal system is required to continually absorb the oxygen permeating from outside through, for example, can-end seam compounds, glass closure-gaskets, heat-seal imperfections , pinholes, cracks in aluminum foils or even through sophisticated 'high oxygen barrier' laminates like PVdC (poly(vinylidene chloride)) 10 μm on PET (polyethylene terephthalate) 60 μm, which commonly display a combined OTR of 12–18 mL O_2 m^{-2} day^{-1} at 25 °C (Brody et al., 2001; Vermerein et al., 2003; Cichello, 2014).

The scavenging process involves irreversible chemical absorption of molecular oxygen by reactive species or reactive functional groups, capable

of irreversibly binding the solute or converting it into other (neutral) species during the course of a chemical reaction. (Solovyov, 2014).

The scavenging reaction can include, for example, chemisorption, enzymatic reactions, catalyzed oxidation of unsaturated hydrocarbons or reduction of transition metals.

Oxygen scavengers and antioxidants are among the most common and widespread active packaging technologies, and their global market is expected to be worth USD 2.67 billion by 2025, at a compound annual growth rate (CAGR) of 4.9% from 2017 to 2025 (Anonymous, 2017).

This direction is confirmed by the publication trend of antioxidants and oxygen scavengers in food packaging reported Figure 5 (A) and (B). In particular, the antioxidant packaging field showed an increase in the number of publications equal to 197% in the last five years, and 476% in the last ten years, while the oxygen scavengers field has witnessed an increase equal to 75% in the last five years, and 160% in the last ten years.

Key market players include BASF SE (Germany), Baker Hughes (USA), Innospec Inc. (USA), Arkema Group (France), Artibal SA (Spain), Accepta Ltd. (UK), Clariant International Ltd. (Switzerland), Sealed Air Corporation (USA), PolyOne Corporation (USA), Kemira OYJ (Finland); Mitsubishi Chemical Corporation (Japan), and Plastichem (Pty) Ltd (South Africa). Commercial devices include independent, separate elements (such as sachets, cards, strips, closure liners, caps or labels, placed into the inner space or adhesively bonded to the packaging walls) or systems integrated into the packaging material itself, not visually perceptible as distinct elements (such as ready-to-apply absorbing films and coatings with oxygen scavenging properties, or sandwich configurations incorporated with scavenging layers).

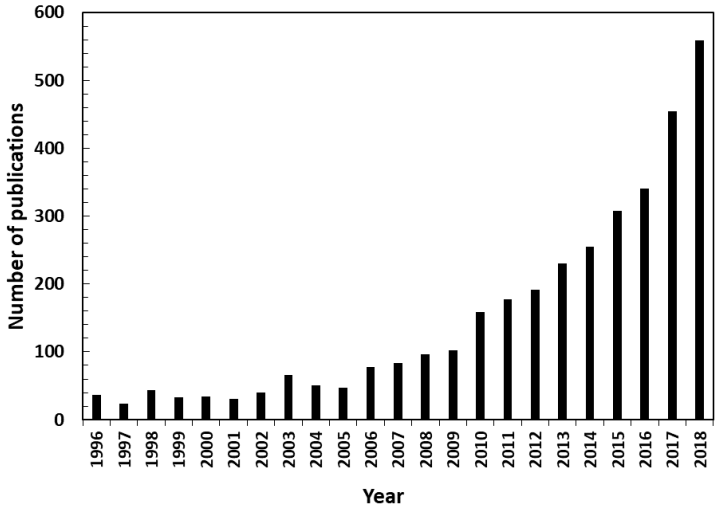

(A)

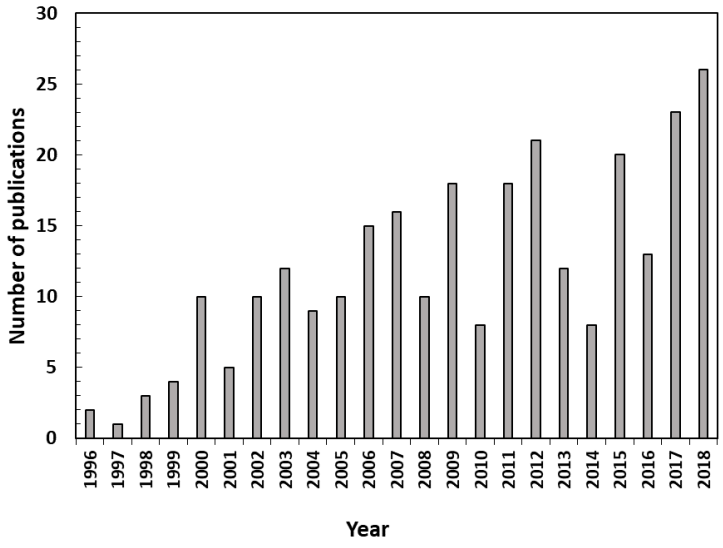

(B)

Figure 5 Publication trends of antioxidant packaging (A) and oxygen scavenging packaging (B) from 1996 to 2018. Data collected from Web of Science using the keywords "antioxidant packaging"-"antioxidant food packaging" and "oxygen scavenging packaging"-"oxygen scavenging food packaging", respectively (https://www.webofknowledge.com).

Classification of oxygen scavengers and antioxidants, reaction mechanisms and applications

Oxygen reactive substrates are each characterized by an activation mechanism, an absorption rate, a scavenging capacity (i.e. the total amount of oxygen absorbable per unit weight of the scavenger), an exhaustion time (i.e. the time required to saturate all the scavenger reactive sites, when the scavenger is incapable of binding more oxygen). These features, together with price and safety, describe the range of suitable candidates for food packaging applications.

Oxygen scavengers can be classified according to different characteristics or properties, related to their triggering mechanism, reaction speed or form (Galdi, 2010).

In principle, any oxidizing substrate, organic or inorganic, can be an oxygen scavenger (Gaikwad et al., 2018; Sun, 2016). Some of them can start absorbing oxygen immediately after exposure to oxygen or air, at ambient humidity and temperature. On the other hand, some oxygen scavengers have an activation mechanism (water vapor, ultra-violet light or magnetic fields, for example), that helps to control the initiation of the reaction, allowing the OS system to be stable before use with food and avoiding its premature activity.

The reaction speed (fast, 0-1 days; medium, 1-4 days; slow, 4-10 days) may depend not only on the chemical nature of the scavenger, but also on its interaction with oxygen and/or other reagents (i.e. the water), the storage conditions, and the packaging layout (Galdi, 2010).

Existing O_2-scavenging technologies are commonly based on iron powder, ascorbic acid, un-saturated fatty acids (i.e. oleic and linoleic acids), enzymes (i.e. glucose oxidase, alcohol oxidase), hydrocarbons, unsaturated polymers, co-polyamides and transition metals, photosensitive dyes, and immobilized yeasts in solid materials (Floros et al., 1997). The classification proposed in Table 2 tabulates the absorbing agents on the basis of their nature and reaction mechanisms.

Metallic oxygen scavengers

Iron-based oxygen scavengers are the most common and widely used scavenging agents for commercial applications. The great success of these systems arises from their easy-to-produce and cheap technology, and their high scavenging capacity and rapid rate of oxidation: theoretically, 1g of iron is capable of absorbing 300 mL oxygen (Miltz & Perry, 2005; Vermerein et al., 2003). However, this value can be achieved only in the case of iron dispersed as a single layer, such that each iron atom is available for oxygen reaction (Foltynowicz, 2018).

Table 2 Classification of the oxygen scavenging agents depending on their nature and reaction mechanism.

Classification	Oxygen scavenging agents	Oxidation mechanisms
Metallic	Iron powder, activated iron, ferrous oxide, iron salt, nano-iron, Co (II), Zn, platinum, palladium	Oxidation of iron with supply of moisture and action of optional catalyst
Organic	Ascorbic acid, ascorbic acid salts, isoascorbic acid, tocopherol, hydroquinone, catechol, rongalite, sorbose, lignin, gallic acid, lecithin, rosemary extracts, polyunsaturated fatty acids, threonine	Oxidation of organic substrate with metallic catalyst or alkaline substance
Inorganic	Sulfite, thiosulfate, dithionite, hydrogen sulfite, titanium dioxide	Oxidation of inorganic substrate by UV light
Polymer based	Oxidation–reduction resin, polymer metallic complex	Oxidation of polymer components with metallic catalyst (mostly cobalt)
Enzyme based	Glucose oxidase, laccase, ethanol oxidase	Immobilization

The oxidation mechanism is based on the following reactions (Cruz et al., 2012):

$$Fe \rightarrow Fe^{2+} + 2e^{-} \quad (1)$$

$$\frac{1}{2}O_2 + H_2O + 2e^{-} \rightarrow 2OH^{-} \quad (2)$$

$$Fe^{2+} + 2OH^{-} \rightarrow Fe(OH)_2 \quad (3)$$

$$Fe(OH)_2 + \frac{1}{4}O_2 + \frac{1}{2}H_2O \rightarrow Fe(OH)_3 \quad (4)$$

The reaction needs a specific level of humidity and it can be accelerated by the presence of electrolytes. Some scavengers may contain water in their carrier materials in order to self-activate upon exposure to oxygen, or use moisture from the food and therefore are suitable for moist products only. Catalysts are commonly used, and the most popular is the chlorine ion, which is usually added in the form of salts such as NaCl, $CaCl_3$ or KCl (Cruz, 2006).

Iron-based sachets were widely used in the past in combination or not with vacuum technology or MAP, are available in different sizes and normally designated by a number representing their scavenging capacity..

Oxygen scavenging films with impregnated iron powder in the polymeric structure have also been developed by incorporation into polypropylene (Lehner et al., 2015), polyethylene terephthalate (Saengerlaub and Muller, 2017), low-density polyethylene (Galotto et al., 2009) or thermoplastic starch (Mahieu et al., 2015). These solutions result in an increased surface area and higher scavenging capacity (Miltz et al., 2005), and some of them are already commercialized under well-known trade names.

A further innovative approach to obtain larger surface areas available for the reaction is the use of iron nanoparticles having surface areas in the range of 20–40 $m^2\ g^{-1}$ and providing 10–1000 times greater reactivity than granular iron, which has a surface area less than 1 $m^2\ g^{-1}$ (Mu et al., 2013).

Nano-iron can be encased into polymers such as polysiloxanes, modified cellulose acetate butyrate, polyamide, polyethylene, polyethylene terephthalate, cellulose derivatives, modified starch, and biodegradable polymers as polylactic acid, polyhydroxybutyrate, and polyoxymethylene (Foltynowicz, 2018).

Films based on other oxidizable transition metals are also known, for example, based on copper, zinc, magnesium, manganese, aluminum, palladium, titanium nanotubes or nanocrystalline titania particles (Yildrim et al., 2015; Matche et al., 2011; Mills et al., 2006; Tulsyan et al., 2017).

The major drawbacks of these systems include potential metal contamination, limitations on the use of food metal detectors, X-ray inspection machines, incompatibility with microwave ovens, as well as the possibility to form rust upon contact with high-moisture foods. In addition, iron oxidation is temperature-dependent, and therefore premature oxygen scavenging exhaustion can occur at high temperatures, as well as excessive slowing of the scavenging rate at low temperatures, creating technical difficulties for food packaging applications.

Inorganic oxygen scavengers

Non-metallic scavengers can be a solution when metallic systems are not permitted; among these, sulfites are very effective oxidation compounds. Sulfite salts, such as potassium or sodium sulfites, can be incorporated into sachets, paper layers, plastic gasket liners of bottle closures, flexible sheets

in trays, or directly integrated into plastic film structures to pack products such as wine or ketchup (Brody et al., 2001). The scavenging reaction is trigged by high humidity and temperature, and the steps involved are :

$$Na_2S_2O_4 + Ca(OH)_2 + O_2 \rightarrow Na_2SO_4 + CaSO_3 + H_2O \quad (5)$$

$$Na_2S_2O_4 + O_2 \rightarrow Na_2SO_4 + SO_2 \quad (6)$$

$$Ca(OH)_2 + SO_2 \rightarrow CaSO_3 + H_2O \quad (7)$$

For example, potassium sulfite can be readily activated by the moist high temperature of the retorting process, and it also has enough thermal stability to be employed during conventional thermoplastic processes. Recently, a sulfite-based oxygen scavenger was developed for kimchi packaging, as a potential alternative to iron powder scavengers, which rust in contact with the high-moisture of the food, and to organic scavengers containing ascorbic acid, which produce additional CO_2 to that coming from kimchi fermentation, thus increasing the package volume and pressure (Lee et al., 2018).

However, end-product compounds such as sulfates and sulfur dioxide are viewed with concern, because of the changes exerted on flavor and sensory profile of the food or even an allergic effect on a susceptible consumer (Brody et al., 2001). Moreover, a sudden catastrophic release of SO_2 could result from water condensation on pads or wettable packaging surfaces

Organic oxygen scavengers

In recent years, some novel non-metallic agents have received considerable attention, including natural organic agents such as ascorbic acid, α-tocopherol, catechol, lecithin, organic acids, gallic acid, polyunsaturated fatty acids, threonine and rosemary extracts, due to their lower perceived risk (Damaj et al., 2015; Gaikwad et al., 2016; Cardona et al. 2011; Janjarasskul et al., 2011).

The natural antioxidant α-tocopherol is receiving a lot of interest from researchers, thanks to its lower sensitivity to high temperatures and its higher molecular weight in comparison with other natural antioxidants (i.e. ascorbic acid, citrus extract, etc.), which make it suitable to be eventually incorporated in natural polymer matrices such as polylactic acid, methylcellulose and whey protein isolate (Scarfato et al., 2015; Jamshidian et al., 2012).

In its scavenging mechanism, α-tocopherol is generally combined with a catalyst, which enhances the scavenging activity thanks to the reaction between oxygen and the transition metal followed by free radical scavenging by tocopherol. Scavenging capacity values were found to increase from

0.69 mL O_2 g^{-1} up to 6.72 mL O_2 g^{-1} without and with a transition metal catalyst, respectively (Scarfato et al., 2015, Byun et al., 2011). Some commonly-used catalysts include iron(II), copper, manganese and cobalt. The proposed steps for the absorption reaction are :

$$O_2 + Fe(II) \rightarrow O_2^{\circ -} + Fe(III) \quad (8)$$

$$O_2^{\circ -} + TocH \rightarrow Toc^{\circ} + HO_2^{\circ} \quad (9)$$

$$HO_2^{\circ} + TocH \rightarrow H_2O_2 + Toc^{\circ} \quad (10)$$

$$2Toc^{\circ} \rightarrow dimer\ and\ other\ products \quad (11)$$

$$Fe(II) + H_2O_2 \rightarrow Fe(III) + HO^{\circ} + OH^{-} \quad (12)$$

$$O_2^{\circ -} + HO^{\circ} \rightarrow {}^1O_2{}^{*} + OH^{-} \quad (13)$$

$${}^1O_2{}^{*} + TocH \rightarrow Tocopherol\ quinone \quad (14)$$

$$Fe(III) + H_2O_2 \rightarrow Fe(II) + O_2^{\circ -} + H^{+} \quad (15)$$

Gallic acid (2,3,4-trihydroxybenzoic acid) is another biobased oxygen scavenger which is receiving increasing attention, due to its strong free radical scavenging activity which makes it commonly used to prevent lipid oxidation in processed foods. This plant phenol is suitable for packaging food with high water activity (a_w > 0.86), as the scavenger activates on contact with moisture (Langowski & Wanner, 2005). Moreover, it absorbs large amounts of O_2 under alkaline conditions, so it must therefore be combined with a base such as sodium ascorbate or sodium hydroxide. Recently, the application of gallic acid into packaging systems has been investigated through incorporation in thermoformed multilayer bio-trays, integration into adhesive layers or film coatings, or addition into the polymer matrix during melt compounding process (Pant et al., 2017; Ahn et al., 2016). The produced systems exhibited a scavenging capacity ranging up to 447 mg O_2 g^{-1}, significantly dependent on environmental temperature and relative humidity.

The oxygen scavenging reaction between gallic acid and potassium carbonate is proposed in the following equations:

Activation step:

$$KCO_3 + H_2O \rightarrow 2KOH + CO_2 \quad (16)$$

Scavenging step:

$$GallicH + O_2 \rightarrow Gallic^{\circ} + HO_2^{\circ} \quad (17)$$

$$HO_2^{\circ} + GallicH \rightarrow Gallic^{\circ} + H_2O_2 \quad (18)$$

$$2Gallic^{\circ} \rightarrow Gallic\ acid\ dimer \quad (19)$$

$$Gallic\ acid\ dimer + O_2 \rightarrow Quinone\ of\ dimer + 2H_2O_2 \quad (20)$$

$$Quinone\ of\ dimer + 2O_2 \rightarrow Open-ring\ product\ of\ dimer \quad (21)$$

Natural oxygen scavengers and antioxidants exhibit the potential for the development of new packaging formats with numerous desirable qualities and advantages, concerning both consumer perception and sustainability.

Wrona et al. (2015) studied several natural compounds, including green tea extract, cinnamon essential oil, α-tocopherol and purple carrot extract, impregnated onto paper sheets or coated on PET substrates, to inhibit enzymatic browning of fresh mushrooms. Results showed the effectiveness of the green tea extract in maintained the white colour of mushrooms during storage, and appreciable positive results for cinnamon essential oil in reducing the bacterial blotching during the mushrooms shelf-life.

The addition into plastic materials of plant and fruit extracts, rich in nutritive properties, has an advantage: the possible migration of these compounds into the food improves the nutritional characteristics of the foods with a nutraceutical benefit. Moreover, the incorporation of natural extracts coming from the revaluation of food industry wastes such as olive pomace, leaves, milling wastewaters, as well as potato, grapes or tomato peelings, represents not only a way to restore their economic and commercial value, but also solves a burdensome problem of environmental impact.

However, the amount of antioxidant added to the polymer must be controlled, since high concentrations can affect the barrier or mechanical properties of the polymeric matrix (Wessling et al., 1998), Further research should focus on improvements in technical and commercial feasibility, including processing issues, thermal stability, cost, effective oxygen scavenging capacity and migration constraints, which actually represent the main hurdles to the commercialization of these active agents.

Enxyme-based oxygen scavengers

Enzyme-based oxidation is another approach to regulate the oxygen concentration in the food package. The most commonly used enzymes for oxygen scavenging in food packaging are glucose oxidase, used in combination with catalase (Johansson et al., 2011). The scavenging reaction takes place according to the following mechanism, where glucose must be

present in food or in the scavenger formulation as a substrate (Cruz et al., 2012; Mabeck & Malliaras, 2006):

$$2\ glucose\ +\ 2O_2\ +\ 2H_2O \xrightarrow{Gox} 2\ gluconic\ acid\ +\ 2H_2O_2 \quad (22)$$

$$2H_2O_2 + catalase \rightarrow 2H_2O + O_2 \quad (23)$$

The formation of gluconic acid lowers the pH, and the effect of pH reduction could have adverse effects since these enzymes are very sensitive to pH, water activity, salt concentration, and temperature (not higher that 60 °C). The presence of $CaCO_3$ has a positive effect as it neutralizes the gluconic acid formed. Moreover, the addition of water is required for activation, and therefore they cannot be effectively used for low-water foods (Graf, 1994).

Enzymes can be either directly incorporated into the packaging structure or put into an independent sachet. The immobilization occurs by adsorption, encapsulation or coating onto different substrates, including polystyrene, polyethylene, and polypropylene (Gaikwad et al., 2018). However, when the coated enzymes are immobilized, the surface carrying the active enzyme must be in direct contact with the food to activate the redox reaction, in order to consume the glucose in the food. This restricts the application of enzyme-based films in food packaging (Brody et al., 2001). In addition, the release of reaction intermediates and end products could promote undesirable changes within the food , affecting the food composition.

Oxygen scavengers in the polymer matrix and polymer-based oxygen scavengers

Although iron-based oxygen scavengers still occupy a leading position among commercialized systems, and the performance of oxygen-absorbing sachets was quite satisfactory for a wide range of food storage conditions, a number of limitations to their use in practice were recognized.

The main concerns are related to (Brody et al., 2001):

- the potential health risks, due to accidental ingestion of the scavenging agent or to food contamination by possible sachet leakage;
- the consumer acceptability of visible devices, which can be perceived as harmful;
- the difficulty of inserting sachets into packages with a very small inner space, or having a narrow opening, or containing liquid foods and beverages;

- the tendency of oxygen scavenging powders in the sachets to coagulate into a lumpy shape, with a consequent reduction in the surface area for oxygen reaction and the need for larger quantities of oxygen-scavenging powder than the theoretical amount to ensure gas absorption at the desired rate.

All these major drawbacks prompted research into new promising approaches for the realization of oxygen active packaging; one of these consists of the incorporation of the oxygen-scavenging compound directly into the packaging material.

The design and development of non-visible, integrated OS systems, easy to blend with the polymer matrix and to process through conventional technologies, is creating growing interest, and new patents are being continuously registered.

Polymers show advantages over materials such as glass and metal. Most popular features include light weight, ease of forming, fast production, good chemical resistance, high toughness, and ease of designing tailor-made solutions. Some of these features are further emphasized in flexible packaging: plastic films involve reduced use of raw materials, reduced waste and disposal issues, and therefore reduced costs for production, handling and transport.

However, attention must be paid to the barrier properties of plastics, which are poorer than those of metal and glass. The polymers used in food packaging applications should provide a sufficient barrier to gas and moisture, otherwise the quality and shelf life of packaged foods will be directly affected (Robertson, 2013). The addition of a scavenging compound to the plastic matrix provides an active protection by markedly reducing the oxygen transmission rate and resulting in the same advantages of heavier and more expensive packaging materials.

The first attempts consisted of the incorporation of the main active compounds employed for the sachets directly into the polymers: patent bibliography describe the use of iron powder plus a metal halide or other kind of electrolytes (Inoue & Komats, 1990a; Inoue et al., 1990b; Nakae et al., 1990; Tung et al., 2004). The most common matrices include polyolefins, polyamides and aromatic polyamides, polyesters, polyfluoro-olefins, etc. Organic oxygen scavengers show much better dispersion and compatibility with polymeric matrices compared to the dispersion of inorganic powders. However, the direct addition of powders or more or less liquid mixtures can often cause degradation of the matrix, loss of transparency, drop of functional properties, and considerably affect the processing and scavenging performance, especially in the fabrication of thin layers (Galdi & Incarnato, 2011). For this reason, this technology is mainly applied to the production of thicker polymeric packages such as trays, bottles, labels and layers for caps.

The newer approach is to add polymer-based scavengers to plastic materials in order to produce both rigid and flexible integrated packages by means of conventional processing technologies. Oxygen scavenging polymers typically lack adequate structural properties, so they are generally added to polymer blends. Polymer-based oxygen scavengers include ethylenic-unsaturated hydrocarbons, such as squalene, fatty acids, or polybutadiene, where the ethylenic unsaturation (-CH=CH-) is subject to catalytic autoxidation and can be used to scavenge molecular oxygen (Solovyov, 2014). These unsaturated hydrocarbons are usually functionalized with chemical end-groups to improve the compatibility with packaging materials such as polyamides, polyolefins, polyesters, and polyfluoro-olefins, in order to form an oxygen scavenging polymer that can be used in the walls of a package. This technology is widely reported in the patent literature (Cochran et al., 1991; Speer et al., 1993; Blinka et al., 1998; Venkateshwaran et al., 1998; Venkateshwaran et al., 1999; Cahill & Chen, 2000; Adur et al., 2000; Gauthier & Speer, 2001; Tung et al., 2004; Miranda & Speer, 2005; Bheda & Moore, 2007; Tibbit et al., 2007; Evans et al., 2010; Share et al., 2012; Fava et al., 2014).

This innovative solution offers a further advantage, namely the possibility of producing monomaterial polymeric packages which can be easily recycled in the post-consumer phase, with no additional environmental impacts. This approach, driven by the growing attention to sustainability and the rational use of resources, allows the rejection of the linear economy model, in favor of the more advantageous circular economy model, capable of being self-sustaining and self-regenerating.

Polybutadiene is recognized as one of the most important hydrocarbons for O_2-scavenging purposes. This synthetic rubbery polymer is readily oxidized upon exposure to even low levels of atmospheric oxygen at room temperature; moreover, it exhibits transparency, mechanical properties and processing characteristics similar to those of polyethylene.

Applications of polybutadiene in oxygen scavenging materials typically include the addition of a small amount of a transition metal catalyst in order to accelerate the oxidation (Li et al., 2012). In this regard, cobalt II neodecanoate (or octoate) is a popular choice in the patent literature (Devlieghere et al., 2004; Cahill & Chen, 2000; Ching et al., 2006). Moreover, photoinitiators can be added to further facilitate and control the initiation of the scavenging process, as well as the addition of antioxidants to prevent premature oxidation and cross-linking.

The reaction mechanism of cobalt-catalyzed polybutadiene, as suggested by Li et al. (2012), is:

$$O_2 + RH \rightarrow ROOH \tag{24}$$

$$Co^{2+} + ROOH \rightarrow Co^{3+} + OH^{-} + RO\cdot \quad (25)$$

$$Co^{3+} + ROOH \rightarrow Co^{2+} + H^{+} + ROO\cdot \quad (26)$$

RH refers to the allylic carbon-hydrogen bonds of the polymer, which are most susceptible to undergo oxidative degradation, and both Co^{2+} and Co^{3+} species are reported to participate in the oxidation steps and help generate free radicals. Upon increasing cobalt neodecanoate concentration, the free radical generation rate increases.

The main issues are related to the formation of oligomeric reaction by-products such as organic acids, aldehydes, or ketones, which can migrate to the food thus affecting its sensory quality, including color changes and development of rancid off-flavors (Devlieghere et al., 2004; Floros et al., 1997). This problem can be minimized by using functional barriers to limit the migration of undesirable oxidation products, or by adding absorber materials such as silica gel and zeolites, or by containing the ethylenic unsaturation within a cyclic group (Ching et al., 1997; Bacskai et al., 1997; Ching et al., 1999).

Another example of polymer-based oxygen scavenger is represented by poly(m-xylylene adipamide), a low permeability aromatic polyamide also known as MXD6, with reducing properties once doped with an appropriate transition metal salt. It is commercially used in high oxygen barrier packaging applications, both for oxygen and CO_2, usually in combination with PET due to similar thermal and rheological properties (Bacskai et al., 1997).

The autoxidation reaction of polyamides such as MXD6 proposed by several authors hypothesize the conversion of molecular oxygen to oxidizing ions (ions of super oxides or peroxides) under the influence of temperature, light or active metal complexes. Once activated, the oxygen is able to attack the polymer chain, creating organic radicals. Propagation may continue through a variety of parallel reactions. Another proposed mechanism suggests decomposition of the polyamide when used along with the catalyst. In this case, an internal electronic shift breaks the bond next to the oxyl-function; the decomposition likely occurs near the carbon atom contained in the amide group, as the C-N bond is usually weaker, but the side of the aromatic ring is also possible (Ball, 1995; DeRoover et al., 1996).

According to the above mechanism, the risks of producing by-products such as aldehydes and carboxylic acids is very high for these systems. The issue can be overcome by designing multilayer structures or blending small amounts of MXD6 directly into the PET, and these solutions are frequently applied in the PET bottle market for beer, wine and sensitive juices (Cahill & Chen, 2000; Tibbitt et al., 2007; Collette et al., 1998).

Other disadvantages are related to haze effects due to the MXD6 immiscibility in PET, forming micron-sized islands, and the potential yellowing of the final package due to the condensation of aldehyde-groups to amine end-groups, forming azomethine groups. (Michelis et al., 2017). Recently, low molecular weight variants of MXD6 have been marketed. These monomeric components are much better distributed inside the PET-matrix. The result of this new technology is the manufacture of clear bottles without any loss in oxygen scavenging (Behrendt et al., 2013; Deshpande, 2014).

The more recent patent literature describe the new generation of oxygen scavengers for food packages as polymeric systems integrated with micro/nano-iron or zero-valent iron doped with boron (Foltynowicz et al., 2012), sodium/potassium sulphite/ascorbate for carbonated beverages (Peirsman & Valles, 2016), active polyamide or copolyamide, polyolefinic unsaturated systems functionalized, as above described, and usually combined together. Many of these applications are currently commercially available under well-known trade names, as reported in Table 2 (Gaikwad et al., 2018; Ravishankar Rai & Jamuna Bai, 2017).

The introduction of inorganic powders, salts, enzymes, and natural extracts from plants is also widely discussed in the recent scientific literature, as reported in the previous paragraph, and the innovations are often related to the improvements in processability or the optical and functional properties of the products.

Table 3 Commercial oxygen scavengers in polymer matrices for food packaging applications.

Manufacturer	Commercial name	Scavenger form	Product form
Ciba specialty chemicals	SHELFPLUS® O_2	Iron based	Plastic film and bottle
Chevron chemicals	–	Benzyl acrylate	Plastic film
CMB technologies	OXBAR	Cobalt catalyst	Plastic bottle and film
Toyo Seikan Kaisha., Ltd.	Oxyguard	Iron based	Plastic tray
Aptar CSP technologies	Active-Film™	UV radiation	Plastic film
Cryovac Division, Sealed Air	Cryovac® OS2000	Light-activated scavenger	Plastic film

Corporation			
Mitsubishi Gas Chemical Co.	AGELESS OMAC	Iron based	Plastic film
Bioka Ltd	-	Enzyme based	Plastic film
Clariant	Cesa®-absorb masterbatch	Organic/ co-polyester	Plastic bottle and film
Colormatrix™, PolyOne Corporation	Amosorb™, Amosorb SolO2™, HyGuard™	PET co-polyester	Plastic bottle
Mossi & Ghisolfi	Poliprotect™	PET co-polyester	Plastic bottle
Amcor	Bind-Ox™	-	PET bottle
Constar	Oxbar™ (multilayer), MonoOxbar™ (monolayer)	-	PET bottle
Mossi & Ghisolfi	ActiTuf™	Moisture-activated scavenger resin	PET bottle
Invista	PolyShield™	PET/MXD6 blend + compatibilizer	PET bottle
Valspar	ValOR®	Moisture-activated scavenger resin	PET bottle

Nevertheless, there are many unsolved problems that have limited the application of these technologies, especially in the flexible packaging markets. Together with the previously mentioned risks for the formation of migrating oligomers such as aldehydes and ketones, other common drawbacks include scavenging speed and capacity which are considerably lower than those of iron-based oxygen scavenger sachets and labels (Kruijf et al., 2002), and the difficulty of guaranteeing constancy in the functional performances of the package, both in terms of ongoing scavenging activity and preserving the mechanical and optical properties.

I.3 Strategies to improve food packaging sustainability

In Europe, the plastic industry ranks 7th in industrial value added contribution, with a production of almost 62 million tonnes per year and a turnover of more than 360 billion euros in 2018. Packaging by far represents the largest end-use market, and accounts for 39.9% of the total plastic required (Anonymous, 2019b).

In particular, the flexible packaging sector is one of the fastest growing sectors of the packaging industry, thanks to its combination of product safety and protection performance with ease of use, large marketability, excellent printability, reduced volumes, ease of transport and storage.

A large part of this market is engaged in food packaging production. Packaging is a central element to food quality preservation, and has been recently identified as essential element to address the key challenge of sustainable food consumption (Guillard et al., 2018). In particular, significant benefits are expected in terms of reduction of food waste thanks to shelf life extension offered by active packaging solutions, especially by using a well dimensioned packaging material.

However, packaging is usually wrongly considered as an additional economic and environmental cost rather than an added value for food waste reduction. After an exclusively single and very short use inherent as food packaging, 40% ends up in landfill, corresponding to 9 million tons of plastic packaging waste that is fated to accumulate in soils. 32% leak out of collecting and sorting systems and finally end in marine and soil litter.

Therefore, public concerns toward waste-management issues and shortage of resources, have recently shifted the research focus towards the development of new eco-compatible and sustainable packaging solutions, in order to create "a world in which packaging is designed to be effective and safe during its life cycle, meets the market's needs in terms of costs and performance, is made by renewable resources and, once used, is efficiently recycled/reused in order to provide valuable resources for future generations" (Buonocore et al., 2016).

To develop sustainable packaging it is important to follow some precise guidelines, such as:

- the respect for the primary functions of containment, protection and preservation of the product, guaranteeing total transparency about the life cycle of the product and its packaging;
- the use of the least possible quantity of material, without reducing the functionality and the fulfillment of its functions;
- the compliance with the main quality requirements provided by the legislation;

- the optimization of the recycling processes of plastics of synthetic origin, in order to reduce their volume over time and minimize the use of new raw materials;
- the compliance with the legislation requirements for waste materials disposal, the implementation of suitable protocols and the creation of adequate infrastructures.

In this context, food and packaging waste reduction means more rather than less packaging, or oil-based resources substitution by renewable resources.

In response to these needs, the interest of packaging scientists and industry mainly focuses on development of eco-sustainable solutions with high performance and smart materials, with particular attention to the use of new technologies, nanotechnologies and natural degradable polymer matrices and additives. In this scenario, innovations in the food packaging sector can be grouped into the following macro-lines of research:

Development of 100% mono-materials packaging as an alternative to multi-materials packaging

As a matter of fact, functional requirements imposed on packaging are so complex that, especially in case of flexible packaging, multiple material combinations are needed to fulfil them.

Multi-material flexible films contain different layers of materials (paper, plastic, aluminum foil, metallized or coated paper). These carefully engineered materials provide many of the properties that consumers and businesses love – adding durability, product safety, extending product life – but their construction also makes them very difficult to recycle.

The development of new multi-layer, mono-material structures, providing the same barrier protection but consisting all of a single material (for example, a single polymer) significantly simplifies sorting in the recycling phase. This would increase the recycling quota and reduce the need for new resources, also simplifying the reuse of materials during the manufacturing phase.

Moreover, the compelling necessity to satisfy high gas barrier performance can be further achieved through development of mono-material active-barrier composites, i.e. through the addition of specific polymeric oxygen-scavengers.

The polymeric nature of the oxygen scavengers would not affect the recyclability of the plastic packaging. At the same time, they are capable to actively control oxygen permeation, offering the same protection as heavier, more expensive and non-polymeric materials.

The action is concretely applicable to packaging sectors related to toiletry, medical, pharmaceutical, and food industries. Data available from studies in European countries implies that approximately 20% (estimated range between 0.52 and 1.4 mt) of the flexible packaging is multi-material (Kaiser et al., 2017). Re-designing multi-layer flexible packaging makes them potentially recyclable via the infrastructure for recycling conventional plastics.

Some examples of mono-materials packaging systems have been launched in 2019 on the market: in Japan, Toppan Printing has developed all-PET (polyethylene terephthalate) laminate mono-material films, providing outstanding oxygen and moisture barrier performance as well as low adsorption and packaging sealability. In Italy, Termoplast has developed all-PE (polyethylene) multilayer structures for pouches and top-lids, which provide mechanical characteristics similar to those of PET and BOPP laminates, and excellent barrier to oxygen and water vapor. In USA, ProAmpac is developing a mono-material PE stand-up pouch, for L'Oréal's REDKEN Flash Lift, within the ProActive Sustainability initiative, which was honored as a Diamond Finalist for the Packaging Innovation Awards by Dow.

The recently launched Circular Plastics Alliance (CPA) aims to ensure that ten million metric tons of recycled plastics are used in EU products by 2025. However, it also calls for the development of recycling technologies and infrastructure throughout the EU.

In fact, despite the ability of researchers to develop mono-material solutions, the lack of recycling infrastructure can still be a challenge, and the necessity for more agile and aligned recycling systems has been highlighted by many industry players.

Therefore, it is also up to governments and the recycling industry to establish the infrastructure that can appropriately collect and recycle those newly developed packaging solutions.

Development of biodegradable packaging as an alternative to petroleum-based materials, and revaluation of food industry waste materials

The use of biodegradable and/or compostable materials aims at minimizing the environmental impact induced by post-consumer synthetic plastic wastes.

According to the latest market data compiled by European Bioplastics, in 2018 the global production capacities of bioplastics amounted to about 2.11 million tonnes, with almost 65 percent (1.2 million tonnes) of the volume

destined for the packaging market – the biggest market segment within the bioplastics industry (Anonymous, 2019b).

However, bio-polymeric systems are only used for some specific applications, due to their limiting characteristics, such as high cost and scarce mechanical and thermomechanical properties, with respect to traditional commodity polymers.

A challenging opportunity, in this sense, is represented by the development of 100% green and eco-friendly bio-composites, obtained from biopolymers incorporated with natural compounds, deriving from agricultural and industrial waste materials. As an example, vegetable and lignocellulosic fibers can be applied as polymer fillers and reinforcements, with potential cost savings deriving from the less employment of raw materials.

At the same time, bioactive compounds with antioxidant or antimicrobial effectiveness, deriving from plants and fruits, can be successfully employed in active packaging technologies.

The synergic combination of biopolymers with natural additives, therefore, would represent not only a way to improve the packaging's functionalities and reduce the dependence on fossil fuels, but also allows the valorization of crop or food-processing waste streams, restoring their economic and commercial value.

Furthermore, encouraged by a favorable European regulation (EU Circular Economy Package, EU Waste legislation, etc.), recent innovative research has focused on developing bio-plastics from organic waste streams (crop residues, agro-food by-products, sewage sludge, etc.) seeking to enter a circular economy concept that does not compete with food usage and that is fully biodegradable to respond to the overwhelming negative externalities of our plastic packaging.

The proposed action is concretely applicable to packaging sectors related to food packaging, food-services, agriculture-horticulture, consumer goods and pharmaceuticals.

Biodegradable flexible packages are particularly suitable for fresh and perishable food products. The shelf-life requirements for food packaging are as different and numerous as there are different types of food. However, the use of additives such as natural antioxidants and antimicrobials, incorporated into the polymer matrix or added into coating layers, could improve the barrier properties of bio-plastics, ensuring the same performance and protection of existing conventional packaging.

Up to now, the major obstacle to bio-based growth is cost-effectiveness, with greater investment and government support needed for the European bioplastics industry. However, more and more investments and experimentation in the space of bioplastics are expected, in particular from Asian countries.

In Italy, the turnover deriving from bio-plastics is constantly growing: +26% in 2018, with respect to 2017, about 685 million euros more in turnover, with a production that sees an increase of 21%, equal to 88,500 tons, and an increase in companies and employees of +4% (Anonymous, 2018a).

In particular, two Italian companies, Novamont and Bio-On, are concentrating their efforts to bring new products to market. Bio-On has already joined forces with Unilever to use patented bio-technologies for natural, biodegradable plastics production.

100% natural and biodegradable packaging solutions are particularly attractive within niche applications, such as sandwiches, nuts, snacks and confectionery, which are also likely to gain more favor with the smaller "challenger brands".

By increasing the number of materials, applications, and products, the number of manufacturers, converters and end-users also would increases steadily. Significant financial investments needs to be made into production and marketing to guide and accompany this development. Legal framework conditions should provide incentives for the use of bioplastics worldwide, providing stimulus to the market.

These strategies go in the direction of supporting the development of a circular economy in the packaging sector, by closing the loop and using wastes as resources, approach that is also being encouraged by recent policies in Europe (Ellen Mac Arthur Foundation, 2015).

According to the latest market data compiled by European Bioplastics in cooperation with the research institute nova-Institute, global bioplastics production capacity is set to increase from around 2.11 million tonnes in 2018 to approximately 2.62 million tonnes in 2023. In particular, production capacities of PLA (polylactic acid) are predicted to grow by 60 percent by 2023, compared to 2018 (Anonymous, 2018a).

The forecast also predicts the budding bioplastics industry to unfold an immense economic potential over the coming decades. Moreover, according to a recent job market analysis conducted by EuropaBio (2016), the European bioplastics industry could realize a steep employment growth. In 2013, the bioplastics industry accounted for around 23,000 jobs in Europe. With the right framework conditions in place, this number could increase more than tenfold by 2030, with up to 300,000 high-skilled jobs being created in the European bioplastics sector. At the same time, opportunities have already been identified to apply industrial symbiosis in valorizing food wastes from the food manufacturing industry. Consequently, food waste valorization has a great deal of potential to provide economic, social and environmental benefits.

I.4 Design strategies for food packaging films: Processing Technologies

Depending on the physiochemical properties of both the active phase and the polymer matrix, different incorporation technologies can be applied to realize active packaging films. These include:

- blending into the polymer matrix (Figure 6 (A) and (B));
- realization of multilayer structures (Figure 6 (C) and (D)).
- dispersing the active agent into a thin coating layer (Figure 6 (E) and (F));
- chemical immobilization of the active agent on the package surface (Figure 6 (G) and (H));

The choice of the processing method and processing parameters may considerably affect the final release behavior of the active compound, in case of controlled release systems, or the absorption performance, in case of scavenging films.

Polymer blending

One of the most straightforward ways to incorporate an active agent into a film layer is to simply blend it with the polymer matrix (Figure 6 (A) and (B)).

This approach is applicable for the development of active membranes by either casting (Janjarasskul et al., 2011; Byun et al., 2012; Fortunati et al., 2016), or extrusion (Arrieta et al., 2014, Jamshidian et al., 2012; Marcos et al., 2014; Byun et al., 2010; Ahn et al., 2016; Busolo & Lagaron, 2012; Shin et al., 2011; Scarfato et al., 2015; Galdi & Incarnato, 2010; Galdi & Incarnato, 2011).

Extrusion compounding is useful in case of blending two or more different polymers, or a polymer with a plasticizer, to modulate the release rate of active compounds (Chen et al., 2019; Arrieta et al., 2014).

Extrusion is also widely applied in the case of oxygen scavenging polymers which typically lack adequate structural properties, so they are usually employed as composites (Carranza, 2010a). Many examples of polyamide or polybutadiene-containing polymers blended with polyethylene terephthalate are reported in the literature, mainly focusing on rigid applications for wine or juice (Dombre et al., 2015; Ros-Chumillas et al., 2007; Bacigalupi et al., 2013; Dombre et al., 2015; Di Felice et al., 2008; Saengerlaub and Müller, 2017).

The active agent compatibility with the selected matrix and its stability play a crucial role in the selection of the polymer blending configuration and processing conditions.

Partial or complete immiscibility involves the formation of active agent particles (spherical in the simplest case) or aggregates within the dispersing matrix, whose size varies depending on the rheology, the mass ratios, and the compounding conditions. Thus, the functional properties and the active performance of the final active packaging are further related to these settings. In addition, large amounts of active phase are needed to ensure homogeneous dispersion throughout the whole package, and major mass and activity losses can occur during the manufacturing process (Johnson & Decker, 2015).

Encapsulation is a possible strategy to circumvent obstacles related to the active agent decomposition due to light, heat or pressure exposure, or to reduce losses by evaporation of highly volatile compounds such as essential oils. Encapsulation involves the entrapment of the antioxidant or antimicrobial within an additional material which has a protective function, while providing a controlled release or/and stimuli-responsive release in a given medium over time. Encapsulation may also improve the compatibility between the packaging polymer and the active substance, reduce changes in food sensorial properties or comply with the legal restriction limits (Becerril et al., 2020).

A broad range of delivery systems or carriers have been developed to encapsulate bioactive compounds in the food sector, such as cyclodextrins, liposomes, emulsions, nanoparticles or microcapsules.

As example, novel active packaging was developed by encapsulating green tea extract (GTE) in inorganic capsules, incorporated in PE films by extrusion process. Inorganic capsules protected GTE against degradation during extrusion processing, while the antioxidant effectiveness of the packaging was verified by *in-vitro* release tests and *in-vivo* experiments on shelf-life extension of fresh minced pork meat (Wrona et al., 2017a). Hydroxypropyl-methylcellulose (HPMC) containing poly(lactic acid) (PLA) nanoparticles (NPs) loaded with green tea extract were also realized to achieve controlled antioxidant release, generally dependent on the size of the nanoparticles (Wrona et al., 2017b).

α-tocopherol-loaded PLA microparticles containing 40 wt% were realized by Scarfato et al. (2015a) to be used as biodegradable oxygen scavenger system. The preparation procedure ensured high encapsulation efficiency and the microcapsules showed satisfactory oxygen scavenging capacity and suitable flowability to be used as active powder additive in conventional polymer extrusion technologies.

Another recent strategy was developed by Silva et al (2019b) and Simionato et al. (2019) to encapsulate antimicrobials in cyclodextrin nanosponges. Nanosponges are cross-linked cyclodextrin polymers nanostructured within a three-dimensional network, ensuring a higher loading capacity, and better controlled released with respect to monomeric native cyclodextrins. This approach was used to encapsulate cinnamon and

coriander essential oil, demonstrating antimicrobial activity against foodborne Gram positive and Gram negative bacteria and a controlled EO release. However, the incorporation of these novel structures in packaging materials has not been tested yet.

Multilayer structures

Multilayer structures (Figure 6 (C) and (D)) represent multipotential, synergic systems, each layer providing different functionalities not achievable through single-layer layouts.

Multilayer configurations are capable of extending the shelf life of the food while, at the same time, ensuring primary functions and customer-driven features of the packaging (mechanical properties, transparency, sealability, printability, etc.), comply with regulatory limitations on food contact layers, and extend the duration of the oxygen scavenger.

For instance, Fe-based films may allow migration of iron into the food, accelerating lipid-oxidative reactions (Gaikwad et al., 2018), while the main risk of polymer-based scavengers is the aforementioned formation of oligomers such as organic acids, aldehydes, or ketones imparting an undesirable flavor and affecting the sensory quality.

Additional inert layers can be used to improve oxygen barrier properties of the package (Granda-Restrepo et al., 2019; Di Maio et al., 2015), creating a synergistic system in which the central layer traps and reacts with oxygen, thus providing an active protection, whereas the outer layers improve the passive protection, controlling the O_2-diffusive flux and therefore the rate at which the scavenger exhausts (Figure 6 (C).

At the same time, an inner, barrier layer between the active layer and the food matrix may be useful in controlling the release of the antimicrobial compound (Figure 6 (D)).

Multilayer packaging refers to laminated, coextruded and/or metallized films, coated and surface treated packaging materials, rigid co-injected containers, multilayer preforms for bottle blow molding, and sheets for thermoforming produced from several different materials and made into a layered heterogeneous structure (Solovyov & Goldman, 2008).

The scientific literature contains a variety of examples regarding this technology. Shin et al., (2011) reported the development of three-layer co-extruded blown films, with the inner and outer layers composed of high density polyethylene (HDPE) and the core layer containing an iron oxygen scavenger mixed with the HDPE or linear low density polyethylene (LLDPE).

Anthierens et al., (2011) proposed the production of oxygen scavenging, multilayer PET bottles using an endospore-forming bacteria *Bacillus amyloliquefaciens* as the active ingredient. Spores were incorporated in poly(ethylene terephthalate, 1,4-cyclohexane dimethanol) (PETG), an

amorphous PET copolymer having a considerably lower processing temperature and higher moisture absorption compared to PET.

Recently, active thermoformed multilayer bio-trays were also produced by incorporating gallic acid and sodium carbonate into the core layer of a biopolyethylene/polylactic acid (BioPE/BioPE+15% oxygen scavenger/PLA) film, prepared by extrusion and lamination (Pant et al., 2017).

A novel approach involves the incorporation of antioxidants or antimicrobials within the adhesive layer that joins different laminating materials. This simple methodology ensures the active agent preservation from degradation or evaporation, without increasing processing costs or complexity, since it does not require additional steps or technical changes in the manufacture process.

Multilayer antimicrobial films were developed by Gherardi et al. (2016) inserting six different antimicrobials (benzoic acid, sodium metabisulphite, tert-butylhydroquinone, LAE, cinnamon and oregano essential oils) within the solvent based adhesive layer joining the aluminum (Al) and PE layers of a PET/Al/PE structure. The produced films were tested for the shelf life extension of tomato puree, and the materials containing polyurethane adhesive free of isocyanates and different concentrations of cinnamon essential oil showed high efficiency against *Escherichia coli* O157:H7 and *Saccharomyces cerevisiae*.

Antioxidant compounds successfully incorporated into adhesive formulations also include green tea extract in OPP/OPP structures (Carrizo et al., 2016), *Arctostaphylos uva-ursi* leaves extract in PET/LDPE (Wrona et al., 2019), olive leaf and cake extracts in PE/PE and PE/paper multilayers (Moudache et al., 2016; Moudache et al., 2017), selenium nanoparticles in PET/PE films (Vera et al., 2016; Vera et al., 2018), sage and bay leaves extracts in LDPE/PET (Oudjedi et al., 2019), demonstrating strong antioxidant effectiveness with no need of direct contact with foodstuffs.

The compatibility between the active phase and the adhesive (if laminated) or the polymeric matrix (if coextruded), as well as the compatibility between the polymers of which the layers are made (if the structure is heterogeneous) plays a crucial role in the success of this application in order to avoid the delamination of the final product.

Coating on a film substrate

Coatings are defined as non-self-supporting layers (usually in liquid form) applied on a substrate in order to impart special properties or improve technical performances of the finished article after drying. Oxygen scavengers, antimicrobials or antioxidants can be physically adsorbed or coated onto food packaging materials to bring additional scavenging functionality to the surface they are applied to (Figure 6 (E) and (F)) (Demicheva, 2015).

Coating layers are commonly produced through precipitation, induced by solvent evaporation, of a coating solution, incorporated with the active phase, spread on a plastic support layer. Active agents can work with or without direct contact with foods or by generating a vapor phase that transfers the antioxidant activity to the headspace (Gaikwad, 2018).

Examples of oxalate oxidase or glucose oxidase entrapment in a polymer-based dispersion coating in active packaging were reported by Nestorson et al., (2008), and Winestrand et al., (2013). Gohil & Wysock (2013) also investigated the effectiveness of oxygen scavenging coatings and flexographic printing ink formulations made using water soluble and water insoluble ascorbate enzyme systems.

Demicheva (2015) developed a novel oxygen scavenging material based on polybutadiene suitable for use in functional coatings. Two polybutadiene types of different isomeric structures and various amounts of additives were tested and the results pointed out the effectiveness of the developed systems, possessing high oxygen scavenging capacity of approximately 26% (mass of oxygen to mass of polybutadiene used).

Recently, a moisture-activated oxygen scavenging film with pyrogallol (a natural phenolic compound) coated onto a LDPE/sodium carbonate substrate was developed by Gaikwad et al., (2017b), resulting in an effective scavenging capacity of 0.443 mL g^{-1} at 20% w/w pyrogallol content.

Coating technology offers the advantage of avoiding thermal stresses to heat sensitive active phases and alterations to the rheological behavior and functional properties of the substrate. In addition, the reduced thickness of the coating allows the use of lower amounts of active agents.

Coatings based on alginate, carrageenan, gelatin, zein, gluten, whey, carnauba, beeswax and fatty acids, proteins and lipids show advantages such as biodegradability, biocompatibility, good look and high barrier to oxygen and physical stress (Fakhouri et al. 2015).

Nevertheless, good compatibility of the active phase with the polymer matrix and the solvent is essential to avoid precipitation of the active agent in the mixing phase, and the affinity of the coating layer with the substrate is fundamental to avoid delamination.

Immobilization on packaging surface

Immobilization of active agents is an alternative to their incorporation into the polymer when extruding or casting. It allows incorporating on packaging surfaces those agents that are not capable of withstand the mechanical stresses and high temperatures of extrusion processes, or which may be altered due to the presence of certain solvents used in the preparations of cast films and coatings (Appendini and Hotchkiss 2002).

This way of incorporating the active agent has the advantage of reducing the amount of the compound added to the polymer matrix, minimizing the loss of activity and helping to maintain the concentration of the active

compound in the food surface at appropriate levels to ensure its inhibitory effect. This type of immobilization requires the presence of functional groups on both the active phase and the polymer. Examples are peptides, enzymes, polyamines and organic acids.

Immobilization on the package surface is widely applied with enzyme-based oxygen scavengers. The immobilization occurs by different processes such as adsorption and encapsulation.

In the case of chemical immobilization, a covalent union between the polymer and the enzyme takes place by chemical activation of the package surface and the attachment of protein nucleophilic groups (Figure 6 (G) and (H)). LDPE, HDPE, PP, PET, PVA, and polystyrene are recognized as good substrates for immobilizing enzymes (Labuza & Breene, 1989). Chemical activation of the polymer surface is obtained through several techniques, including UV irradiation (Goddard & Hotchkiss 2007). Immobilization in this case is irreversible, and the enzymes are not intended to migrate into the food. In some cases, specific crosslinkers such as glyoxal, glutaraldehyde, formaldehyde, or transglutaminase are used to attach the enzymes to the packaging.

The immobilization of oxalate oxidase and catalase on active films as oxygen and oxalic-acid scavengers was investigated by Winestrand et al., (2013).

Enzymes can be also adsorbed in the packaging material by weak secondary forces such as hydrogen bonds, ionic or hydrophobic interaction, or van der Waals forces, or encapsulated in small particles or droplets coated by a carrier material compatible with the chemical characteristics of the package; however, these technologies are more related to the development of enzyme-based antimicrobial applications.

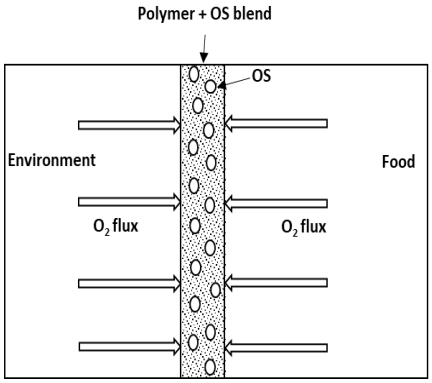
Polymer + OS blend
OS
Environment
Food
O_2 flux
O_2 flux

(A)

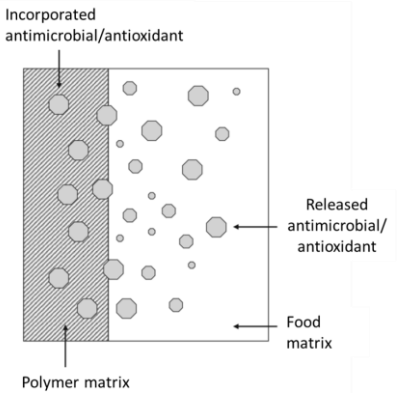
Incorporated antimicrobial/antioxidant
Released antimicrobial/ antioxidant
Food matrix
Polymer matrix

(B)

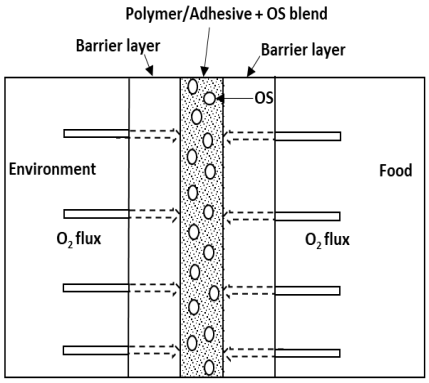
Polymer/Adhesive + OS blend
Barrier layer
Barrier layer
OS
Environment
Food
O_2 flux
O_2 flux

(C)

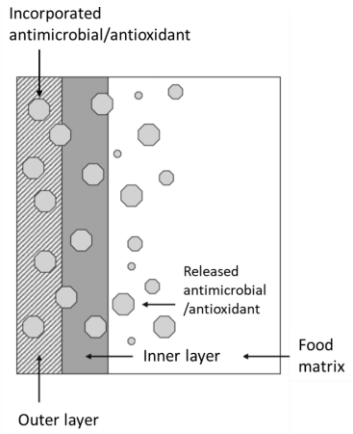
Incorporated antimicrobial/antioxidant
Released antimicrobial /antioxidant
Inner layer
Food matrix
Outer layer

(D)

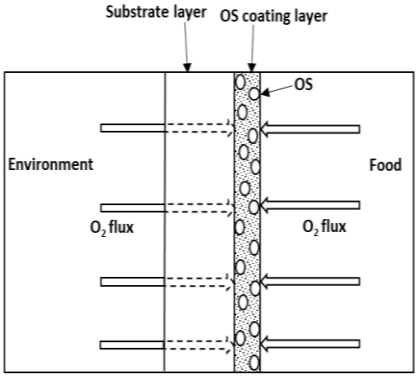
Substrate layer
OS coating layer
OS
Environment
Food
O_2 flux
O_2 flux

(E)

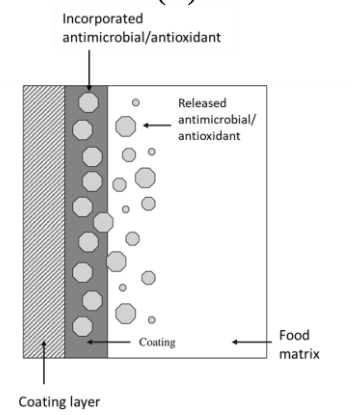
Incorporated antimicrobial/antioxidant
Released antimicrobial/ antioxidant
Coating
Food matrix
Coating layer

(F)

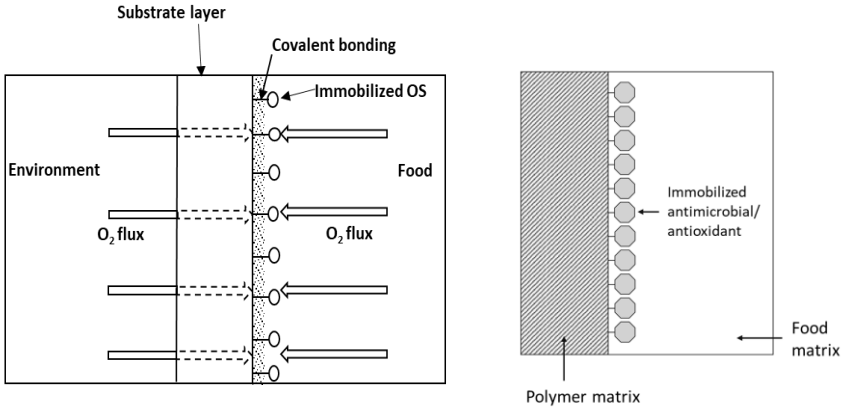

(G) (H)

Figure 6 Different incorporation technologies for the realization of oxygen scavenging films (left coloumn) and controlled release films (right coloumn): (A) and (B): Polymer blend; (C) and (D): Multilayer structures; (E) and (F): Coating on film substrate; (G) and (H): Immobilization on packaging surface.

I.5 Sizing and optimization of oxygen scavenging films

The rationale for the correct design of an oxygen scavenging packaging is to ensure an oxygen concentration within the package environment below a determined critical value, and to keep it constant over the entire food shelf life.

Therefore, the first step in sizing calculations is to determine the total volume of O_2 that must be scavenged over time (V_{SC}), which is generally the sum of the O_2 volume in the package headspace (V_H) plus the volume of oxygen which permeates through the packaging during the shelf life period (V_{IN}) (Cruz et al., 2012).

The O_2 headspace volume V_H can be evaluated according to the following Equation:

$$V_H = \frac{(V_p - W_p) * [O_2]}{100} \quad (27)$$

Where V_P is the volume of the finished pack, determined by immersion in water and expressed in g (assuming water density is 1 mL g^{-1}), W_P is the weight of the finished pack (g), and $[O_2]$ is the initial O_2 concentration in the headspace, which can normally be measured via invasive analyzers during the packaging process (equal to 21% if air).

Once the O_2 headspace volume is known, if the product has a relatively short shelf life, then removing this initial oxygen may be all that is required. However, if the food shelf life is longer and no nearly absolute barriers like aluminum foils are employed, an additional volume of oxygen would permeate through the package over time, and it can be calculated according to Equation (28):

$$V_{IN} = \mathrm{A} * \mathrm{P} * d_S \quad (28)$$

Where P is the packaging material permeability (mL m^{-2} day^{-1} atm^{-1}), A is the surface area of the pack (m^2) and d_S is the expected shelf life of the product (days).

Nevertheless, oxygen dissolved in the food should not be neglected and is normally calculated by expert consultants in their field (Cichello, 2014). Then, knowing the scavenging capacity of the oxygen absorber, the proper amount of OS required for that application can be determined.

The main goal in the selection of the oxygen scavenger and the design of the most appropriate configuration is to adapt the performances of the package to the requirements of the specific food, in terms of respiration rate, sensitivity to environmental conditions and shelf life parameters.

The choice of the reactive layer thickness, the concentration and dispersion of the scavenger loaded into the layer, particle size and specific surface area, scavenger activation method and reaction kinetics, retained scavenging capacity and stability, OS compatibility with the polymer matrix, material transport properties, and the permeabilities of the active and passive layers are some of the factors controlling the performance of the whole structure.

In particular, the relationships among system layout, processing conditions, developed morphology and oxygen transport properties and scavenging performances (initial oxygen scavenging rate, amount of oxygen absorbed, scavenging capacity and exhaustion times) should be extensively investigated.

Figure 7 summarizes all the properties and parameters related to the packaging, food and oxygen scavenger which should be taken into account for the proper sizing and optimization of the performance of an oxygen scavenging packaging system.

For an oxygen scavenging package to be effective, some conditions have to be fulfilled, as the commercial application of oxygen scavenging packaging requires a rigorous evaluation of its functionality and efficacy.

In principle, an ideal oxygen scavenger should exhibit good processability by conventional processes, high compatibility with the polymers commonly used in food packaging design, and an adequate thermal stability. For example, most organic agents are unstable at the high

processing temperatures commonly used in extrusion; thus, it is challenging for researchers to incorporate such materials into polymer matrices (Gaikwad et al., 2018). On the other hand, some scavengers, such as iron-based ones, absorb more oxygen at high temperatures, so it is critical to minimize the absorption of oxygen during the processing stage, in order to avoid rapid saturation of oxygen scavenging films.

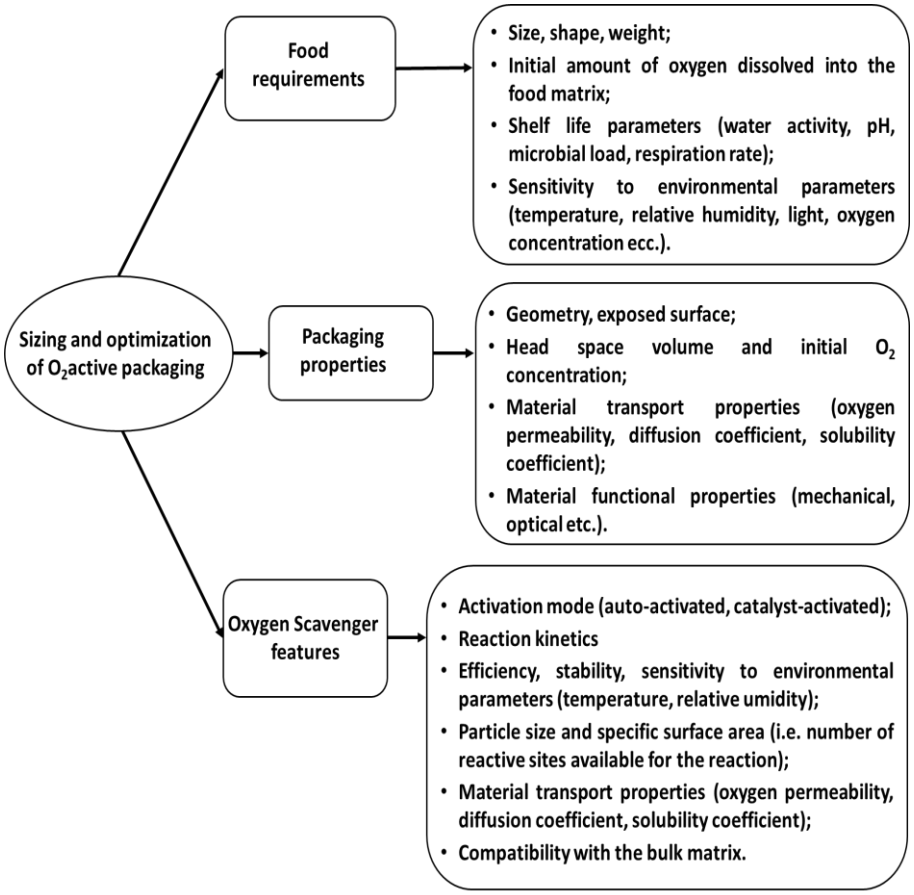

Figure 7 Food requirements, packaging properties and oxygen scavenger features involved in the proper sizing and performance optimization of an oxygen scavenging package.

The scavenger should also be capable of preserving a high scavenging capacity and a fast O_2-reaction rate after processing. The retained scavenging capacity tends to decrease after manufacturing, as the high temperatures, shearing force, and high pressure involved may result in deterioration of the active agent (Suppakul et al., 2003), and the optimal storage conditions

should be chosen for maximum activity retention. At the same time, quantitative evaluation of the scavenger reaction kinetics, by varying the final storage conditions (e.g. relative humidity and temperature) should be known (Pant at al., 2018).

Moreover, the active package should not release by-products that could affect the sensory or nutritional characteristics of the food or contaminate it with harmful substances.

The ideal OS system should be also stable in air prior to use, have some kind of activation mechanism to control initiation of the scavenging activity, and have inherently good control of the reaction rate over time. In fact, the oxygen scavenger should scavenge oxygen slowly and over an extended period, otherwise the active packaging will rapidly reach saturation and lose its capacity to trap more oxygen from the headspace of the package, as well oxygen permeating from the outside environment.

Another important property of oxygen scavengers is the number of reactive sites available for the oxidation reaction. A strategy to increase the number of reactive sites available per unit surface, and therefore the scavenging effectiveness, is to control the diameter of the particles. For instance, the surface area of spheres increases by a factor 10 when the particle diameter decreases by a factor 10. Iron powder with a particle diameter of 10 nm instead of 10 mm would have a 1000 times greater surface area (Foltynowicz, 2018).

Regarding the packaging material, a careful evaluation must be performed by considering the final application and feasibility of commercialization on an industrial scale. The incorporation of oxygen scavenging systems into the polymer matrix may affect the functional properties of the plastic, including the tensile strength, elongation, gas barrier, thermal properties, and optical properties. Therefore, the chemical and physical compatibility with the scavenger and the stability with the active phase during the manufacturing processes must be taken into account, and a proper dispersion of the agent by sufficient shear during processing must be achieved.

Polymer matrices with an oxygen permeability not exceeding 20 mL m^2 d^{-1} atm^{-1} are recommended, as the designers have to consider that the reactive capacity of these barriers is inherently limited, because the scavenger is consumed in the chemical reaction binding the oxygen, and its premature oxidation should be avoided. As better oxygen barrier packaging materials and structures become available, the oxygen permeation rates through packages can be reduced, and smaller sized scavengers are then needed to offset the ingress of oxygen (Solovyov, 2014).

As mentioned above, most of the patents and applications for active packages are focused on polymer families that already have high barrier properties, such as polyester and polyamide packaging. PET is widely

applied, thanks to its good barrier against oxygen, high inertia to migrating by-products, high mechanical and optical properties, and easy recyclability.

Secondly, for flexible packaging, heat sealing should be of such quality that no air enters the package through the seal. Lastly, the quantity of oxygen scavenger must be commensurate with the size of the package, head space volume and initial oxygen concentration.

I.6 Sizing and optimization of controlled release films

The fundamental concept of controlled release systems design is the focus on the kinetics and mechanism of controlled release - what to release, when and how to trigger the release, how much to release, and how fast to release (Chen et al., 2018).

The release rate should closely match the requirement of the kinetics of food deterioration. A rate too slow would result in insufficient amount of active compound to retard food deterioration, and a rate too fast would result in excessive amount of active compounds and their loss due to degradation.

Controlled release systems can have many possible “release rate profiles”, defined as plots of rate of release of active compound versus time. Generally, when an active compound is incorporated into a film, its release is often governed by diffusion of the active compound in the film, following the diffusion-controlled release rate profile, characterized by fast release initially with progressively slower release as time passes.

From a commercial point of view, changing concentration with time has practical value: for example, it is desirable to have a higher concentration of antimicrobials or antioxidants in the beginning to retard microbial and oxidative deterioration at the beginning to extend shelf life of the product during distribution and storage, but to have a lower concentration when the product reaches the consumer.

Achieving the optimum concentration profile requires to develop a package with the desired release rate profile of active compound. Once the package volume is specified, a mathematical relationship between concentration profile and release rate profile can be obtained through unsteady mass balance analysis.

Many of the design parameters of controlled release systems, as shown in Figure 8, are in common with the ones mentioned above about oxygen scavenging packaging.

The active agent is the first design factor, and its selection depends on efficacy, regulatory compliance, and cost. The molecular shape, size, polarity, and weight of an active compound are important properties that determine its release from the package (Nerin et al. 2016). For example, active agents with different polarities (BHT, BHA, pyrogallol, α-tocopherol etc.) incorporated within the same polymer matrix (PLA) will interact

differently with a certain food simulant of given polarity (water/ethanol mixture), exhibiting different release rate.

At the same time, two active agents with the same polarity (e.g., BHT and BHA) show different release rate depending on their molecular weight (Jamshidian et al., 2013).

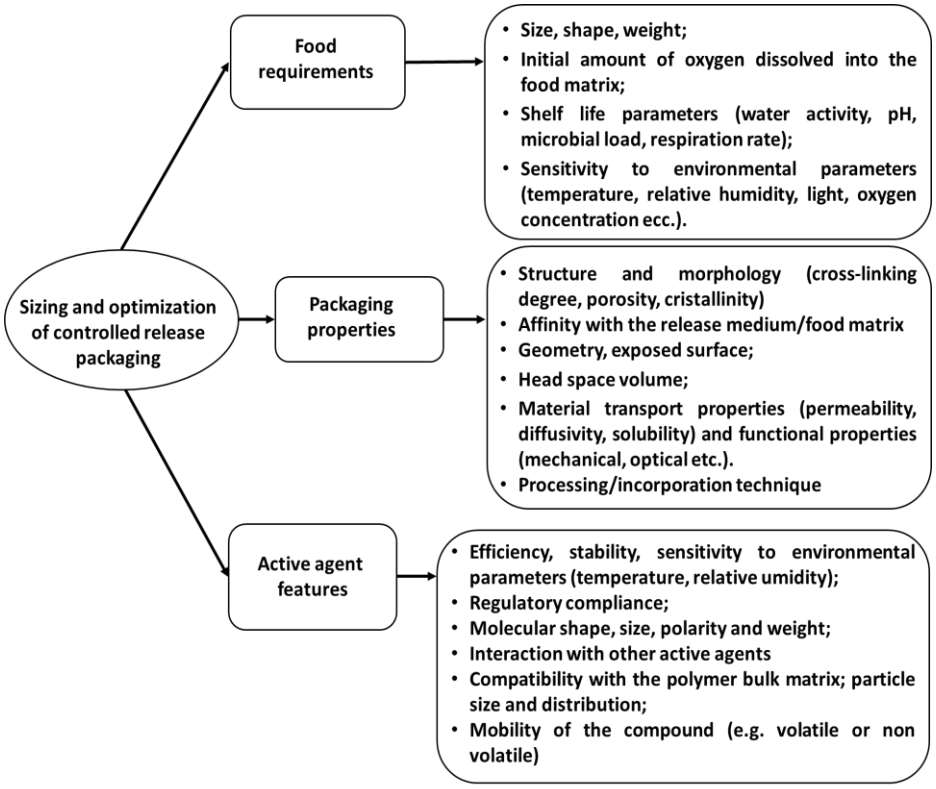

Figure 8 Food requirements, packaging properties and antioxidant/ antimicrobial features involved in the proper sizing and performance optimization of a controlled release package.

Furthermore, when two active compounds are incorporated into a packaging polymer, the presence of one compound may influence the release rate of the other compound, due to plasticizing effects (Chen et al., 2012).

The compatibility (or molecular affinity) of the active agent with the packaging material also plays a crucial role in the packaging effectiveness, and greatly affecting its release from the packaging material. The compatibility cannot be too high resulting in too slow release, or too low leading to immiscibility of the active compound in the packaging material.

The mobility of the active compound also largely affects the selection of the processing conditions and of the final food/package configuration. For example, both volatile and non-volatile agents may be used where there is direct food/package contact (e.g., in a vacuum packed fresh meat pouch), but only volatile antimicrobials may be used where there is no direct food/package contact (e.g., in a fresh produce bag where there is air space between the product and the bag). In general, volatile compounds are usually more effective than non-volatile compounds for retarding microbial growth and oxidation. However, this mobility can also cause undesirable loss of volatile compounds during processing (such as in film extrusion process where high temperature and shear are involved) and during storage due to premature release of the volatile compound.

The second design factor is the package composition and structure. The packaging film or coating serves as reservoir of the antioxidant/ antimicrobial, and as carrier for its release at an appropriate time.

The structure and morphology of the polymer matrix should be adequate, so that the active agent can migrate outside under the driving force of a concentration gradient, but at the same time a certain entrapment should be achieved, in order to avoid the easy and immediate release of the compound.

In this sense, the release rate can be tuned by manipulating the polymer morphology, in terms of cross-linking, porosity or stereochemical isomers composition. Gemili et al., (2009) reported that by manipulating the cellulose film morphology from dense to porous, the release rates of L-ascorbic acid, tyrosine, and lysozyme from the films, as well as the partition coefficients, can be altered greatly. Arabi (2012) reported that by manipulating the composition of stereochemical isomers of PLA, as well as processing methods including drying, annealing, solution casting and extrusion, the crystallinity of the resulted film can be controlled and a wide range of tocopherol release rate profiles can be obtained. Rohini (2008) reported that by controlling the degree of crosslinking in low methyl pectin film using calcium ion as a crosslinker, both release rate and the released amount of nisin can be altered.

The third design factor is the processing methods, which serve the purpose of incorporating the active compound into the packaging polymer and creating an appropriate morphology or structure to allow the release of the active compound. Depending on the processing methods, the release behavior of active compounds can be quite different (Jamshidian et al., 2012; Jamshidian et al., 2013). By utilizing different processing methods, a wider range of release profiles can be obtained for various applications. Processing technologies were widely discussed above in Paragraph II.1.

Both synthetic polymers and biobased polymers have been studied for controlled release packaging applications. In the last years, a great attention

was focused on the realization of antioxidants/antimicrobials release systems based on biopolymers: PLA incorporating thymol (Wu et al. 2014), PLA incorporating antioxidants including BHA, BHT, pyrogallol, tert-butylhydroquinone (Jamshidian et al., 2012), zein film incorporating lauryl arginate (LAE) (Kashiri et al. 2016), cassava starch film incorporating bixin nanocapsules (Pagno et al. 2016), pectin-carboxymethyl cellulose films incorporating potassium sorbate (Yu et al., 2017), whey protein film incorporating essential oil (Ribeiro-Santos et al. 2017), starch film incorporating green tea extract (u Nisa et al. 2015).

In general, most of the systems reported in the literature seems to release too fast, so there is a need to develop systems that can release active compounds in a slower and more sustained manner (Chen et al., 2018).

Moreover, information from the literature is of little value to develop commercial biobased films, because most studies used the solution casting method to produce films in petri dishes, not a commercial viable process to produce large volume of films. Therefore, the morphology and properties of the film depends on the film production process, so the usefulness of results from studies using petri dishes and solution casting method is questionable.

Finally, incorporation of active compounds into the package may facilitate unintended migration of other packaging additives into food, especially for the systems involving micro and nanoencapsulation of active compounds, as some of the encapsulants may migrate with active compounds into the food. The possible migration of undesirable compounds may cause product safety and regulatory compliance issues, presenting major hurdles that must be dealt with in order to transfer CRP technology from benchtop to reality.

I.7 Mathematical modelling of active packaging.

Modelling of absorption performance of oxygen scavenging films

In recent decades, there has been a considerable effort devoted to the development of mathematical models for software-based packaging design. In fact, there is a need for a rapid and reliable method for evaluating, comparing, and optimizing the scavenging performance of such structures, and to confidently extrapolate predictive data. Mathematical modelling could be a useful tool to describe the transport phenomena occurring in the designed active packaging, leading to advanced knowledge of the optimal parameters, both in terms of barrier and scavenging properties (Di Maio et al., 2017a).

The scientific literature reports several gas transfer models to study the reactive-diffusive transport in solid media, and different approaches are mentioned (Paul & Kemp, 1973; Paul & Koros 1976; Crank, 1975; Fogler, 1999; Cussler, 1997; Yang et al., 2001; Charles et al., 2006; Solovyov &

Goldman, 2005a; Solovyov & Goldman, 2005b; Solovyov & Goldman, 2005c; Nuxoll & Cussler, 2005; Ferrari et al., 2009; Carranza et al., 2010b; Carranza et al., 2010c; Carranza at al., 2012; Di Maio et al. 2017b). These papers include numerical and analytical solutions describing the permeation through a reactive membrane barrier with immobilized catalytic or non-catalytic scavengers, dispersed within the layer, where the oxygen scavenger is consumed in chemical reaction by binding the solute.

Early models consisted of relatively simple and accurate schemes to predict only the steady state, or analytical estimates of transient behavior limited to narrow ranges of applicability (Paul & Kemp, 1973; Paul & Koros 1976; Yang et al., 2001; Solovyov & Goldman 2005b).

Recent papers, on the other hand, have focused on the study of the transient behavior of reactive membranes, and the description of the time-dependent absorption of O_2 considering different reactive barrier configurations.

General steps to develop and run a mathematical model able to describe the transport phenomena and to predict the scavenging performance of an oxygen scavenging packaging configuration, are (Di Maio et al., 2017b):

- definition of the system geometry and the different subdomains;
- definition of the mathematical system: identification of the transport mechanisms involved in each subdomain (e.g. diffusion, diffusion and reaction), and writing the appropriate transport equations;
- assignment of initial and boundary conditions;
- definition of parameters and variables;
- selection of the proper mesh and post-processing of the results.

Possible reactive barrier configurations for mathematical modeling include homogeneous films, or heterogeneous structures such as polymer blends and multilayer composites, as suggested by Carranza (2010a), and shown in Figure 9.

The homogeneous model (Figure 9 (a)) represents a pure reactive membrane, where the reactive sites are confined to the molecular structure of the polymer bulk, and a single polymer phase is present. The uniformly distributed, reactive sites are consumed as the reaction with the mobile solute progresses. The polymer blend model (Figure 9 (b)) consists of an inert matrix with uniformly dispersed oxygen scavenger particles. In this case, the bulk polymer is inert, and the reaction is confined to the scavenging particles. The particle size distribution and possible non-spherical shapes of the particles may be taken into account, and design equations based on the surface area to volume ratio could be applied (Ferrari et al., 2009). The multilayer model (Figure 9 (c)) represents composite films consisting of multiple alternating inert and reactive polymer layers. Permeation through such heterogeneous reactive-passive structures is an even more complex

process than permeation through single-layer reactive membranes, and, in general, the dynamics of solute permeation and consumption cannot be obtained analytically.

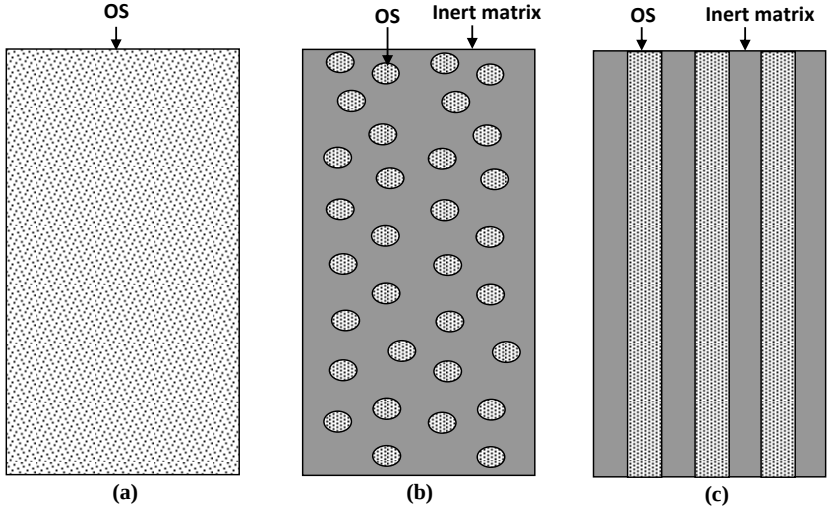

Figure 9 Schematic illustration of three possible configurations of oxygen scavenging packaging structures that can be considered for modeling: (a) homogeneous; (b) polymer blend; (c) multilayer.

The selection of the most suitable configuration for a particular application depends on the inherent properties of both the inert matrix and the reactive polymer. In general, all the models should include material balances for the mobile species and immobilized reactive sites of the scavenger. The rate of change in the concentration of the mobile solute is balanced with diffusive and reactive contributions, while the rate of change in concentration of the scavenger is due to reaction only, since the reactive species are immobilized.

The framework of the homogeneous model can also be used to approximate polymer blends or films where inorganic reactive particles have been uniformly dispersed within the film, paying due attention to the calculation of parameters such as the bulk reaction rate k_R and the diffusion coefficient of the reactive and inert layers D (Carranza et al., 2010c). This matching approach is also effective to estimate modeling results of a multilayer system where the reactive layers are blended polymers, without the need to develop more complex models.

Once the model has been validated, the simulation results can be used to predict the performance of the active packaging, in terms of exhaustion time, time lag, and total amount of absorbable oxygen, or to analyze the time

evolution of oxygen profiles inside the active film or its surroundings. Furthermore, it is possible to evaluate the effect of the configuration and composition of the layers, or of the physical parameters on the barrier/scavenging properties.

On the basis of these considerations and of the possible approximations described above, a mathematical model has been developed to describe the scavenging performance of a symmetrical, three-layer I/A/I active film. The mathematical model, the set of governing equations and the simulation results are reported and extensively discussed in Chapter II.

On the other hand, a mathematical model was also developed and applied to describe the 2nd order reaction kinetics of polyphenols in natural oxygen scavenging compounds. The mathematical description and the simulation results and predictions are reported in Chapter V.

Modelling of kinetic data of controlled release films

The release of active compounds from a polymeric packaging film involves three steps: (1) molecular diffusion within the film towards the film/food interface, (2) mass transfer across the interface, and (3) dispersion into food or desorption into package headspace (Chen et al., 2018).

Mathematical models are useful to summarize release kinetic data, predict release behavior, and provide mechanistic insights.

Diffusivity and partition coefficient are the two model parameters commonly used to describe the release behavior of an active compound from a polymer film to a food or a food simulant. Diffusivity indicates how fast the active compound moves within the film, while the partition coefficient indicates how much the active compound is released from the film to the food at equilibrium.

The most popular mathematical models to describe release behavior are derived from differential equations based on one dimensional Fickian diffusion with appropriate initial and boundary conditions (Crank 1975).

The diffusion coefficient (D) can be determined by fitting the release versus time data with Fick's second law for an infinite slab in contact with an infinite volume of solvent (Crank, 1975):

$$\frac{M_t}{M_\infty} = 1 - \sum_{n=0}^{\infty} \frac{8}{(2n+1)^2\pi^2} \exp\left[-\frac{D(2n+1)^2\pi^2 t}{L^2}\right] \qquad (29)$$

Where M_t is the mass of active agent diffused at time t, M_∞ is the concentration of active agent diffused at equilibrium, L is the thickness of the film and D (m^2/s) is the diffusivity of the active agent in the substrate.

This equation has valid solution when the diffusion of active compound in polymer film is the rate determining step in the release process. Other boundary conditions have to be satisfied: the active agent is homogeneously distributed into the matrix, no structural change in the polymer film occur during the release process, the active compound can be readily desorbed from the film into the food, , the initial concentration of active compounds in food is zero, no concentration gradient of active compound exists in food, the partition coefficient and diffusivity are constant at a given temperature, the interactions between food simulant and film are absent or negligible, and no degradation of active compound occurs.

For short times (M_t/M_∞ is lower than 2/3), the equation above can be simplified as follows:

$$\frac{M_t}{M_\infty} = 4\left(\frac{Dt}{4\pi L^2}\right)^{1/2} \tag{30}$$

and the diffusion coefficient can be determined by the equation:

$$D = \left(S \cdot \frac{L}{2}\right)^2 \pi \tag{31}$$

Where S is the slope of the plot representing M_t/M_∞ against $t^{1/2}$.

The partition coefficient K is defined as the ratio of migrant equilibrium concentration in the polymeric material, C_P, to its equilibrium concentration, in the food phase, C_S:

$$K = \frac{C_P}{C_S} \tag{32}$$

It is important to validate the model before accepting it. If the model does not fit the data, this fact suggests that the release kinetics does not follow Fickian diffusion and/or some of the model assumptions are violated. For example, liquid from the food or food simulant may cause swelling of the polymer film especially if the film is made of a biopolymer, and the swelling may in turn cause the active compound to move faster and deviate from Fickian behavior.

If the deviation is small, Fickian models may still be marginally acceptable. If the deviation is large, a non-Fickian model accounting for the swelling effect must be used.

In most of the cases, the theoretical concepts are not completely fulfilled, and some empirical equations have proved to be more appropriate to describe mass diffusion phenomena following mixed mechanism of release.

Some of the kinetic model describing the active agent release from a matrix include zero-order kinetics, first order kinetics, Higuchi model, Hixson-Crowell model, Weibull model, Baker-Lonsdale model, Korsmeyer-Peppas and Ritger-Peppas model and Hopfenberg model.

Section I

Mono-material, active films based on polyethylene-terephthalate (PET) and co-polyester oxygen scavengers (OS) with extended effectiveness

Chapter II - *Mono-material, oxygen scavenging PET films with multilayer configuration to extend their effectiveness*

Chapter III - *Monolayer PET active films combining oxygen scavenger with high barrier constituents to extend their effectiveness*

Chapter II

Mono-material, oxygen scavenging PET films with multilayer configuration to extend their effectiveness

II.1 Introduction

The state of the art discussed in Chapter I underlined as oxygen scavengers (OS) systems have revolutionary changed the approach to the shelf life extension of sensitive foods, simplifying the process of gas reduction inside the package and also eliminating costly equipment and technologies.

In particular, the design and development of non-visible, integrated OS systems, easy to blend with the polymer matrix and to process through conventional technologies, is raising growing interest, and new patents are continuously registered.

Currently, polymeric OS are widely used to improve barrier properties of Poly(ethylene terephthalate) containers. PET is relevant for packaging foods, such as beverages and oils, thanks to its capability to ensure good protection from environmental contamination, the good optical and mechanical properties, the recyclability advantages, and the ease of use with traditional processing technologies (Mahajan et al., 2013; Barbaro et al., 2015). Despite its intrinsic low oxygen permeability with respect to other commercial polymers (Robertson, 2013), efforts are still made to increase its barrier performance, especially in those cases where particularly compelling requirements are imposed by the nature of the packaged food. The addition of a scavenging compound to the plastic matrix provides an active

protection, which results in the same advantages of heavier and more expensive packaging materials.

However, many literature studies were interested in the development of integrated OS systems for PET rigid packaging (Dombre et al., 2015; Ros-Chumillas et al., 2007; Bacigalupi et al., 2013; Dombre et al., 2014; Di Felice et al., 2008; Sängerlaub et al., 2017), and only few have dealt with the application of these scavengers to flexible packaging.

The integration of the OS inside polymeric films to achieve a significant active barrier is still facing some practical difficulties, particularly in case of self-activating oxygen scavengers. Major issues concern the necessity: (i) to adopt precautions during material storage and handling, to avoid premature depletion of the OS films as soon they are manufactured, prior to filling the package; and (ii) to prevent the excessively fast oxidation of the scavenger, delaying the exhaustion of the active phase until the end of the food shelf life is reached.

Among all possible strategies, joining the active and the passive barrier in a multilayer structure represents an interesting solution to control the diffusive flux of the oxygen and to modulate the performance of the active system.

The realization of a multilayer structure, by inserting the active layer between two or more inert, barrier layers, would create a synergistic system in which the central layer traps and reacts with oxygen, thus providing an active protection, whereas the outer layers improve the passive protection, controlling the rate at which the OS exhausts.

There is still little research regarding active multilayer systems development, or deeply studying the optimization of the layer thicknesses or the effects of the active phase on the transport and functional properties of the polymer (Carranza et al., 2012; Ferrari et al., 2009; Tung et al., 2012; Di Maio et al., 2017; Yildirim et al., 2015; Di Maio et al., 2015; Pant et al., 2017).

These considerations inspired the aim of the part of PhD research discussed in this Chapter, which focused on the production and characterization of PET active multilayer films, intended for food packaging applications.

Figure 10 shows the flow diagram of the experimental set-up and of the activities carried out in this part of the PhD work, which will be discussed in this chapter.

Multilayer, “IAI” samples were produced by co-extrusion process by inserting the active layer (A), containing the oxygen scavenger at an optimized composition, between two PET inert layers (I).

The careful design and selection of the materials would allow mono-material multi-layer structures, all in PET, easily recyclable in the post-consumer phase.

Four multilayer films were obtained with different relative thicknesses of both the active and the inert layers. The scavenging performance of the films was assessed in terms of initial oxygen scavenging rate, exhaustion time, scavenging capacity and total volume of oxygen absorbed per unit surface.

A detailed analysis was conducted in order to discriminate the individual contributions of the active and the inert layers on the oxygen permeation and scavenging phenomena in terms of scavenging capacity, exhaustion time and oxygen absorption rate. This enables the necessary information for the design of active multilayer structures with tunable OS performances to be obtained.

The systems were characterized in order to ascertain the effect of the scavenger phase on the morphology and functional properties of the polymeric films.

Shelf life tests were also conducted on *Brassica oleracea* florets, in order to highlight the effectiveness of the OS systems in inhibiting vegetables senescence.

A mathematical model was developed and applied to the data set in order to investigate, at mathematical level, oxygen diffusion and sorption phenomena through the layers and to predict the scavenging performance of the films with different multilayer configurations.

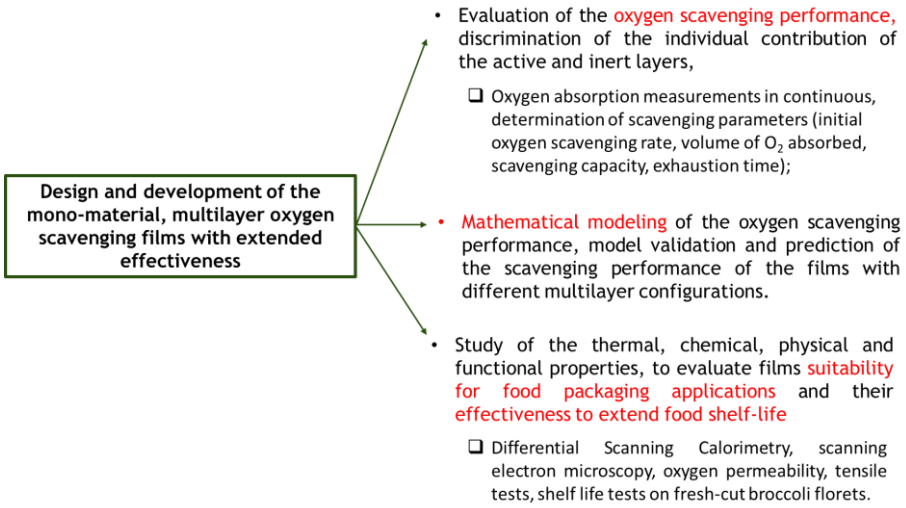

Figure 10 Experimental set up and activities discussed in Chapter II.

II.2 Multilayer films production

Materials

The selected polymeric matrix is the film grade PET resin Cleartuf P60 (M&G Polimeri S.p.A., Patrica (FR), Italy), having intrinsic viscosity 0.58 dL/g. The active phase is a new generation of polymeric oxygen scavenger, named Amosorb DFC 4020 (AMS_DFC4020, supplied by Colormatrix Europe, Liverpool, UK). This is a copolyester-based polymer designed for rigid PET containers, characterized by an auto-activated scavenging mechanism. Both PET and AMS_DFC4020 comply fully with FDA and EU food contact legislation.

Process conditions

For the preparation of the active systems, the PET was dried under vacuum at 130 °C for 16 h, before processing. The AMS_DFC4020, delivered dried in aluminum bags sealed under vacuum, was used as received. The percentage of the oxygen scavenger added to the active layer, equal to 10% w/wt, was already optimized by previous published studies [56].

The multilayer active films were produced by using a laboratory co-extrusion cast film line (Collin, Teach-line E20T), equipped with two single screw extruders (D=20, L/D=25) one feeding the active layer (A) and one feeding the inert layers (I), a flow convergence system (feed-block), a coat-hanger type head (slit die of 200 x 0.25 mm^2) and a take-up/cooling system (chill rolls) thermally controlled by water circulation at 50°C. The temperature profile for the two extruders was set at 280°C from the hopper to the die. The chill roll speed was 7 m/min, thus allowing the films to be stretched to their final dimensions of about 170 mm wide and variable thicknesses.

The mass flow rates of both the extruders was varied in order to obtain a set of four multilayer films with a combination of two thicknesses for the active layer (a smaller one, equal to 13.5, and a larger one, equal to 23.5 µm) and two for the inert layers (a smaller one, equal to 6.75 and a larger one, equal to 11.75 µm).

Films were named A_LI_S, A_SI_S, A_LI_L and A_SI_L, depending on the thickness of each layer (where "*S"* stands for Small and "*L"* stands for Large), as resumed in Table 4. Single layer films inert I (i.e. made of pure PET) and active A (i.e. made of PET + 10% w/wt AMS_DFC4020) were also produced, for comparison, using the same apparatus and processing conditions.

Table 4 Nominal thicknesses of the inert and active layers for I, A, A_LI_S, A_SI_S, A_LI_L and A_SI_L samples, calculated from the screw speed of extruders feeding layers I and A.

Sample	Total thickness [µm]	Inert layer 1 [µm]	Active layer [µm]	Inert layer 2 [µm]	Speed extruder A [rpm]	Speed extruder I [rpm]
I	35	35	-	-	-	40
A	25	-	25	-	25	-
A_LI_S	37	6.75	23.5	6.75	40	27
A_SI_S	27	6.75	13.5	6.75	27	27
A_LI_L	47	11.75	23.5	11.75	40	40
A_SI_L	37	11.75	13.5	11.75	27	40

II.3 Characterization techniques

Thermal analyses on the produced films were performed using a Differential Scanning Calorimeter (DSC mod. 822, Mettler Toledo). The specimens were heated at a rate of 10°C/min from 25°C to 300°C under a nitrogen gas flow (100 mL/min), in order to minimize thermos-oxidative degradation phenomena. The crystallinity degrees, Xc, were calculated from first heating parameters, according to the following formula (Equation 33):

$$Xc = \frac{\Delta H_m - \Delta H_{cc}}{(1 - \phi * \omega) * \Delta H_\infty} \quad (33)$$

Where ΔH_m and ΔH_{cc} are the heat of melting and the heat of cold crystallization of the samples respectively, ΔH_∞ is the heat of melting of purely crystalline PET, that is equal to 140 J/g, ϕ represents the fraction of active film, calculated as the ratio between the thickness of the active layer and the total thickness, and ω represents the content of oxygen scavenger phase.

The experimental X_C values of multilayer samples, evaluated according to Equation (33), were also compared to crystallinity degree Xc_{calc} calculated, for the same films, starting from the general mixing rule expressed in Equation (34). Xc_{calc} was expressed as the average between the crystallinity degree of the films I and A ($X_{C\,I}$ and $X_{C\,A}$ respectively),

weighted on the mass fractions of the active and inert layers, assuming equal density for both.

$$Xc_{\,calc} = X_{C\,I} * (1 - \phi) - X_{C\,A} * \phi \quad (34)$$

Field Emission Scanning Electron Microscopy (FESEM) was performed on film sections cut normally to the extrusion direction by cryofracture of the films in liquid nitrogen; then, they were sputter coated with gold (Agar Auto Sputter Coater mod. 108A, Stansted, UK) at 30 mA for 160 s, and analyzed using a FESEM microscope (mod. LEO 1525, Carl Zeiss SMT AG, Oberkochen, Germany). Sigma Scan Pro 5.0 (Jandel Scientific, San Rafael, Canada) and Origin 8.5 (Microcal, Northampton, USA) softwares were used for length evaluation and to determine the average diameter of the membrane pores.

Oxygen absorption measurements were carried out at 25 °C in continuous mode by means of the fiber optical oxygen meters Minisensor Oxygen Fibox 3-Trace V3 and Stand-alone Oxygen Meter Fibox 4 (PreSens GmbH, Regensburg, Germany), equipped with a polymer optical fiber and oxygen sensor spots SP-PSt3-NAU (detection limit 15 ppb, 0–100% oxygen). Experiments were conducted on cut film samples with a defined geometry (8 x 4,5 cm^2), which were introduced in glass measurement cells, having volume equal to 9 mL, and hermetically capped. Oxygen consumption inside the closed glass vial was measured over time. From the oxygen absorption parameters, it was possible to calculate the main absorption properties of the active films, such as the total volume of oxygen absorbed V_{Ox}, the exhaustion time t_E (i.e. as the time at which the O_2 concentration becomes constant), the initial oxygen scavenging rate k (i.e. the slope of the curves at short times, determined through a linear regression model by applying the ordinary least squares method to the experimental data of O_2 concentration versus time). The scavenging capacity of the films at complete exhaustion was also evaluated, calculated as the ratio between the total volume of oxygen absorbed and the total thickness of the samples (μ_1) and the ratio between the total volume of oxygen absorbed and the thickness of only the active layer (μ_2). In addition, the scavenging activity was calculated, defined as the same as the scavenging capacity, but at different time intervals.

Oxygen permeability tests were performed by means of a gas permeabilimeter (GDP-C, Brugger, Munchen Germany). The tests were carried out in triple at 23°C and 0% R.H., with the oxygen flow rate of 80 mL/min (ASTM D1434). In order to reach the equilibrium value of permeability, the films were analyzed after the complete scavenger saturation. The standard deviation of the permeability coefficient results is in the worst case contained within 4% of the reported values.

Mechanical tensile tests were carried out according to the standard ASTM D 882-91 using the SANS (mod. CMT 4000 by MTS, China) tensile

tester equipped with a 100 N load cell. Test samples were cut, along the extrusion direction, with a rectangular geometry of 12.7 x 80 mm^2. The crosshead speed of the test was kept at 5 mm/min for the duration of each test.

The effectiveness of the active films in preserving the quality of fresh vegetables was verified by analysing the yellowing over the time of untreated, fresh-cut broccoli florets (Brassica oleracea L. var. Italica).

Broccoli were cut in florets by using knives, mixed thoroughly in order to ensure a random selection and precooled overnight prior to packaging. Then, florets of uniform size and visual appearance and free of defects were divided into single bags, each one measuring 10 x 10 cm^2 in size, and approximatively of the same weight (ca. 40 g), thermally sealed and then stored in a refrigerator at 5 °C for 10 days. The colour of fresh-cut broccoli florets was measured on homogeneous spot areas of 4 mm in diameter, by means of a colorimeter Minolta CR-300 (Konica Minolta International, Japan). The measurements were taken on all the samples at day 0 and after 10 days of storage. Ten measurements were performed on each floret, in order to homogeneously cover the whole surface, and then an average value was calculated for each parameter.

The colour variation of the broccoli florets over time was evaluated by means of the colour-difference equation CIELAB ΔE^*_{ab}, based on the coordinates L*, a* e b*.

II.4 Results and discussion

Morphological and thermal characterization

In order to verify the uniformity of the layers' thickness and the quality of the interlayer adhesion, SEM analyses were carried out on the produced film. Figure 11 shows the cross-section micrographs of the multilayer film A_LI_S taken as an example.

Image analysis exhibits the presence of prints of spheroidal shape well distributed in the central part of the film, referable to the presence of AMS_DFC4020 particles detached, whose size (equal or less than 1 µm in size) is comparable to the data reported in previous studies on active films with the same percentage of active phase (Galdi & Incarnato, 2011). The absence of boundary lines or voids in the whole cross-sectional area of the investigated films points out the obtainment of good inter-layer adhesion.

The calculation of the active/inert layers thicknesses ratio underlined a good agreement with the nominal ones, pointing out the good control of the relative layer thickness during the co-extrusion process.

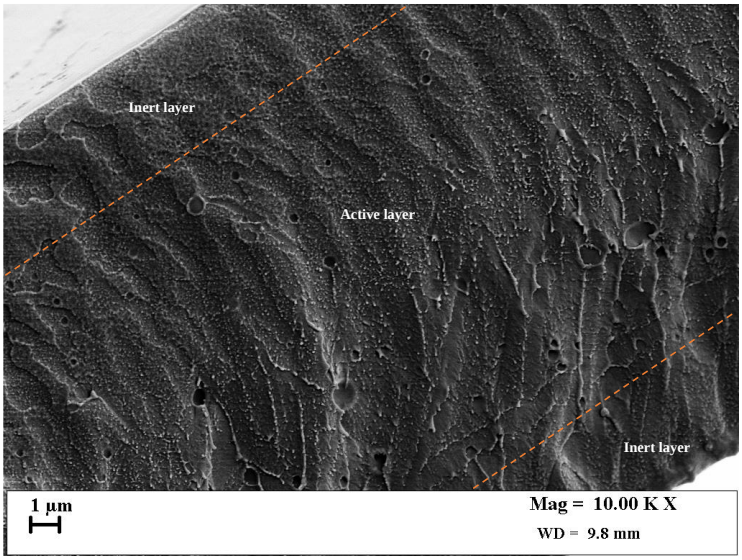

Figure 11 Scanning Electron Microscopy image of A_LI_S multilayer sample (Mag = 10.00 KX).

Thermal analyses were performed on all the single layer and multilayer films, in order to investigate the effect of the oxygen scavenger and of the film structure on crystallinity behavior of the polymer. Data are shown in Table 5 and Table 6.

From the comparison between A and I samples, it is possible to observe that the presence of AMS_DFC4020 in the active monolayer film results in an increase in the polymer crystallinity degree, acting as nucleating agent on PET, as also comes out from the shift in Tc value towards higher temperature (ca. 7°C) as reported in Figure 12. Similar outcomes were already reported in our previous work on monolayer PET active films at different percentages of AMS_DFC4020, in which the significance of the effect was found proportional to the AMS_DFC4020 loading (Galdi & Incarnato, 2011).

An increase in crystallinity percentage due to AMS_DFC4020 presence was also observed in all multilayer films. Of course, in these cases the variation is less relevant with respect to the active monolayer film, since only the active layer of the multilayer structures can contribute to it.

Table 5 Thermal parameters of the single layer and multilayer films related to the first heating cycle.

Sample	First heating						
	T_g [°C]	T_{cc} [°C]	T_m [°C]	ΔH_{cc} [J/g]	ΔH_m [J/g]	X_C [%]	X_{Ccalc} [%]
I	78.6	136.5	251.3	26.6	-40.8	9.7	-
A	77.3	133.9	252.9	20.5	-43.0	12.6	-
$\mathbf{A_LI_S}$	78.1	135.4	252.3	27.7	-42.8	11.5	11.6
$\mathbf{A_SI_S}$	78.1	136.0	251.1	26.6	-40.5	11.4	11.2
$\mathbf{A_LI_L}$	77.9	137.7	252.0	29.2	-42.1	11.1	11.2
$\mathbf{A_SI_L}$	78.4	137.3	251.2	27.8	-44.7	10.7	10.8

Table 6 Thermal parameters of the single layer and multilayer films related to the cooling cycle.

Sample	Cooling	
	T_c [°C]	ΔHc [J/g]
I	189.6	37.2
A	196.1	39.9
$\mathbf{A_LI_S}$	196.4	40.9
$\mathbf{A_SI_S}$	196.5	38.7
$\mathbf{A_LI_L}$	195.1	39.3
$\mathbf{A_SI_L}$	195.8	39.8

Experimental Xc values of multilayer samples are in good agreement with the ones calculated by applying the general mixing rule expressed in Equation (34) (Van Krevelen & Nijenhuis, 1997). Concerning the melt crystallization behavior, all multilayer systems respond to the nucleating effect of AMS_DFC4020 in the core layer and start to crystallize at temperatures similar to the one of active monolayer system.

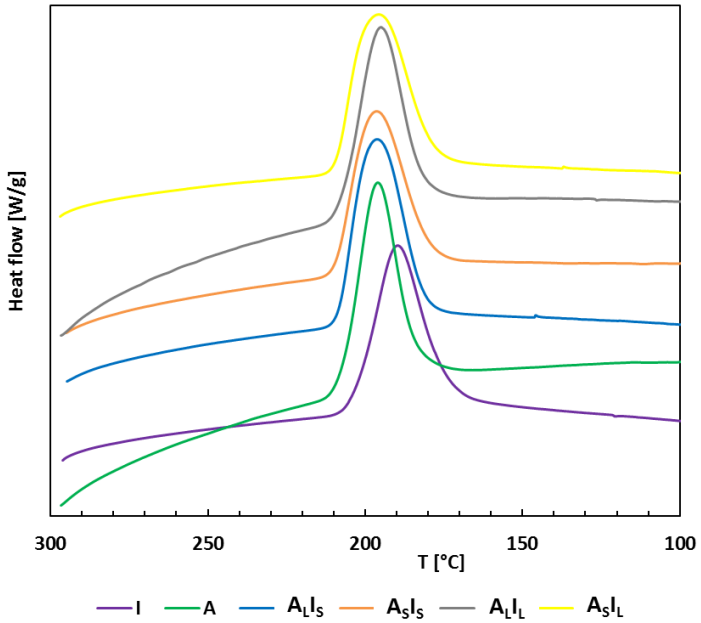

Figure 12 Cooling DSC thermograms for the single layer films (I and A) and for the multilayer samples (A_LI_S, A_SI_S, A_LI_L and A_SI_L).

Effects of layers configuration on O_2 absorption curves, absorption parameters and permeability coefficients

In order to evaluate the oxygen scavenging performance of the films, continuous O_2 absorption measurements were performed. Figure 13 shows oxygen absorption curves for all the films investigated, expressed as the volume of gas absorbed as function of the time, while the O_2 absorption parameters are reported in Table 7.

With respect to the active monolayer A, all the multilayer films show a slower absorption kinetics at short times, as evident from the calculated initial oxygen scavenging rate k reported in Table 7, and both the inert and active layer thicknesses influence the evolution of the scavenging phenomenon.

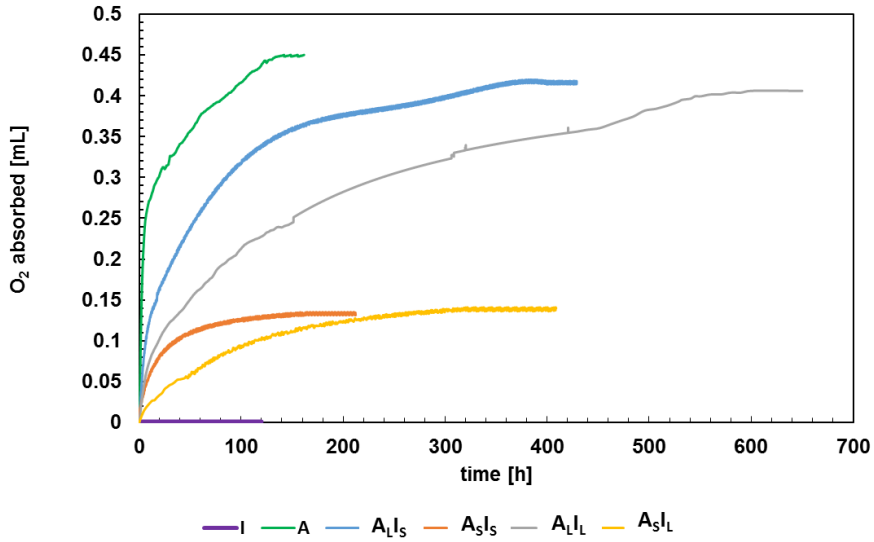

Figure 13 Oxygen absorption curves at 25°C for the single layer films (I and A) and for the multilayer samples (A_LI_S, A_SI_S, A_LI_L and A_SI_L).

Table 7 Initial oxygen scavenging rate k, exhaustion time t_E, volume of O_2 absorbed at exhaustion V_{ox}, scavenging capacity and O_2 permeability coefficients for inert (I) and active (A) monolayer and multilayer films (A_LI_S, A_SI_S, A_LI_L and A_SI_L).

Sample	k	t_E [h]	V_{ox} [mL/dm^2]	Scavenging capacity μ_1 $[\frac{mL\ O2}{\mu m\ film}]$	Scavenging capacity μ_2 $[\frac{mL\ O2}{\mu m\ active\ layer}]$	P_{O2} $\frac{cm^3 mm}{m^2 d\ bar}$ $[\frac{cm^3 mm}{m^2 d\ bar}]$
I	n.d.	n.d.	n.d.	n.d.	n.d.	2.97
A	0.257	130	1.25	0.0180	0.0180	1.93
A_LI_S	0.094	400	1.15	0.0112	0.0177	2.22
A_SI_S	0.086	170	0.364	0.0049	0.0097	2.34
A_LI_L	0.041	550	1.12	0.0086	0.0172	2.34
A_SI_L	0.046	315	0.386	0.0038	0.0103	2.48

These effects are well emphasized in the Figure 14, which reports the comparison between oxygen absorption curves at constant thickness of the

inert layer (Figure 14 (A) and (B)) and at constant thickness of the active layer (Figure 14 (C) and (D)).

At constant thickness of the inert layers

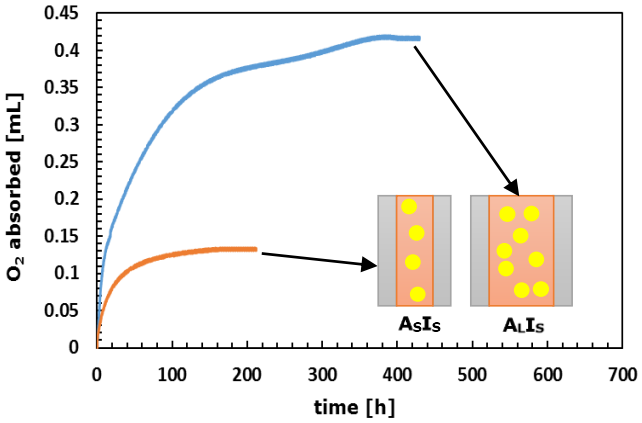

(A)

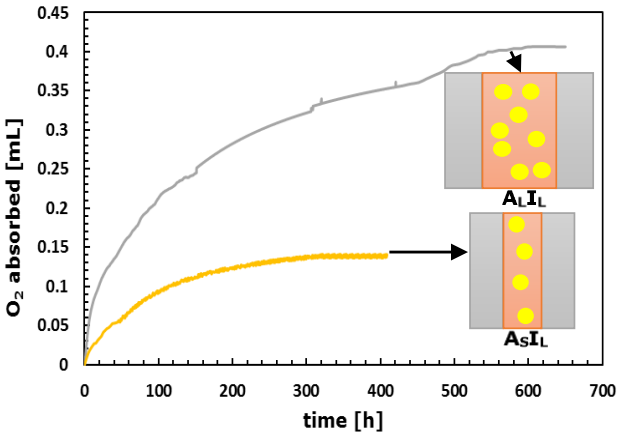

(B)

At constant thickness of the active layer

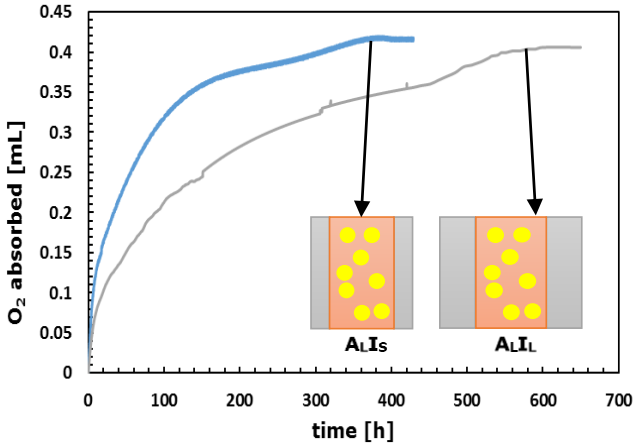

(C)

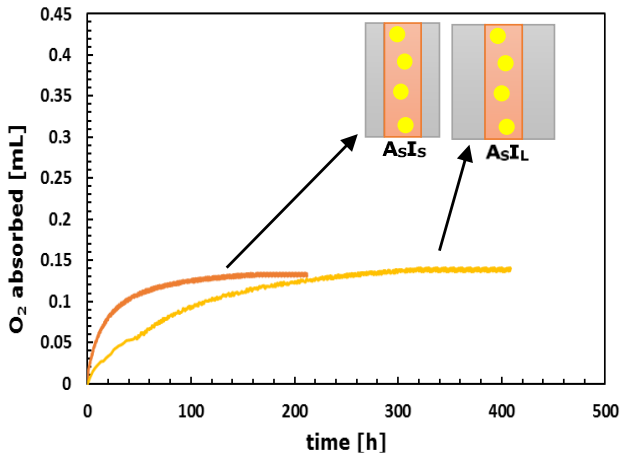

(D)

Figure 14 Comparison among oxygen absorption curves of multilayer films, at constant thickness of the inert layers ((A) and (B)) and at constant thickness of the active layer ((C) and (D)).

At constant thickness of the inert layers (Figure 14 (A) and (B)), the total volume of oxygen absorbed per unit surface of the film increases by increasing the thickness of the active layer, and therefore the amount of scavenger available for the oxidation reaction. In particular, by increasing the thickness of the active layer of ca. 74% (A_LI_S-A_SI_S and A_LI_L-A_SI_L couples), an increase of absorbed O_2 of 217% and 191% respectively is observable. The increase is quite comparable for both the film pairs considered, showing that there exists a reproducible scavenger performance

of the active layer, regardless of the multilayer configuration. On the other hand, looking at the kinetic constants of the same pairs considered, no significant variations can be noticed for samples having the same thickness of the inert layers, and therefore providing the same resistance to the oxygen diffusive transport.

Conversely, multilayer films with the same thickness of the active layer (Figure 14 (C) and (D)) absorb almost the same amount of oxygen per unit surface at equilibrium, but they reach the plateau stage at different times, because of the different thickness of the inert layers. It is important to underline how the exhaustion time parameter is influenced by both the thickness of the active and of the inert layers. However, for the film pairs A_LI_S-A_LI_L and A_SI_S-A_SI_L, an increase of the thickness of the inert layer of 5 μm per side leads, in both cases, to the same increase in exhaustion time, equal to ≈ 150 hours, highlighting the reproducible barrier performance of the inert layers, independently from the thickness of the reactive layer.

The proportionality between the kinetic constant of the same pairs is observable: in particular, the k value almost halves by almost doubling the thickness of the inert layers.

In order to better analyze the scavenging performance of the films, in relationship with their layout, the scavenging capacity values were evaluated for all the active films on both the total thickness of the films (μ_1) and on the thickness of only the active layer (μ_2) and data are reported in Table 7. Moreover, Figure 15 shows the scavenging activity as function of the time for the same films, evaluated on their total thickness.

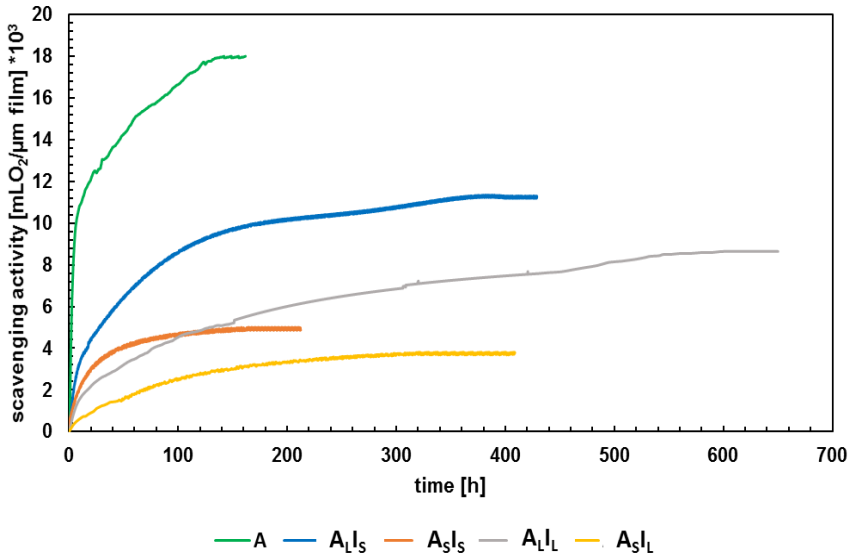

Figure 15 Scavenging evaluated as the volume of O_2 absorbed by the total thickness of the sample, for active monolayer A and multilayer films (A_LI_S, A_SI_S, A_LI_L and A_SI_L).

The μ_1 parameter gives information on the overall scavenging performance of the films, and is affected by both the thickness of the active and inert layers. In fact, as it is possible to observe from Figure 15 and Table 7, the A film shows the highest values in all the time interval, as the total thickness of the sample exactly corresponds to the thickness of the active layer, which controls the oxygen scavenging reaction. For all the multilayer systems, the presence of the inert layers, which affect the total thickness but do not participate in the scavenging reaction, leads to a decrease of the scavenging parameters with respect to the active monolayer sample.

Therefore, comparing the films at constant thickness of the active layer (A_LI_S-A_LI_L and A_SI_S-A_SI_L pairs), the scavenging activity values are higher in all the time interval for those samples with thinner inert layers (A_LI_S and A_SI_S), which have less impact on the total thickness.

Comparing the samples with the same thickness of inert layers (A_LI_S-A_SI_S and A_LI_L-A_SI_L pairs), the scavenging activity values are higher for samples with larger thickness of the active layers (A_LI_S and A_LI_L), which effectively react with the oxygen. As expected, among all the multilayer samples, the best scavenging performance are observed for A_LI_S sample, the one with the maximum thickness of active layer (23.5 microns) and the minimum

thickness of the inert layers (6.75 micron), for the same considerations as before. In the same way, the worst scavenging performances are the observed for the A_SI_L sample, the one with the minimum thickness of the active layer (13.5 microns) and the maximum thickness of inert layer (11.75 micron). In particular, for a time interval comprised between zero and 100 hours, the scavenging activity of A_SI_S is greater than the one that A_LI_L. At the beginning of the scavenging reaction, the thinner inert layers of A_SI_S provide less resistance to the oxygen diffusion towards the active center of the film. However, the smaller thickness of the active layer of A_SI_S sample let it exhaust rapidly (in 170 hours), while the scavenging action of A_LI_L remains for up to 550 hours.

As for the μ_2 parameter, values do not significantly differ among A, A_LI_S and A_LI_L samples, suggesting that the structure and properties of the active layers are almost identical, independently from the film structure and composition. However, this reasoning does not apply to A_SI_S and A_SI_L samples, the ones with smaller thickness of the active layer, whose μ_2 value is almost one half than the expected one. A possible explanation might be the partial inactivation of these films already during the extrusion process, where the high temperatures have led to a rapid diffusion of the oxygen through the inert layers towards the core layer which, being thinner with respect to the other two multilayer films, inactivated faster. Processing conditions (such as the chill roll temperature, the cooling conditions), as well as the thickness of the active layer, could play an important role in determining the residual activity of the samples.

To better summarize the impact of both the active and inert layer thicknesses on the performance of the multilayer films, the trends of t_E and of μ_1 as a function of the films' configuration are reported in Figure 16 (A), (B), (C) and (D).

Figure 16 (A) and (B) show how, at constant thickness of the inert layers (A_SI_S-A_LI_S and A_LI_L- A_SI_L pairs), both exhaustion time and scavenging capacity increase by increasing the thickness of the active layers, because a larger number of reactive sites are available for the oxidation reaction, allowing the depletion of the films activity in longer times.

Moreover, the scavenging capacity increases by the same percentages in both cases (128% for A_SI_S-A_LI_S pair and 126% for A_LI_L- A_SI_L), as is also observable from the same slope of the trend lines; this confirms previous conclusions, according to which there exists a good reproducibility of the scavenging performance of the active layer independently from the multilayer configuration.

Figure 16 (C) and (D) show the effects of thickness variation of inert layers, at constant thickness of the active layer.

At constant thickness of the inert layers

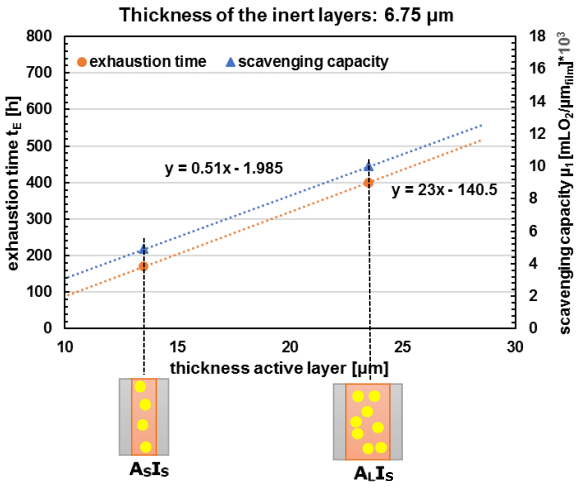

(A)

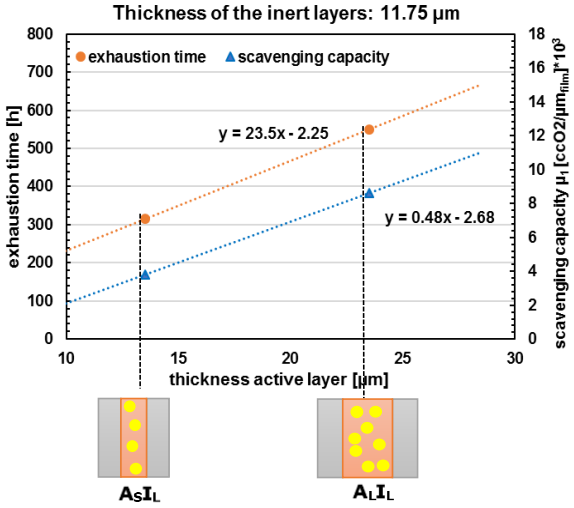

(B)

At constant thickness of the active layer

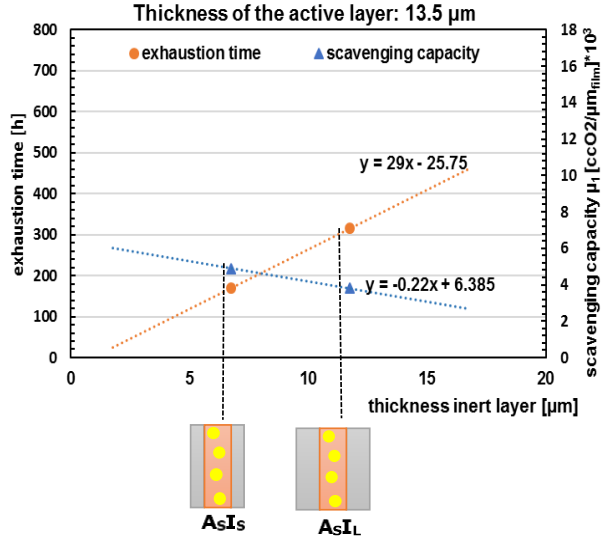

(C)

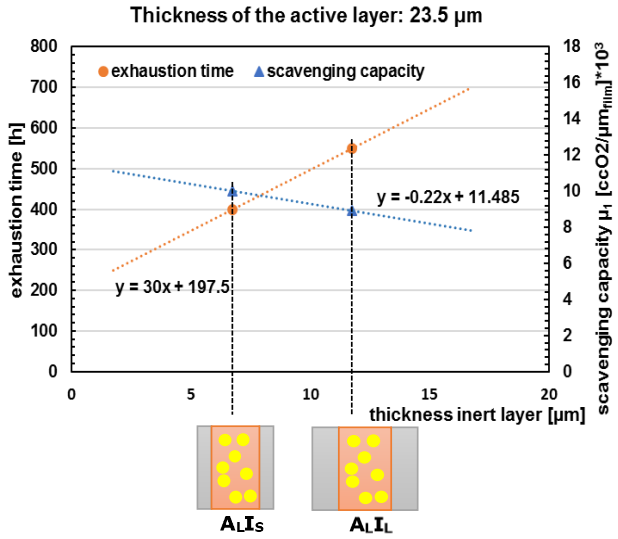

(D)

Figure 16 Dependence of exhaustion time and scavenging capacity μ_1 on the multilayer layout; (A) and (B): on the thickness of active layer, at constant thickness of the inert layers; (C) and (D): on the thickness of inert layer, at constant thickness of the active layer.

By increasing the thickness of pure PET layers, the decrease of the scavenging capacity is explained by the same reasons as before, whereas the increase of the exhaustion time is due to the increase of the hindering effect

on the oxygen diffusion through the inner active layer offered by the inert polymer. In addition, as also previously said, the exhaustion time increase follows the same trend by increasing the thickness of the inert layers (A_SI_S-A_SI_L and A_LI_S-A_LI_L pairs), confirming the good reproducibility of the passive barrier behavior of the multilayer films too.

To evaluate the steady-state oxygen transport properties of the multilayer films, oxygen permeability measurements were performed on the samples after the O_2 scavenging activity exhaustion. The same measurements were also conducted on the single layer films, both active and inert, and the results are reported in Table 7.

From the comparison between A and I samples, it is possible to observe that the presence of AMS_DFC4020 in the active monolayer film results in a slight reduction in the permeability value of the PET. As regards the multilayer films, the permeability values are intermediate with respect to those of samples A and I, and the amount of these changes depends on the layers configuration. However, the differences among the multilayer samples are negligible in order to assess the performances of the films in the real working conditions.

Evaluation of the effectiveness of the Active films on sensitive foods preservation

Amosorb DFC 4020E is a commercial product aimed at oxygen sensitive products and, as reported previously, it is permitted to be in direct contact with food according to US and European legislation. Global migration analyses on active films, ranging from 5 to 10% OS, showed migration values below the maximum limit of 10 mg/dm^2, defined by current legislation (Galdi, 2010).

In order to verify the effectiveness of the active films in preserving the quality of oxygen sensitive foods, shelf life tests on broccoli florets were performed.

Broccoli have a limited shelf life because of their relatively high metabolism rate. Broccoli heads deteriorate rapidly after harvest, and its visual and organoleptic qualities greatly depend on its storage conditions. In order to lower the metabolism of the vegetable and extend its shelf life, it is recommended to decrease the oxygen concentration in the headspace of the package (Izumi et al., 1996). An active device can quickly modify the gas composition inside the packaging, and can be combined with the fruit metabolism to control the equilibrium of oxygen in the headspace around the product (Adobati et al., 2015).

To this aim, fresh untreated broccoli florets were cut and packaged into the active monolayer and multilayer films and into pure PET film (I),used as control, according to the method previously described. Packages were thermally sealed and stored at 5°C for 10 days.

The packaged broccoli in neat PET film and in active monolayer film, taken as example, after 1 day of storage at 5°C are reported in Figure 17.

(A) (B)

Figure 17 Broccoli florets packaged in neat PET film (I, left) and in active monolayer film (A, right) taken as example, after 1 day of storage at 5°C.

Colour is one of the most important quality attributes of broccoli (Shouten et al., 2009). Yellowing due to senescence of broccoli florets is the main external quality problem in the broccoli production chain, and it is caused by caused by sepal chlorophyll degradation (Corcuff et al., 1998).

The colour of broccoli florets was measured in order to evaluate and quantify chromatic alterations undergone by the vegetables during the storage in active bags, and was assumed as the index for the effectiveness of the active film in preserving food from oxidation processes.

Figure 18 shows the images of broccoli florets packed in the single layer films (I and A) and in the active multilayer samples (A_LI_S, A_SI_S, A_LI_L and A_SI_L) after 10 days storage at 5°C, while Figure 20 shows L*, a*, b* parameters evaluated by colour measurements. ΔE^*_{ab} was also calculated for each sample, in comparison with Time 0, whose reference values (L^*_0, a^*_0, b^*_0) consisted of the average color measured on the florets before packaging. Finally, in Table 4 the weight loss (%) is reported.

As it is possible to observe from Figure 18 (A) and Figure 20, broccoli florets stored in PET neat package (I) show the most consistent yellowing of the sample, as also indicated by the highest increase of the b*coordinate with respect to Time 0 (equal to 21.0 and 12.0, respectively), while L* and a* parameters indicate a slight decrease in lightness and an increase in redness of the sample. The ΔE^*_{ab} value, in comparison with Time 0, is equal to 10.9.

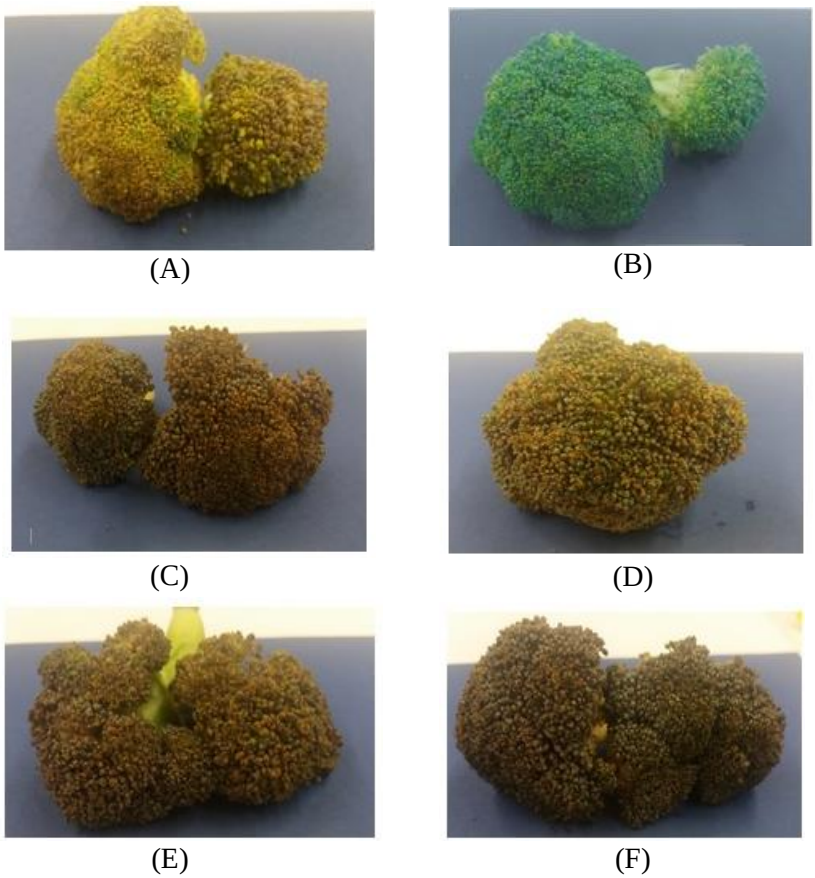

Figure 18 Images of broccoli florets packed in the single layer films PET inert (A) and active (B), and in the active multilayer samples A_LI_S (C), A_SI_S (D), A_LI_L (E) and A_SI_L (F), after 10 days storage at 5°C

The sample also shows the highest weight loss, equal to 13.3%, and a proliferation of moulds on the vegetables surface by visual observation.

On the other hand, florets stored in the single layer active film (A) exhibit the best overall features, regarding the visual appearance, the colour and the weight retention. In particular, in comparison with Time 0, the b* value (equal to 12.0) remains unaltered during the storage, while only a slight decrease in L* and a* parameters (equal to 50.0 and -9.3, respectively) is observable. The ΔE^*_{ab} is the smallest, and is equal to 4.6, just as weight loss is the least, and is equal to 6.2%.

Vegetables stored in multilayer active films all tends to a general browning and darkening of the surface, marked by the decrease of the L*

parameter (equal to 37.4, 38.5, 37.2 and 34.4 for the A_LI_S, A_SI_S, A_LI_L and A_SI_L films, respectively) and by the sharp increase in a* value (equal to -0.6, -2.4, 0.3 and -0.5 for the A_LI_S, A_SI_S, A_LI_L and A_SI_L films, respectively), consistently turning towards red colour. This results in a significant increase in the ΔE^*_{ab} parameter, which is in all cases comparable to or higher than the value observed for the inert PET film.

Although no visible mold proliferation is observed on the surface of the vegetables stored in the active multilayer films, and the weight loss is in all cases lower than that found in the inert PET film, the results show a not optimal configuration of multilayer films for the selected food.

In particular, looking at the oxygen absorption curves (Figure 13) and considering the respiration rates and the oxidative phenomena occurring into the vegetable, it is reasonable to hypothesize that the gas absorption rate of the OS at early times becomes relevant in this case. The vegetable requires a rapid oxygen reduction (as the one offered by the of active single layer film A), instead of the gradual, slower oxygen reduction offered by the active multilayer samples, in order to maintain its brilliant green colour and visual appearance.

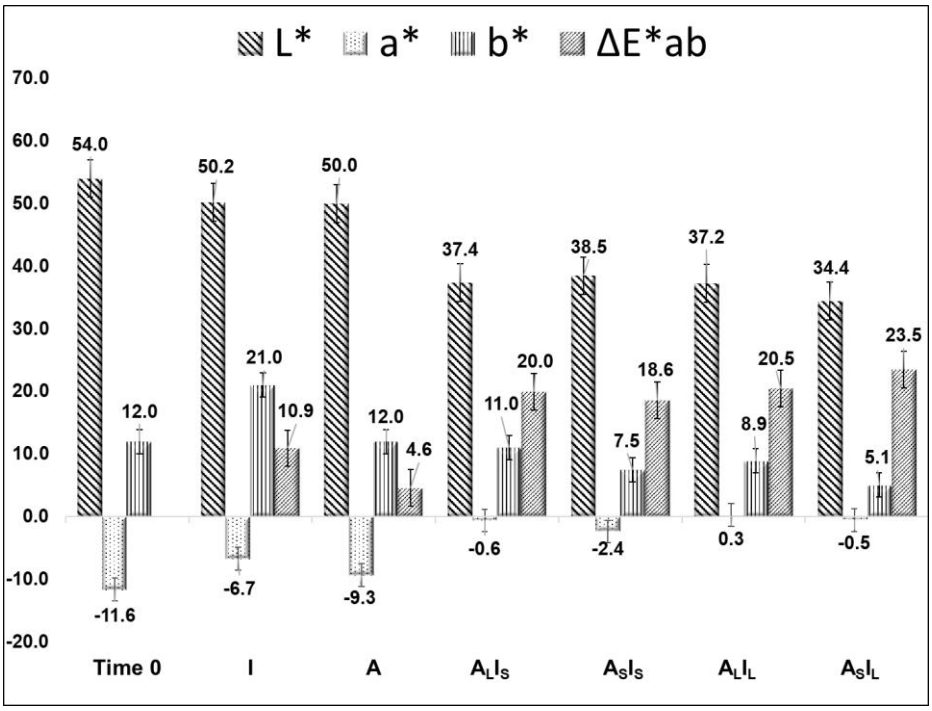

Figure 19 Cielab L, a*, b* and ΔE*ab parameters for broccoli samples stored at 5°C for 10 days in the single layer films (I and A) and in the active multilayer samples (A_LI_S, A_SI_S, A_LI_L and A_SI_L).*

Therefore, these results suggest the possibility to customize the application of the films depending on their scavenging performance, and that the monolayer active film may find application for the packaging of sensitive foods with fast oxidation rate and limited shelf life, while multilayer films could be more suitable in applications for sensitive foods with slow oxidation rate and medium-long storage term.

Table 8 Weight loss (%) of broccoli samples packaged in the single layer films (I and A) and in the active multilayer samples (A_LI_S, A_SI_S, A_LI_L and A_SI_L), after 10 days storage at 5°C.

Sample	Weight loss [%]
I	13.3
A	6.2
A_LI_S	12.7
A_SI_S	9.4
A_LI_L	10.3
A_SI_L	10.2

Evaluation of tensile properties

With the aim to better demonstrate the effects of the system composition on the mechanical performances of the samples, tensile properties of the monolayer and multilayer films are compared in Figure 20, in terms of elastic modulus E, stress at break σ and strain at break ε. No variation was highlighted in yield properties among all the samples.

The histograms of Figure 20 (A), (B) and (C), show a general decline in tensile properties of active films, if compared to the PET neat film I. This worsening, due to the presence of the second phase in the polymer matrix, is partially recovered in multilayer samples thanks to the external layers made by the pure polymer.

Among the multilayer films, the thinnest one, A_SI_S, shows the least value of elastic modulus and stress at break, whereas the ε value is the highest. On the contrary, the thickest film, A_LI_L, shows the largest value of E and σ, and the worst performances in terms of strain at break.

Multilayer films with the same total thickness (A_LI_S and A_SI_L) exhibit comparable values in terms of elastic modulus, stress at break and strain at break values.

In general, at constant thickness of the active layer (the pairs A_LI_S-A_LI_L and A_SI_S- A_SI_L), the increase of pure PET layer thickness leads to an increase in E and σ parameter, and a decrease in ε parameter. The same behaviour is observable by keeping constant the thickness of the external layers (the pairs A_LI_S-A_SI_S and A_LI_L-A_SI_L) and increasing the one of the central layer.

The trends observed (of which an example is reported in Figure 20 (D) for σ and ε parameters) allow a general consideration, according to which the elastic modulus and the stress at break proportionally increase when increasing the thickness of the layers, regardless of whether they are active or not. Conversely, the strain at break increases by decreasing the thickness of the layers.

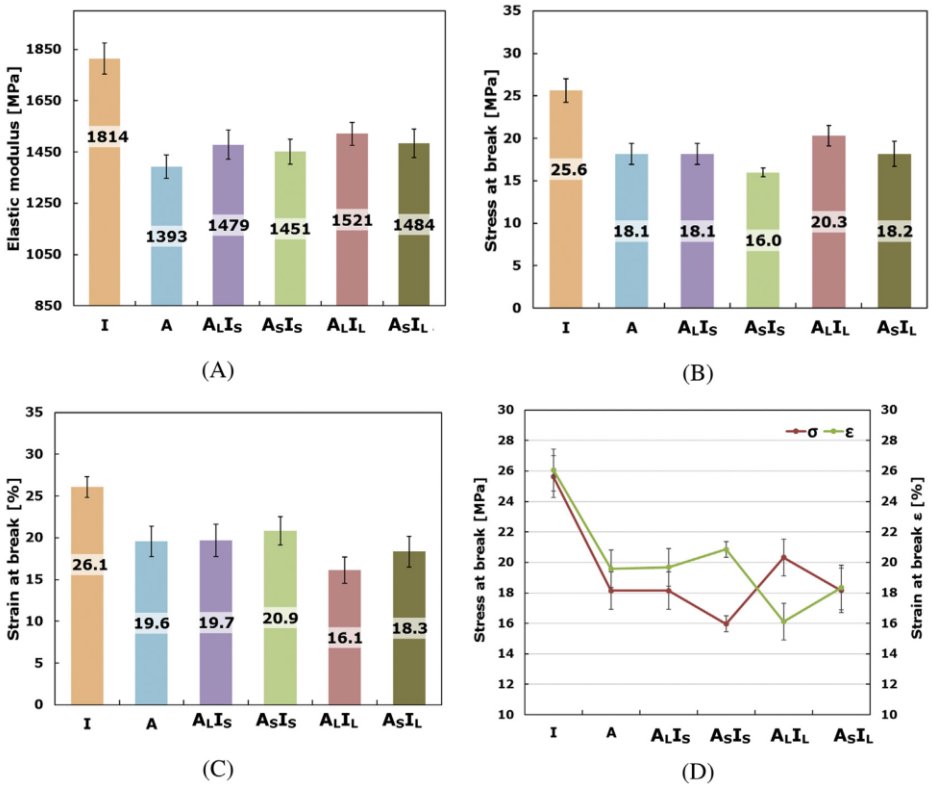

Figure 20 (A), (B), (C) and (D): Tensile properties for active monolayer and multilayer samples.

II.5 Modelling of oxygen scavenging performance of the active films

Model description

A multilayer Inert/Active/Inert (I/A/I) film layout, composed of three layers (two inert layers and one scavenging layer) arranged in an alternating pattern, with total thickness L and surface S, is considered. Literature studies, aimed at finding the best placement of reactive and inert layers and the optimal number of layers, indicated that this layout is preferable for food and pharmaceutical applications, as the external inert layer slows the oxygen diffusion towards the reactive layer, extending its durability, while the internal inert layer avoids contact between the scavenging layer and the product (Carranza et al., 2012).

The schematic representation of the multilayer film configuration under scrutiny is illustrated in Figure 21.

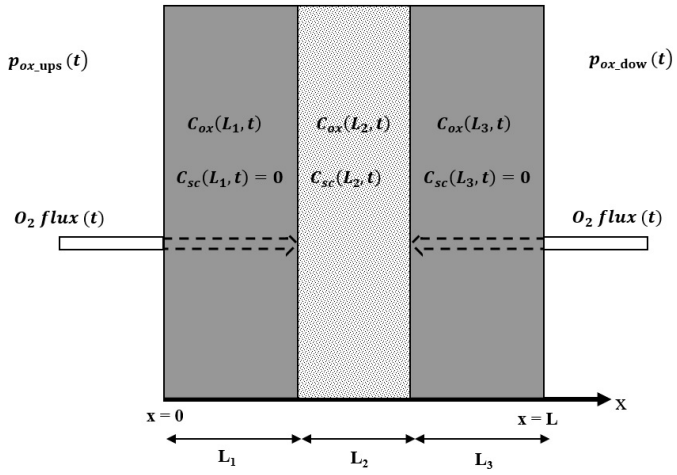

Figure 21 Schematic illustration of the symmetrical, multilayer I/A/I film layout under scrutiny. L1, L2, L3 are the thicknesses of each of the three layers considered.

An unsteady-state, one-dimensional (1D) reaction-diffusion mass transfer is considered. Oxygen is assumed to diffuse only through the plane faces, with a negligible amount through the edges.

The upstream and downstream sides of the film are exposed to environments having oxygen partial pressures equal to $p_{ox\_ups}(t)$ and

$p_{ox\_down}(t)$, respectively. In packaging applications, the upstream side is typically exposed to an infinite source of oxygen, normally air, with $p_{ox\_ups}(t)$ equal to ambient partial pressure, while the downstream side could have vanishing oxygen partial pressure $p_{ox\_dow}(t)$~0 (Carranza, 2010a).

At initial time, all the layers of the film are assumed to be devoid of oxygen, and both the scavenger and the reaction products are assumed to be immobile.

Oxygen transport trough the film is assumed to obey Fick's first law (Eq. 35), for which the transfer rate of a diffusing substance through a unit area is proportional to the concentration gradient normal to the section (Crank, 1975):

$$J = -D\,\frac{\partial C}{\partial x} \tag{35}$$

where J is the molar flux, D is the diffusion coefficient, C is the concentration of diffusant, and x is the film thickness.

Under unsteady state conditions, the three-dimension general equation of diffusion-reaction across a material can be written as:

$$\frac{\partial C}{\partial t} = D\left(\frac{\partial^2 C}{\partial x^2} + \frac{\partial^2 C}{\partial y^2} + \frac{\partial^2 C}{\partial z^2}\right) \pm R \tag{36}$$

where x, y and z are the spatial coordinates, t is the process time and R is the reaction rate.

To describe the oxygen reaction with the scavenger, first-order or second-order kinetic models can be applied. The first-order approach is based on the assumption that the reaction rate depends solely on the concentration of one reactant, i.e. the oxygen or the scavenger. This is a reasonable approximation when there is a large excess of either O_2 or scavenger (pseudo first-order reaction). However, this assumption may be not valid in many packaging applications. In this case, second-order reaction models should be applied (Pant et al., 2018).

With this aim, the oxygen consumption due to scavenging reaction can be described as a pseudo-second order reaction (Eq. 5):

$$R_{ox} = -k_R\, C_{ox}\, n \tag{37}$$

where k_R is the reaction rate constant, C_{ox} is the oxygen concentration, and n is the concentration of reactive sites.

The transient mass balances for oxygen and the reactive sites are given by Eq. 38 and Eq. 39:

$$\frac{\partial C_{ox}}{\partial t} = D(x)\,\frac{\partial^2 C_{ox}}{\partial x^2} - k_R\, C_{ox}\, n \tag{38}$$

$$\frac{dn}{dt} = -\nu\, k_R\, C_{ox}\, \mathrm{n} \tag{39}$$

Where ν is the stoichiometric coefficient for the oxidation reaction, x is the position along the film thickness and t is the time. Oxygen mass transfer (Eq. 36) accounts for both diffusion and reaction, and therefore it is described by a partial differential equation. The diffusion coefficient D(x) differs from layer to layer, depending on the constituent material and the presence of the scavenger that will affect the diffusion of oxygen into the film; therefore, it will assume a certain value D_i in the inert layers, and D_a in the reactive layer.

The reaction rate constant is null in the inert layers, so that in these portions of the domain the oxygen mass transfer is due only to diffusion.

At initial time, the film is devoid of any oxygen in all the layers, and the reactive sites are considered uniformly distributed throughout the active layer, with initial concentration of reactive sites equal to n_0 (Eq. 40).

$$C_{ox}(x,0) = 0;\;\; n(L_2,0) = n_0; \tag{40}$$

As for the boundary conditions, the oxygen concentration at the gas/polymer interface is assumed to obey Henry's law. Therefore, the oxygen concentration at the upstream and downstream boundaries are given by Eq. 41:

$$C_{ox}(0,t) = s\, p_{ox\ ups}(t);\;\; C_{ox}(L,t) = s\, p_{ox\ dow}\,(t) \tag{41}$$

where $C_{ox}(0,t)$ and $C_{ox}(L,t)$ represent the oxygen concentrations at system boundaries in the film side, and *s* is the solubility coefficient of oxygen in the polymer matrix.

At the interfaces between reactive and inert matrix layers, the flux and oxygen partial pressure are continuous, but the oxygen concentration on the reactive and inert sides should obey the equilibrium partitioning relationship, as described by Carranza et al., (2012), that constitutes the boundary conditions for the oxygen balance at the interfaces between the layers.

The total amount of oxygen permeating through the film per unit area is also a quantity of interest, and is defined as follows:

$$Q = \int_0^t J(t)|_{x=L}\, dt \qquad (42)$$

Where the downstream flux J at time t is given by:

$$J(t)|_{x=L} = -D \left.\frac{\partial C}{\partial x}\right|_{x=L} \qquad (43)$$

Equations 38-41 have been numerically solved using an explicit finite difference method, by applying the initial and boundary conditions listed and by entering the parameter set required for case-specific calculations. FEM based commercial software Comsol 5.0 (Comsol AB, Stockholm, Sweden) was used, and a multiphysics module for transport of diluted species involving reaction was selected.

The parameters and constants used to run the model are listed in Table 9.

Table 9 List of parameters and constants used to run the model.

Description	Parameter	Value	Units
Oxygen diffusivity coefficient in inert PET layers	D_i	5.27×10^{-9}	cm^2/s
Oxygen diffusivity coefficient in reactive layer	D_a	4.85×10^{-9}	cm^2/s
Volume of the testing cell	V_{cell}	9	mL
Initial concentration of scavenger at t=0	C_{sc0}	1.186×10^{-2}	mol/L
Initial concentration of O_2 at t=0 in the test cell	C_{ox0}	8.561×10^{-3}	mol/L
Oxygen solubility coefficient	s	7.16×10^{-2}	$cm^3/cm^3/bar$
Surface of the film	S	36	cm^2
Reaction rate constant	k_R	1×10^4	$cm^{3/}(mol\ s)$
Stoichiometric coefficient	ν	2	mol_{OX}/mol_{SC}

Oxygen solubility values among inert and reactive layer are assumed to be equal, as their differences experimentally measured remain within very narrow range (Carranza et al., 2012; Di Maio et al., 2017).

Model prediction and comparison with experimental results

The mathematical model was applied to the data set in order to verify its effectiveness in predicting the transport phenomena occurring in the active systems. Mathematical modelling of oxygen scavenging process in polymeric films should take into account both physical and chemical phenomena involved, such as the physical dissolution and diffusion of the gas through the polymer and the reaction of oxygen with the active phase (Gillen and Clough, 1992). Scavenging performances of the films depend on a number of parameters, such as the diffusion and solubility coefficients, the concentration of the scavenger added to the polymer, the number of sites available for the oxidation reaction, as well as the thickness of the layers.

Figure 22 shows the comparison between experimental (continuous line) and simulated (dotted line) oxygen absorption curves for multilayer samples under scrutiny. The comparison between experimental and simulated exhaustion time and final oxygen concentration in the test cell is also shown in Table 10.

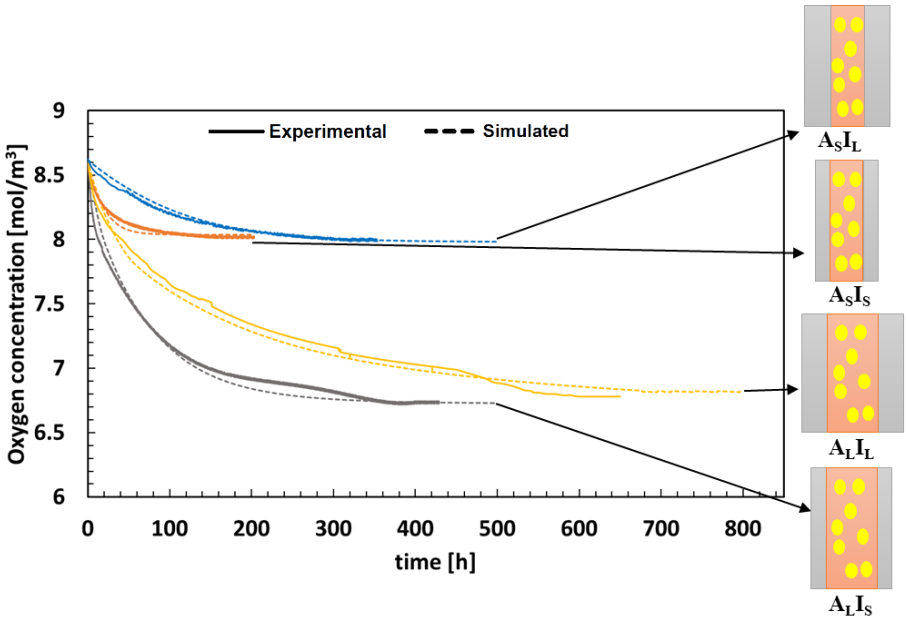

Figure 22 Comparison between simulated and experimental time evolution of oxygen concentration in the test cell with A_LI_S, A_SI_S, A_LI_L and A_SI_L multilayer films configurations.

Simulated oxygen absorption curves show an immediate reaction of the samples with the oxygen, whose concentration decreases to reach a plateau value, in correspondence of the relative exhaustion time, dependent on the configuration of the multilayer films. The scavenging activity in the active layer is mainly dependent on the amount of OS concentration loaded in the matrix and, therefore, the number of active sites found in the matrix of the film.

Table 10 Comparison of Exhausting Time and Final Oxygen Concentration, for the A_LI_S, A_SI_S, A_LI_L and A_SI_L multilayer films configurations (exp, Experimental; sim, Simulated)

Configuration	**A_LI_S**		**A_SI_S**		**A_LI_L**		**A_SI_L**	
	exp	sim	exp	sim	exp	sim	exp	sim
Exhaustion time (h)	400	397	170	150	550	630	315	317
Residual oxygen conc. (mol/m^3)	6.73	6.74	8.02	8.05	6.75	6.83	7.99	8.00

The trends of changes in oxygen concentration over time in the test cell provided by the model numerical solution are in quite close agreement with the experimental data, both in terms of the time evolution of oxygen depletion and oxygen consumption kinetics (i.e. the slope of the curves).

In terms of comparison of exhaustion time (i.e. the time at which the residual oxygen concentration becomes constant and the curve reaches a plateau) and final oxygen concentration in the test cell, Figure 22 and Table 10 show a good agreement between simulated and experimental values in all tested cases.

The residual oxygen concentrations calculated by the model are 6.74, 8.04, 6.83 and 8.00 mol/m^3 (vs. 6.73, 8.02, 6.75, 7.99 mol/m^3 estimated experimentally), obtained for the A_LI_S, A_SI_S, A_LI_L and A_SI_L configurations, respectively, with a discrepancy less than 2% in all the cases.

The exhaustion times calculated by the model, instead, are 397, 150, 630 and 317 h (vs. 400, 170, 550 and 315 estimated experimentally) obtained for the A_LI_S, A_SI_S, A_LI_L and A_SI_L configurations, respectively. Some discrepancy observed for A_LI_L film is probably due to an increasing oxygen depletion in the last 20–30 h of the process.

The results obtained suggested that the proposed model could be used to predict quite accurately the exhaustion time and the oxygen amount that the active multilayer film can remove, configuration by configuration.

II.6 Summary and conclusions

In this part of the research, multilayer flexible active films, with extended effectiveness of the OS performance and tunable OS kinetic and capacity, were successfully produced by conventional co-extrusion film production technology, properly designing and optimizing the layers' configuration.

Oxygen absorption measurements showed the effectiveness of the inert layers in decelerating the oxygen permeation through the core layer, as demonstrated by the increased exhaustion times and the slower absorption kinetics of multilayer films, compared to the active monolayer.

From the comparison among all the multilayer films, it was possible to discriminate the individual contributions of the layers, and the influence of the multilayer layout on the scavenging parameters.

In particular, at constant thickness of the inert layers, the total volume of oxygen absorbed per unit surface of the film increases by increasing the thickness of the active layer. The increase is comparable for both the film pairs considered, leading to a reproducible scavenger performance of the active layer, regardless of the multilayer configuration. Conversely, at constant thickness of the active layer, the same increase of the thickness of the inert layer leads, in both the film pairs, to the same increase in exhaustion time, highlighting the reproducible barrier performance of the inert layers, independently from the thickness of the reactive layer. Concerning the kinetic constant k, no significant variations can be noticed for samples providing the same resistance to the oxygen diffusive transport, while it decreases proportionally to the increase of the thickness of the inert layers. Results on the scavenging capacity μ_1 underlined a proportional decrease of the parameter by increasing the thickness of the sample not contributing to the scavenging reaction, while the μ_2 parameter suggests that the structure and properties of the active layers are almost identical, independently from the film configuration.

Steady-state oxygen transport tests conducted on the exhaust multilayer films have shown that in all cases the permeability values show only minor changes with the layer configuration.

Shelf life tests conducted on fresh-cut broccoli florets confirmed the helpful role of the oxygen scavenger in retarding oxidation reactions, thus inhibiting vegetable senescence. Results also pointed out the necessity of designing the food package basing on the requirements of each food, in terms of respiration rates, sensitivity to environmental parameters and shelf life parameters.

Mechanical tests exhibited a decrease in tensile parameters of the active films, if compared to the neat PET. This worsening, due to the presence of

the second phase in the polymer matrix, is partially recovered in multilayer samples thanks to the external layers made by the pure polymer.

Finally, the simulation results obtained by mathematical model agreed with the experimental data, highlighting the efficacy of the model in predicting the scavenging activity of the multilayer films, and its wide potential for characterization, designing and optimization of their scavenging performances.

Chapter III

Monolayer PET active films combining oxygen scavenger with high barrier constituents to extend their effectiveness

III.1 Introduction

In the previous chapter it was demonstrated how the realization of multilayer configurations can represent an effective solution in in decelerating the oxygen permeation through the core layer, extending the oxygen scavenger durability over the time.

However, multilayered technologies may require specific equipment not immediately available, adding to the total cost.

Therefore, in this chapter, another solution is analyzed to improve the passive barrier in monolayer systems.

In particular, the effectiveness of the oxygen scavenger can be enhanced by blending it with high barrier constituents (mainly aromatic polyamides), which further reduce the amount of oxygen permeating from the environment and simultaneously extend the exhaustion time of the scavenger.

Barrier polymer such as the nylon poly(m-xylene adipamide) (MXD6) has been proven to be effective as an oxygen barrier at concentrations starting from 10 wt % (Hu et al., 2005a; Hu et al., 2005b). The oxygen that attempts to enter the package will encounter a high tortuosity, increasing the diffusion pathway. The effect on solubility is minimal, but the diffusion can be halved in a blend of 10 wt % MXD6 (Hu et al., 2005b).

Both PET-oxygen scavengers and PET-aromatic polyamides blends have given good results in terms of barrier properties, the aim of this part of the research was to combine the two approaches, thus developing monolayer

active PET films with a new formulation of the Amosorb oxygen scavenger, added with a second phase with high barrier constituents of copolyamide nature, claimed to provide enhanced protection from gas diffusion for a wide range of foods and beverages (Anonymous, 2018b).

Figure 23 shows the flow diagram of the experimental set-up and of the activities carried out in this part of the PhD work, which will be discussed in this chapter.

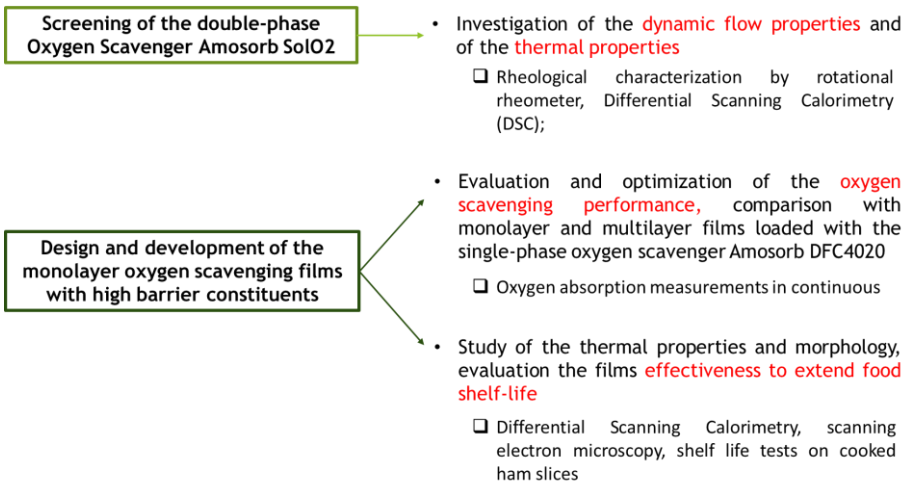

Figure 23 Experimental set up and activities discussed in Chapter III.

Since MXD6 is immiscible in PET, forming micron-sized islands, the oxygen scavenger was opportunely designed to increase the affinity between the two polymers.

The dynamic flow properties of the double-phase scavenger were investigated and compared to those of the single-phase scavenger, in order to evaluate possible differences in macromolecular structure among active agents,

Single layer PET films were produced at different concentrations of the boosted OS (ranging from 0 to 20%) by cast extrusion process. The effect of the OS on the thermal, morphological and oxygen absorption properties was investigated, and the film composition was optimized.

The scavenging performance of the optimized system were also compared to that of the monolayer film, loaded with the same concentration of the single-phase oxygen scavenger, analyzing the absorption kinetic, the total volume of oxygen absorbed and the exhaustion time.

Furthermore, the comparison was carried out among the films with the best performance in terms of prolonged exhaustion time obtained from both approaches, investigated in this chapter and the previous one.

Finally, shelf life tests on cooked ham slices were conducted to evaluate the effectiveness of the films in prolonging the shelf life of sensitive food matrices.

III.2 Materials and methods

Materials

PET resin Cleartuf P60 (M&G Polimeri S.p.A., Patrica (FR), Italy), was selected as polymer matrix. The active phase is Amosorb SolO2 (named AMS_SOLO, supplied by Colormatrix Europe, Liverpool, UK), an auto-activated polymeric oxygen scavenger designed for PET bottles and food contact approved from FDA and EU legislation. The scavenger is characterized by the presence of a double phase: a violet, active phase, of copolyester nature, which effectively reacts with the oxygen (named SOLO2_V), and a white phase of copolyamide nature, which gives enhanced gas barrier properties (SOLO2_W) [19]. The measured weight percentages for the violet and white phases inside Amosorb SolO2 are 60% and 40%, respectively.

Monolayer films production

Before films processing, the PET was dried under vacuum at 130 °C for 16 h, to avoid hydrolytic degradation. The SOLO, delivered in aluminum bags sealed under vacuum, was used as received. Single layer active PET films were produced using the same extrusion equipment and processing conditions described in the previous chapter. Only one of the extruders was employed to produce the films.

Table 11 shows a recap of the produced systems. Single layer film made of pure PET was also produced for comparison.

Table 11 List of the prepared systems, at different percentages of SOLO, with their nominal thicknesses.

Sample	O2-scav. concentration [% wt]	Total thickness [µm]
PET	0	47
PET+5%SOLO2	5	45
PET+10%SOLO2	10	45
PET+20%SOLO2	20	46

Characterization of the materials and active films

The dynamic flow properties of the raw materials at molten state were measured with a rotational rheometer (ARES, Rheometric Scientific, New

Jersey, US), using parallel plates geometry (plate diameter = 25 mm, gap = 1 mm). Frequency sweep tests in an angular frequency range of 1–100 rad/s, were performed at 260°C and at a constant strain amplitude 10%, under nitrogen gas purge, in order to minimize thermo-oxidative degradation phenomena.

Thermal analyses on the two phases of the pure oxygen scavenger and on the produced films were performed using a Differential Scanning Calorimeter (DSC mod. 822, Mettler Toledo). Experiments were carried out under nitrogen gas flow (100 ml/min) in order to minimize thermo-oxidative degradation phenomena. The samples were first heated at a rate of 10°C/min, from 25°C to 300°C, and held at this temperature for 5 min to allow the complete melting of the crystallites; then they were cooled from 300°C to 25°C at a rate of 10°C/min. The values of glass transition, cold crystallization and melting temperature (Tg, Tcc, Tm), the enthalpy of cold crystallization and melting (ΔHcc and ΔHm) and the percentage of crystallinity (Xc) were evaluated from the first heating scan; the values of crystallization temperature and enthalpy (Tc, ΔHc) were calculated from the cooling scan. The crystallinity degree Xc was calculated according to Equation (33), imposing ϕ equal to 1.

Scanning Electron Microscopy (SEM) analyses were conducted to investigate the morphology of the produced films. Film sections were cut cryofracturing them in liquid nitrogen normally to the extrusion direction, sputter coated with gold (Agar Auto Sputter Coater mod. 108A, Stansted, UK) at 30 mA for 160 s, and analyzed using a field emission scanning electron microscope (mod. LEO 1525, Carl Zeiss SMT AG, Oberkochen, Germany). Sigma Scan Pro 5.0 (Jandel Scientific, San Rafael, Canada) was used for image analysis.

Oxygen absorption measurements on the active films were carried out at 25 °C in continuous mode by means of the fiber optical oxygen meters Minisensor Oxygen Fibox 3-Trace V3 and Stand-alone Oxygen Meter Fibox 4 (PreSens GmbH, Regensburg, Germany), equipped with a polymer optical fiber and oxygen sensor spots SP-PSt3-NAU (detection limit 15 ppb, 0–100% oxygen). Experiments were conducted on cut film samples with a defined geometry (8.0 x 4.5 cm^2), which were introduced in glass measurement cells, having volume equal to 9 mL, and hermetically capped.

Oxygen consumption inside the closed glass vial was measured over time. From the oxygen absorption curves, it was possible to calculate the main absorption properties of the active films, such as the total volume of oxygen absorbed V_{O2}, the exhaustion time t_E and the scavenging capacity μ, calculated as the ratio between the total volume of oxygen absorbed and the weight of the films.

The effectiveness of the active films in extending the shelf life of oxygen-sensitive foods was verified by preliminary shelf life tests, using slices of cooked ham as test food. Ham was purchased on the local market, and stored at 4 ± 1°C overnight before slicing and packaging. On the day of packaging, the ham was cut in slices of (10 x 10) cm^2 area and 0.3 cm thickness, and individually sealed inside the bags made of neat and active PET. After packaging, samples were stored at 4 ± 1°C, both in illuminated (24 h/day) or in darkness conditions. A LED light with natural light (4000 K), luminous intensity equal to 750 lumens and an emission angle of 120° was used as light source. The red color of ham slices was measured by means of a tri-stimulus colorimeter Minolta CR-300 (Konica Minolta International, Japan), and the CIE Δa* parameter ($\Delta a^* = a^*_t - a^*_{t=0}$) was calculated. The measurements were taken on the ham slices by opening the packaging films at 1, 3 and 7 days, and 2 different locations on the ham surface were measured. Measurements were performed in triplicate.

III.3 Results and discussion

Rheological characterization

Oscillatory shear mode tests, within viscoelastic range, were conducted on both on the mixed composition of AMS_SOLO2 and on each individual component of the double-phase scavenger (named SOLO2_V and SOLO2_W, respectively). The results were also compared to those obtained for AMS_DFC4020 scavenger, to evaluate differences in macromolecular structure among the two polymeric oxygen scavengers. Indeed, possible differences could influence the morphology and viscoelastic properties of the polymer blends or induce possible degradation phenomena.

In Figure 24, the complex viscosity curves (Figure 24 (a)) and the storage moduli G' versus frequency (Figure 24 (b)) are reported.

AMS_SOLO2 shows a higher complex viscosity with respect to AMS_DFC4020 in all the range of frequencies investigated. Despite the similarities in shape, color and size among AMS_DFC4020 and SOLO2_V pellets, the rheological behavior suggests different chain structures, as underlined by the higher complex viscosity values and the more pronounced shear thinning behavior of SOLO2_V with respect to AMS_DFC4020.

SOLO2_W shows the highest complex viscosity and a Newtonian behavior in most part of the frequency range. The G' analysis confirms the differences in macromolecular structure between AMS_DFC4020 and SOLO2_V, as underlined by the higher G' value for SOLO2_V sample, compared with AMS_DFC4020, and a slightly lower G' frequency-dependence at low frequencies, which suggests a reduced mobility of the polymeric chains.

AMS_DFC4020 shows similar G' with respect to SOLO2_W at low frequencies, while AMS_SOLO2 and SOLO2_V storage moduli show a very similar behavior in all the investigated range of frequencies.

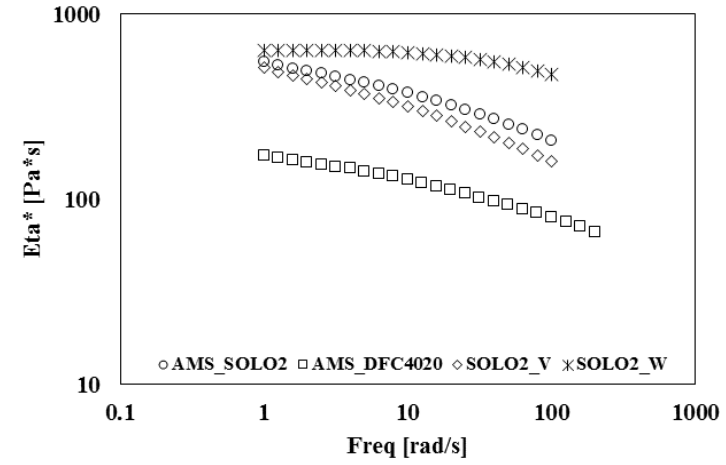

(A)

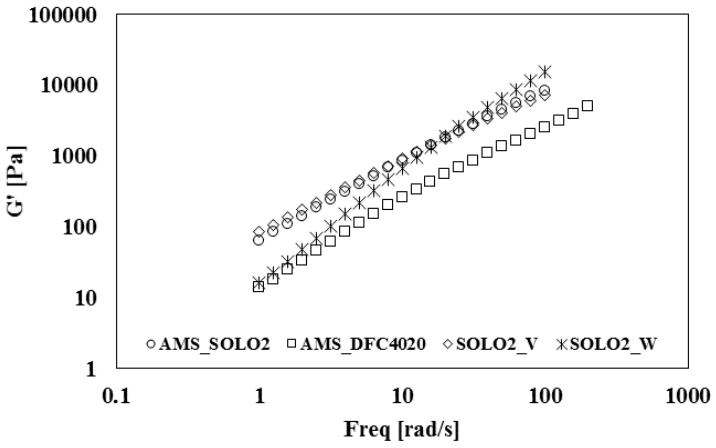

(B)

Figure 24 Complex viscosity curves (A) and Storage moduli (G') versus frequency (B) at 260°C of AMS_DFC4020, AMS_SOLO2 and single phases SOLO2_V and SOLO2_W.

Thermal and Morphological characterization

The results of thermal analyses carried out on the AMS_SOLO2 single components and on the active films are reported in Table 12 and Table 13.

Table 12 Thermal parameters of the SOLO2_V and SOLO2_W single components of the oxygen scavenger and of the active films, related to the heating cycle.

Sample	T_g [°C]	T_{cc} [°C]	T_m [°C]	ΔH_{cc} [J/g]	ΔH_m [J/g]	X_c [%]
SOLO_V	n.d.	n.d.	248.4	n.d.	38.8	n.d.
SOLO_W	n.d.	n.d.	194.5 , 239.2	n.d.	2.8 , 56.9	n.d.
PET	78.5	134.0	252.8	32.5	44.8	9
PET + 5% SOLO2	77.0	134.0	251.5	32.1	46.6	11
PET + 10% SOLO2	76.8	133.7	250.9	31.6	45.9	11
PET + 20% SOLO2	76.3	130.9	249.7	34.3	47.3	12

Table 13 Thermal parameters of the SOLO2_V and SOLO2_W single components of the oxygen scavenger and of the active films, related to the cooling cycle.

Sample	T_c [°C]	ΔH_c [J/g]
SOLO_V	158.6	25.2
SOLO_W	182.1	40.3
Film PET	192.4	40.7
PET + 5% SOLO2	197.3	42.8
PET + 10% SOLO2	198.5	42.2
PET + 20% SOLO2	199.9	43.5

The DSC data confirmed the copolyester nature of the violet phase SOLO_V of the oxygen scavenger, which shows a single melting peak, at a temperature of 248°C, comparable to the one of neat PET. The white phase SOLO_W shows two melting peaks - the first one, quite small, centered at c.a. 194°C, which falls within the melting range of polyamides (Messin et al., 2017), and the second one at 239°C - suggesting a more complex nature of both copolyester and copolyamide composition.

For all the active films, only a single melting peak is observed, at T_m around 250°C, while the melting peak imputable to the copolyamide phase is no longer appreciable, due to the small concentrations of scavenger dispersed inside the polymer matrix. Moreover, with respect to the PET film, all active systems feel the nucleating effect of the oxygen scavenger. Therefore, a slight crystallinity increase from 9% to 12% at increasing SOLO amount, a slight decrease of the cold crystallization temperature Tcc, and the shift of the crystallization temperature Tc towards higher values, whose significance increases by increasing the percentage of OS can be observed.

The distribution and dispersion of the active phase inside the polymer matrix was investigated through SEM analyses. Figure 25 shows the cross-section micrographs of the active films at 5% and 20% of the oxygen scavenger.

The presence of the polymeric oxygen scavenger inside the PET matrix is highlighted by the occurrence of spheroidal domains, which size and arrangement vary depending on the composition of the samples. In particular, the films at low percentage of SOLO show an uneven layout of the OS particles, which diameter is less or equal to 1 micron ((Figure 25 (A)), while the film at 20% of SOLO shows the presence of big voids related to OS aggregates with diameter larger than 1 micron ((Figure 25 (B)).

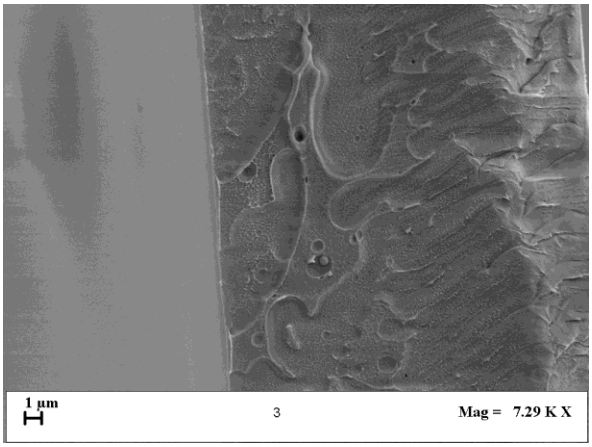

(A)

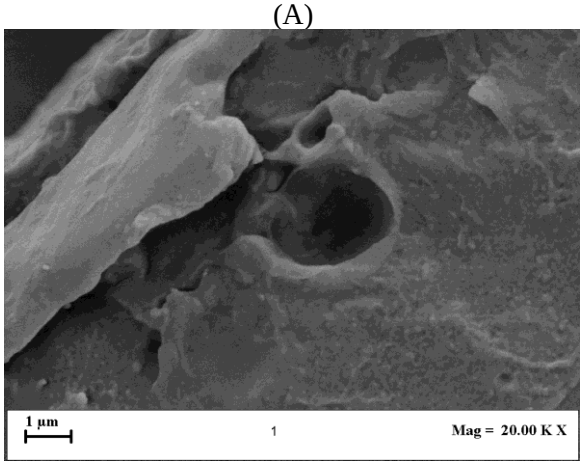

(B)

Figure 25 SEM micrographs of: (A) PET + 5% SOLO2 film; (B) PET + 20% SOLO2 film.

Evaluation and comparison of Oxygen absorption kinetic and parameters

Continuous oxygen absorption measurements were performed to evaluate the oxygen scavenging capacity and the absorption rate of the active films produced. The obtained curves are compared in Figure 26 and the scavenging parameters calculated from the curves are listed in Table 14.

The oxygen absorption kinetics of Figure 26 show an immediate reaction of all the active films with the oxygen inside the vial, absorbing it during the time, up to reach the film exhaustion displayed by the plateau stage. At short times, the oxygen absorption rate increases inversely proportional to the OS

concentration. The phenomenon can be due to the presence, in the OS formulation, of the copolyamide phase that, acting as passive gas barrier, hinders the oxygen diffusion towards the reactive sites, the higher is the OS loading.

At long times, the absorption kinetics progressively slow down to activity exhaustion. In particular, the PET film at lowest AMS_SOLO2 content shows the lowest scavenging capacity (2.02 ccO2/g film) and the shortest exhaustion time (ca. 70 hours). The film at 10% AMS_SOLO2 has an almost doubled scavenging capacity and a much longer exhaustion time, thanks to the higher amount of copolyamide phase as passive barrier that delay the oxygen diffusion across the film. Nevertheless, the film at 20% AMS_SOLO2 shows only a small increase of scavenging capacity and a reduction of the exhaustion time with respect to the PET + 10%SOLO2 film.

This is related to the non-homogeneous film morphology, characterized by the presence of large particles of oxygen scavenger phase. This leads to a slowing of the absorption rate, due to the fewer reactive sites exposed on the surface and a more difficult O_2 diffusion towards the inner reactive sites, causing a premature depletion of the film.

These results are consistent with those obtained in the previous chapter with AMS_DFC4020, where it was found that the scavenging performance depends not only on the percentage of oxygen scavenger added, but also on the morphology developed upon processing in terms of dispersion, distribution and size of the active phase.

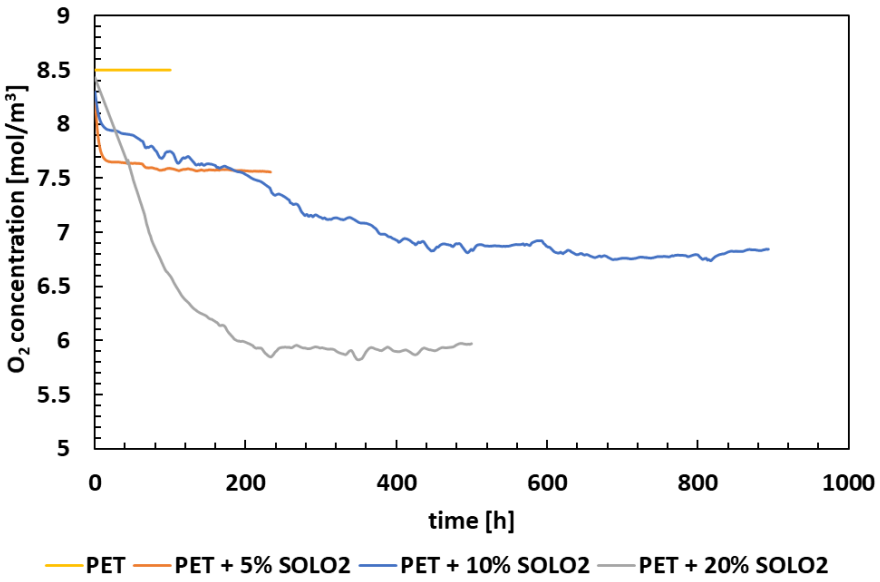

Figure 26 Oxygen absorption kinetics at 25°C for the PET films at 0, 5, 10 and 20% AMS_SOLO2.

Table 14 Exhaustion time t_E, total volume of oxygen absorbed V_{O2} and scavenging capacity μ for PET films loaded at 5, 10 and 20% AMS_SOLO2.

Sample film	t_E [h]	V_{O2} [mL]	μ [cc O_2/g film]
PET + 5% SOLO2	70	0.19	2.02
PET + 10% SOLO2	600	0.34	3.93
PET + 20% SOLO2	250	0.56	4.48

With the aim of comparing the scavenging performance of the films loaded with the two different oxygen scavengers AMS_DFC4020 and AMS_SOLO2, Figure 27 displays the comparison among the oxygen absorption curves of the two monolayer PET films, of comparable thicknesses, both loaded at 10% of the oxygen scavengers. In Table 15 the exhaustion time t_E and total volume of oxygen absorbed V_{O2}', normalized with respect to the percentage of active phase in the scavenger, are also reported.

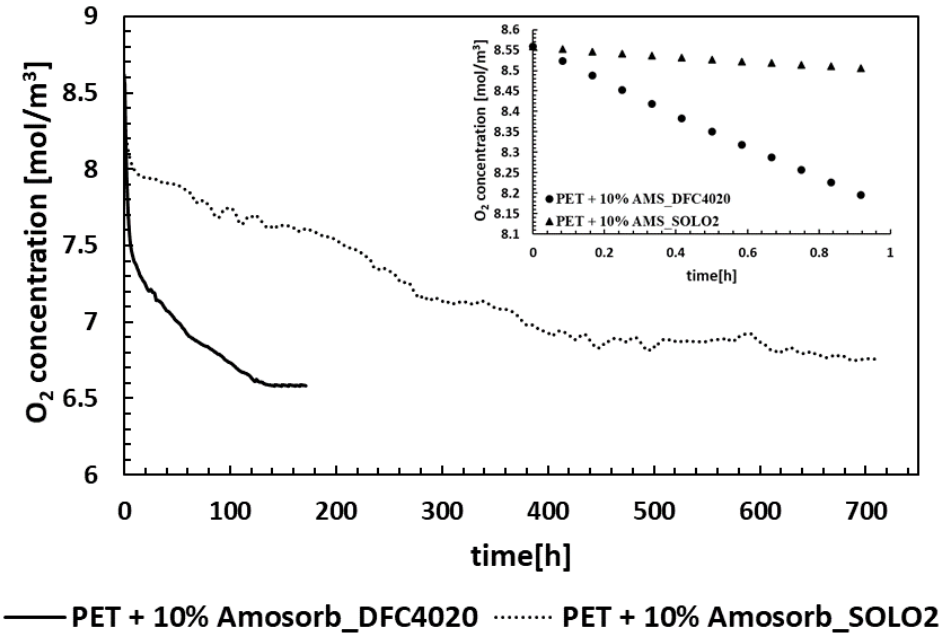

Figure 27 Comparison among oxygen absorption curves of the single layer PET films loaded with 10%wt oxygen scavengers AMS_DFC4020 and AMS_SOLO2. Inset graph: zoom of the region at short times.

Table 15 Exhaustion time t_E and total volume of oxygen absorbed V_{O2}' for PET films loaded with 10% oxygen scavengers AMS_DFC4020 and AMS_SOLO2.

Sample film	t_E [h]	V_{O2}' [mL]*
PET + 10% AMS_DFC4020	130	0.450
PET + 10% AMS_SOLO2	600	0.550

**normalized with respect to the percentage of active phase in the scavenger.*

Oxygen absorption curves and parameters highlight the effect of the different composition of the two active phases on the absorption kinetics. With respect to the PET + 10% AMS_DFC4020 sample, the PET + 10% AMS_SOLO2 film shows a slower absorption kinetics since initial times, as reported in Figure 27, and an increase of the exhaustion time (of almost 384%), as reported in Table 15. These results confirm the increase of the

resistance to the oxygen diffusive transport provided by the copolyamide phase.

Regarding the total volume of oxygen absorbed, normalized on the basis of the effective content of active phase in both scavengers (e.g. 100% in case of AMS_DFC4020 and 60% in case of AMS_SOLO2), it is worth to underline an increase of almost 30% of oxygen absorbed by the PET + 10% AMS_SOLO2 film, with respect to the PET + 10% AMS_DFC4020 sample. This result suggests an enhanced scavenging power AMS_SOLO2 with respect to of AMS_DFC4020, and then a more concentrated composition of the active phase, confirming the difference in molecular structure reported before.

Finally, the last comparison was carried out among the PET + 10% AMS_SOLO2 and the A_LI_L films, e.g. the films with the best performance in terms of prolonged exhaustion time obtained from both approaches investigated in this chapter and the previous one, respectively (Figure 28 and Table 16). Films have comparable nominal total thicknesses.

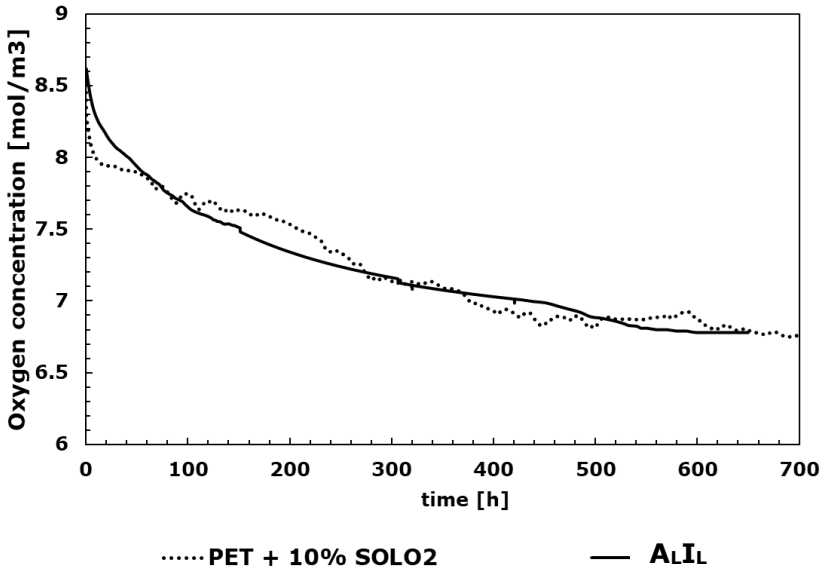

Figure 28 Comparison among oxygen absorption curves of the single layer PET + 10% SOLO2 film and the multilayer film A_LI_L.

Table 16 Nominal total thickness, relative thickness of Inert/Active layers, exhaustion time t_E and total volume of oxygen absorbed V_{O2}' for the single layer PET + 10% SOLO2 film and the multilayer film A_LI_L.

Sample	Total thick. [µm]	Thick. layers I/A/I [µm]	t_E [h]	V_{O2}' [mL]*
PET+ 10% AMS_SOLO2	45	-/45/-	600	0.550
A_LI_L	47	11.75/23.5/11.75	550	0.405

**normalized with respect to the percentage of active phase in the scavenger.*

As expected, the short-term absorption kinetics (t < 50 h) is faster for the PET+ 10% AMS_SOLO2 film than for the A_LI_L sample. This is because, in the monolayer film, the active phase is homogeneously distributed throughout the whole thickness of the film, while in the multilayer the external layers of inert PET slow down more effectively the diffusion of oxygen molecules towards the active core layer.

For longer times, the barrier effect of the copolyamide phase and the multilayer configuration is comparable, and the two films show similar depletion times, equal to 600 h and 550 h for the PET+ 10% AMS_SOLO2 and A_LI_L, respectively.

Finally, as regards the total volume of absorbed oxygen, normalized on the effective content of the active phase, a slightly higher value for the PET+ 10% AMS_SOLO2 film is obtained, but in any case the V_{O2}' values are comparable and of the same order of magnitude.

Therefore, both the approaches used, i.e. the development of a multilayer configuration and mixing with a high barrier polymeric phase, are effective in extending the exhaustion time of the scavenger, prolonging its durability over the time.

Evaluation of the effectiveness of the Active films on sensitive foods preservation

In order to verify the effectiveness of the active films in preserving the quality of oxygen sensitive foods, preliminary shelf life tests were performed on slices of cooked ham. For meat products, color is one of the most important aspects that influences the purchase and the assessment of quality and palatability. Several works pointed out the oxygen impact on discoloration of cooked ham, due to the oxidation of denatured nitrosomyoglobin (dMbNO) to metymioglobin (MMb), catalyzed by the

presence of light, resulting in a grey color of the product surface (Hutter et al., 2016; Møller et al., 2003; Andersen et al., 1988; Haile et al., 2013).

This discoloration is reflected in a decrease in the value of the CieLab a* parameter, which has been investigated through colorimetric measurements. For this purpose, Table 21 shows the changes in redness (Δa*=a*t - a*t=0) for all the samples with the different packaging films and storage conditions, while Figure 29 shows the images of the cooked ham slices at time 0 (A) and after 7 days storage at 4°C in darkness in the films of neat PET (B) and PET + 20% SOLO2, taken as example.

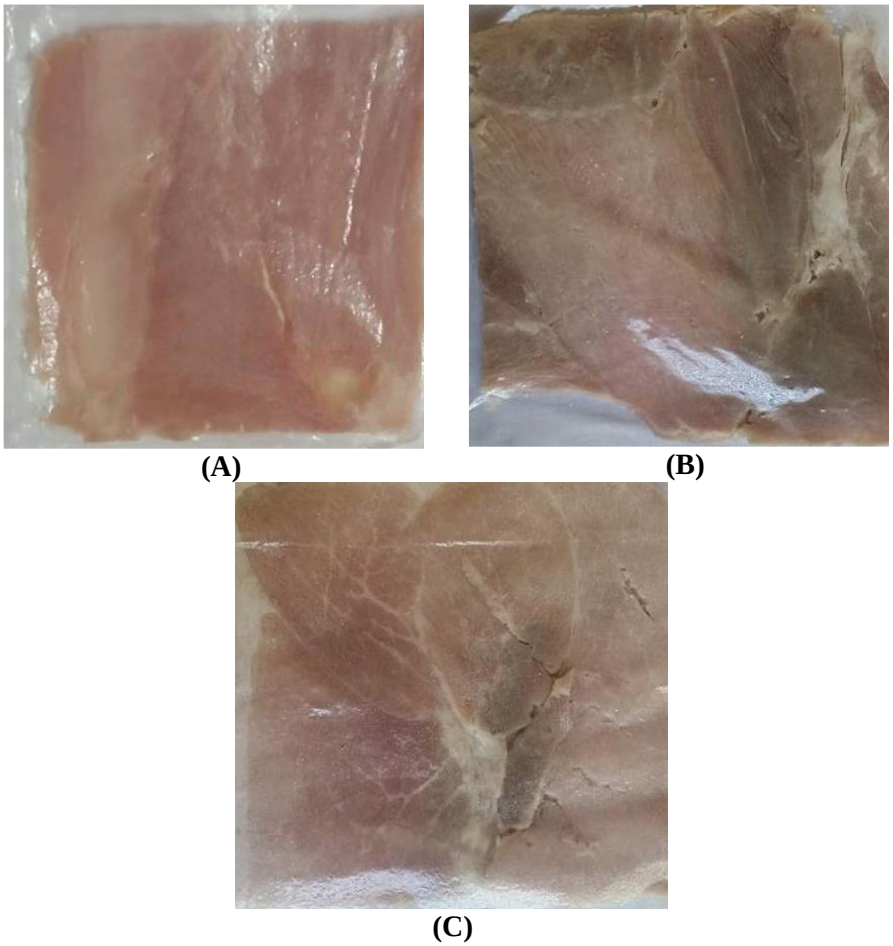

(A) **(B)**

(C)

Figure 29 Comparison among the cooked ham slices at time 0 (A) and after 7 days storage at 4°C in darkness in the films of neat PET (B) and PET + 20% SOLO2.

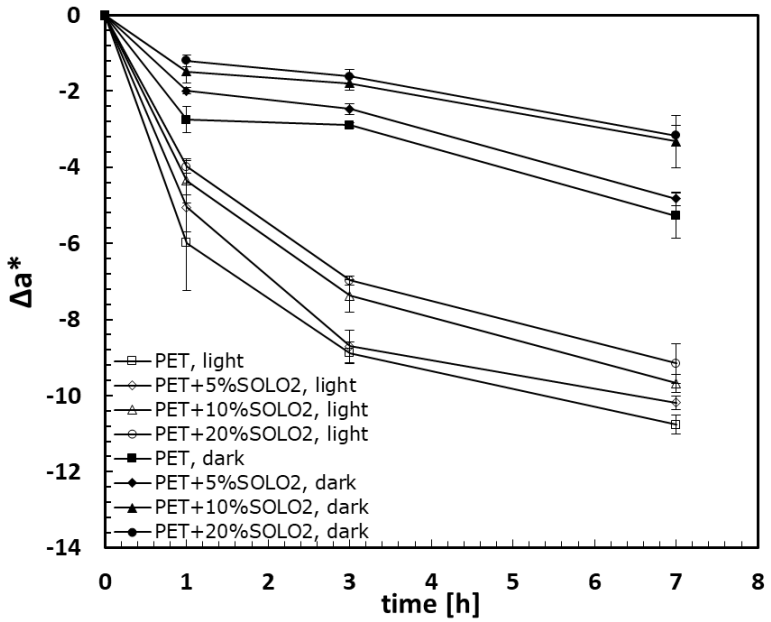

Figure 30 Changes in redness ($\Delta a^* = a^*_t - a^*_{t=0}$) of ham slices packaged in neat PET and active films at different percentage of oxygen scavenger, during 7 days storage at 4 ± 1°C. Filled symbols indicate the samples stored in dark, while unfilled symbols indicate samples stored at illuminated conditions. Mean value ± standard deviation.

As noticeable from Figure 29, all illuminated samples show a quick discoloration, started immediately after packaging, as well as the most significative decrease in Δa* parameter, pointing out the crucial role of light in catalyzing the oxidative reaction, as also confirmed by other authors (Møller et al., 2003; Andersen et al., 1988; Haile et al., 2013).

On the other side, all the samples stored in darkness show a less pronounced decrease in redness, especially between day 1 and 3, during which the a* parameter is almost constant for all the films.

The maximum discoloration rate is observed, in both cases, between day 0 and day 1, indicating that the product just cut and packaged is very sensitive to environmental conditions, while instead, in the following two days, the darkness condition favors a slowing of the discoloration reaction, such that the a* parameter remains almost constant.

Moreover, samples stored in neat PET, both in light and dark conditions, exhibit the most consistent graying, while a better color retention is observed for samples stored in active films by increasing the scavenger percentage, with the best behavior for the film at 20% SOLO2 (Figure 29). These results

can be explained taking into account the oxygen absorption curves seen before, particularly in the first 200 hours, in which it is clear how the 20% SOLO2 system rapidly lowered the oxygen concentration inside the headspace of the pack, effectively slowing down the ham discoloration, pointing out the importance of scavenger absorption kinetics to extend the durability of the foods depending on the specific requirements.

III.4 Summary and conclusions

In this chapter, a second approach aimed at avoiding the rapid exhaustion of the oxygen scavenger in flexible packaging was investigated.

This approach involved the use of a new formulation of the oxygen scavenger, added with a second phase with high barrier constituents of copolyamide nature, capable to slow down the O_2 diffusive mechanism through the active film.

The results obtained from rheological investigations pointed out the difference in molecular structure among AMS_DFC4020 and AMS_SOLO2. In particular, different chain structure was found for AMS_DFC4020 and the violet phase of Amosorb $SOLO_2$ (named SOLO2_V) despite the similarities in shape, color and size between the pellets.

Single layer PET films were then produced at 5, 10 and 20% of the oxygen scavenger AMS_SOLO2, by cast extrusion process. Thermal analyses highlighted the influence of the scavenger phase on the crystallization behavior of the polymer matrix, acting as a nucleating agent. SEM images confirmed the impact of scavenger concentration and processing conditions on the morphology of the PET films, playing a crucial role on their final scavenging performance oxygen absorption kinetics.

As in the case of AMS_DFC4020, the 10% AMS_SOLO2 concentration was the optimal one with the best dispersion and distribution of the reactive domains in the matrix, leading to the best performance of the film in terms of prolonged exhaustion time.

Oxygen absorption measurements conducted on the films loaded with 10% of each oxygen scavengers revealed an enhanced formulation for the AMS_SOLO2 with respect to AMS_DFC4020, with an increased scavenging power. Moreover, the high barrier performance offered by the copolyamide component in the AMS_SOLO2 allowed to obtain an increased exhaustion time and a slower absorption kinetic.

The shelf life tests conducted on cooked ham slices showed the potential of the active films in retarding the oxidation reactions, thus prolonging the shelf life of sensitive food matrices.

The outcomes obtained by the two different approaches are comparable, when composition and configuration are optimized, and both technologies

represent a valid solution to effectively extend the durability of the scavenger over the time.

The alternative choice of one or the other approach can be made on the basis of the ease of realization (i.e., if specific equipment for multilayer films production is not available) or on the specific requirements of the food, especially at short time. Furthermore, the results could represent a starting point for new interesting insights for the development of new hybrid systems.

Section II

Sustainable active films based on PET functionalized by Antimicrobial Bio-coatings

Chapter IV - *Sustainable active films based on PET functionalized by Antimicrobial Bio-coatings*

Chapter IV

Sustainable active films based on PET functionalized by Antimicrobial Bio-coatings

IV.1 Introduction

In this chapter, the possibility to functionalize PET films with antimicrobial bio-coatings is evaluated. The state of art previously reported highlighted the potential use of polymers as carriers for the controlled release of active agents during the storage and distribution of food packaging, with less antimicrobial concentration, tunable release and tailor-made applications.

The main challenges are related to the production of effective packaging systems, with good functional properties, realized through easy-scalable, conventional technologies in use in food packaging industry and with high eco-sustainability.

At the same time, the selection of the proper antimicrobial, as well as the choice of its optimal loading, is an important and not an easy task in the design and application of antimicrobial packaging (Wicochea-Rodríguez et al., 2019; Becerril et al., 2013). Some of these substances can modify the organoleptic profile of the packaged foodstuff, or can be used only for a small variety of foods, or can affect the functional properties (i.e. gas permeability, tensile strength, transparency, thermal stability, etc.) of the packaging material, or can have migration limits (Aznar et al., 2013; Muriel-Galet at al., 2014; Bugatti et al., 2019; European Commission, 2009).

One of the most innovative and powerful antimicrobial compounds, not showing much of these drawbacks, is Ethyl-Nα-dodecanoyl-L-arginate (LAE). LAE is a derivative of lauric acid, L-arginine and ethanol, which showed an extensive spectrum of antimicrobial activity against Gram

positive and Gram-negative bacteria, as well as yeasts and molds (Infante et al., 1997; Bakal and Diaz, 2005; Pezo et al., 2012). It interacts, as a cationic surfactant, on the cytoplasmic membrane of microorganisms increasing the cell permeability without causing lysis (Nerin et al., 2016). Among the major positive features, LAE has been classified as GRAS (Generally Recognized as Safe) and food preservative by the Food and Drug Administration (FDA), is chemically stable, has low cost, and does not provide any taste or odor, in compliance with European Regulation on active food packaging materials (Otero et al., 2014).

Previous published researches already addressed the realization of packaging films incorporated with LAE, realized by solvent casting technique (Moreno et al., 2017; Haghighi et al. 2019; Rubilar et al, 2016; Muriel-Galet et al. 2012). Many authors have also highlighted LAE interesting performance when used in combination with other technical procedures: Silva et al. (2019a) described the preparation of cellulose nanofibril (CNF) films and hydrogels, demonstrating the hydrogels ability to inhibit bacterial swimming motility and, in the form of films, the potent antimicrobial activity against *L. monocytogenes* at concentrations as low as 1% LAE.

However, limited information is available concerning the development of sustainable packaging solutions based on PET films, functionalized with LAE-activated bio-coatings, and produced with conventional techniques easy-scalable at industrial level.

On the basis of the aforementioned considerations, the goal of this part of the PhD work was to develop antimicrobial, multifunctional and sustainable food packaging films, based on LAE, by means of coating technology.

Figure 31 shows the flow diagram of the experimental set-up and of the activities carried out in this part of the PhD work, which will be discussed in this chapter.

The multilayer films were realized by spreading an amorphous PLA coating layer (C), incorporated at different concentrations of LAE, on a Bi-oriented PET substrate (S).

PET was selected as web layer thanks to its excellent functional properties, as oxygen and water vapor barrier, high tensile strength, and complete recyclability. The amorphous PLA coating already demonstrated to provide sealant layer to polyester films (Barbaro et al., 2015), in addition to its good optical properties, good processability and environmental benefits (Scarfato et al., 2017). In addition, the biodegradable layer is easy to be removed by non-toxic solvents, ensuring the complete recovery of the recyclable substrate (Bugnicourt et al., 2013), and the coating technology ensures to avoid thermal stresses to heat sensitive active compounds.

The antimicrobial effectiveness of the active films was assessed by means of microbiological tests, using E. Coli CECT 434 strain as pathogenic agent.

Release tests were carried out to investigate the diffusion kinetics of the active films in aqueous food simulant, checking the compatibility of the film release times with the shelf life of the target foods, to be an attractive solution from practical and commercial point of view.

Finally, the produced systems were characterized in order to ascertain the effect of the active phase on the thermal stability, chemical and morphological properties of the films. The wetting and adhesion properties, the barrier, tensile and optical performance were also investigated.

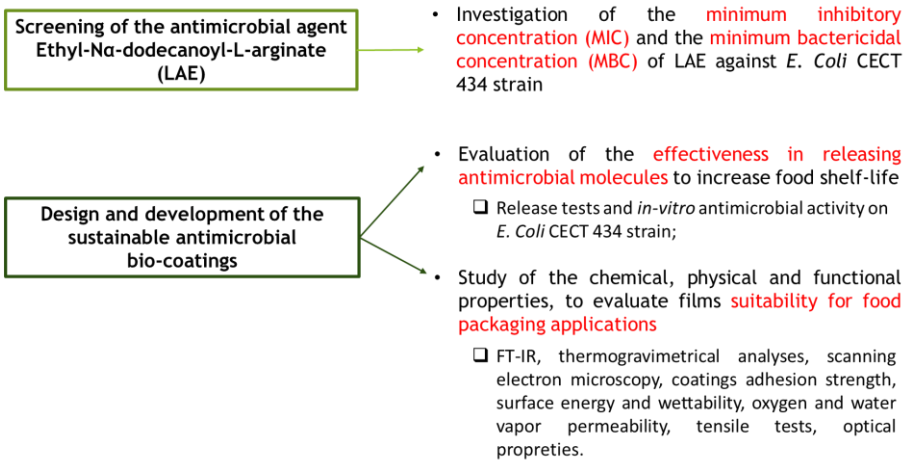

Figure 31 Experimental set up and activities discussed in Chapter IV.

IV.2 Materials and Methods

Realization of the antimicrobial biocoatings

Commercial biaxially oriented poly(ethylene terephthalate) (BOPET) film (Nuroll S.p.a, Italy), with 23 μm thickness and corona treated surface, was used as substrate (S). PLA4060 (Natureworks, Minnetonka, USA), characterized by a D-lactide content of 12 wt%, was used for the coating layer (C). Ethyl-Nα-dodecanoyl-L-arginate (LAE) was provided by Vedeqsa Grupo LAMIRSA (Terrassa, Barcelona, Spain). All the solvents used were analytical grade.

Antimicrobial coated films were realized according to the method explained by Barbaro et al., 2015, with some modifications. The PLA coating solution was prepared by dissolving the polymer in acetone (mass ratio 20:80) and subsequently adding LAE at different percentages (0, 5, 10 and 20% w/wt). The casting mixture was spread on the BOPET substrate by means of a K Hand Coater (RK, Printocoat Instruments Ltd., Litlington, UK), equipped with stainless steel closed wound rod, with wire diameter equal to 0.64 mm, yielding final coatings with an average thickness of the coating layer comprised between 7 and 10 microns.

Table 17 resumes the list of the prepared films (named SC, SC5, SC10, SC20). The PET substrate (S) was also used as comparison.

Table 17 List of the prepared systems, at different percentages of LAE.

Sample Film	LAE concentration [wt %]	Thickness of the coating layer [μm]	Total Thickness [μm]
S	0	0	23
SC	0	7 ± 0.5	30 ± 0.5
SC5	5	7 ± 0.9	30 ± 0.9
SC10	10	8 ± 1.0	31 ± 1.0
SC20	20	10 ± 1.2	34 ± 1.2

Characterization techniques

Fourier Transform Infrared spectra of the films were collected by a Thermo Scientific Nicolet 600 FT-IR, equipped with a Smart Performer accessory for attenuated total-reflection (ATR) measurement using a ZnSe

crystal. The operating spectral range was set at 650–4000 cm^{-1}, with a resolution of 4 cm^{-1} and 64 scans per sample. Normalization and peak integration was performed using Omnic software.

Thermogravimetric analyses (TGA) were performed with a Q500 TA Instruments apparatus, heating specimens (10–30 mg) at 10°C/min up to 600°C in N_2 atmosphere. The thermograms were analyzed to determine the temperature at the maximum rate of weight loss (DTGmax).

Field Emission Scanning Electron Microscopy (SEM) analyses were conducted on the film sections, which were cut cryofracturing them in liquid nitrogen normally to the extrusion direction, sputter coated with gold (Agar Auto Sputter Coater mod. 108A, Stansted, UK) at 30 mA for 160 s, and analyzed using a field emission scanning electron microscope (mod. LEO 1525, Carl Zeiss SMT AG, Oberkochen, Germany).

In order to evaluate the adhesion strength of the PLA coatings, delamination tests were carried out by SANS tensile tester (mod. CMT 4000 by MTS, China), equipped with a 10 N load cell, according with the standards ASTM F88-00 and ASTM 2029. In particular, the coated films were cut in strips of 200 x 25 mm^2 area, sealed with a Brugger HSG-C (Germany) heat sealing machine at 120 °C for 1s, by applying a force of 690 N, and stored for 48 h in environmental condition prior to analysis. Then, the bonding strength was evaluated in tensile mode at 250 mm/min until delamination failure of the seal. The maximum load reported is considered as the maximum bond strength of the coating on a specific substrate (expressed as N/25 mm). For each sample type, at least 10 measurements were performed to assess the reproducibility of the results.

Static contact angle measurements were performed with a First Ten Angstrom Analyzer System 32.0 mod. FTA 1000 (First Ten Angstroms, Inc., Portsmouth, VA, USA), according to the standard test method ASTM D5946. The drop volume was taken within the range where the contact angle did not change with the variation of the volume (2 ± 0.5 μL). Each reported value of the contact angle is the average of at least ten replicate measurements. The dispersion (γ_s^d) and polar (γ_s^p) components of the surface energy (SE) for all the samples were calculated according to the Owens-Wendt geometric mean equation (Owens and Wendt, 1969), using distilled water and ethylene glycol as testing liquids. According to this method, the surface energy is assumed to be composed by dispersive and polar forces. Therefore, it is necessary to measure the contact angles with at least two liquids of known surface tensions, in order to calculate the dispersive and polar part of interfacial tension between liquid and solid (Lindner et al., 2018). The SE components (mN/m) for water are: γ = 72.1, γ^d = 19.9, γ^p = 52.2, and for ethylene glycol are: γ = 48, γ^d = 29, γ^p = 19 (here γ is the total SE, and γ^d and γ^p are the dispersion and polar components, respectively) (Zonder at al., 2014).

The antimicrobial effectiveness of the films was tested against the Gram-negative bacteria E. Coli CECT 434 (ATCC 25922), selected because of its relevance in food industry. Stock culture was stored at -18 °C in Nutrient Broth (Sigma-Aldrich, Missouri, USA) with 40% Glycerol. Subcultures were grown overnight in Tryptic Soy Broth (TSB, Sigma-Aldrich) plus 0.6% Yeast Extract (YE, Sigma-Aldrich) at 37 ºC prior to each experiment.

The minimum inhibitory concentration (MIC) and the minimum bactericidal concentration (MBC) of LAE against the selected strain was determined in TSBYE. 1.2 g of LAE was diluted in 100 mL of Milli-Q water to obtain a concentration of 12000 ppm, and then serial dilutions between 80 and 4 µg/mL were made up in sterile TSBYE to study MIC and MBC.

100 µL of approximately 10^4 CFU/mL of microorganism in exponential phase was inoculated in each test tube. The tubes were incubated at 37 °C overnight, then, 100 µL from each tube was plated and incubated at 37 °C overnight (M100-S18, 2008). MIC was reported as the lowest antimicrobial concentration that inhibited the growth of the pathogen microorganism, while the MBC was defined as the lowest concentration at which no colonies growth was observed in the medium (TSBYE), and they were not culturable after plating onto Tryptic Soy Agar (TSA, Sigma-Aldrich) (Muriel-Galet et al., 2012; Higueras et al., 2013).

In vitro microbial tests on the films were performed by cutting 3 x 3 cm^2 of multilayer film samples at different LAE concentration (0%, 5%, 10% and 20%), sterilizing them by UV lamp on both sides, and placing them in a sterile tube containing 5 mL of TSBYE medium. Aliquots containing 100 µL of approximately 10^4 CFU/mL of microorganism in exponential phase were inoculated in each test tube, and incubated at 37°C and 300 rpm overnight. Depending on the turbidity of the tubes, serial dilutions with physiological saline were made and plated in Petri dishes with 20 mL TSA culture medium. Colonies visible to naked eye were counted after incubation at 37°C overnight (Paciello et al., 2013). The negative controls (i.e. films in liquid medium without E. Coli) were also prepared. Counts were performed in triplicate.

A study of the release kinetic of LAE from PLA coated films was also carried out by determining the agent concentration in distilled water, which was used as aqueous food simulant. Total immersion migration tests were performed at 23°C, by placing 10x10 cm^2 of each film sample in 50 mL of food simulant, with an area-to-volume ratio equal to 20 dm^2/L, similar to that of microbiological tests performed, and in compliance with the range established by the European Legislation (European Commission, 2011)
Water samples were taken periodically during 13 days, and LAE concentration was measured by the method described by Pezo et al. (2012), with some modifications. Briefly, the procedure is based on the formation of a ionic pair between the LAE and the organic complex $Co(SCN)_4^{2-}$, followed by a liquid-liquid extraction with 1,2-dichloroethane and by the absorbance

measurement by molecular absorption spectrophotometry. Ionic pair formation occurs according to the following equation:

$$2LAE^{+} + Co(SCN)_4^{2-} \rightarrow (LAE)_2Co\,(SCN)_4 \quad (44)$$

50 mL of the food simulant at native pH were placed in a 100-mL capacity extraction funnel, and added with 7 mL of a stock $Co(SCN)_4^{2-}$ reagent solution, prepared by mixing 23.0 g of NH_4SCN and 11 g of $Co(NO_3)_2$ in 26 mL of H_2O. Then, 10 mL of 1,2-dichloroethane as extracting solvent was added, and the mixture was vigorously hand-shaken in order to separate the two phases. After 5 minutes, the organic extract was recovered and filtered by Whatman 1 PS filters to guarantee the absence of water in the organic phase. The blue dichloroethane extract containing the complexed LAE was measured by UV-Vis spectrophotometer by using quartz cuvettes. Blank extractions of distilled water were performed, and the recovered 1,2-dichloroethane phase was used as reference in all cases. One liquid-liquid extraction was performed for each aliquot. Optimized extraction parameters (i.e. volume of reagent solution and 1,2-dichloroethane, extraction time and number of extractions) were derived from Pezo et al. Three independent aliquots were measured for each individual point.
The concentration of LAE released was determined by means of a calibration curve previously obtained by analyzing known amounts of the compound.

Water vapor permeability coefficient was measured by M7002 Water Vapor Permeation Analyzer (Systech Instruments Ltd, Oxfordshire, UK) according to the standard ASTM F 1249.

Films were tested at 23°C and 50% R.H., and the results, performed in triplicate, were expressed as P_{WV} (g m/(m^2 Pa s)), calculated as the following equation (Li et al., 2015):

$$P_{wv} = \frac{WVTR \times L}{\Delta P} \quad (45)$$

where WVTR is the water vapor transmission rate (g/m^{2}s) measured through the film, L is the average film thickness (m), and ΔP is the partial water vapor pressure difference (Pa) across the two sides of the film.

Oxygen permeability tests were performed by means of a gas permeabilimeter (GDP-C, Brugger, Munchen Germany).

The tests were carried out in triple at 23°C and 0% RH, with the oxygen flow rate of 80 mL/min (ASTM D1434).

Mechanical tensile tests were carried out according to the standard ASTM D 882-91 using the SANS (mod. CMT 4000 by MTS, China) tensile tester equipped with a 100 N load cell. Test samples were cut, along the

extrusion direction, with a rectangular geometry of 12.7x80 mm^2. The crosshead speed of the test was kept at 5 mm/min for the duration of each test.

The optical properties of the films were evaluated by measuring the UV-Visible transmittance of the films from 200 nm to 800 nm with Perkin Elmer UV-Visible Spectrophotometer Lambda 800. The transparency of the films was evaluated by measuring the Transmittance % of visible light at 550 nm, according to the ASTM D1746-03.

IV.3 Results and discussion

ATR-FTIR analyses

Possible changes in intra- and intermolecular interactions due LAE addition into the PLA matrix were explored by Fourier transform infrared spectroscopy (FT-IR), which is sensitive to the structural conformation and local molecular motions. Due to the limited penetration depth of infrared radiation into the sample in the ATR-FTIR measurement geometry, the spectra were collected on the thin PLA coating layers (namely C, C5, C10 and C20), at different percentages of antimicrobial, and compared to the spectrum of LAE, which is shown in Figure 32 (A). The absorption band at 3320 cm^{-1} corresponds mainly to the ν(N-H) stretching vibration of hydrogen bonded N-H functionalities. The double peaks at 2927 and 2850 cm^{-1} can be assigned to antisymmetric and symmetric stretching vibrations of CH_3 and CH_2 functionalities, $\nu_{as}(CH_3/CH_2)$ and $\nu_s(CH_3/CH_2)$, respectively. The small peak around 1740 cm^{-1} suggest the presence of carbonyl groups, the one at 1560 cm^{-1} corresponds to the δ(N-H) bending vibrations (amide-II) combined with ν(C–N) stretching, the peak at 1655 cm^{-1} is due to the ν(C=O) stretching vibration (amide-I), while the band situated around 1027cm^{-1} can be assigned to a ν(C–O) stretching vibration. Similar outcomes were shown by other authors (Haghighi et al., 2019).

As it is possible to observe from Figure 32 (B), (C) and (D), the PLA characteristic absorption peaks remain essentially unaltered, and the LAE characteristic absorption peaks are observable only by increasing the antimicrobial content in the coating layers. In particular, for the samples at 10% and 20% LAE (C10 and C20, respectively), the absorption bands at 2927, 2850, 1655 and 1027 cm^{-1} are detectable. The absence of changes in the intensities and positions of the major PLA and LAE bands suggests the realization of a physical mixture, with no chemical interaction between the two phases. Similar results were also reported by other authors (Gaikwad et al., 2017; Rubilar et al. 2016).

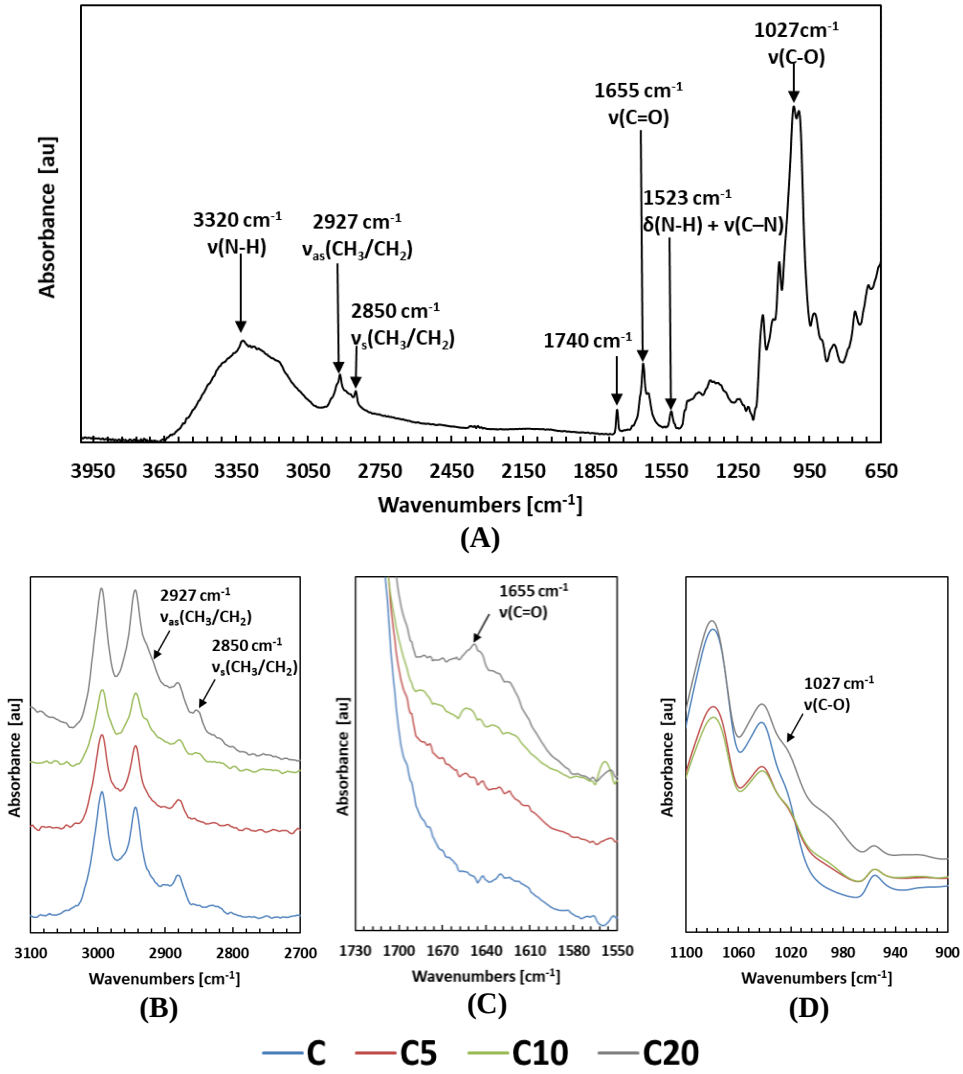

Figure 32 ATR-FTIR spectra of LAE (A) and of the thin PLA coating layers C, C5, C10 and C20, loaded at 0, 5, 10, 20% LAE, respectively (B, C, D).

Thermogravimetrical and morphological analyses

In order to evaluate the effect of LAE addition on thermal stability of the PLA matrix, thermogravimetrical analyses were conducted on only the PLA coating layers (namely C, C5, C10 and C20).

Figure 33 shows the thermogravimetric curves of PLA coating layers at different percentages of the active phase, compared with LAE powder. Table 18 shows the results of the temperature at which the maximum rate of weight loss (DTGmax) occurs.

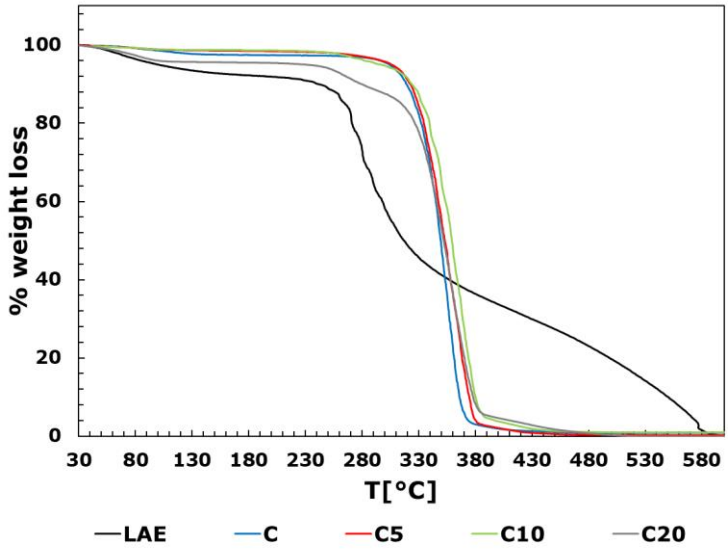

Figure 33 Thermogravimetric curves of LAE and PLA coating layers at 0, 5, 10 and 20% LAE concentration.

Table 18 Temperature at the maximum rate of weight loss (DTGmax) for LAE and PLA coating layers at 0, 5, 10 and 20% LAE concentration.

Sample Film	DTG_{max} [°C]
LAE powder	278
C	354
C5	361
C10	365
C20	266, 359

Thermal degradation of PLA coating layers occurred in a single step up to 10% LAE, and a slight increase of the thermal stability of the active coatings with respect to the neat PLA is observable from the shift of the DTG_{max} towards higher temperatures (from 354 °C to 361°C and 365 °C for

PLA, PLA + 5% LAE and PLA + 10% LAE, respectively). At larger content of antimicrobial phase, conversely, a double stage decomposition pattern occurs, with two different degradation steps at DTG_{max} equal to 266 °C and 359 °C, respectively.

The influence of added filler depends on its amount. At LAE concentration up to 10%, a protective effect on the polymer matrix prevails, as the LAE absorbs the thermal energy of the system and degrades first. At 20% LAE, instead, the antimicrobial decomposition products act as a trigger, inducing an acceleration of the polymer degradation mechanisms.

Similar outcomes were also found in literature, in which the protective effect of fillers, both organic and inorganic, on the thermal stability of PLA was investigated (Liu et al., 2014; Abdullah et al., 2019; Yee et al., 2016; Vidovic et al., 2016). In particular, it has been emphasized the role of the concentration, the size, the distribution and the intrinsic characteristics of the filler in the increase of thermal stability of polylactide composites (Vidovic et al., 2016).

As it is known, the microstructural properties of composite films depend on the compatibility between all the film components, affecting the final physical, mechanical, barrier and optical properties (Attaran et al., 2015). To this aim, the distribution of the active phase inside the PLA matrix and the quality of the interlayer adhesion were investigated through SEM analyses.

Figure 34 (A) and (B) show the cross-section micrographs of SC and SC10 films, respectively, taken as an example.

Images analyses display the PLA coating layer, in which few small voids are recognizable due to solvent evaporation, over the BOPET substrate, characterized by an oriented morphology. The absence of visible LAE powder domains inside the coating layer highlights the good dispersion and homogeneous distribution of the antimicrobial into the polymer matrix.

The absence of voids in the cross sectional area of the investigated films pointed out the good adhesion of the coating layers on the substrate.

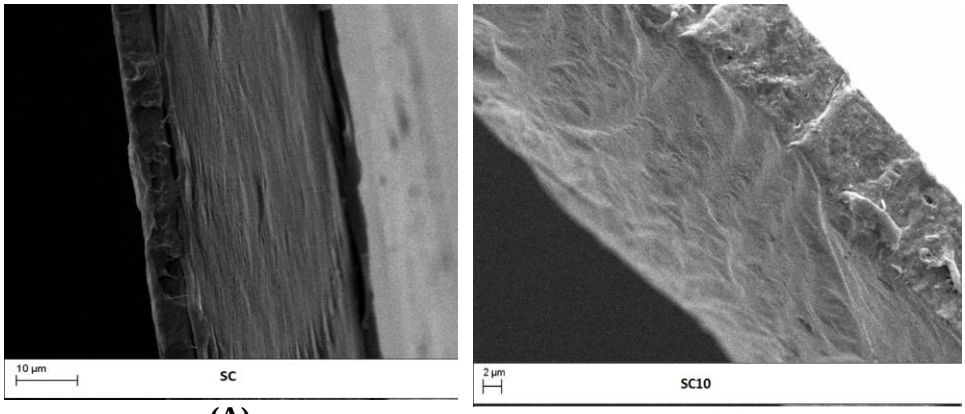

(A) **(B)**

Figure 34 Cross-sectional SEM micrographs of: (A) SC and (B) SC10 films.

Evaluation of adhesion strength and surface wettability

To determine the adhesion strength, delamination tests were performed as described in the methods section. The delamination occurred by separating the coating, thermally sealed at the defined temperature, by means of a tensile tester. The bonding strength, reported in Table 19, represents the force required to delaminate the PLA coating from the web.

Table 19 Bonding strenght (N/25mm), static water CAw) and ethylene glycol (CA_{EG}) contact angles, and dispersion (γ_s^d) and polar (γ_s^p) components of the surface energy for the neat PET substrate film (S) and for the SC coated films at 0, 5, 10 and 20% LAE concentration.

Sample Film	Bonding Strenght [N/25mm]	CA_w [°]	CA_{EG} [°]	γ_s^d [dyne/cm]	γ_s^p [dyne/cm]
S	Not sealable	65.3 ± 2.8	39.5 ± 0.9	18.8	19.3
SC	3.20 ± 0.4	65.8 ± 1.0	54.3 ± 1.3	7.4	28.6
SC5	3.12 ± 0.3	55.9 ± 1.1	43.1 ± 1.2	7.9	36.5
SC10	3.10 ± 0.8	54.2 ± 1.3	41.3 ± 1.1	7.9	38.1
SC20	2.56 ± 0.3	46.4 ± 2.2	40.5 ± 1.3	4.2	51.4

The results show that the adhesion strength of the PLA coating layers was not significantly affected by the antimicrobial addition up to LAE concentrations equal to 10% (SC10 sample), whereas a decrease in the bonding strength for the SC20 film, equal to 2.56 ± 0.35 N/25mm, was observed.

The adhesion strength strictly depends on the amount of polar and dispersion bonds between the substrate film and the coating (Lindner et al., 2017).

To this aim, the polar (γ_s^p) and dispersion (γ_s^d) components of the surface energy were calculated from water and ethylene glycol static contact angle measurements, as described in the "Materials and Methods" section of this chapter, and displayed in Table 19.

The adhesion force is optimal when the γ_s^p and γ_s^d values are of the same order of magnitude, and maximum when their ratio is close to unity. When the difference between the γ_s^p and γ_s^d values is more pronounced, as in the case of SC20 sample, where it is of one order of magnitude, a significant drop in bonding strength is observable, which however remains acceptable for the film application in food packaging.

Antimicrobial activity and release kinetics of the active bio-coated films with LAE

The antimicrobial efficiency of LAE incorporated materials is mainly based on the effective release of the compound into the food (Muriel-Galet et al., 2013). Moreover, in the real packaging applications, the different layout of systems can determine differences in the mass transport of the active agent. Therefore, it is necessary to study in depth the release kinetics and the antimicrobial activity of the active multilayer films in real geometry and application conditions.

The antimicrobial activity of the multilayer films against *E. Coli* growth was then determined by the liquid medium method described in the previous section.

In first analysis, the MIC and the MBC for LAE were evaluated. The corresponding values are reported in Table 20, and are equal to 51 and 63 ppm, respectively. These values, different from previous results reported in the literature, highlight the influence of medium composition, of the method used (in terms of incubation time, inoculum concentration, temperature), as well as of the strain used, in the quantification of the activity of the antimicrobial agent (Muriel-Galet et al., 2012).

Afterwards, the microbiological tests were conducted on the SC samples, at different LAE concentrations (0, 5, 10 and 20%) and with exposed surface area equal to 6.25 cm^2. The results are reported in Table 20, and are expressed as logarithm of colony forming units (Log(CFU)) and log

reduction value (LRV). Data regarding the control sample are also reported as reference.

Table 20 Minimum inhibitory concentration (MIC) and minimum bactericidal concentration (MBC) of LAE against E. Coli, and antimicrobial activity for the SC coated films at 0, 5, 10 and 20% LAE concentration., expressed as logarithm of colony forming units (Log(CFU)) and log reduction value (LRV).

Sample	*Escherichia Coli CECT 434*			
	MIC [ppm]	**MBC [ppm]**	**Log(CFU)**	**LRV**
LAE	51	63	-	-
Control	-	-	10.96 ± 0.69	-
SC	-	-	10.88 ± 1.22	0
SC5	-	-	5.79 ± 0.60	5.17
SC10	-	-	Total inhibition	
SC20	-	-	Total inhibition	

To further demonstrate this, Figure 35 shows the pictures of the tested tubes after incubation at 37°C overnight, in comparison with the control sample.

To better investigate the agent migration mechanism, a characterization of the release from the PLA coatings into water (used as food simulant) was also carried out at room temperature (23 ± 1°C), according to the procedure described above in the experimental section.

Figure 36 and Figure 37 show the results of the release test of SC, SC5, SC10 and SC20 films, expressed both as concentration of LAE released (g/L) and as the ratio between the amount of LAE released at time t and that obtained at equilibrium (M_t/M_∞), respectively.

Since the main interest is to evaluate the release of LAE for a time compatible with the duration of a packaged food product, the analyses were conducted starting from a minimum time of 3 hours, up to a maximum of 13 days of observation.

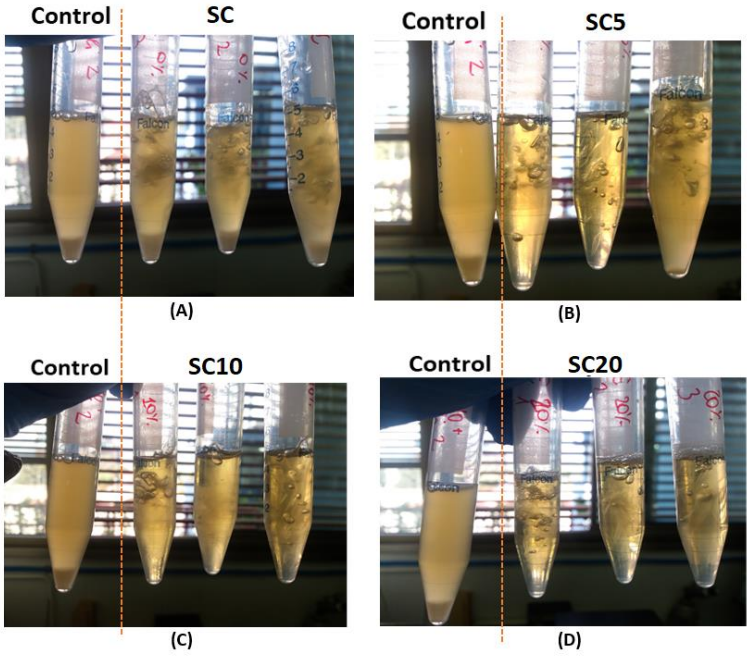

Figure 35 Images of the tested safe-lock tubes inoculated with E.Coli and containing multilayer BOPET/PLA films produced at different concentration of active phase: 0% LAE (A), 5% LAE (B), 10% LAE (C) and 20% LAE (D), after incubation at 37°C overnight, in comparison with the control sample.

As can be seen from Figure 36, the SC film shows no significant LAE release over time, whereas all the active films exhibit similar migration profiles, with an initial "burst effect" due to the rapid migration of LAE, localized on the coating surface, in the aqueous medium.

After 3 hours, the concentration of antimicrobial released is equal to 0.25 g/L, 0.33 g/L and 0.62 g/L for the SC5, SC10 and SC20 films, respectively, with a percentage of LAE released between 71% and 85% of the total.

A release between 70% and 90% of the active phase for times shorter than 200 minutes has also been reported by other authors (Higueras et al., 2013; Muriel-Galet et al., 2014), in similar release conditions (temperature, release medium) but with more hydrophilic polymeric matrices. Several factors influence the release of low molecular weight substances from a solid polymer matrix inside a simulant solution: the polymer morphology, the molecular weight distribution, the polymer-active interactions, the polarity, the temperature, as well as the antimicrobial solubility within the release solution and its distribution within the polymer matrix. Therefore, the

reported outcomes could suggest that the high solubility of the migrant in water plays a crucial role in the release of the antimicrobial at short times, also facilitated by the LAE dispersion in a layer of such reduced thickness as the coating.

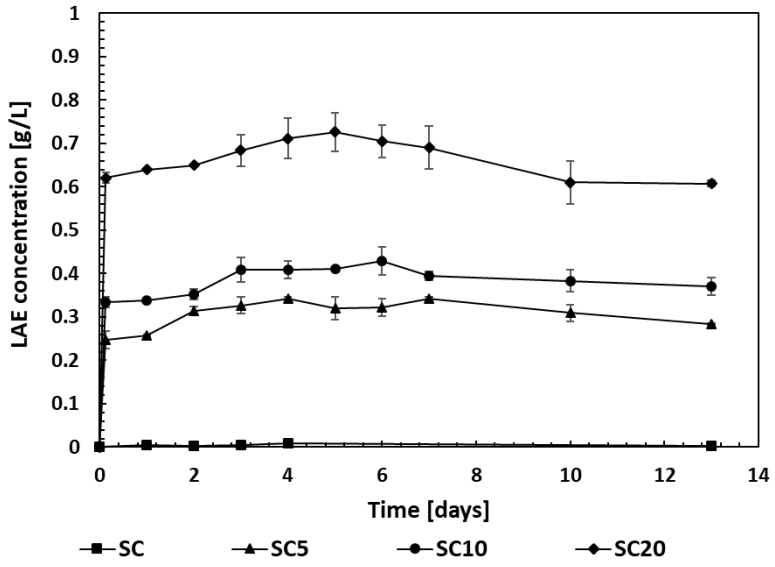

Figure 36 Migration kinetics of LAE from coated films SC, SC5, SC10 and SC20 to distilled water, at 23°C.

After the initial burst release, there is a decrease in the release rate, meaning a slow diffusion path through the high molecular weight polymer matrix. Hence, the antimicrobial compound is desorbed in water following a much slower release kinetic, advancing towards full migration, up to reach a maximum concentration of LAE released equal to 0.34 g/L after 4 days, 0.43 g/L after 6 days and 0.73 g/L after 5 days for the films loaded at 5%, 10% and 20% LAE, respectively.

The extent of LAE release into the food simulant at equilibrium can be characterized by the partition coefficient K, defined as the ratio between the compound concentrations in the polymeric phase and in the food phase (Muriel-Galet, 2013). An indication of the release approaching full migration, that is, K approaching to zero, are the intermingled values of the antimicrobial release rate (M_t/M_∞) observed in Figure 18 for SC5, SC10 and SC20 samples at t > 2 days, highlighting comparable release kinetics for all the investigated samples.

The minimum LAE concentration analyzed, i.e. that released by the SC5 film after 3 hours, is already higher than the results reported in the literature by other authors (Higueras et al., 2013) and higher than the MIC and MBC reported above.

From a practical point of view, the films are able to immediately release an antimicrobial amount sufficient to inhibit a pathogenic microbial load already at the lowest LAE concentration incorporated within the polymer matrix. In addition, the measurements carried out even at longer times show that a high concentration of LAE still remains within the simulant after several days, when the protection is really necessary. Consequently, the obtained results make the developed LAE active films an attractive and efficient solution for antimicrobial protection of high water content packaged foods.

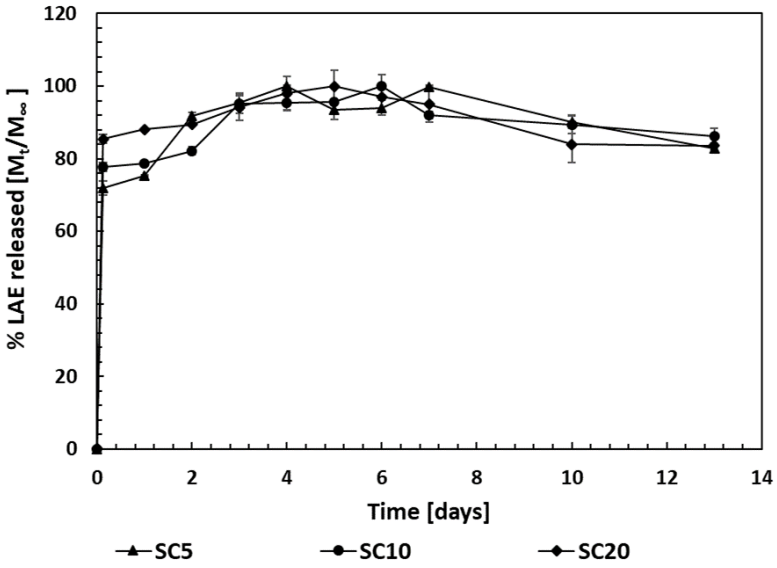

Figure 37 Antimicrobial release rate (M_t/M_∞) from coated films SC, SC5, SC10 and SC20 to distilled water, at 23°C.

Evaluation of barrier, tensile and optical properties

In order to better investigate the effects of the systems composition on the functional performance of the samples, oxygen and water vapor permeability analyses, mechanical tests and optical measurements were carried out.

Outcomes are reported in Table 21 in terms of oxygen permeability P_{O2}, water vapor permeability P_{WV}, elastic modulus E, stress at break σ_b, strain at break ε_b and transmittance percentage T_{550} %.

All the coated films (SC), with respect to the PET substrate (S), show an increase in the oxygen and water vapor permeability values. However, this is mainly due to the normalization over the total thickness of the films, in which the amorphous PLA layer does not offer any resistance to the transport of oxygen and water molecules and is inherently fragile with scarce tensile properties (Robertson, 2013).

Table 21 Oxygen (P_{O2}) and water vapour permeability (P_{WV}), elastic modulus E, tensile properties at break (stress σ_b and strain ε_b) and UV-Vis transmittance at 550 nm (T_{550} %) for the neat PET substrate (S) and for the SC coated films at 0, 5, 10 and 20% LAE concentration.

Sample Film	P_{O2} $[\frac{cm^3 mm}{m^2 d\ bar}]$	$P_{WV} \cdot 10^{13}$ $[\frac{g\ m}{m^2 d\ Pa}]$	E [MPa]	σb [MPa]	εb [%]	T_{550} (%)
S	1.6 ± 0.3	7.4 ± 0.1	4149 ± 150	115 ± 19.3	36.7 ± 9.3	84.3
SC	2.2 ± 0.1	11.1 ± 0.4	3822 ± 376	38.5 ± 12.3	38.5 ± 12.3	84.3
SC5	2.4 ± 0.1	11.2 ± 0.2	3808 ± 224	36.3 ± 12.9	36.3 ± 10.8	73.2
SC10	2.6 ± 0.7	11.4 ± 0.2	3689 ± 222	34.3 ± 3.07	35.3 ± 13.2	69.1
SC20	3.1 ± 0.4	12.5 ± 1.2	3663 ± 213	33.3 ± 22.0	35.9 ± 3.78	60.1

This leads to an apparent worsening of the functional performance, but actually the films maintain the properties of the uncoated PET, and the further LAE keeps them essentially unaltered, with only slight further decrease of barrier and tensile properties observable at the highest LAE content, i.e. in the SC20 sample.

In packaging applications, the transmission of visible and ultraviolet light are important parameters to preserve and protect food products until they

reach the consumer, as well as to get an attractive transparent package. To evaluate the transparency of samples, UV-Vis measurements were carried out. PET and PLA are known to have excellent optical properties, in this sense the LAE effect on transparency was investigated. In UV-Vis spectra reported in Figure 38, the transmittance percentage T% is reported as a function of wavelength for the neat substrate (S) the coated SC films at different content of the active phase. The transparency of the multilayer films, defined as the transparency of visible light in short range of 540-560 nm, was therefore evaluated measuring the transmission at 550 nm (T_{550} %), and the values for the investigated samples are reported in Table 21.

The PLA coating did not affect the transparency of the PET substrate, which remains the highest, with a T_{550} % value equal to 84.3 % in both films. The further LAE addition to the polymer matrix determines a slight decrease in the transmittance at 550 nm, which becomes more significant at LAE concentration equal to 20% (T_{550} % of SC20 equal to 60.1%). In this latter case, the increase in film cloudiness, with respect to the SC, SC5 and SC10 samples, is also visible in Figure 39.

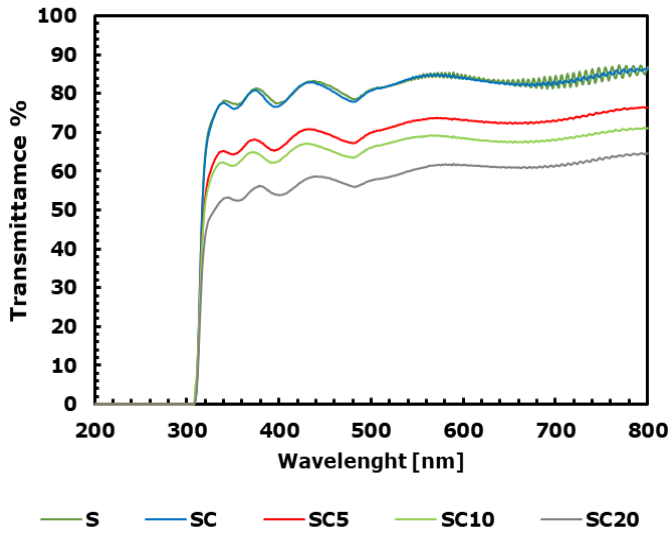

Figure 38 UV-Vis transmission spectra of the neat PET substrate film (S) and for the SC coated films at 0, 5, 10 and 20% LAE concentration.

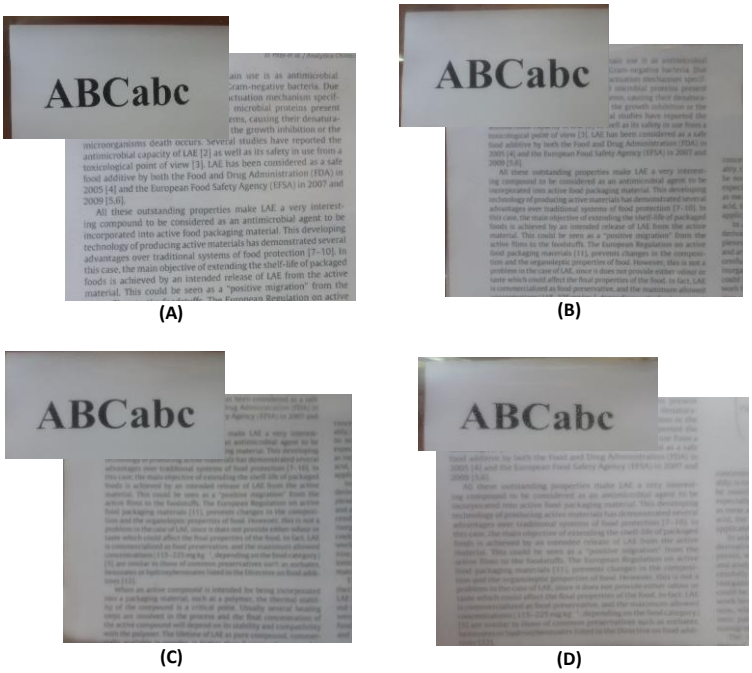

Figure 39 Pictures of the SC coated films at different concentration of active agent: 0% LAE (A), 5% LAE (B), 10% LAE (C) and 20% LAE (D).

IV.4 Summary and conclusions

In this part of the research, innovative multifunctional and eco-sustainable antimicrobial packaging solutions have been successfully developed, through a conventional technique commonly applied in packaging industry. The produced films combine the structural and barrier performance of PET with the PLA sealing capacity and the LAE antimicrobial activity.

The chemical, physical and functional analyses carried out on the active multilayer films showed the good dispersion and homogeneous distribution of LAE into the polymer matrix, as well as the good adhesion of the coating layer on the substrate. Moreover, LAE addition did not modify the macromolecular structure of PLA.

Films were found able to release the antimicrobial agent when exposed to highly humid media. Microbiological tests pointed out the effectiveness of the produced systems in releasing the antimicrobial agent and inhibiting microbial growth. In particular, the inhibition of microbial strain was found proportional to the LAE concentration into the PLA matrix, with 5.17 log

decrease of viable counts at 5% LAE and total inhibition measured for coating formulations at higher LAE content. This antimicrobial activity is comparable with or higher than currently commercially available antimicrobial packaging solutions for foods and pharmaceuticals.

The migration kinetics have proved that the films are able to immediately release an antimicrobial amount sufficient to inhibit a microbial load already at the lowest LAE concentration within the polymer matrix, and a sustained release is reached for a period of at least 6 days.

Furthermore, by increasing the LAE concentration up to 10%, a slight increase of the thermal stability of the PLA matrix was obtained. The functional performance of the films, in terms of adhesion, barrier, tensile and optical properties, were not significantly affected. On the other hand, increasing LAE content at 20%, a slight worsening of the PET film functionalities was observed. On the basis of these results, the 10% LAE configuration produced the best performance in terms of total microbial inhibition, delivery time and functional properties.

The results obtained make the developed LAE active films an attractive and efficient solution for antimicrobial packaging, and the shelf life of numerous foodstuffs could be significantly improved. To this extent, shelf life tests on poultry minced meat are currently ongoing to test the effectiveness of the active films in extending the shelf life of meat-based food products, as part of future work related to the thesis project.

Section III

Antioxidant films with natural extracts from valorization of olive industry wastes: PET functionalization by high performance bio-coatings and development of 100% biodegradable structures

Chapter V - *Development of high performance, eco-sustainable antioxidant films, based on Whey Protein Isolate coatings with natural extracts from olive pomace*

Chapter VI - *Development of 100% biodegradable antioxidant films, based on Poly(lactic acid) coatings and natural extracts from olive milling wastewaters*

Chapter V

Development of high performance, eco-sustainable antioxidant films, based on Whey Protein Isolate coatings with natural extracts from olive pomace

V.1 Introduction

In this chapter, the PhD research aimed at exploring new possibilities to develop eco-sustainable active PET coatings, through the valorization of natural bioactive compounds deriving from food industry wastes. Innovative routes were investigated for the revaluation of olive pomace extract (OPE) in high barrier, whey protein isolate (WPI) antioxidant coatings.

As stated in Chapter I, the incorporation of natural antioxidants represents an innovative approach for the development of antioxidant packaging, through the use of plant and fruits extracts, rich in nutritive properties (Adiletta et al., 2015), or essential oils derived from herbs or spices, which can be successfully applied if food sector, as well as in pharmaceuticals, nutritionals or cosmetics uses (Sillero et al., 2018).

Recent innovative research has focused on the extraction of these bioactive compounds directly from industrial organic waste streams, seeking to enter the circular economy concept, and a growing interest is dedicated to the use of antioxidant extracts from olive oil industry wastes.

The olive oil industry produces a large quantity of waste and by-products, such as pomace, vegetation waters and leaves. These products are rich in phenolic compounds, including oleuropein, luteolin, tyrosol, hydroxytyrosol,

verbascoside, capable to interfere with the oxidation of lipids and other molecules by rapid donation of a hydrogen atom to radicals (Ajila et al. 2010), thus showing a strong antioxidant activity which makes them very attractive for the active packaging industry.

Olive pomace (OP) is one of the major olive oil processing byproducts, reaching 2,881,500 tonnes/year worldwide (Ravindran & Jaiswal, 2016). It is an heterogeneous biomass composed by polysaccharides, proteins, fatty acids, pigments and polyphenols (Mirabella et al., 2014).

In order to eliminate its harmful impact in environment, OP is usually disposed of by combustion. However, this method can be considered a waste reduction strategy and not a recovery of valuable components. Recent studies aimed at recovering polyphenols and proteins using different extraction methodologies, such as pulsed electric fields, high voltage electrical discharges, and ultrasound-assisted extraction (Rubio-Senent et al., 2015). The recovery of tocopherols and squalene from olive pomace using supercritical fluid extraction has also been studied (Roselló-Soto et al., 2015). OP is extraordinary rich in polyphenols, especially hydroxytyrosol, but also have a significant content in oleuropein, tyrosol, caffeic acid, *p*-coumaric acid, vanillic acid, verbascoside, elenolic acid, catechol, and rutin. Therefore, it is a promising source of antioxidants that have potential uses not only in the food industry, but also, for instance, in pharmaceutical areas.

Another by-product showing very promising properties for food packaging applications is the whey protein, derived from cheese-production.

Whey protein is currently underused, as only 50% of the accruing cheese-whey is treated and transformed into different food and feed products, while the 25% of the whey produced is disposed as waste (Schmid et al., 2014).

Therefore, whey protein is a readily available and economically interesting raw material, representing a promising alternative for the development of bio-plastics from waste streams not competing with food usage as other biodegradable polymers (Guillard et al., 2018). Whey application as a barrier film is particularly interesting: various studies have shown that whey protein has high potential for enhancing the aroma, fat, water vapour and oxygen barrier, with superior barrier properties compared to other bioplastics and approached those of synthetic barrier layers, such as ethylene vinyl alcohol (EVOH) (Cinelli et al., 2014).

All these consideration inspired the aim of this part of the PhD work, which deals with the design, realization and verification of the effectiveness of high performance, bio-active coatings, on PET substrate, with antioxidant properties, based on raw materials deriving from food industry by-products.

Figure 40 shows the flow diagram of the experimental set-up and of the activities carried out in this part of the PhD work, which will be discussed in this chapter.

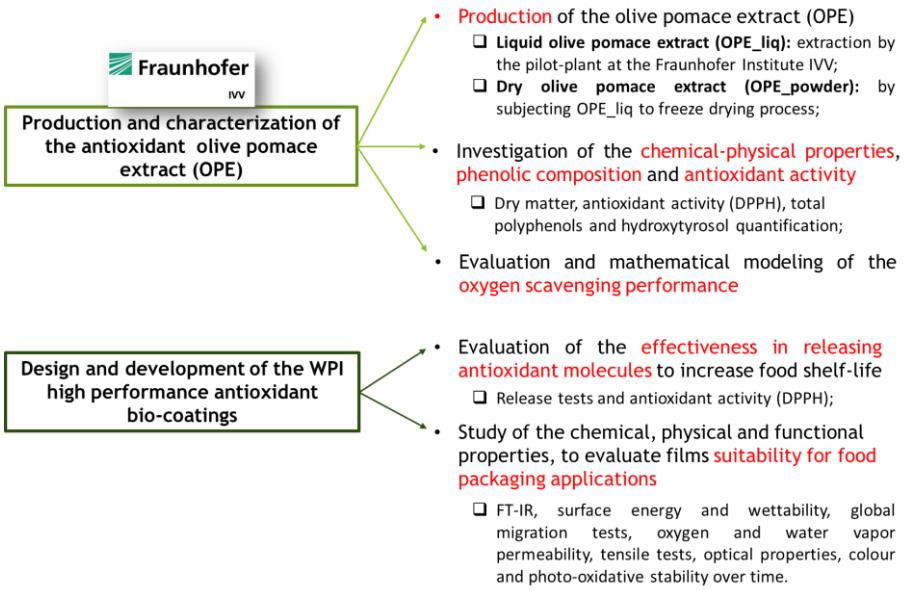

Figure 40 Experimental set up and activities discussed in Chapter V.

The first part of the activities, involving the production of the olive pomace extract (OPE), the chemical-physical characterization and the evaluation and modelling of the oxygen scavenging properties, was carried out during the six-months internship at the Fraunhofer Institute for Processing Engineering and Packaging (IVV) in Munich. The activities were also part of the EU Horizon2020 Project AgriMax- "Agri & food waste valorization co-ops based on flexible multi-feedstocks biorefinery processing technologies for new high added value applications".

The study of the antioxidant and O_2-scavenging potential provided basic knowledge for tailor-made packaging design. A second-order mathematical model was then applied to describe the oxidation-kinetics of polyphenols, and the modeling parameters were determined.

Active bio-coatings were realized by incorporating the OPE at different percentages (ranging from 0 to 10%) of the active phase into a biodegradable Whey Protein Isolate (WPI) coating, spread on a corona-treated PET substrate. This created a functionalized PET with a bio-based material, easily removable by washing, and to preserve its intrinsic excellent properties without losing recyclability.

Release tests in a selected food simulant and DPPH radical scavenging measurements were carried out to investigate the effectiveness of the produced systems as antioxidant carriers, as potential new packaging for

extending O_2-sensitive foods shelf-life. The effect of the films configuration on the mass diffusive transport was evaluated, and the different polymer/antioxidant/food simulant interactions were evaluated.

The films were also characterized by infrared spectroscopy, to evaluate possible chemical interactions of the active phase with the polymer matrix.

The barrier, tensile, optical and surface properties of the produced systems were then evaluated, in order assess possible effects of OPE on the functional performance, surface wettability and inter-layer adhesion of the films.

Finally, global migration analyses were performed to assess the films compliance with European regulation on food contact applications, and the foto-oxidative stability of the films under natural light exposure was also evaluated over time.

V.2 Materials and Methods

Materials

The olive pomace was gently supplied by a Spanish farming company, partner of the AgriMax project. Whey Protein Isolate (WPI) powder was supplied by BiProDavisco Foods International Inc. (Le Suer, MN, USA). Commercial biaxially oriented poly ethylene terephthalate (PET) film (Nuroll S.p.a, Italy), with 23 μm thickness and corona treated surface, was used as substrate. Glycerol, DPPH (2,2-diphenyl-1-picrylhydrazyl), Trolox (6-Hydroxy-2,5,7,8-tetramethylchromane-2-carboxylic acid) and Folin-Ciocolteau reagents were obtained from Sigma Chemical Co. (St. Louis, Mo., USA). All organic solvents used were analytical grade.

Olive Pomace Extract Preparation

The olive pomace extract was produced on the extraction pilot-plant located at the Fraunhofer Institute. The dried olive pomace was loaded in a 300L vessel, equipped with a water jacket for the temperature control and a MIG (multi-stage pulse counter-current) stirrer. It was used water as extracting solvent, to maximize the extraction of antioxidant polar compounds such as hydroxytyrosol and tyrosol, with a solid to liquid ratio equal to 1:8. The temperature was adjusted to 80°C. The mixture was continuously stirred for 90 minutes after reaching the extracting temperature.

After stopping stirring, the slurry was transferred to a buffer tank and decanted to remove large solids, then concentrated by means of a rotary evaporator, with a concentration percentage of 60.6%. The scheme of the extract production is reported in Figure 41.

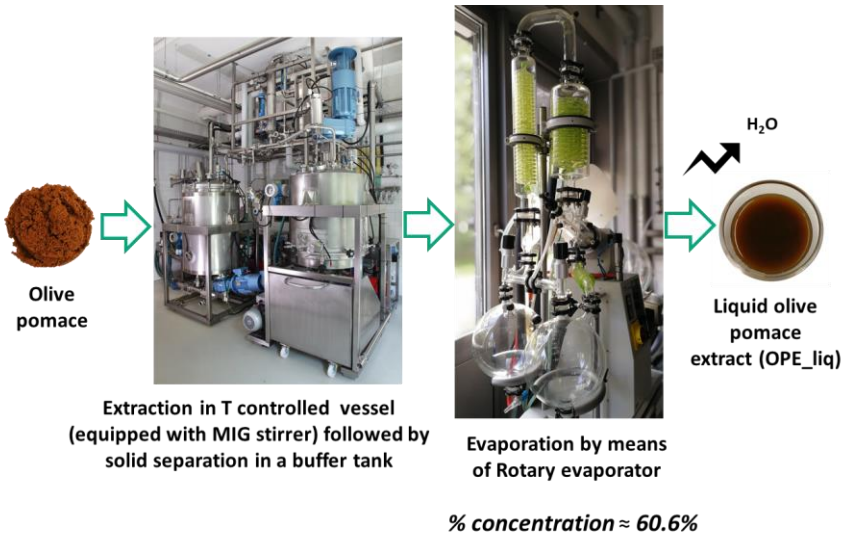

Figure 41 Scheme of the pilot-plant scale extraction.

The liquid olive pomace extract (OPE_liq) was eventually subjected to freeze drying process (Figure 42), in order to obtain a freeze dried powder, according to the following processing parameters:

temperature condenser = -56°C; temperature heating plate = from 5°C up to 30°C; time = 3 days; vacuum pressure = 1.03 mbar.

Both the liquid and the freeze dried extracts were stored under nitrogen in -18°C cold chamber prior to use.

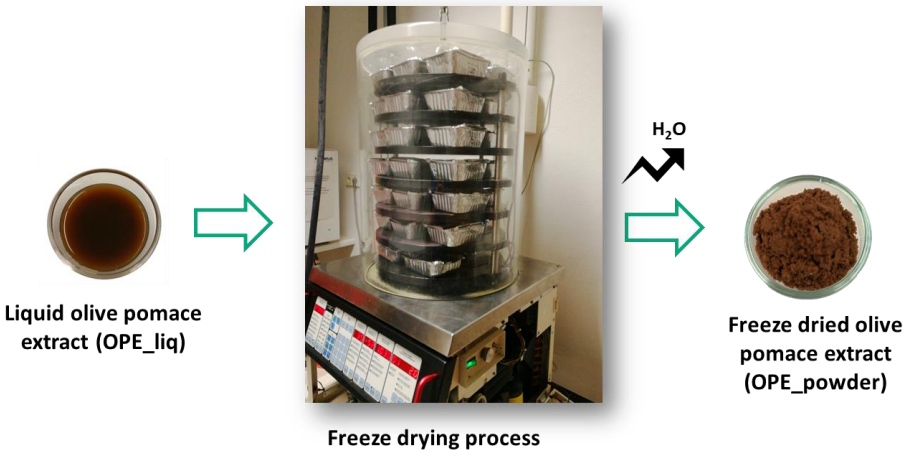

Figure 42 Scheme of the freeze drying process.

Olive Pomace Extract Characterization

The OPE_liq was characterized in terms of dry matter, antioxidant activity, total polyphenols and hydroxytyrosol quantification.

The dry matter content was determined by means of Sartorius Moisture Analyzer MA100 (Sartorius AG, Göttingen, Germany).

The total phenols (TP) were quantified using Folin–Ciocalteu assay. The olive extract was centrifuged at 5000×g for 10 min and an aliquot equal to 20 µL was mixed with the Folin–Ciocalteu reagent in sodium carbonate solution (20% w/v), and stored in the dark for 30 min. The absorbance was read at 765 nm using a UV–Vis spectrophotometer (Lambda Bio 40, Perkin Elmer, Waltham, MA, USA). Calibration curve, with a concentration range between 0.1 and 1 g of gallic acid/L, was used for the quantification of TP. The results were expressed as mg of gallic acid equivalents per grams of dry matter (mg GAE/g of dry matter).

HPLC analyses for the identification and quantification of hydroxytyrosol were carried out by using a Hewlett Packard (Palo Alto, CA, USA) HP1100 series instrument, fitted with a HP1100 series variable wavelength detector Or Agilent DAD detector, and equipped with an HPLC column: 5 µ ACE 5 C18 column (25 cm× 4.6 mm ID; Apex Scientific, Ireland). The set program was: Temp: 22ºC: Flow rate 1 mL/min; Sample injection volume: 20 µL; Mobile phase: A) 0.1% phosphoric acid and B) methanol; Wavelength: 278 nm (absorption wavelength for hydroxytyrosol). The samples were dissolved in water. The ratio of phosphoric acid to methanol was set at a gradient of 90:10 for the first 10 min and then increasing to 62.4:37.6 in next 10 min and maintaining at this ratio for another 5 min. The hydroytyrosol was quantified by means of a standard calibration curve.

The antioxidant activity was analyzed using the stable radical 2,2-diphenyl-1-picrylhydrazyl (DPPH). 50 µL of extract was mixed with 1.95 mL of ethanolic solution of DPPH (6×10^{-5} M) in a capped cuvette. The mixture was shaken vigorously at room temperature and allowed to stand at room temperature in the dark for 20 min. The absorbance of the solution was measured at 517 nm with a UV–Vis spectrophotometer (Lambda Bio 40, Perkin Elmer, Waltham, MA, USA). The blank was conducted using distilled water instead of the sample. All analyses were performed in triplicate, and the obtained values were expressed as millimoles of Trolox equivalents (mmolTrolox/g dry matter), based on a standard curve of Trolox (6-Hydroxy-2,5,7,8-tetramethylchromane-2-carboxylic acid).

The absorption of oxygen by both liquid and powder OPE was measured in hermetically closed stainless-steel cells with a free headspace volume of 112 cm^3, as shown in Figure 43 (A) and (B)). Petri dishes containing 5 mL of OPE_liq or 0.675 g of OPE_powder, calculated on the equivalent dry matter content of the liquid extract, were placed in the cells hermetically closed with a glass lid and sealed with a viton O-ring.

A preliminary pasteurization treatment at 85°C for 10 minutes was conducted on OPE_liq samples, then 0.05% w/w of NaN_3 was added to both OPE_liq and OPE_powder, in order to avoid O_2-consuption interference due to microbial proliferation during the measurements. The addition of NaN_3 did not affect the pH of the samples.

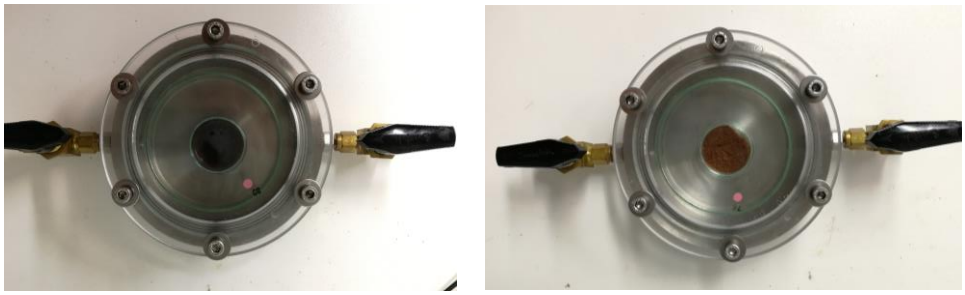

(A) (B)

Figure 43 Experimental setup for oxygen absorption measurements of OPE_liq (A) and OPE_powder (B).

The O_2 uptake from the headspace (initial gas atmosphere: air) was monitored for 50 days at 23°C using Fibox 4 Trace (PreSens Precision Sensing GmbH, Regensburg, Germany). An optical sensor spot (PSt3) was placed inside the cell at the glass top, as shown in Figure 43.

The p_{ox} absorption data in hPa were converted to concentrations C_{ox} using the ideal gas law:

$$C_{ox} = \frac{n_{ox}}{V_{HS}} = \frac{p_{ox}}{RT} \quad (46)$$

Where n_{ox} is the amount of substance of O_2, V_{HS} is the headspace volume of the cell, R =8.314 J/(mol K) is the ideal gas constant, and T is the temperature in Kelvin.

The effect of the pH and of the relative humidity on the oxygen scavenging phenomenon was investigated. In particular, measurements were carried out on OPE_liq at pH native (i.e. 6.5), 8, 10, 12, respectively, by adjusting it with NaOH 1M solution. On OPE_powder, tests were performed on 55% RH and 100% RH.

Each experiment was carried out at least four times and the results are presented as the arithmetic mean with standard deviations.

The mean square deviation for each experimental condition was then calculated as follows:

$$MSE_{exp} = \sqrt{\frac{1}{N}\sum_{i=1}^{m}\sum_{l=1}^{q}([O2]_{exp} - [O2]_{\text{mean}})^2} \quad (47)$$

where N is the total number of observations, m is the number of parallel experiments, q the number of observations in one experiment, $[O2]_{exp}$ the observed oxygen concentration and $[O2]_{mean}$ the arithmetic mean of all *m* observations for each *l*.

Modeling of the oxidation kinetics of the olive pomace extract

For the mathematical model description, the following overall reaction was assumed, by following the approach used by Pant et al., 2018:

$$OPE + \nu O2 \longrightarrow OPE_{ox} \quad (48)$$

where OPE represents all non-oxidized species, ν is the stoichiometric factor and OPE_{ox} accounts for the various reaction products. In this approach, the oxygen reaction was assumed to be irreversible.

The kinetic law of this reaction was approximated as a second-order elementary reaction, and the reaction rate *r* was expressed as shown:

$$r = k * [OPE] * [O2] \quad (49)$$

Here, the reaction rate depends on the concentration of both reactants, $[OPE]$ and $[O2]$, and k is the reaction rate coefficient.

The net consumption rates of OPE and O_2 can be described with a system of ordinary differential equations (ODEs), as shown in Equations (50) and (51):

$$\frac{d[OPE]}{dt} = -k * [OPE] * [O2] \quad (50)$$

$$\frac{d[O2]}{dt} = -\nu * k * [OPE] * [O2] \quad (51)$$

The ODE system given in Equations (50) and (51) was solved in MATLAB R2014a (The MathWorks, Inc., Natick, MA, USA) using the multistep solver *ode15s* with the default tolerances AbsTol = 10^{-6} and RelTol =10^{-3}.

The model was fitted to the experimental data to determine the kinetic parameters k and n. The fit was optimized based on the minimization of the sum of squared residuals (SSQ):

$$SSQ = \sum_{i=1}^{m}\sum_{l=1}^{q}([O2]_{sim} - [O2]_{\mathbf{exp}})^2 \quad (52)$$

where *m* is the number of parallel experiments, *q* the number of observations in one experiment, and $[O2]_{sim}$ and $[O2]_{exp}$ the predicted and the observed O_2 concentrations, respectively.

For the minimization of the SSQ objective function, the MATLAB function *fminsearch* was used. The function a simple and widely used algorithm for local optimization, and it is based on the Nelder-Mead downhill-simplex algorithm, as described by Pant et al. (2018).

The stoichiometric coefficient *n* is a measure for the O_2 absorption capacity and gives the number of absorbed molecules O_2 per molecule of OTE. Therefore, n must not be negative. The reaction rate coefficient k, by definition, must also not be negative. The termination tolerance of the function value was 10^{-4} and the lower bound on the size of a step was 10^{-4} (MATLAB default settings). The optimization terminates when both stopping criteria are fulfilled.

Since the downhill-simplex optimization is known to be sensitive to the chosen starting values, the initial k and n values were varied systematically in equidistant steps over the whole parameter space so that in total 231 different combinations of k and n were tested. For all optimization results, the root mean square error (RMSE) was calculated as a measure of the goodness of fit:

$$RMSE = \sqrt{\frac{SSQ}{N-p}} \quad (52)$$

where N is the total number of experimental observations and p the number of fitted parameters.

Realization of the active biodegradable coatings

The active bio-coatings coatings were realized on a PET substrate by precipitation, induced by solvent evaporation, of a Whey Protein Isolate (WPI, BiPro, Davisco Foods International) aqueous solution (with mass ratio 10:90), incorporated with 5 and 10 wt%, based on the protein content, of the freeze dried olive pomace extract (OPE_powder).

Ten percent of WPI was added to deionized water and stirred in a cold bath for 30 minutes; then, it was heated up to 90°C for 30 minutes, in order to guarantee protein denaturation. This temperature is above the denaturation temperature of β-lactoglobulin (75-80°C), α-lactoalbumin (70-90°C) and bovine serum albumin (about 60°C), facilitating the formation of intermolecular disulphide bonds.

During denaturation, the reactive units (i.e. the amino groups of the protein's lysine and glutamine units) are exposed, and their steric accessibility increases. In aqueous solutions, these amino acids are able to form intramolecular and intermolecular links by chemical and physical interactions (van der Waals forces, hydrogen bonds, electrostatic and hydrophobic interactions). The result is a crosslinked structure (Schmid et al., 2014).

In particular, the denaturation of proteins makes them insoluble in water and, depending on the heat load applied, is divided into two different processes: unfolding and aggregation (DeWit and Klarenbeek, 1984). During the first heating, the protein molecules unfold and some of the inner structures interact with those of other molecules. In this step only non-covalent interactions are involved and, if the proteins are cooled down, the structures could return to their original states. In order to obtain non-reversible intermolecular bonding, a further heating is needed, inducing aggregation and bridging reactions into insoluble clumps (Cinelli et al., 2016).

The mixture was then cooled down to 50°C, and 6.7% w/w_{WPI} of glycerol was added as plasticizer. External plasticizers addition is fundamental to avoid excessive brittleness of WPI films, due to the large amount of chain interactions involved.

The OPE_powder was also added in this step, and first trials were carried out adding from 0% up to 20% w/w_{WPI}. As it is possible to observe from Figure 44, at the maximum concentration of OPE the solution viscosity increased greatly, and it lost its flowability because of gel formation. Because of this, the final coatings were produced by adding only up to 10% of the active phase. A strong thickening of the WPI mixture was also obtained by adding the OPE powder before the heating step, suggesting an interaction of the olive pomace extract with the protein molecules during denaturation and cross linking mechanism.

Before the coating deposition, the solution was sonicated for 15 minutes using an ultrasonic bath to eliminate the air bubbles formed during the stirring process. Afterwards, the casting mixture was spread on the bi-oriented PET substrate by means of a K Hand Coater (RK, Printocoat Instruments Ltd., Litlington, UK), equipped with stainless steel closely wound rod, with wire diameter equal to 0.64 mm, yielding final coatings with comparable thicknesses, as listed in Table 22. The corona pre-treatment was performed in order to obtain sufficient wettability and adhesion of the coating layer on the substrate.

Table 22 List of the prepared systems, at different concentration of OPE_powder. The neat substrate (PET) was used as reference.

Sample Film	OPE concentration [%w/w_{WPI}]	Thickness of the coating layer [µm]	Total Thickness [µm]
PET	0	0	23.0 ± 0.3
PET/WPI	0	9.2 ± 2.5	32.2 ± 2.5
PET/WPI-5%OPE	5	10.1 ± 2.1	33.1 ± 2.1
PET/WPI-10%OPE	10	10.2 ± 2.2	33.2 ± 2.2

Solvent was evaporated at room conditions overnight, then the coated films were stored under vacuum sealing in aluminium bags before analysis. The coating layer thickness was evaluated as difference among the total thickness of the coated films and the BOPET substrate thickness.

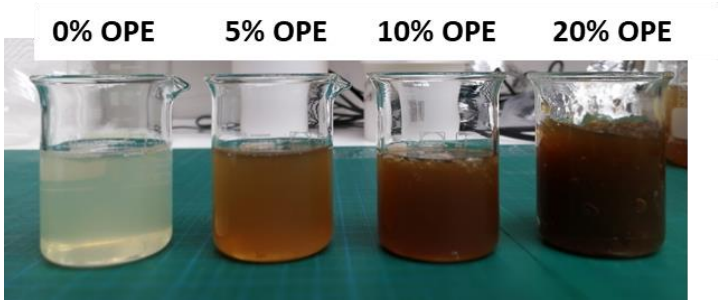

(A)

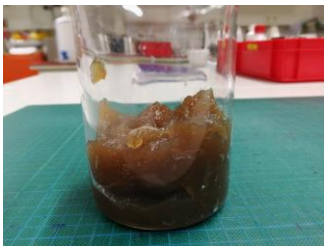

(B)

Figure 44 Image of the WPI coating mixture at 0%, 5%, 10% and 20% w/w$_{WPI}$ OPE (A) and of the WPI coating mixture with OPE addition before the heating process (B).

Characterization of the active coated films

Fourier Transform Infrared spectra of the films were collected by a Thermo Scientific Nicolet 600 FT-IR, equipped with a Smart Performer accessory for attenuated total-reflection (ATR) measurement using a ZnSe crystal. The operating spectral range was set at 650–4000 cm^{-1}, with a resolution of 4 cm^{-1} and 64 scans per sample. Normalization and peak integration was performed using Omnic software.

Static contact angle measurements were performed with a First Ten Angstrom Analyzer System 32.0 mod. FTA 1000 (First Ten Angstroms, Inc., Portsmouth, VA, USA), according to the standard test method ASTM D5946. Moreover, the dispersion (γ_s^d) and polar (γ_s^p) components of the surface energy (SE) for all the samples were calculated according to the Owens-Wendt geometric mean equation, using distilled water and ethylene glycol as testing liquids. According to this method, it is necessary to measure the contact angles with at least two liquids of known surface tensions, in order to calculate the dispersive and polar part of interfacial tension between liquid and solid (Lindner et al., 2018). The drop volume was taken within the range where the contact angle did not change with the variation of the volume (2 ± 0.5 µL). Each reported value of the θ angle is the average of at least ten replicate measurements.

The PET/WPI films were submitted to global migration tests by total immersion method, according to the Regulation (EU) 10/2011 and (EU) 2017/752. Film specimens (surface area = 1 dm^2) were put in a glass vial, in contact with 100 mL of food simulant. Distilled water and isooctane were selected as food simulants (A and D2, respectively). Films were stored at 40°C for 10 days in the case of distilled water, and at 20°C for 48 hours in the case of isooctane. At the end of test period, the samples were removed and the extracted solutions were transferred to quartz evaporation capsules and concentrated on a hot plate. The concentrated solutions were further evaporated to dryness in a thermostatically controlled chamber at 100±5°C for 30 minutes, then cooled for 30 min in a desiccator and weighted. The procedure was repeated until a constant weight of the residue was reached, to the nearest 0.1 mg. The amount of extractive obtained was calculated and expressed in mg/dm^2. Duplicate film samples were set up.

Total immersion method was also used to study the release kinetic of antioxidants from WPI coated films. Isooctane was selected in order to evaluate the antioxidant release in fatty foods simulants. In this case, film samples were cut in rectangles of surface area equal to 2 dm^2 and immersed in 100 mL of isooctane in 250 mL flasks. The flasks were kept in the dark under magnetic stirring, to minimize mass transfer resistance of antioxidants from the film, at room conditions for 10 days. Two milliliters of the food simulant were periodically sampled for quantification, and then reinserted. The concentration of antioxidants released into the simulant was quantified using a UV-Vis spectrophotometer (Lambda Bio 40, Perkin Elmer, Waltham, MA, USA) at 279 nm, on the basis of a standard curve (0-2000 ppm). The selected wavelength was the one at which the maximum absorbance of the olive pomace extract was found. To account for background interferences (i.e. light losses due to scattering or absorption by the solvent), a blank sample with the release medium was used as reference in the measurements.

The antioxidant activity released into the simulant solution was also assessed by DPPH method, using the same method as described in the "Olive Pomace Extract Characterization" paragraph. The blank was conducted using the pure release medium instead of the sample. All analyses were performed in triplicate, and the obtained values were expressed as µmolTrolox/L, based on the standard curve of Trolox. The maximum antioxidant activity was also expressed per unit volume of the coating, in $mmolTrolox/dm^3$.

Oxygen permeability tests were performed by GDP-C gas permeabilimeter (Brugger, Munchen Germany) at 23°C and 0% R.H., with the oxygen flow rate of 80 mL/min, according to the ASTM D1434 procedure. Resulting oxygen permeability of the PET/WPI coated film was used for further calculations of the permeability of the single whey protein

layer, assuming the film as 2-layer structure. The following equations can be used:

$$\frac{x_{tot}}{P_{tot}} = \frac{x_1}{P_1} + \frac{x_2}{P_2} \quad (53)$$

$$\frac{1}{Q_{tot}} = \sum \frac{x_i}{P_i} = \frac{1}{Q_1} + \frac{1}{Q_2} + \cdots \quad (54)$$

Where x and P represent the thickness and the permeability of each layer i. Subscript 1 stands for the PET substrate, subscript 2 for the whey protein coating and subscript tot for the whole multilayer structure.

Oxygen permeability of the whey coating was then converted to a thickness of 100 mm (Q_{100}) in order to allow direct comparison of different materials independently of the thickness, according to the following equation (55):

$$Q_{100} = Q * \frac{x}{100} \quad (55)$$

Water vapor permeability was measured by M7002 Water Vapor Permeation Analyzer (Systech Instruments Ltd, Oxfordshire, UK) according to the standard ASTM F1249. Films were tested at 23°C and 50% RH, and the results, performed in triplicate, were expressed as PWV (g m/(m^2 Pa s)) according to Equation (45) .

Mechanical tensile tests were carried out according to the standard ASTM D 882 using the a CMT 4000 Series tensile tester (SANS, China) equipped with a 100 N load cell. Film specimens were cut with a rectangular geometry (12.7x80 mm^2) along the coating direction. The crosshead speed of the test was kept at 5 mm/min for the duration of each test.

The films transmittance within the range 200 nm to 800 nm was evaluated by a Perkin Elmer UV-Visible Spectrophotometer Lambda 800. The transparency of the films was evaluated by measuring the Transmittance % of visible light at 550 nm, according to the ASTM D1746-03.

Colour measurements were carried out the films by using a colorimeter CIE-Lab (Chroma Meter II Reflectance CR-300, Minolta, Japan) and the results were expressed according to colour coordinates L* (darkness /lightness), a* (greenness/redness), b* (blueness/yellowness). The chromatic parameters were evaluated soon after the coatings production (i.e. at time 0) and at regular time intervals (up to 70 days) exposing films to natural light, in order to evaluate possible effects due to photo-oxidation phenomena. The colour variation of the films over time was evaluated by Δa* Δb*

parameters, and by means of the colour-difference equation CIELAB ΔE*ab, based on the coordinates L*, a* e b*.

V.3 Results and discussion: Olive Pomace Extract

Dry matter, total polyphenols, hydroxytyrosol content and antioxidant activity of the Olive Pomace Extract

Olive pomace is mainly constituted by sugars (polysaccharides), proteins, fatty acids, pigments, and polyphenols (Mirabella et al., 2014). Of the latter, phenols with two or more hydroxyl groups showed high antioxidant capacity in vitro, whereas phenols with one hydroxyl group have little or none (Vissers et al., 2004).

In particular, olive pomace is rich in hydroxytyrosol, but also has a significant content in oleuropein, tyrosol, caffeic acid, *p*-coumaric acid, vanillic acid verbascoside, elenolic acid, catechol, and rutin (Ghanbari et al., 2012; Rigane et al., 2012; Uribe et al., 2013). The polar compounds hydroxytyrosol and tyrosol are the end products of hydrolysis of oleuropein- and ligstroside-aglycones or their derivatives in olives and olive oil. Hydroxytyrosol demonstrated to have the highest antioxidant potency compared to the other olive polyphenols, with an activity in the micro-molar range (Cinar et al., 2011). Phenolic compounds act as antioxidants by different pathways. The most important is likely to be by free radical scavenging in which the phenol can break the free radical chain reaction (Delgado-Adámez et al., 2016)

With the aim of evaluating the potential of the produced olive pomace extract to develop an effective active packaging, the total polyphenols, hydroxytyrosol content and antioxidant activity were quantified on OPE_liq sample, and the outcomes are reported in Table 23. Results are expressed in terms of dry matter content, in order to better compare the properties with literature data.

Total phenols content of the pomace extract is equal to 34.2 ± 0.3 mg GAE/g dry matter, and the concentration of hydroxytyrosol is equal to 589 ± 4.6 mg HyTy/kg dry matter. The antioxidant activity of the OPE_liquid, determined by DPPH method, is equal to 158.4 ± 0.5 mmol Trolox/g dry matter.

Table 23 Dry matter content (DM), total polyphenols (TP), hydroxytyrosol content (HYTY) and antioxidant activity (AA) of the liquid olive pomace extract. Results are expressed as mean ± SD (standard deviation) of three determinations.

Sample	**DM [g/L]**	**TP** $\left[\frac{mg\ GAE}{g\ dry\ matter}\right]$	**HYTY** $\left[\frac{mg\ HyTy}{kg\ dry\ matter}\right]$	**AA** $\left[\frac{mmol\ Trolox}{g\ dry\ matter}\right]$
OPE_liq	135 ± 2	34.2 ± 0.3	589 ± 4.6	158.4 ± 0.5

Compared to literature data of other research groups, the phenolic composition and hydroxytyrosol concentration of OPE_liq are in line with or higher than those of other polyphenolic extracts deriving from olive leaves and pomace, reported inTable 24; moreover, OPE shows a remarkably high antioxidant activity.

Although the concentration and composition of polyphenols, as well as the antioxidant activity, are largely affected by the sample origin (cultivar, ripening stage, geographic origin of olives), these results suggest a good preservation of the bioactive components during the extraction process, which makes OPE suitable for the development of active packaging to preserve and/or extend the shelf life of sensitive foods.

Table 24 Literature references of total polyphenols, hydroxytyrosol concentration and antioxidant activity of natural extracts deriving from olive leaves and pomace.

Sample	**Total polyphenols**	**Ref.**
Olive leaves extract (Sevillane, EtOH:H2O)	$73.05 \pm 15{,}52 \frac{\text{mg } GAE}{\text{g dry matter}}$	Ben Salah M. et al. 2012.
Sample	**Hydroxytyrosol Concent.**	**Ref.**
Olive leaves extract (water, T=100°C)	$411 \pm 11 \frac{\text{mg } Hyty}{\text{kg dry matter}}$	Luo H. 2011.
Olive pomace "La Pepa"	$10.4 \pm 0.24 \frac{\text{mg } Hyty}{\text{kg dry matter}}$	Cioffi et al., 2010.
Olive pomace "Severini"	$8.4 \pm 0.56 \frac{\text{mg } Hyty}{\text{kg dry matter}}$	Cioffi et al., 2010.
Sample	**Antioxidant activity**	**Ref.**
Olive leaves extract	$0.930 \left[\frac{mmol\ Trolox}{g\ dry\ matter}\right] \frac{\text{mmol Trolox eq}}{\text{g dry extract}}$	Amaro Blanco et al. 2017.
Olive pomace flour	$0.143 \left[\frac{mmol\ Trolox}{g\ dry\ matter}\right]$	de Moraes Crizel et al. 2017.
Pomace extract microparticles	$0.109 \frac{\text{mmol Trolox eq}}{\text{g dry matter}}$	de Moraes Crizel et al. 2017.

Oxygen scavenging performance of the Olive Pomace Extract: effect of pH and relative humidity

In order to provide basic knowledge about the O_2 absorption kinetics of the olive pomace extract, gas absorption measurements were carried out.

The effect of pH on the oxygen scavenging reaction is shown in Figure 45, where the pH of the OPE_liq sample was increased from 6.5 (i.e., native pH) up to 12. The absorption parameters, evaluated after 50 days measurements, are also reported in Table 25. Oxygen scavenging capacity values are both expressed over of grams of dry matter and grams of gallic acid equivalents (GAE), derived from total polyphenols analysis.

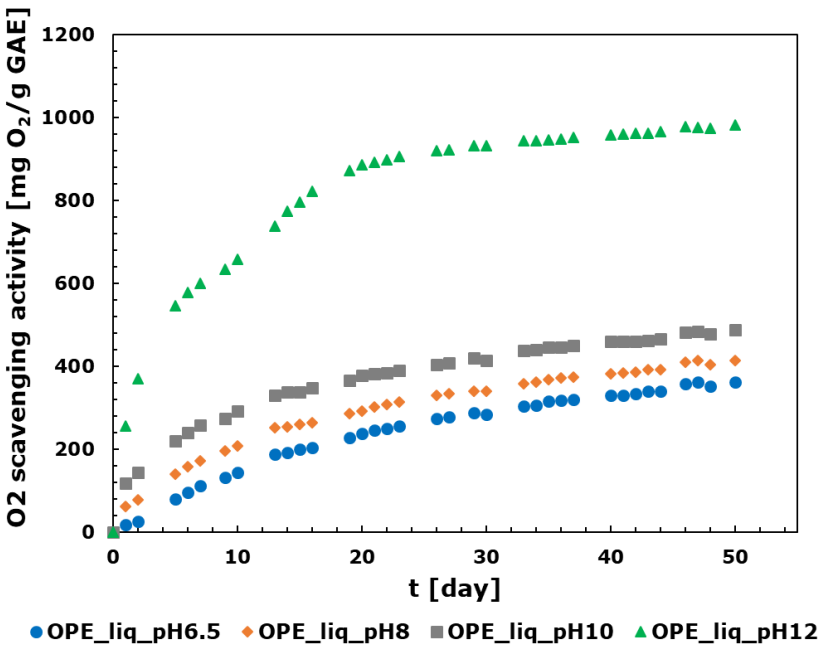

Figure 45 O2 scavenging activity curves by OPE_liq samples at different pH and at 23°C. Standard deviation bars are not visible on the graph.

All the olive extract samples immediately reacted with the oxygen inside the cell, absorbing the gas over the time up to reach a semi-plateau value, at which the reaction kinetic becomes very slow.

The pH has an effect on the scavenger kinetics: the addition of the base speeds up the scavenging reaction, and an increased amount of sodium hydroxide enhances both the reaction rate and the volume of the oxygen absorbed.

In particular, the sample at pH 12 showed the highest oxygen absorption activity compared to others, with a maximum scavenging capacity equal to 26.2 mLO_2/g dm (or 982.3 mgO_2/g GAE), and a total volume of gas absorbed increased by 165%, with respect to the OPE at native pH.

Table 25 Volume of O2 absorbed V_{O2}, % increase of Vox and scavenging capacity for the OPE liquid samples at different pH and 23°C. Results were taken after 50 days measurements.

Sample	V_{O2} [mL]	% Increase V_{ox}	Scavenging capacity	
			$[\frac{mL\ O2}{g\ dry\ matter}]$	$[\frac{mg\ O2}{g\ GAE}]$
OPE_liq_pH6.5	6.67	-	9.88	362.3
OPE_liq_pH8	7.54	13%	11.2	412.8
OPE_liq_pH10	8.92	34%	13.2	488.2
OPE_liq_pH12	17.7	165%	26.2	982.3

By comparing the obtained results with literature data, a good agreement with the scavenging capacity values obtained for pure gallic acid (GA) was found. In particular, the scavenging capacity of the OPE at pH=8 (i.e. 412.8 mgO2/g GAE) matches the one of GA found by Pant et al. (2017) at the same pH and 21°C (i.e. 448 mgO2/g GA), suggesting that mainly the polyphenols in OPE are responsible for the O_2 scavenging effect.

Moreover, it is reasonable to hypothesize that the base interacts with the chemical structure of the polyphenols, leading to polyphenols deprotonation and therefore affecting the oxidation phenomenon.

Other authors also described the effect of alkaline environment in enhancing the oxygen scavenging capacity of natural polyphenols.

Pant et al. (2019) described the effect of deprotonation on the reaction kinetics of gallic acid, that is a weak polyprotic acid with four acidic protons that can be transferred to an acceptor base. Chemically, the scavenging function relies on the auto-oxidation of gallic acid in alkaline solution, therefore oxygen scavengers based on this polyphenol usually contain a base that establishes the conditions necessary for the humidity-induced scavenger reaction. The study revealed that both the reaction rate coefficient k and the scavenger capacity n were significantly affected by the degree of deprotonation (DoD), with a maximum at pH 10-11 (DoD=0.6-0.7).

Gaikwad et al. (2017b) observed that a system utilizing pyrogallol and sodium carbonate can be an effective oxygen scavenger, with highest oxygen scavenging capacity and rate for the sample at 1:1 ratio of reactant and base. The scavenging phenomenon described involves the formation of oxygen free radicals from the non-enzymatic reactions of O_2 along with an alkaline solution. Pyrogallol can donate its electrons to scavenge the oxygen free

radical, which returns to its ground state and is eliminated, leading to the reduction of gas amount in the headspace.

Cilliers and Singleton (1989) also studied O_2 absorption of caffeic acid in the pH range 4-8, and reported raising reaction rate constants at higher pH values.

All the OPE samples analyzes showed enough oxygen scavenging activity required to use as oxygen scavengers for packaging application.

They exhibit a scavenging capacity range (i.e. 9.88 – 26.2 mLO2/g dry matter) which not only complies the aforementioned values of gallic acid/sodium carbonate systems, but also those of pyrogallol/sodium carbonate at the same temperature and relative humidity (i.e. 27.12 – 36.8 mLO2/g dry matter; Gaikwad et al., 2017b). Generally, the capacity of most traditional oxygen scavengers could be as low as 1 mL O2/g with an oxygen scavenging rate of 0.1 mL O2/g day (Jerdee et al., 2003), and the oxygen scavenging capacity of an iron sachet is within the range of 39–79 mL O2/g (Charles et al., 2006).

In order to assess the effect of relative humidity on the scavenging phenomenon, measurements were also carried out on the OPE_powder sample, which were stored up to 50 days in the closed cells by conditioning the headspace environment at 55% and 100% RH.

The outcomes are shown in Figure 46.

At 55% RH the oxygen concentration remains constant at its initial value (8.2 mol/m^3) over time, and no oxygen absorption is observable.

At 100% RH, soon after the beginning of the test, the OPE powder started dissolving, enabling the scavenging reaction.

The water content inside the head space volume plays a crucial role in the activation of the oxygen scavenging reaction of the OPE polyphenols; they also corroborate the upshots of other authors, describing the humidity as an important trigger of the scavenging reaction for other polyphenols (Pant et al., 2018; Ahn et al., 2016; Langowski and Wanner, 2005).

On the same pathway, it could be hypothesized that the OPE polyphenols follow similar activation mechanism, which involves their deprotonation prior to the reaction with O_2, and describes the presence of water as fundamental medium for the proton transfer.

Thereafter, the amount of available water determines if the reaction takes place and, in combination with the base, can also determine the extent of deprotonation, influencing the subsequent oxidation route. This effect can be utilized for the application of OPE based scavengers in packaging: packaging films containing the scavenger could be stored under typical room conditions (55% RH) without losing their capacity.

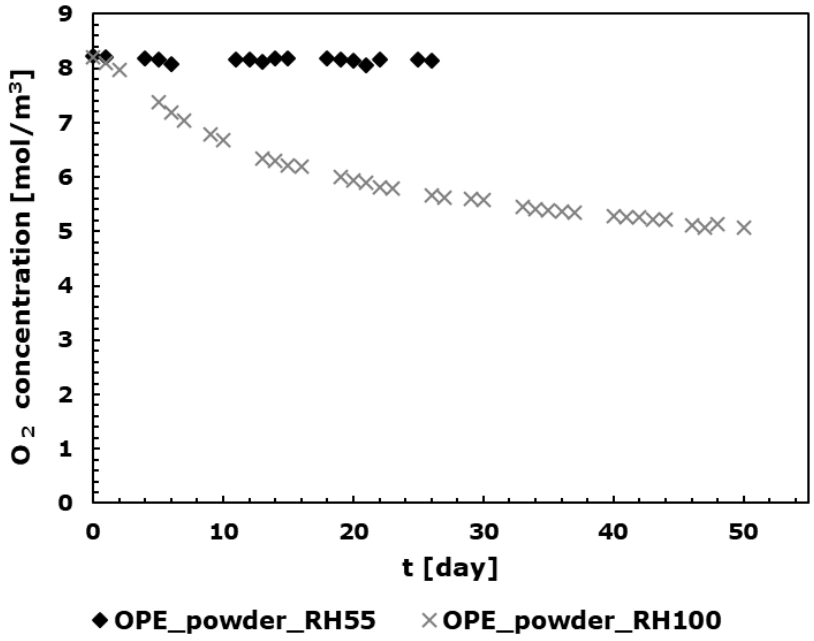

Figure 46 Oxygen absorption curves by OPE powder at 23°C and at 55% and 100% RH. Standard deviation bars are not visible on the graph.

Model prediction of OPE oxidation kinetics and comparison with experimental results

In order to have a closer look at the modeling of the scavenging reaction and to determine the kinetic parameters, each experimental data set obtained for OPE_liquid was fitted by the second-order kinetic model described in the previous section.

The fitted curves are shown in Figure 47, while Table 26 gives an overview of the obtained model parameters, compared with the experimental scavenging capacity expressed in mol O_2/mol GAE.

The trends of time evolution of oxygen concentration in the cell provided by the model numerical solution are in close agreement with the empirical values. In particular, the calculated root-mean square error (RMSE) is in the same order of magnitude as the experimental error MSE_{exp}.

Table 26 Experimental scavenging capacity (in molO2/molGAE) and kinetic model parameters n, k, MSE_{exp} and RMSE for the OPE_liq samples at different pH.

Sample	Scavenging capacity μ $[\frac{\text{mol O2}}{mol\ GAE}]$	n $[\frac{\text{mol O2}}{mol\ GAE}]$	k $[\frac{m^3}{mol\ s}]$	MSE_{exp} $[\frac{mol}{m^3}]$	RMSE $[\frac{mol}{m^3}]$
OPE_liq_pH6.5	1.926	2.273	$6.335 \cdot 10^{-8}$	0.061	0.067
OPE_liq_pH8	2.194	2.261	$1.028 \cdot 10^{-7}$	0.019	0.088
OPE_liq_pH10	2.539	2.501	$1.592 \cdot 10^{-7}$	0.038	0.156
OPE_liq_pH12	5.222	5.325	$2.799 \cdot 10^{-7}$	0.086	0.199

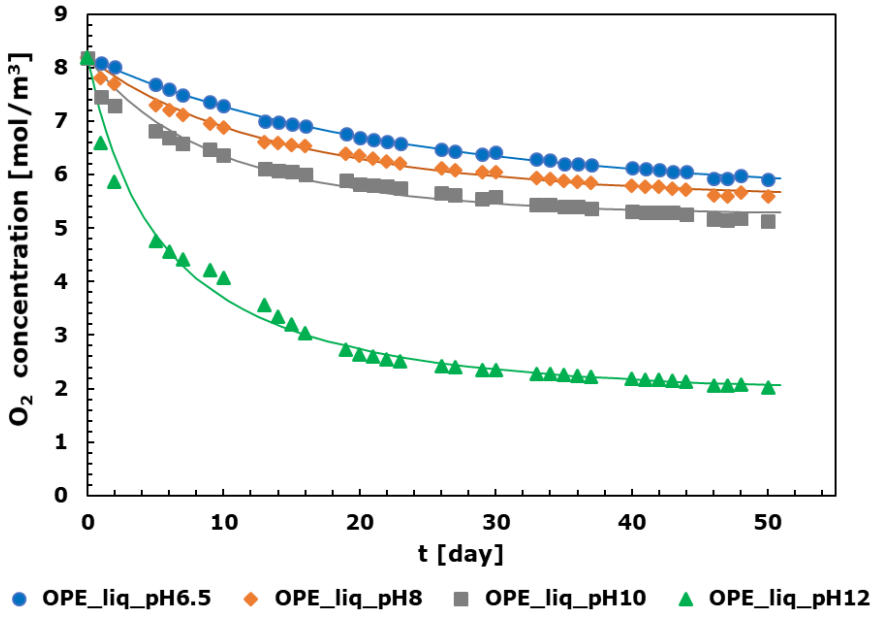

Figure 47 Comparison among experimental and simulated oxygen absorption curves by OPE liquid extract at different pH at 23°C. Symbols show the experimental data and lines show the simulation results.

The reaction rate constant *k* and the absorption capacity *n* were also determined from the fitting using the multiple-step downhill simplex optimization, and in Figure 27 are shown as function of the pH.

The kinetic parameter k increases in line with the pH, and is equal to $6.335 \cdot 10^{-8}$, $1.028 \cdot 10^{-7}$, $1.592 \cdot 10^{-7}$, $2.799 \cdot 10^{-7}$ $m^3/(mol \cdot s)$ for the OPE samples at pH 6.5, 8, 10 and 12, respectively.

The number of oxygen molecules reacting per molecule of scavenger remains almost constant within the pH range 6.5-10 (and is equal to 2.273, 2.261 and 2.501 mol O_2/mol GAE, respectively), then sharply increases at pH 12, being equal to 5.325 mol O_2/mol GAE. This clearly confirms the effect of the base on the autoxidation reaction of the polyphenols, inducing their deprotonation. As future work, O_2 scavenging measurements at larger pH (~14) are in progress to verify if the maximum degree of deprotonation has been reached.

Finally, from the comparison between the simulated scavenging capacity *n* and the empirical one μ, a good agreement was found. Since n is evaluated at complete exhaustion of the scavenger, after 50 days of test, when the semi-plateau value was reached, the end of the reaction was very close.

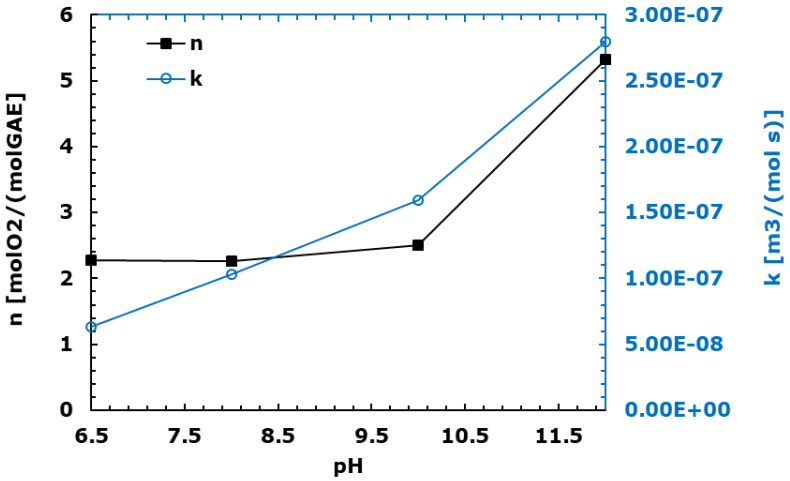

Figure 48 Effect of the pH on the reaction rate coefficient k and on the absorption capacity n. Connecting lines are shown for clarity.

The proposed mathematical model was also applied to fit the O_2 absorption data of a gallic acid-based oxygen scavenger, demonstrating its suitability for describing the oxygen absorption in a range of different

temperatures (from 5 to 38 °C), relative humidity (from 0 to 100% RH) and pH (from 2.9 to 13.8). For most of the experiments, the simulation results were in good agreement with the empirical data (Pant et al., 2018; Pant et al., 2019). The positive outcomes obtained from the modeling of the OPE data set further validate the model. This simple second-order model can be applied to describe the O_2 uptake by a variety of polyphenols, and to predict quite accurately their scavenging capacity under different conditions.

V.4 Results and discussion: Active biodegradable coatings based on the Olive Pomace Extract

ATR-FTIR analyses

The Fourier transform infrared spectroscopy (FT-IR) was used to investigate possible alterations in the intra- and intermolecular interactions due to OPE_powder addition into the WPI coating layer. Figure 49 shows the absorption spectra of the olive pomace extract OPE_powder (A) and of only the pure WPI coating layer (B). Figure 50 shows their comparison with the WPI coating at the intermediate concentration of 5% OPE, taken as an example.

For the OPE_powder (Figure 49 (A)), the broad absorption band in the 3700-3000 cm^{-1} region is attributable to νOH stretching vibrations of oleuropein, cellulose, organic acids etc., whereas bands centred at 2920 and 2851 cm^{-1} involve the asymmetric and symmetric stretching vibrations of aliphatic C-H in CH_2 and terminal CH_3 groups, respectively. The region comprised between 1780 and 1480 cm^{-1} corresponds to C=O and C=C stretching vibrations (esters, acid, carboxylate, aromatic ring), and the peak observed at 1745 cm^{-1} corresponds to the C=O stretching vibration of carbonyl groups of the triglycerides. The bands in the 1400-1200 cm-1 region are mainly attributed to bending vibrations of CH_2 and CH_3 aliphatic groups, like symmetric HCH bending at 1375 cm^{-1}. Bands in the 1150-900 cm^{-1} region correspond to endocyclic and exocyclic C–O stretching vibrations, like the stretching vibration of C-O groups of carbohydrates at 1012 cm^{-1} . Similarities were found with MIR absorption spectra of olive leaf and olive oil samples (De La Mata et al., 2012; Aouidi et al., 2012).

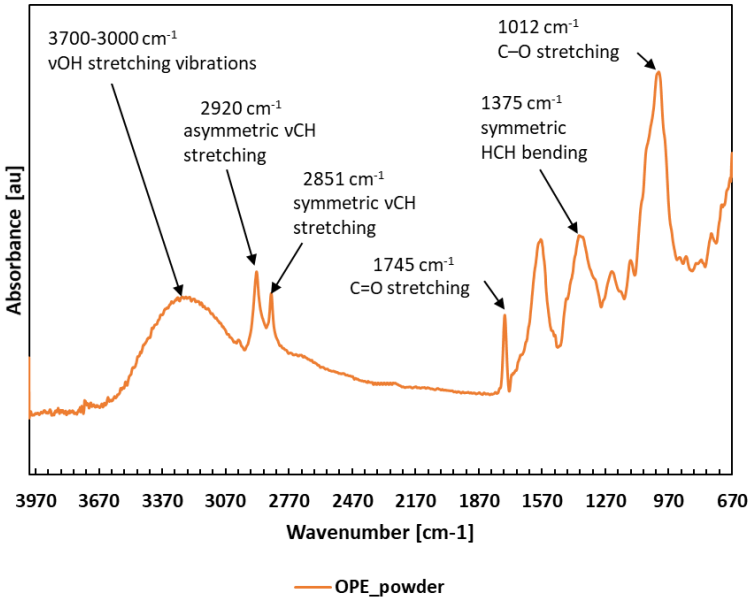

(A)

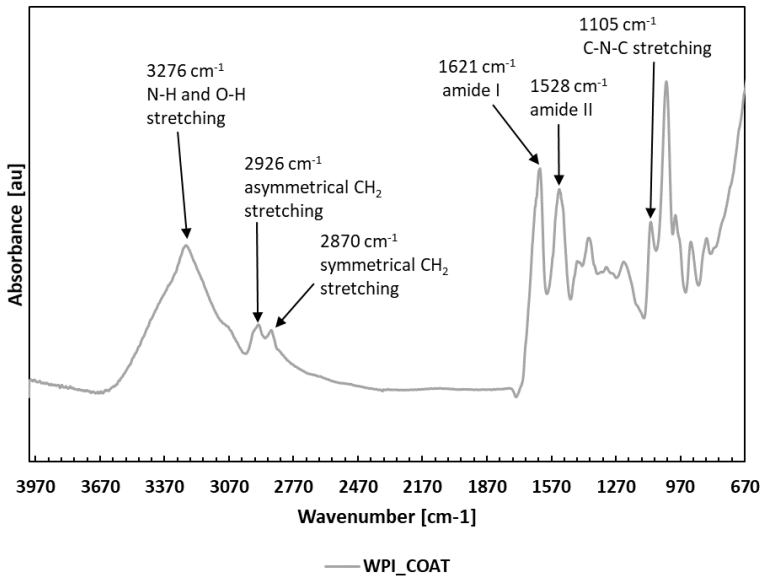

(B)

Figure 49 ATR-FTIR spectra of OPE_powder (A) and of the neat, thin WPI coating layer (B)

In the spectrum of the WPI coating layer (Figure 49 (B)) the band at 3276 cm^{-1} is ascribable to the stretching vibration of hydroxyl groups of the protein, and to asymmetric and symmetric stretching vibrations of the N-H bonds in amino groups. The peaks at 2926 and 2870 cm^{-1} correspond to asymmetrical and symmetrical CH_2 stretching of lipids in the protein, while typical amide I and amide II bands are observed at 1621 cm^{-1} and 1528 cm^{-1}, and are due to the C=O stretching and N–H bending, combined with C-N stretching, respectively. Generally, the amide I band is centered near 1650 cm^{-1} when the protein is unfolded, and is characteristic of an unordered structure. Conversely, the displacement of the band at lower wavenumbers (as in this case) is characteristic of the α-helix to β-sheet interconversion, and reveals the heat induced aggregation of protein molecules (Farjami et al., 2015). Finally, the peak at 1220 cm^{-1} corresponds to the C-O stretching, and the band at 1105 cm^{-1} is attributable to the C-N-C stretching of the peptide bond.

As it is possible to observe from Figure 50, after the OPE addition the WPI characteristic peaks remain substantially unchanged. Although the WPI and OPE patterns overlap in some regions, no displacement of the absorption bands is detectable from the comparison between the WPI_COAT and WPI_COAT_5%OPE spectra. This outcome was also visible for the whey protein coating at 10% of active agent (data not shown) suggesting that, at the percentages investigated, a good solubilization of OPE in the protein network is obtained, with no chemical interactions between the two phases.

A more in-depth study at the highest OPE concentration examined in the preliminary applications studies (i.e. 20% w/w_{WPI}) will be carried out in future work, in order to investigate the gel formation phenomenon in the coating mixture during the films process.

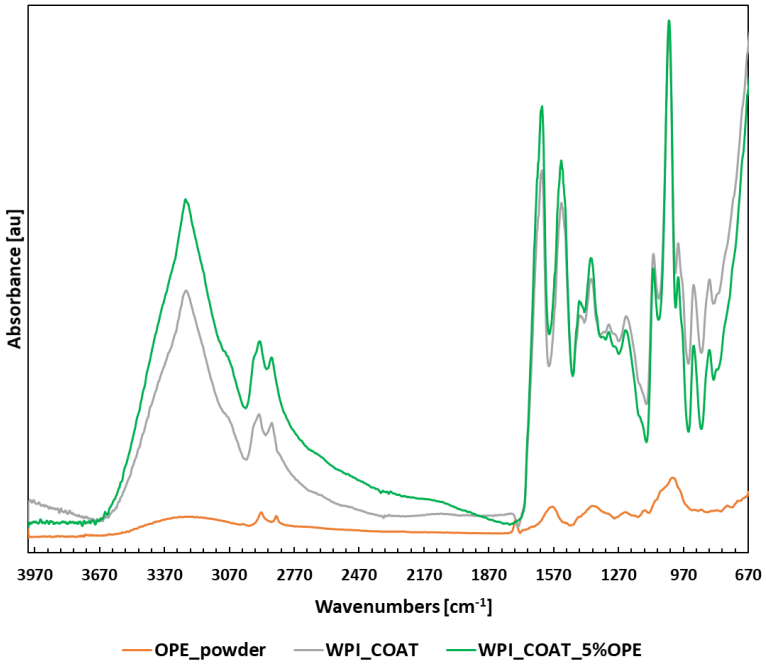

Figure 50 ATR-FTIR spectra of the OPE_powder and of the thin WPI coating layers loaded at 0 and 5% of olive pomace extract.

Evaluation of wettability and surface energy

The surface wettability of the PET/WPI coated films was estimated by contact angle measurements, and by evaluating the surface energy and its polar (γ_s^p) and dispersive (γ_s^d) components (Table 27).

For the PET/WPI sample, the surface energy of the protein layer (38.0 dyne/cm) is in the range of that of synthetic polymers (Schmid et al., 2014). The polar part γ_s^p is comparable to that of the corona treated PET substrate (equal to 25.4 dyne/cm and 24.5 dyne/cm, respectively), indicating a high number of free polar units (-OH and -NH groups) on amino acids which can interact with the polar groups of the corona treated PET substrate (as C=O, -COOH, and -OH groups), improving the coating adhesion.

The addition of the OPE_powder leads to a dramatic decrease of the polar component of the coatings, whose significance increases by increasing the active phase concentration (13.9 dyne/cm and 11.4 dyne/cm for PET/WPI-5%OPE and PET/WPI-10%OPE samples, respectively), while the dispersive

component γ_s^d changes only slightly (16.1 dyne/cm and 17.1 dyne/cm for PET/WPI-5%OPE and PET/WPI-10%OPE samples, respectively).

The lower polarity of the active surfaces is also confirmed by the increase of the CA_W values with respect to the PET/WPI sample, and could be attributable to the presence of non-polar groups, of lipid and triglyceride origin, in the active agent. The decrease of the number of hydrophilic groups ultimately leads to a decrease in the intermolecular force between the substrate and the coating, entailing a worsening of the adhesion strength. Nevertheless, no significant delamination problems occurred, and the extent of interlayer adhesion, which will be object of further investigations by coating topography, still remained qualitatively acceptable for the films application in food packaging.

Table 27 Static water (CAw) contact angle, surface energy and dispersion (γsd) and polar (γsp) components for the neat PET substrate film and for the WPI coated films at 0, 5 and 10 % OPE content

Sample Film	CA_w [°]	Surface energy [dyne/cm]	γ_s^p [dyne/cm]	γ_s^d [dyne/cm]
PET	62.8 ±2.3	38.6	24.5	14.1
PET/WPI	63.7 ±3.1	38.0	25.4	12.6
PET/WPI-5%OPE	75.8 ±1.2	30.0	13.9	16.1
PET/WPI-10%OPE	79.1 ±1.3	28.5	11.4	17.1

Study of the antioxidant activity of the films and Overall migration analyses

The potential of the active bio-coatings in extending the shelf-life of foods was evaluated both through oxygen absorption measurements and antioxidant release tests, downstream the promising results obtained from the OPE preliminary characterization, discussed in the previous paragraphs.

However, it was not possible to appreciate any significant oxygen scavenging activity on the active coatings. The tests were carried out both at RH 55% and 100%, after UV sterilization to eliminate the interference of any microbial proliferations in the oxygen absorption mechanisms. This is probably due to the inactivation of the agent during the coating

manufacturing process, which leads to a rapid exhaustion of the scavenging effect.

Conversely, it was possible to evaluate both the antioxidant release phenomenon and the radical scavenging capacity of the films, using isooctane as simulant for fats, oil and fatty foods (European Commission, 2011).

Figure 51 displays the comparison among the release curves of PET/WPI-5%OPE and PET/WPI-10%OPE in the fat simulant. For a better understanding of antioxidant release kinetic, the graph is presented as the percent ratio of M_t/M_∞, where M_t is the concentration of antioxidant (mg/mL) diffused at time t, and M_∞ represents the concentration of antioxidant diffused at equilibrium.

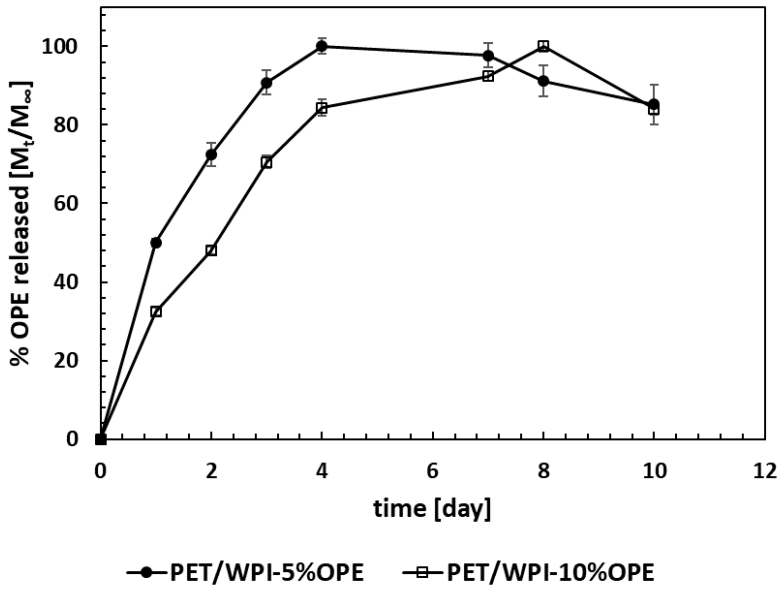

Figure 51 OPE release rate (Mt/M∞) from active coated films in isooctane, at 23°C.

Both the active multilayer samples show an increasing trend in the migration mechanism over time, with a faster initial kinetics, followed by a sustained release at longer times. The slight reduction for both curves (~16%) observed after 10 days could be due to the degradation of the phenolic components reacting with the oxygen dissolved in the medium.

In particular, the release rate is higher (and faster) for the PET/WPI-5%OPE film almost in the whole measurement range analyzed. For this sample, the percentage of antioxidant released on day 1 is ~50%, and in 4 days the film reaches the equilibrium. On the other hand, the PET/WPI-10%OPE sample releases ~32% of antioxidant on day 1, and a maximum release of active agent is obtained after 8 days.

The results are in compliance with the antioxidant activity measured in the food simulant over the time, expressed as µmolTrolox/L (Figure 52). Table 28 also shows the maximum antioxidant activity per unit volume of the coating (in mmolTrolox/dm^3), and the time at which the maximum antioxidant activity is reached.

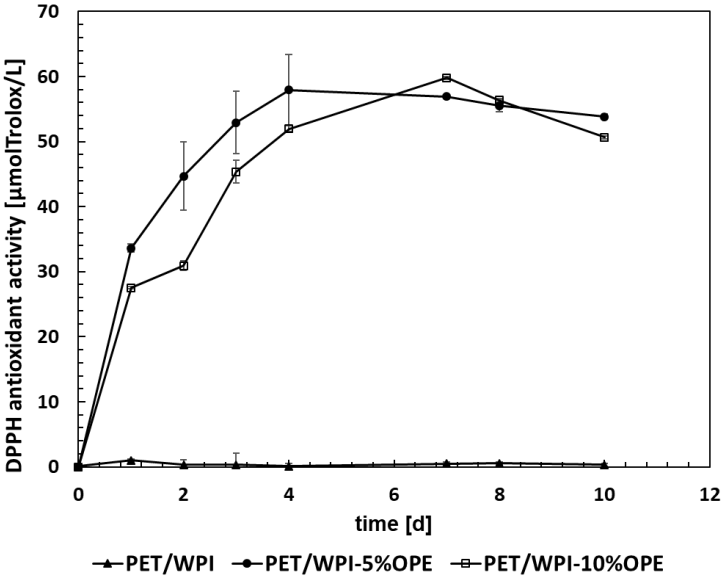

Figure 52 DPPH antioxidant activity (expressed in µmolTrolox/L) released from active coated films in isooctane, at 23°C.

Table 28 Time at which the maximum antioxidant activity is reached, and average maximum antioxidant activity (expressed as mmol Trolox/dm^3) for the active coated films.

Sample Film	Time at max antioxidant activity [d]	Average max. antioxidant activity [mmolTrolox/dm^3]
PET/WPI-5%OPE	4	28.96 ± 2.73
PET/WPI-10%OPE	7	29.89 ± 0.12

In particular, a maximum antioxidant activity equal to 28.96 ± 2.73 mmolTrolox/dm^3 is observed for the PET/WPI-5%OPE film after 4 days. Only a slightly higher value is reached for the PET/WPI-10%OPE film (29.89 ± 0.12 mmolTrolox/dm^3) after 7 days, at the test conditions investigated.

By increasing the concentration of antioxidant extract in the coating layer, a slower diffusion kinetics is obtained.

This effect could be attributed to the formation of OPE clusters at the highest concentration, which increase the resistance to diffusive transport, or to a higher entrapment of the antioxidant molecules within the whey protein network. The most important factor for the diffusion of a migrant from a solid polymer phase into a simulant liquid phase is the migrant solubility in the simulant. The other factor is the rate of molecule involvement and/or entrapment within the polymer matrix: a higher molecule involvement in the polymer reduces its release to the simulant. In this case, the film preparation method can directly influence the migrant incorporation into the polymer, as the process provides a more or less structured film, and consequently a more or less dispersed migrant.

In general, the more the protein network is crosslinked, the slower would be the diffusion. The changes in physicochemical properties of the filmogenic solution, as the viscosity changes observed in the preparation of the active coatings, may be considered as indicator of interactions among the WPI and OPE, which can influence the retention of the active compound (Wicochea et al., 2019).

However, in both cases the active bio-coatings are capable of releasing the antioxidant through a biodegradable matrix in medium-long times, significantly larger than the those obtained by other authors with active

systems based on natural antioxidants and biodegradable polymers (Marcos et al. 2014; Jamshidian et al., 2013).

Modifying the chemical and morphological composition of the coating matrix, it is possible to modulate the release of the active agent, obtaining a faster release more suitable for foods with a short shelf life, or a slower release kinetic preferable for long term stability foods.

Although all the ingredients for the whey coating production were selected among those approved for food contact, the compliance with overall migration limits of the European Regulation was verified. Table 29 shows the results of global migration analyses, using distilled water and isooctane as aqueous and fatty foods simulants, respectively.

Table 29 Global migration analysis results for the WPI coated films at 0, 5 and 10% of olive pomace extract, according to the (EU) 10/2011 and (EU) 2017/752 Regulations.

Sample Film	IsoOctane [mg/dm^2]	Distilled water [mg/dm^2]
PET/WPI	0.75 ± 0.03	5.30 ± 0.10
PET/WPI-5%OPE	0.80 ± 0.05	4.25 ± 0.05
PET/WPI-10%OPE	0.85 ± 0.02	4.00 ± 0.10

From the comparison among the two food simulants, one can observe overall migration values higher in case of contact with distilled water than isooctane. This is attributable to the larger affinity of WPI with water, which acts as swelling agent. The resistance to mass transfer of migrants in a polymer decreases with increasing affinity and contact time between the polymer and the medium. Therefore, water can facilitate the migration of whey protein oligomers because of interface solubilization phenomena, penetrating and spreading in the first layers of the matrix through the non-crosslinked regions. This allows a consequent decrease in the resistance to mass transfer of potential migrants.

However, in both cases the coatings fulfilled food safety regulation, since the measured values in the two specified simulants were below the migration limits of 10 mg/dm^2. Taking into account the uncertainties of the analytical method, only minor changes occur in global migration after the OPE incorporation in the coating layer.

Evaluation of barrier and tensile properties

Oxygen and water vapor permeability tests were carried out to investigate the barrier properties of the whey coated films, and the effect of OPE addition on their final performance (Table 30).

As a result of oxygen permeability analyses, the pure WPI coating layer addition decreases the oxygen permeability of the PET substrate, thanks to its excellent oxygen barrier properties (Hong and Krochta, 2004; Schmid et al., 2012). A ~ 40% reduction of P_{O2} was registered by comparing the PET/WPI film (0.86 ± 0.3 cm^3/m^2 d bar) and the pure substrate (1.42 ± 0.3 cm^3/m^2 d bar).

Table 30 Oxygen (P_{O2}) permeability, diffusivity coefficient (D) and water vapour permeability (P_{WV}), for the neat PET substrate and for the WPI coated films at 0, 5 and 10 and OPE concentration.

Sample Film	P_{O2} $[\frac{cm^3 mm}{m^2 d\ bar}]$	$D \cdot 10^9$ $[\frac{cm^2}{s}]$	$P_{WV} \cdot 10^{13}$ $[\frac{g\ m}{m^2 d\ Pa}]$
PET	1.42 ± 0.3	2.19 ± 0.01	7.4 ± 0.1
PET/WPI	0.86 ± 0.3	1.58 ± 0.03	11.1 ± 0.4
PET/WPI-5%OPE	0.77 ± 0.2	1.17 ± 0.05	11.2 ± 0.2
PET/WPI-10%OPE	0.68 ± 0.4	1.14 ± 0.07	11.4 ± 0.2

The incorporation of the OPE in the coating leads to a slight further reduction of P_{O2}, equal to 0.77 ± 0.2 $cm^3/(m^2$ d bar) and 0.68 ± 0.4 $cm^3/(m^2$ d bar) for the PET_WPI-5%OPE and PET_WPI-10%OPE samples, respectively, with a percentage decrease equal to 46% and 52% with respect to the neat PET film. A possible hypothesis could be an effect of OPE on decreasing the chains mobility, with a reduction of the free volume of the protein network, as also confirmed by slightly lower diffusion coefficients obtained for the active coatings.

In addition, the oxygen permeability of only the 10 µm WPI coating layer was calculated, according to the equation mentioned above in the "Materials and methods" section, and the 100 µm normalized value was derived and compared to literature results, as displayed in Table 31.

*Table 31 Comparison of oxygen permeability values (normalized with respect to 100 μm thickness) obtained from different research groups on whey protein films and coating layers. (*Calculated values)*

Sample Film	**Oxygen permeability [cm^3/m^2 d bar] ·100 μm**	**Ref.**
WPI coating, this study	4.5	
WPI coating on PET/nylon/LLDPE laminates	2.6 – 5.8 $\cdot 10^{-4}$*	Joo et al., 2018
WPI coating on biodegradable substrate	9.5	Cinelli et al., 2014
WPI with different transglutaminase concentrations	2.9 - 18.4	Schmid et al., 2014
WPI hydrolized with different glycerol concentrations	36 – 112*	Sothornvit et al., 2000
WPI unhydrolized with different glycerol concentrations	41 – 333*	Sothornvit et al., 2000
WPI coating on PET substrate	0.4 – 7.9	Schmid et al., 2012

The obtained results are in compliance with most of the data derived from existing literature, and underline the effectiveness of whey protein as a barrier material. However, it is important to keep in mind that a variation among permeability values may occur even though the formulations are quite similar, since processing parameters (i.e, curing and drying rate, orientation and crystallinity degree), measurement conditions and raw materials quality have a huge influence on the final outcomes.

As for the water vapor permeability results, an increase of the P_{WV} was observed after the WPI layer addition in the multilayer structure, with respect to the neat substrate ($11.1 \pm 0.4 \cdot 10^{-13}$ g m/(m^2 d Pa) and $7.4 \pm 0.1. 10^{-13}$ g m/(m^2 d Pa) for PET/WPI and PET films, respectively).

This evidence is justified by the high content of hydrogen bonds and hydroxyl and amino groups in the protein layer, as found by the FT-IR and wettability measurements, which makes it sensitive to polar matter such as water. Other authors also reported an increase of water vapor transmission rate with increasing relative humidity (Fang et al., 2002; Kokoszka et al., 2010; McHugh et al., 1994). Possible solutions to improve the material resistance to polar liquids and gases are a high degree of crosslinking (Schmid et al., 2014), lamination (Schmid et al., 2012), hydrophobic coatings such as nitrocellulose or alkyd lacquers or beeswax (Gällstedt and Hedenqvist, 2002).

Furthermore, no significant changes derived by the OPE addition, suggesting the good solubilization of the active phase in the polymer matrix, with no occurence of irregularities or microfractures on the coating surface that may facilitate the water permeation throughout the film.

Mechanical properties of the WPI coated films are summarized in Table 32, and compared to those of neat PET substrate. The elastic modulus, tensile strenght and elongation at break of the PET/WPI film were 3009 ± 140 MPa, 71.0 ± 2.4 MPa and 32.2 ± 1.1%, respectively.

Table 32 Elastic modulus (E), tensile strength (σb) and elongation at break (εb) for the neat PET substrate and for the WPI coated films at 0, 5 and 10 and OPE concentration.

Sample Film	E [MPa]	σb [MPa]	εb [%]
PET	3457 ± 68	75.7 ± 6.5	34.9 ± 4.3
PET/WPI	3009 ± 140	71.0 ± 2.4	32.2 ± 1.1
PET/WPI-5%OPE	2872 ± 118	60.7 ± 7.8	29.4 ± 1.2
PET/WPI-10%OPE	2853 ± 48	66.8 ± 7.6	31.3 ± 4.1

The reduced tensile properties with respect to the PET can be attributed to the low physical strenght of the WPI coating. Other authors reported for free-standing WPI films average values equal to 1.25 MPa, 1.25-1.3 MPa and 35-45%, respectively (Joo et al., 2018; Jiang et al., 2019). A slight further decrease of is observable after OPE addition, probably disrupting the

continuity of the protein matrix, although the final performance still remain within the range of acceptability.

Film optical properties and photo-oxidation stability

As a general observation, the coated films were highly transparent, free of any defects and easy to handle.

Films transparency was evaluated by UV-Vis light transmission rate in the range 200 and 800 nm (Figure 53) and transmittance percentage at 550 nm (Table 33). CieLab color coordinates L*, a* and b* and chromatic variation ΔE*ab are also reported in the table.

As noticeable, the pure WPI coating did not affect the transparency of the substrate, with a T_{550} % value equal to 84.5% and 84% for the PET and PET/WPI films, respectively. No significant differences occurred in the T_{550}% values of the active coatings (equal to 83.9 and 83.4 for the films at 5% and 10% OPE, respectively), which still remained comparable with the previous ones.

The chromatic parameters L*, a* and b* remained substantially unaltered among the PET and the PET/WPI coating. Conversely, a slight yellowing, marked by the increase of the b* coordinate, occurred after the addition of the olive pomace extract in the active coatings (with values equal to 2.54 ± 0.11 and 2.75 ± 0.34 for the PET/WPI-5%OPE and the PET/WPI-10%OPE, respectively).

Table 33 UV-Vis transmittance at 550 nm (T_{550} %), CieLab color coordinates L, a* and b* for the neat PET substrate and for the WPI coated films at 0, 5 and 10% OPE concentration. Chromatic variation ΔE*ab, calculated with respect to the PET substrate, is also reported.*

Sample Film	T_{550} %	L*	a*	b*	ΔE*ab
PET	84.5	98.8 ± 0.3	-0.84 ± 0.10	1.50 ± 0.10	-
PET/WPI	84.0	98.4 ± 1.5	-0.86 ± 0.15	1.70 ± 0.26	0.2
PET/WPI-5%OPE	83.9	98.7 ± 0.2	-0.94 ± 0.10	2.54 ± 0.11	1.1
PET/WPI-10%OPE	83.4	98.2 ± 1.5	-0.95 ± 0.21	2.75 ± 0.34	1.3

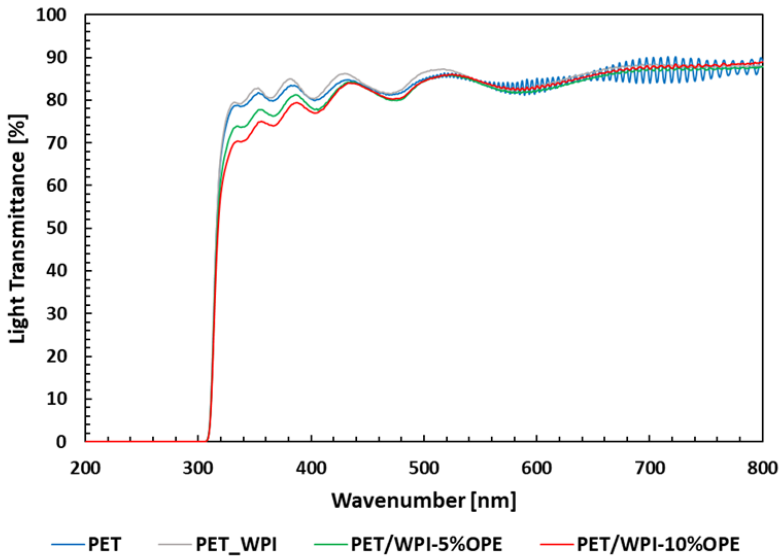

Figure 53 Light transmittance of PET and WPI coated films at 0, 5 and 10% OPE concentration.

For the a* parameter, a progressive decrease came out by increasing the OPE percentage, with a color variation towards green. Likewise, a slight increase of the chromatic variation ΔE*ab, calculated with respect to the neat PET, was found; in any case, values were lower than the perceptibility limit of the human eye (Witzel et al., 1973).

In order to analyze the photo-oxidative stability of the films over the time, the variation of a* and b* coordinates with respect to time 0 was measured up to 70 days. The calculated trends of Δa* and Δb* are shown in Figure 54 (A) and (B).

Both the PET substrate and the pure WPI coating did not undergo any significant colour change over the time.

By contrast, the active surfaces exhibited a sensitivity to photo-oxidative phenomena, with a slight yellowing over the time, which increased by increasing the antioxidant content.

In particular, for the films at 5% and 10% OPE, only minor changes were detectable for Δa* after 70 days (equal to -0.17 and -0.18, respectively), whereas an increase in Δb* equal to 0.86 and 1.01, respectively, was found.

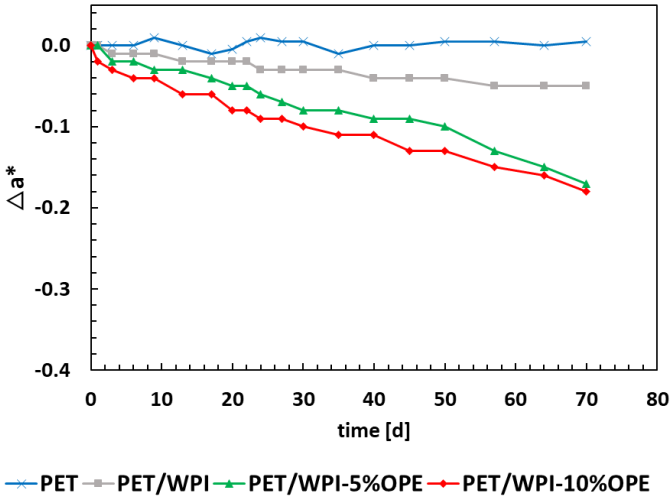

(A)

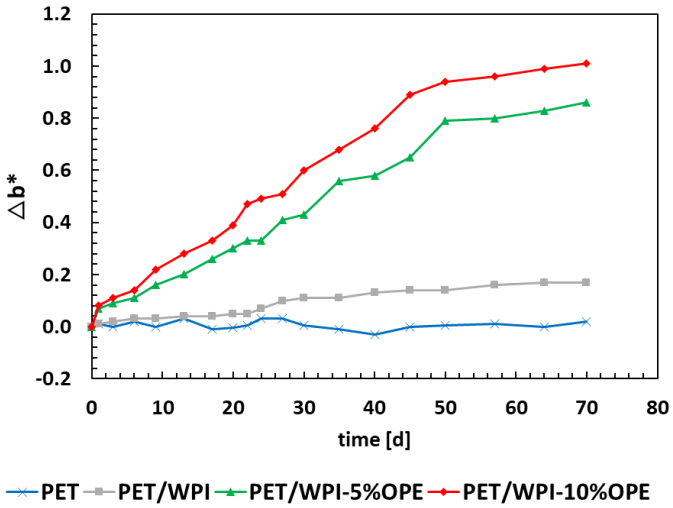

(B)

Figure 54 Change in redness ($\Delta a^*=a|_t - a|_{t=0}$, (A)) and yellowness ($\Delta b^*=b|_t - b|_{t=0}$, (B)) during the time, for the PET and WPI coated films at 0, 5 and 10% OPE concentration.

The progressive yellowing/browning is attributable to the oxidation of the active phase over the time. In fact, polyphenols are widely seen as very unstable and highly susceptible to degradation. The stability of polyphenols may be affected by different factors, involving high temperatures, light, oxygen, solvents, the presence of enzymes, proteins, metallic ions, or association with other food constituents (Volf et al., 2014).

The color of polyphenols is determined by the presence of chromophoric groups that interact with light (Shahidi and Naczk, 2003). Dark reaction products for polyphenol oxidation, for example brown or black polycondensates, can be found in wine or humic substances (Oliveira et al., 2011; Kumada, 1965).

The colorimetric analysis, therefore, can represent an indirect measure of the oxidation of the active phase contained in the films, exposed to the environmental conditions of light, temperature and relative humidity. However, the presence of complex matrices in the plant extracts, such as co-pigments, can inhibit degradation effects, preventing polyphenols from severe UV-degradation effects.

V.5 Summary and conclusions

In this chapter, the PhD research revealed the potential of using whey protein and olive pomace extract in effective antioxidant bio-coatings, with a number of environmental advantages deriving from the revaluation of food industry by-products, while maintaining required technical performance.

The olive pomace extract (OPE), produced by the extraction pilot plant located at the Fraunhofer Institute IVV, highlighted remarkably high hydroxytyrosol concentration and antioxidant activity, higher than the results reported in the literature on olive leaves and pomace extracts. Very good O2-absorption performance was also observed, comparable to that of pure gallic acid and in compliance with those required to use it as effective oxygen scavenger for packaging application. The scavenging reaction was enhanced by the addition of a base, increasing both the reaction rate and the amount of the oxygen absorbed, and trigged by the humidity content. The oxygen scavenging mechanism was well described by a second-order reaction kinetic model, underlining the possibility to use the mathematical model to predict quite accurately the O2-scavenging performance of a variety of polyphenols.

The OPE was successfully incorporated in whey protein (WPI) biodegradable coatings, to produce eco-sustainable, bio-active films for sensitive foods preservation. The processing window for the active coating process was reduced because of the increasing viscosity of the protein solution when the olive pomace extract is added.

Surface energy measurements underlined the good interlayer adhesion among the protein coating and the PET substrate. The sensitivity to polar matter and the scarce tensile properties of the whey protein layer induced only a slight worsening of the PET film functionalities, whereas its excellent gas barrier properties led to a decrease of the oxygen permeability up to 46% with respect to the neat substrate.

OPE addition up to 10% did not substantially modify the functional performance of the films in terms of adhesion, barrier and tensile properties, suggesting a good solubilization of the active phase in the polymer matrix. The colour of the active coatings was slightly impaired due to the presence of polyphenols, and the active surfaces exhibited a sensitivity to photo-oxidative phenomena. Nonetheless, all the coatings were highly transparent to the human eye, as in all cases the overall transmittance level was above 80% in the range 450-800 nm.

The produced coatings were shown to be suitable packaging films for food products since migration values tested for both aqueous and fatty foods simulants were below the migration limits established by the European Union Legislation. Finally, the release and DPPH tests proved that the films are able to release the antioxidant agent within fatty foods simulant, with a diffusion kinetic influenced by the composition and morphology of the bio-active coating. In particular, a comparable maximum antioxidant release was found after 4 days and 7 days for the film at 5% and 10% OPE, respectively. Overall, both the WPI/OPE formulations provided promising results for active packaging applications with medium-long shelf-life terms, with the possibility to tune the release rate and time. This outcome, coupled with the excellent oxygen barrier performance provided by the films, suggests their possible application with foods having high oxygen barrier requirements and medium-long shelf-life. To this aim, shelf life tests are now ongoing using buffalo butter and avocado puree, in order to evaluate their efficacy in preserving oxygen-sensitive greasy food matrices. The intended application of the antioxidant coatings is for direct food contact. Therefore, the shelf life tests were properly designed in order to maximize the packaging surface in contact with the food. The outcomes will be part of future works aimed at proving the success of the technology in this field.

Chapter VI

Development of 100% biodegradable antioxidant films, based on Poly(lactic acid) coatings and natural extracts from olive milling wastewaters

VI.1 Introduction

In the previous chapters, 100% mono-material PET films or biodegradable coatings on PET substrate were realized, all pursuing the concept of eco-compatibility and ease of recycling.

In this part of the research, as further step forward, 100% biodegradable antioxidant films have been realized, all based on biopolymers and natural extracts derived from olive milling wastewaters (OW).

The olive pomace extract characterized in Chapter V already demonstrated its wide potential to be applied in effective antioxidant food packaging.

Olive mill wastewaters represent the liquid fraction of residues in the three phase oil extraction system, which involves the use of a large amount of water (Nunes et al., 2016). Different organic compounds can be found in olive wastewaters as sugars, phenolic compounds, polyalcohols, lipids and pectins. Hydroxytyrosol is the main phenolic compound of OW; others include oleuropein, luteolin, tyrosol, hydroxytyrosol, verbascoside, which have demonstrated several benefits such as inhibition of low-density lipo-protein oxidation, free radical scavenging activity and in-vitro antimicrobial activity (De Marco et al., 2007).

However, the high quantity of phenolic compounds in the olive wastewaters makes them very resistant to microbial degradation, generating phytotoxicity and pollution of the groundwaters. Thus, the possibility to recover bioactive compounds from olive wastewaters represents a challenging task. Several processes have been described in literature to obtain olive polyphenol concentrate, using extraction and membrane separation techniques (Sabatini, 2010).

Therefore, investigating new fields of applications to reuse these products is not only a way to restore their economic and commercial dignity, but also solves a burdensome problem of environmental impact.

To this aim, this part of the research deals with the design, realization and verification of the effectiveness of biodegradable multilayer active films with antioxidant properties, based on natural extracts from olive mills wastewaters (OWE).

Figure 55 shows the flow diagram of the experimental set-up and of the activities carried out in this part of the PhD work, which will be discussed in this chapter.

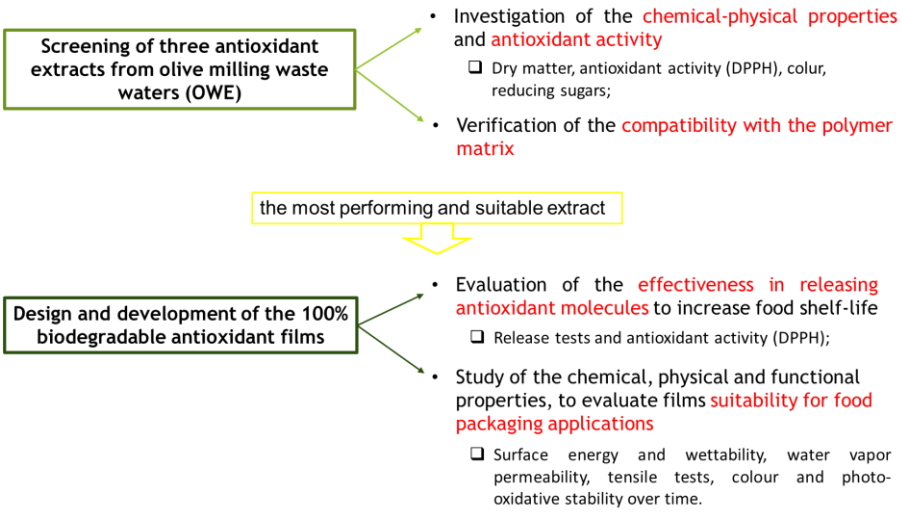

Figure 55 Experimental set up and activities discussed in Chapter VI.

Three phenolic extracts, subjected to different separation pre-treatments, were characterized in terms of the main chemical-physical properties (dry matter content, colour, reducing sugars) and antioxidant capacity. Then, the most performing and suitable extract was selected to produce active multilayer biodegradable films, spreading a PLA coating layer at different percentages of active phase (ranging from 0 to 20%), on a biodegradable substrate made of poly(lactic acid) and poly(butylene adipate terephthalate).

Release tests in fatty food simulant and DPPH radical scavenging measurements were carried out to investigate the effectiveness of the produced systems as antioxidant carriers for extending foods shelf-life.

Moreover, the effect of the active phase on the surface wettability, functional performance and photo-oxidative stability of the films was also evaluated.

VI.2 Materials and Methods

Materials

Three phenolic olive extracts deriving from olives milling wastewaters (named OWE1, OWE2 and OWE3) and subjected to different filtration concentration pre-treatments (data non disclosed), were donated by Fangiano Farming Company (Nocera Terinese, CZ, Italy). A commercial biodegradable blown film, named Bioter (Euromaster, Pistoia, Italy), made by Poly(lactic acid) and Poly(butylene adipate-co-terephthalate) blend, having a thickness of 22 ± 1.0 μm, was used as substrate for the production of the active coatings.

PLA4060 (Natureworks, Minnetonka, USA), characterized by a D-lactide content of 12 wt%, that confers an amorphous morphology to the material, was used for the coating layer. DPPH (2,2-diphenyl-1-picrylhydrazyl), Trolox ((±)-6-Hydroxy-2,5,7,8-tetramethylchromane-2-carboxylic acid), Tween 80 surfactant and Fehling reagents were obtained from Sigma Chemical Co. (St. Louis, Mo., USA). All organic solvents used were analytical grade.

Characterization of the olive milling wastewater extracts

The dry matter content of the phenolic extracts was determined by means of Sartorius Moisture Analyzer MA100 (Sartorius AG, Göttingen, Germany).

Reducing sugars were evaluated by Felhing assay, a volumetric method to define the reducing sugars in food. A mixed Fehling's solution and methylene blue as indicator were used in titration. Fehling solution A is made from copper (II) sulfate pentahydrate ($CuSO_4$, $5H_2O$) dissolved in water and Fehling solution B contains potassium sodium tartrate tetrahydrate (Rochelle salt) ($KNaC_4H_4O_6$,$4H_2O$) and sodium hydroxide (NaOH) in water. 5 ml of Fehling A and 5 ml of Fehling B were put into a 200 mL Erlenmeyer flask and 40 ml of water were added. This mixture was placed in a small furnace and heated to the boiling point in the presence of a few glass beads to prevent bumping. A 25 mL burette was filled up with diluted sample.

From the burette the sample solution was added slowly to mixed Fehling's solution as boiling continued. When the colour has become brick red, three drops of methylene blue indicator was added and the titration was continued. The titration was finished when the colour was became strong brick red or cherry red. The results were expressed in g of reducing sugars in 100 g of phenolic extract (dry basis).

The antioxidant activity of OWEs was analyzed using the stable radical 2,2-diphenyl-1-picrylhydrazyl (DPPH) as reported in the previous chapter in the "Olive Pomace Extract Characterization" paragraph (V.2). The control was conducted using distilled water. All analyses were performed in triplicate, and the obtained values were expressed as millimoles of Trolox equivalents (mmolTrolox/g dry matter), based on a standard curve of Trolox (6-Hydroxy-2,5,7,8-tetramethylchromane-2-carboxylic acid).

Color measurements were carried out on the extracts by using a colorimeter CIE-Lab (Chroma Meter II Reflectance CR-300, Minolta, Japan), equipped with a CIE standard D65 illuminant. The results were expressed according to color coordinates L*, a*, b*, hue value ($\tan^{-1}$ b*/a*) and saturation index, chroma ($(a^2+b^2)^{1/2}$). Chroma indicates the dullness/vividness of a product, while the hue angle is how an object's color is perceived by human eye: red, orange, green or blue (CIEL*a*b* colour system, 1986).

Realization of the active biodegradable coatings

The preliminary investigations on the available phenolic extracts allowed to select the best candidate for the production of the active packaging. Then, antioxidant multilayer films were realized by precipitation, induced by solvent evaporation, of a PLA4060/Acetone coating solution (with mass ratio 20:80), incorporated at different percentages of the selected active phase (0, 1, 3% w/w_{PLA}) under magnetic stirring.

Non-ionic surfactant Tween 80 (HLB value=15) was previously added to the water-based extract (1% w/w_{OE}), in order to enhance solubilization with PLA solution and avoid precipitation.

The casting mixture was then spread on the biopolymer substrate made of PLA and polybutylene adipate terephthalate (PBAT), by means of a K Hand Coater (RK, Printocoat Instruments Ltd., Litlington, UK), equipped with stainless steel close wound rod, with wire diameter equal to 0.64 mm, yielding final coatings with comparable thicknesses, as listed in Table 34.

Solvent was evaporated at room conditions overnight, then the coated films were stored under vacuum sealing in aluminium bags before analysis.

The coating technology avoided thermal stresses to the thermo-sensitive active phase, while PLA coating enabled an all eco-compatible, 100% biodegradable multilayer films. The coating layer thickness was evaluated as

difference among the total thickness of the coated films and the Bioter substrate thickness.

Film samples were stored under vacuum in aluminium bags before the utilization.

Table 34 List of the prepared films with their composition and thicknesses.

Sample Film	OWE concentration [%w/w_{WPI}]	Thickness of the coating layer [µm]	Total Thickness [µm]
Bioter	0	0	22 ± 1.0
Bioter/PLA	0	7 ± 0.4	29 ± 1.4
Bioter/PLA-5%OWE	5	7 ± 0.6	29 ± 1.6
Bioter/PLA-10%OWE	10	7 ± 0.8	29 ± 1.8
Bioter/PLA-20%OWE	20	8 ± 0.4	30 ± 1.4

Characterization of the active coated films

Surface energy and wettability were evaluated by static contact angle measurements, which were performed with a First Ten Angstrom Analyzer System 32.0 mod. FTA 1000 (First Ten Angstroms, Inc., Portsmouth, VA, USA), according to the standard test method ASTM D5946. The dispersion (γ_s^d) and polar (γ_s^p) components of the surface energy (SE) were calculated according to the Owens-Wendt geometric mean equation, using distilled water and ethylene glycol as testing liquids. The drop volume was taken within the range where the contact angle did not change with the variation of the volume (2.0 ± 0.5 µL). Each reported value of the contact angle is the average of at least ten replicate measurements.

The release kinetic of the antioxidant films was evaluated by total immersion method. 95% v/v Ethanol was selected as release medium, as fatty foods simulant (D2) according to the Regulation (EU) 10/2011. Film samples were cut in rectangles of surface area equal to 2 dm^2 and immersed in 100 mL of 95% ethanol in 250 mL flasks. The flasks were kept in the dark under magnetic stirring, to minimize mass transfer resistance of antioxidants from the film, at room conditions for 13 days. Two milliliters of the food simulant were periodically sampled for quantification, and then reinserted.

The concentration of antioxidants released into the simulant was quantified using a UV-Vis spectrophotometer (Lambda Bio 40, Perkin Elmer, Waltham, MA, USA) at 280 nm, on the basis of a standard curve (0-600 ppm). The selected wavelength was the one at which the maximum absorbance of the olive pomace extract was found. To eliminate the influence of other polymer additives, release studies were also conducted on the control films (Bioter and Bioter/PLA) and no significant absorbance at 280 nm was observed. Results were expressed as percent ratio of M_t/M_∞ (M_t is the concentration of antioxidant (mg/mL) diffused at time t, and M_∞ represents the concentration of antioxidant diffused at equilibrium).

The antioxidant activity released into the simulant solution was assessed by DPPH method, using the same method as described in the "Olive Pomace Extract Characterization" paragraph. The blank was conducted using the pure release medium instead of the sample. All analyses were performed in triplicate, and the obtained values were expressed as µmolTrolox/L, based on the standard curve of Trolox. The maximum antioxidant activity was also expressed per unit volume of the coating, in mmolTrolox/dm^3.

Oxygen permeability tests were performed by GDP-C gas permeabilimeter (Brugger, Munchen Germany) at 23°C and 0% R.H., with the oxygen flow rate of 80 mL/min, according to the ASTM D1434 procedure.

Water vapor permeability was measured by M7002 Water Vapor Permeation Analyzer (Systech Instruments Ltd, Oxfordshire, UK) according to the standard ASTM F1249. Films were tested at 23°C and 50% R.H., and the results, performed in triplicate, were expressed as PWV (g m/(m^2 Pa s)), according to Equation (45).

Mechanical tensile tests were carried out according to the standard ASTM D 882 using the a CMT 4000 Series tensile tester (SANS, China) equipped with a 100 N load cell. Film specimens were cut with a rectangular geometry (12.7x80 mm^2) along the coating direction. The crosshead speed of the test was kept at 5 mm/min for the calculation of the Elastic modulus, and at 500 mm/min for the evaluation of the properties at break.

Colour measurements were carried out the films by using a colorimeter CIE-Lab (Chroma Meter II Reflectance CR-300, Minolta, Japan) and the results were expressed according to colour coordinates L* (darkness/lightness), a* (greenness/redness), b* (blueness/yellowness). The chromatic parameters were evaluated soon after the coatings production (i.e. at time 0) and at regular time intervals (up to 70 days) exposing films to natural light, in order to evaluate possible effects due to photo-oxidation phenomena. The colour variation of the films over time was evaluated by Δa* Δb* parameters, and by means of the colour-difference equation CIELAB ΔE*ab, based on the coordinates L*, a* e b*.

VI.3 Results and discussion: Olive Pomace Extract

Dry matter content, reducing sugars, antioxidant activity and color of the Olive Wastewater Extract

All the investigated olive wastewater extracts were in form of liquid samples, with a density comparable to that of an aqueous solution, more or less concentrated. Table 35 shows the dry matter, reducing sugars and antioxidant activity of the olive wastewater extracts under investigation. The results are expressed over dry matter in order to better compare the physico-chemical properties and the antioxidant activity of the phenolic extracts.

Table 35 Dry matter (DM), reducing sugars (RS) and antioxidant activity (AA) of the olive wastewater extracts under investigation. Results are expressed as mean ± SD (standard deviation) of three determinations.

Sample	DM [g/L]	RS $\left[\frac{g}{100g\ of\ dry\ matter}\right]$	AA $\left[\frac{mmol\ Trolox}{g\ dry\ matter}\right]$
OWE1	614 ± 3.1[b]	10.67 ± 0.5[b]	733.13 ± 15.41[a]
OWE2	687 ± 3.2[c]	12.57 ± 0.6[c]	793.53 ± 22.39[b]
OWE3	530 ± 3.1[a]	8.68 ± 0.6[a]	937.20 ± 25.15[c]

[a,b,c] *Values followed by the same letter within the same column were not significantly different according to Duncan's test (P < 0.05)*

The content of reducing sugars has been evaluated because the polar nature of the aldehyde and ketone groups may interfere with the nonpolar nature of the polymeric PLA coating mixture, inducing a precipitation of the active compound and consequently entailing the addition of a higher content of surfactant to stabilize the emulsion. In particular, the reducing sugars content was found proportional to the dry matter of the samples, with values equal to 10.67, 12.57 and 8.68 g/100g of dry matter for the OWE1, OWE2 and OWE3, respectively.

Regarding the antioxidant activity, the results highlighted the higher antioxidant activity for the OWE3 sample (937.20 mmol Trolox/g of dry matter) followed by OWE2 and OWE1 (793.53 and 733.13 mmol Trolox/g of dry matter, respectively).

In all cases, the antioxidant activity of the OWE analyzed was found much higher than that of Olive Pomace Extract (OPE) characterized in the previous chapter (Table 23) and of available literature data reported in Table 24. The highest antioxidant activity of the extract with lower dry matter content suggests a better preservation of the bioactive components in the OE3 extract, and highlighted the critical role of the pre-treatment conditions in preserving the effectiveness of the phenolic components.

The color of the samples was then evaluated by colorimetric analysis, and the associated parameters are shown in Table 36. All the extracts were characterized by a dark brown color, as confirmed by high Hue angle (ranging from 322.50 to 324.20 °) and a saturation value (C^*_{ab}) always lower than 13. The typical color was due to polymerization of tannins and low molecular weight phenolic compounds, as also reported by Otles and Semih, 2012.

Table 36 CieLab color parameters of the olive wastewater extracts.

Sample	L*	a*	b*	h_{ab} [°]	C^*_{ab}
OWE1	19.8 ± 0.02^{b}	9.31 ± 0.18^{a}	-6.71 ± 0.31^{b}	324.20 ± 0.75^{a}	11.48 ± 0.32^{a}
OWE2	20.3 ± 0.06^{c}	8.58 ± 0.32^{a}	-6.42 ± 0.37^{b}	323.21 ± 1.14^{a}	10.72 ± 0.45^{a}
OWE3	18.5 ± 0.24^{a}	10.35 ± 0.75^{b}	-7.93 ± 0.27^{a}	322.50 ± 1.27^{a}	13.04 ± 0.75^{b}

^{a,b,c} Values followed by the same letter within the same column were not significantly different according to Duncan's test ($P < 0.05$)

The results obtained from characterization of phenolic extracts pointed out the highest antioxidant activity and the lowest reducing sugars content of the OWE3 sample, which was then selected as the most suitable for the production of the active multilayer films.

VI.4 Results and discussion: Active biodegradable coatings based on the Olive Pomace Extract

Evaluation of wettability and surface energy

The surface wettability of the Bioter/PLA coated films was estimated by contact angle measurements, and by evaluating the surface energy and its polar (γ_s^p) and dispersive (γ_s^d) components (Table 37).

The pure PLA coated sample (Bioter/PLA) shows a total surface energy and γ_s^p and γ_s^d components comparable with that reported in literature by other authors (Gonçalves et al., 2013).

The addition of the olive wastewater extract leads to an increase of the polarity of the coated surface, as underlined by the decrease of CA_w values (equal to 69.7, 67.9 and 60.7 for films at 5%, 10% and 20% OWE, respectively) and by the increase of the polar component of surface energy (equal to 21.2, 22.1 and 35.9 for films at 5%, 10% and 20% OWE, respectively), with respect to Bioter/PLA sample.

The increase of surface water wettability can be attributable to the high water content of the active phase, and becomes more significant at the highest OWE percentage. As for the dispersive component γ_s^d, no significant variations were observed up to 10%OWE concentration (γ_s^d equal to 12.2 and 12.3 dyne/cm for samples at 0, 5 and 10% OWE, respectively), while a strong decrease up to 5.4 dyne/cm is observed for the Bioter/PLA-20%OWE sample.

Table 37 Static water (CAw) contact angle, surface energy and dispersive (γ_s^d) and polar (γ_s^p) components for the neat Bioter substrate and for the PLA coated films at 0, 5 and 10 % OWE content.

Sample Film	CA_w [°]	SE [dyne/cm]	γ_s^p [dyne/cm]	γ_s^d [dyne/cm]
Bioter	80.6 ± 3.2	25.5	22.6	2.9
Bioter/PLA	70.0 ± 0.5	32.8	20.6	12.2
Bioter/PLA-5%OWE	69.7 ± 1.2	33.5	21.2	12.3
Bioter/PLA-10%OWE	67.9 ± 0.9	34.4	22.1	12.3
Bioter/PLA-20%OWE	60.7 ± 2.5	41.3	35.9	5.4

Study of the release kinetic and antioxidant activity of the films

The films potential as effective carriers for the antioxidant release during the time was evaluated by release tests in 95% Ethanol, as selected simulant for fats, oil and fatty foods.

Figure 56 shows the OWE release kinetic for the active films in 95% Ethanol, expressed as percent ratio of M_t/M_∞. Figure 57 depicts the antioxidant activity measured in the food simulant during the time, expressed as µmolTrolox/L, while Table 38 reports the maximum antioxidant activity per unit volume of the coating, expressed as mmolTrolox/dm^3, and the time at which the maximum antioxidant activity is reached.

In the complex system polymer-active-simulant under investigation, it is important to take into account a number of features, such as the hydrophilic nature of the active phase, but also the strong swelling and penetrating action of ethanol towards the amorphous PLA (Scarfato et al., 2017). Indeed, the release of the antioxidant from the biopolymer coating is the result of many factors, including not only the antioxidant-simulant affinity and the interactions among the polymer chains and the active agent, but also structural changes of the polymer matrix induced by the contact with the food simulant (Wicochea-Rodríguez et al., 2019). All parameters involved in the matrix formulation such as nature of biopolymer, dispersion of the polymer in the solvent used, addition of plasticizers or emulsifiers and drying conditions are key parameter affecting the release kinetic of the active phase.

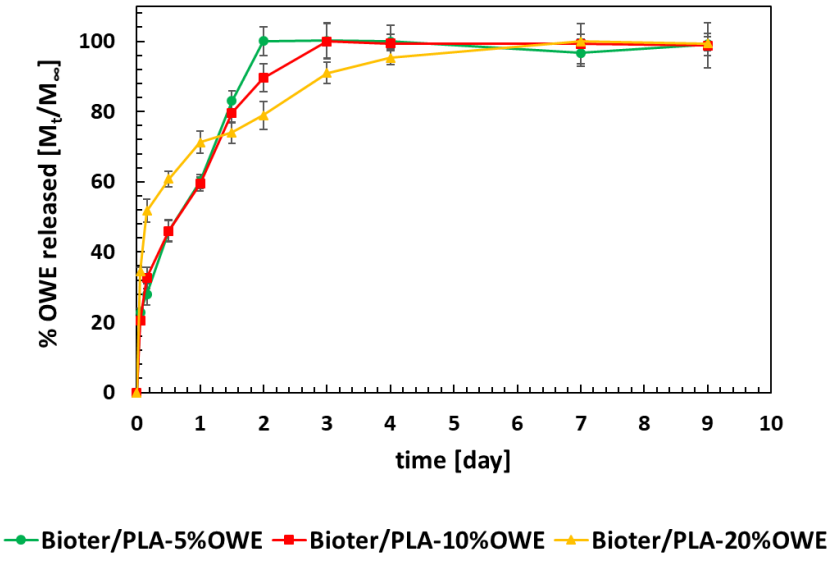

Figure 56 OWE release rate (Mt/M∞) from active coated films in 95% Ethanol, at 23°C.

As it is possible to observe from Figure 56, the films at 5% and 10% OWE follow almost the same release kinetic within the first 36 hours. In particular, the percentage of antioxidant released is equal to 23-20%, 28-32%, 46%, 60% and 83-79% after 1, 3, 12, 24 and 36 hours, respectively, suggesting for these samples similar morphology and mass transport interactions regulating the diffusion mechanism. The equilibrium was reached after 48 and 72 h, respectively.

By contrast, the Bioter/PLA-20%OWE film shows a different release behavior at short (t < 24 h) and long (t > 24 h) times. For t <1 day, the release rate is maximum for this sample, and the percentage of antioxidant released is equal to 34%, 52%, 61%, 71% after 1, 3, 12 and 24 hours, respectively. After 24 hours, slower kinetics are established, and the system reaches the equilibrium after 7 days of test.

For this sample, an uneven distribution of the active phase within the coating thickness is conceivable, being more concentrated on the coating surface, at the interface with the release medium. This leads to a faster initial release of the antioxidant; as the diffusion involves the inner side the coating, the resistance to diffusive transport increases by increasing the concentration of the olive wastewater extract.

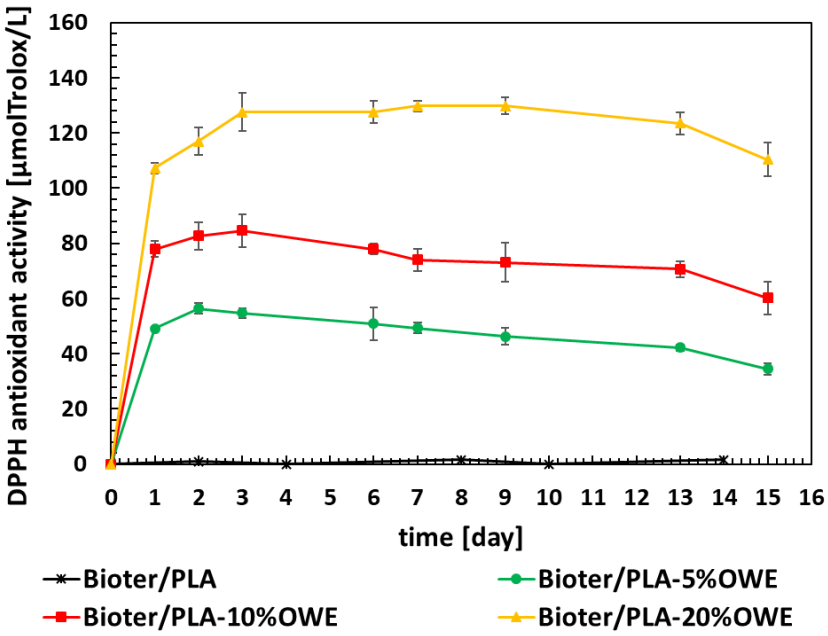

Figure 57 DPPH antioxidant activity (expressed in µmolTrolox/L) released from active coated films in Ethanol 95%, at 23°C.

Table 38 Time at which the maximum antioxidant activity is reached, and average maximum antioxidant activity (expressed as mmol Trolox/dm^3) for the active coated films.

Sample Film	Time at max antioxidant activity [d]	Average max. antioxidant activity [mmolTrolox/dm^3]
Bioter/PLA-5%OWE	2	28.21 ± 1.93
Bioter/PLA-10%OWE	3	42.31 ± 2.2
Bioter/PLA-20%OWE	7	64.86 ± 1.2

Regarding the antioxidant activity (Figure 57) as expected, no significant antioxidant activity was found for the pure PLA coated film. A less than linear increase of antioxidant capacity was observed with increasing OWE content, with a maximum antioxidant activity equal to 28.21 ± 1.93, 42.31 ± 2.2 and 64.86 ± 1.2 mmolTrolox/dm^3 for Bioter/PLA-5%OWE, Bioter/PLA-10%OWE and Bioter/PLA-20%OW samples, respectively (Table 38). Also in this case, as for the WPI/OPE based systems, it is clear how the proper design of the systems composition allows to tune the release kinetic and the final antioxidant activity, offering the possibility of tailoring the films performance according to the shelf-life requirements of the target food.

Evaluation of barrier, tensile properties and optical properties

The results of films characterization in terms of oxygen transport properties are summarized in Table 39. As for the water vapor permeability and the tensile properties, these were investigated among the pure substrate, the pure PLA coated sample and the active film at 5%OWE, taken as example as an intermediate concentration.

Results are summarized in Table 40.

From the comparison between Bioter and Bioter/PLA samples, it is possible to observe that the PLA coating layer addition resulted in a slight reduction in the permeability of the substrate to both oxygen and water vapor (from 51.5 to 40.8 cm^3 mm/(m^2 d bar) and from 9.19 to 8.31 g m/(m^2 Pa s), respectively).

Table 39 Oxygen permeability (P_{O2}) for the neat Bioter substrate and for the PLA coated films at 0, 5, 10 and 20% OWE concentration.

Sample Film	P_{O2} $[\frac{cm^3 mm}{m^2 d\ bar}]$
Bioter	51.5 ± 3.5
Bioter/PLA	40.8 ± 0.9
Bioter/PLA-5%OWE	37.1 ± 2.7
Bioter/PLA-10%OWE	38.5 ± 2.1
Bioter/PLA-20%OWE	33.7 ± 1.2

The further addition of the active agent did not significantly affect the oxygen permeability of the multilayer films, except at 20% OWE content, for which a slight additional reduction in the P_{O2} value (equal to 33.7 ± 1.2 cm^3 mm/(m^2 d bar), is observed.

As for the water vapor permeability, a slight increase in the P_{WV} values among Bioter/PLA-5%OWE and Bioter/PLA was observed. This could be attributed to an increased affinity of the active coating to the permeating water vapor molecules, due to the inherent high polarity of the active phase. However, the increment is negligible, in order to assess the performances of the film in the real working conditions.

Table 40 Water vapor permeability (P_{WV}), Elastic modulus (E), tensile strength (σb), and elongation at break (εb) for the neat Bioter substrate and for the PLA coated films at 0 and 5% OWE concentration.

Sample Film	$P_{WV} \cdot 10^{12}$ $[\frac{g\ m}{m^2 d\ Pa}]$ $[\frac{g\ m}{m^2 d\ Pa}]$	E [MPa]	σb [MPa]	εb [%]
Bioter	9.19 ± 3.5	332 ± 17	22.5 ± 1.2	276 ± 22
Bioter/PLA	8.31 ± 0.9	645 ± 45	23.3 ± 1.4	255 ± 18
Bioter/PLA-5%OWE	9.99 ± 2.7	772 ± 34	21.4 ± 1.7	252 ± 33

Both oxygen and water vapor permeability values obtained for these biodegradable systems are at least two orders of magnitude higher than those obtained for PET/WPI coated films (Table 30). On this basis, as possible applications, the Bioter/PLA-OWE films could be suitable to package sensitive foods as horticultural products, requiring adequate oxygen and water vapor permeability to avoid anoxic conditions and condensation of water vapor inside the package (Robertson et al., 2013).

When comparing the mechanical properties, the main differences were obtained among the pure substrate and the Bioter/PLA coated sample. Bioter substrate is a tear-resistant and flexible film, thanks to the presence of PBAT which increases overall flexibility. The elastic modulus of the pure substrate is equal to 332 MPa, lower than that of PLA (ca. 2220 MPa), and closer to that of PBAT (ca. 120 MPa) (Arruda et al., 2015). The tensile strength and elongation at break for this sample are equal to 34.9 ± 4.3 MPa and 276 ± 20 %, respectively, and are in accordance with the literature data relating PLA/PBAT mixtures with different mass ratios (Coban et al., 2017; Tiimob et al., 2018; Wang et al., 2016).

For the Bioter/PLA sample, the increase of E value to ca. 664 MPa is a consequence of the deposition of the PLA4060 coating layer that is an inherently brittle and fragile polymer, characterized by a high Young's modulus. As for active film, compared to the Bioter/PLA, the incorporation of the active phase at the percentage investigated involves only minor variations in the elastic modulus and the properties at break, which remain substantially unchanged.

The visual examination of the films showed that Bioter substrate was white, opaque and matte, while Bioter/PLA films were white, opaque and opalescent. The effect of antioxidant concentration on colour parameters is shown in Table 41.

Instrumental colour analysis of the films showed that the incorporation of both antioxidants gave a coloured taint to the films. Films containing the antioxidant showed higher a* and b* values with increasing concentration of antioxidant. The presence of the highest OWE concentration also resulted in darker films in comparison with the Bioter/PLA sample (L* coordinate equal to 93.9 ± 0.8 and 97.3 ± 0.8, respectively).

Table 41 CieLab color coordinates L, a* and b* for the neat Bioter substrate and for the PLA coated films at 0, 5, 10 and 20% OWE concentration. Chromatic variation ΔE*ab, calculated with respect to the Bioter substrate, is also reported.*

Sample Film	L*	a*	b*	ΔE*ab
Bioter	96.9 ± 0.2	-0.74 ± 0.12	2.28 ± 0.20	-
Bioter/PLA	97.3 ± 0.8	-0.80 ± 0.25	2.27 ± 0.26	0.4
Bioter/PLA -5%OWE	96.7 ± 0.3	-1.04 ± 0.30	3.98 ± 0.11	1.73
Bioter/PLA -10%OWE	96.2 ± 1.5	-1.51 ± 0.33	6.02 ± 0.44	3.8
Bioter/PLA -20%OWE	93.9 ± 0.8	-1.80 ± 0.56	11.9 ± 0.63	10.1

This was confirmed with ΔE^*_{ab} (total colour change) parameter (Table 41). The films containing olive wastewater extract experienced bigger ΔE^*_{ab} than those added with olive pomace extract (Table 33). Similar outcomes were found by other authors (Marcos et al., 2013; Manzanarez-López et al., 2011) reporting increased yellowness in PLA films containing olive leaves extract or α-tocopherol.

In order to analyze the photo-oxidative stability of the films over the time, the variation of a* and b* coordinates with respect to time 0 was measured over 73 days. The calculated trends of Δa* and Δb* are shown in Figure 58 (A) and (B). Also there is no significant colour change for the Bioter substrate and the pure PLA coating, while the PLA/OWE coatings undergo an increase in redness (Figure 58 (A)) and yellowness (Figure 58 (B)) of the samples, more significant by increasing the antioxidant content. In particular, the total increase in Δa* and Δb* parameters, after 73 days, was equal to -0.23, -0.4, -0.44 and 0.88, 1.46, 2.16 for the films at 5%, 10% and 20% OWE, respectively.

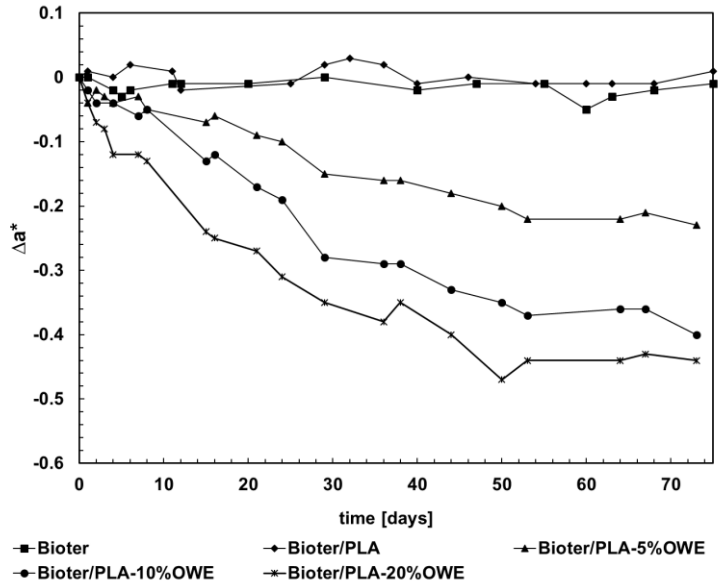

(A)

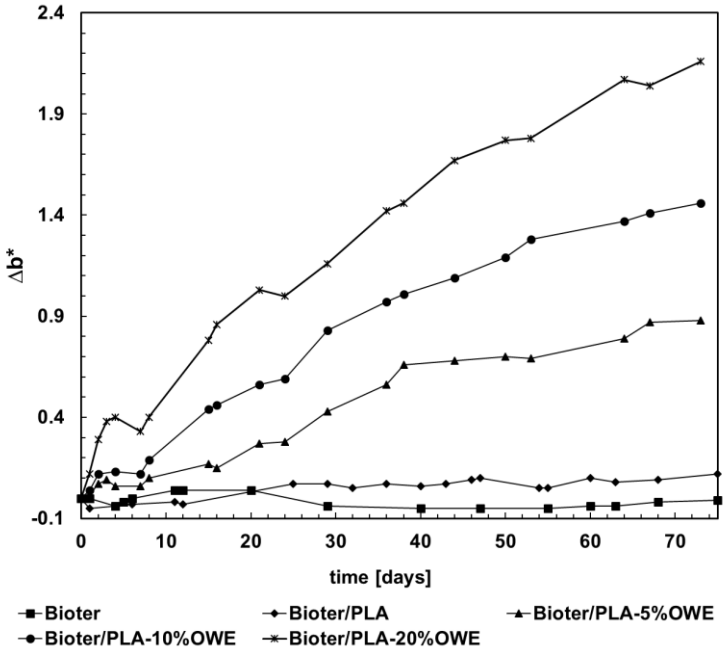

(B)

Figure 58 Change in redness ($\Delta a^*=a|_t - a|_{t=0}$, (A)) and yellowness ($\Delta b^*=b|_t - b|_{t=0}$, (B)) during the time, for the Bioter substrate and PLA coated films at 0, 5, 10 and 20% OWE concentration.

VI.5 Summary and conclusions

This is a further step forward in the realization of eco-sustainable active films, based on revalued food industry waste products. 100% biodegradable antioxidant films, loaded with olive milling wastewater extracts, were successfully produced by coating technique.

The results of the preliminary investigation, carried out on the available phenolic extracts, identified the OWE3 as the best candidate for the development of the active bio-coatings, thanks to its highest antioxidant activity and lowest content of polar functional groups, which allowed an easier incorporation within the PLA non-polar coating solution.

The incorporation of the olive wastewater extract within 5-20% w/w range into the multilayer films did not significantly affect the functional performance of the systems, required for food packaging applications in real working conditions.

The release and DPPH antioxidant activity tests proved that the films are able to be used as carriers for the controlled release of the antioxidant agent. In particular, both the antioxidant activity and the release time increased by increasing the active agent concentration, while the diffusion kinetic is influenced by the composition and morphology of the bio-active coatings.

Also in this case, as for the WPI/OPE based systems, the proper design of the systems composition allows to tune the release kinetic and the final antioxidant activity, offering the possibility to tailoring the films performance according to the shelf-life requirements of the target food.

These results, coupled with the lower barrier performance of the films, suggest their possible application to preserve sensitive foods as horticultural products, requiring adequate oxygen and water vapor permeability to avoid anoxic conditions and condensation of water vapor inside the package. To this aim, shelf life tests are now ongoing using avocado slices, as target food for fresh, oxygen-sensitive fatty food matrices, as part of future works deriving from the thesis project.

Chapter VII

Concluding remarks

VII.1 Conclusions

In recent years, active packaging has revolutionized the concept of food preservation. Packaging is no longer seen as a simple container with generic protection functions, but as the main actor in food shelf-life extension, vigorously contributing to the reduction of spoilage, food waste, food recalls, and foodborne illness outbreaks.

However, achieving the optimum performance of an active packaging is not an easy task, and requires the packaging engineer to take account of a multiplicity of targets. The main goals include the achievement of tailor-made performance, based on the food preservation requirements, and satisfactory functional properties; the use of commercially viable processes, to produce large volume of films; and the compliance with the sustainability requirements dictated by the circular economy model.

Therefore, the proper design plays a crucial role in this process, in order to obtain structures that are truly effective, competitive on the market and that constitute a real added value for food waste reduction, rather than an additional economic and environmental cost.

These considerations constituted the starting point for the development of this PhD work, which involved the design, the realization and the study of effectiveness of new multifunctional, sustainable active films for food packaging applications.

All the active films developed demonstrated their potential, acting as oxygen scavengers or carriers for the controlled release of antimicrobials and antioxidants.

Particular attention was paid to the innovative eco-design of the systems, selecting completely recyclable materials, as PET, or biodegradable polymers, such as PLA, PBAT and WPI. Innovative routes for the

valorization of re-evaluation of food industry wastes and by-products were also investigated.

At the same time, the research project had industrial feasibility as one of its main targets, involving conventional technologies, such as extrusion and coating, widely used in the food packaging industry.

In the first section of the PhD work, mono-material, active films based on polyethylene-terephthalate (PET) and co-polyester oxygen scavengers (OS) were realized by extrusion process. Two strategies were studied to prolong the effectiveness of the OS during the time (Chapters II and III).

The first one involved the realization of multilayer structures by cast co-extrusion, inserting the active layer, at an optimized concentration (10% w/w) of OS, between two PET inert layers, capable to control the oxygen diffusion through the core. Four different configurations were designed, and the scavenging properties were extensively investigated, exploring the influence of the multilayer layout on absorption kinetic and parameters.

The second strategy involved the realization of single layer active PET films, blending the OS with a second, high-oxygen barrier phase.

Single-layer active PET structures were produced by cast extrusion, and the concentration of the 2-phases OS (ranging from 5 to 20%) was optimized. The absorption performances were thoroughly analyzed and compared with those of the multilayer films, highlighting the similarities, the application potentialities and the advantages of each.

Both the investigated approaches were successful in controlling the oxygen scavenger (OS) exhaustion kinetics and prolonging the films effectiveness over time.

As discussed in Chapter II, the active PET multilayer films were effective in decelerating the oxygen permeation through the core layer, with an increase of the exhaustion times from 130 hours, for the active monolayer film, up to 550 hour, for the most performing multilayer layout.

From the comparison among all the multilayer configurations, it was also possible to discriminate the influence of the multilayer layout on the O_2-scavenging parameters.

As showed in Chapter III, also the OS enhancement with a high-oxygen barrier phase demonstrated relevant benefits in extending the films absorption kinetics. The OS composition was optimized at 10%w/w, with a maximum exhaustion time equal to 600 h. As it turned out, both technologies represent a valid solution to effectively prolong the durability of the scavenger over the time, and the alternative choice of one or the other might depend on the available processing facilities or the gas absorption requirements at very short time.

The simulation results of the mathematical model developed were in good agreement with the experimental ones, and highlighted the potential of the virtualization tool as rapid and reliable method for optimizing the

scavenging performance of active films and confidently extrapolating predictive data, thus reducing the experimental matrix to explore.

Moreover, the shelf life tests underlined the suitability of both multilayer and single-layer films to preserve sensitive foods with slow oxidation rate and medium-long storage term.

Among the controlled-release systems, the active bio-coatings loaded with 5, 10 and 20% of LAE antimicrobial (Chapter IV), demonstrated their the effectiveness in releasing the antimicrobial agent and inhibiting microbial growth. In particular, the inhibition of microbial strain was found proportional to the LAE concentration into the PLA matrix, with 5.17 log decrease of viable counts at 5% LAE and total inhibition measured for coating formulations at higher LAE content. The migration kinetics proved that the films were able to immediately release an amount of antimicrobial agent, already at the minimum LAE concentration, sufficient to achieve an antimicrobial effect comparable with or higher than currently commercially available antimicrobial films and coatings for foods and pharmaceuticals. Furthermore, the functional performance of the films, in terms of adhesion, barrier and optical properties, were not significantly affected.

As for the antioxidant bio-coatings loaded with olive pomace extract (OPE) (Chapter V), the preliminary characterization of the produced OPE highlighted remarkably high hydroxytyrosol concentration and antioxidant activity (equal to 589 mgHyTy/kg_{dm} and 158.4 mmolTrolox/g_{dm}, respectively), higher than the results reported in the literature on olive leaves and pomace extracts. Very good O2-absorption performance was also observed, enhanced by pH increase and trigged by humidity, with a scavenging capacity (in the range 362.3-982.3 mgO2/gGAE and 9.88-26.2 mLO2/g_{dm}) comparable to that of pure gallic acid and in compliance with those required for oxygen scavengers in packaging applications. The oxygen absorption mechanism was also well described by a second-order reaction kinetic model, underlining the possibility to use the mathematical model to predict quite accurately the O2-scavenging performance of a variety of polyphenols.

Basing on these promising results, the OPE was successfully incorporated (at 5% and 10% w/w) in whey protein (WPI) biodegradable coatings, to produce eco-sustainable, high-performance films with antioxidant activity. All the active films showed very high transparency and satisfactory functional performance in terms of adhesion and tensile properties, while the excellent gas barrier offered by WPI coating led to a decrease of the oxygen permeability up to 46% with respect to the neat substrate. What is more, films respected the overall migration limits established by the EU Legislation, and the release tests proved their ability to release the antioxidant agent within fatty foods simulant, with possibility to tune the release rate and time. In particular, an average maximum antioxidant release equal to 29 mmolTrolox/dm^2 was obtained, after 4 and 7 days for the films at

5% and 10% OPE, respectively. These outcomes, coupled with the excellent oxygen barrier performance, suggested films application with greasy foods having high oxygen barrier requirements and medium-long shelf-life.

The 100% biodegradable antioxidant films at 5, 10 and 20 % wt of olive milling wastewater extract (OWE) (Chapter VI) also proved their effectiveness to be used as carriers for the controlled release of the antioxidant agent, with larger antioxidant activity (within the range 28.21-64.86 mmolTrolox/dm^2) and release time (from 2 to 7 days) by increasing the OWE concentration. The OWE addition did not significantly affect primary functionalities required for films suitable for food packaging applications. At the same time, the encouraging results obtained endorsed the promising perspectives for films to be used as 100% green alternative for the preservation of oxidative-sensitive food products with high respiration rates.

To conclude, the numerous packaging structures developed have all demonstrated their potential in extending the shelf life of foods, interacting with a multiplicity of deterioration mechanisms. The tailor-made performance of all the films also allow to satisfy the preservation needs of a wide range of foods (fresh-cut vegetables or fruits, dry or fat products) with short, medium or long storage time.

The approach used ensured to obtain highly eco-compatible and sustainable packages, with multiple satisfactory functional properties, allowing to overcome the linear economic model "take-make-dispose", in favor of the adoption of the most advantageous model of circular economy, capable of self-sustaining and regenerating.

Future research efforts needs to keep on focusing on testing the films effectiveness on real food matrices, as well as organoleptic tests are recommended.

To this aim, shelf life tests on minced poultry meat, buffalo butter and avocado are currently ongoing on the antimicrobial and antioxidant films, with encouraging preliminary results, and the future outcomes will be part of future works deriving from the thesis project.

Literature cited

Abdullah N.A.S., Mohamad Z., Che Man S.H., Baharulrazi N., Majid R.A., Jusoh M., Ngadi N., 2019. Thermal and toughness enhancement of poly (lactic acid) bio-nanocomposites, Chem. Eng. Trans. 72, 427-432.

Adobati A., Uboldi E., Franzetti L., Limbo S., 2015. Shelf life extension of raspberry: passive and active modified atmosphere inside master bag solutions, Chem. Eng. Trans. 44, 337-342.

Adiletta G., Russo, P., Proietti N., Capitani D., Mannina L., Crescitelli A., Di Matteo, M., 2015, Characterization of pears during drying by conventional technique and portable non invasive NMR, Chem. Eng. Trans. 44, 151-156.

Adur, A.M., Marano, G.A., Volpe, R.A., Mei, H.L. 2000. Oxygen-Scavenging Filled Polymer Blend for Food Packaging Applications. U.S. Patent 6,037,022.

Ahn B.J., Gaikwad, K.K., Lee, Y.S. 2016. Characterization and properties of LDPE film with gallic-acid-based oxygen scavenging system useful as a functional packaging material. J. Appl. Polym. Sci. 133, 1–8.

Ajila C.M., Brar S.K., Verma M., Tyagi R.D., Godbout S., Valero J.R., 2010, Extraction and Analysis of Polyphenols: Recent trends. Critical Reviews in Biotechnology, 31. 227-49.

Amaro-Blanco G., Delgado-Adámez J., Martín M. J., Ramírez R., 2018, Active packaging using an olive leaf extract and high pressure processing for the preservation of sliced dry-cured shoulders from Iberian pigs. Innovative Food Science and Emerging Technologies, 45, 1–9.

Amorati, R., Foti, M. C., & Valgimigli, L. 2013. Antioxidant activity of essential oils. J. Agric. Food Chem. 61, 10835–10847.

Andersen, H.J., Bertelsen, G., Boegh-Soerensen, L., Shek, C.K., Skibsted, L.H. 1988. Effect of light and packaging conditions on the colour stability of sliced ham. Meat Science, 22, 283-92.

Anonymous, 2019a. Active And Intelligent Packaging Market - Growth, Trends, And Forecast (2020-2025).

https://www.mordorintelligence.com/industry-reports/active-and-intelligent-packaging-market-industry.
Anonymous, 2019b. Plastics – the Facts 2019. An analysis of European plastics production, demand and waste data. https://www.plasticseurope.org/it.
Anonymous, 2018. Rapporto Annuale Assobioplastiche. http://www.assobioplastiche.org/
Anonymous, 2018b. PolyOne Amosorb, Amosorb Plus and Amosorb SolO_2 Product Information & Technical Data Sheet, http://www.polyone.com/products/polymer-additives/oxygen-scavengers/colormatrix-amsorb-solo2-co2-barrier-pet, (Accessed 21/01/2018).
Anonymous, 2017. Oxygen Scavengers Market. Market research report, Grand View Research. https://www.grandviewresearch.com/press-release/global-oxygen-scavengers-market.
Anthierens, T., Ragaert, P., Verbrugghe, S., et al. 2011. Use of endospore-forming bacteria as an active oxygen scavenger in plastic packaging materials. Innov. Food Sci. Emerg. Technol. 12, 594-599.
Aouidi, F., Dupuy, N., Artaud, J., Roussos, S., Msallem, M., Perraud Gaime, I., & Hamdi, M. (2012). Rapid quantitative determination of oleuropein in olive leaves (Olea europaea) using mid-infrared spectroscopy combined with chemometric analyses. Ind. Crop. Prod., 37(1), 292–297.
Appendini, P., Hotchkiss, J., H., 1997. Immobilization of Lysozyme on Food Contact Polymers as Potential Antimicrobial Films. Packag. Technol. Sci. 10(5), 271-279.
Arabi, S.-A. A., Chen, X., and Shen, L. (2012). Flavor-release food and beverage packaging. In: Emerging Food Packaging Technologies, pp. 96-107. Woodhead Publishing Limited.
Arrieta, M.P., Castro-López, M. del M., Rayón, E., Barral-Losada, L.F., López-Vilariño, J.M., López, J., González-Rodríguez, M.V. 2014. Plasticized poly(lactic acid)–poly(hydroxybutyrate) (PLA–PHB) blends incorporated with catechin intended for active food-packaging applications. J. Agric. Food Chem. 62, 10170–10180.
Arruda, L.C., Magaton, M., Bretas, R.E., Ueki, M.M., 2015. Influence of chain extender on mechanical, thermal and morphological properties of blown films of PLA/PBAT blends. Polym. Test. 43, 27-37.
Attaran, S. A., Hassan, A., Wahit, M. U. (2015). Materials for food packaging applications based on bio-based polymer nanocomposites. J. Thermoplast. Compos. Mater. 30(2), 143–173.
Aziz, M., & Karboune, S. (2018). Natural antimicrobial/antioxidant agents in meat and poultry products as well as fruits and vegetables : A review. Crit. Rev. Food Sci. Nutr., 58(3), 486–511.

Aznar, M., Gómez-Estaca, J., Vélez, D., Devesa, V., Nerín, C. (2013). Migrants determination and bioaccessibility study of ethyl lauroyl arginate (LAE) from a LAE based antimicrobial food packaging material. Food Chem. Toxicol., 56, 363–370

Bacigalupi, C., Lemaistre, M. H., Boutroy, N., Bunel, C., Peyron, S., Guillard, V., Chalier, P. 2013. Changes in nutritional and sensory properties of orange juice packed in PET bottles: An experimental and modelling approach. Food Chem. 141, 3827–3836.

Bacskai, R., Ching, T.Y., Katsumoto, K. 1997. Oxygen Scavenging Homogeneous Modified Polyolefin-Oxidizable Polymer-Metal Salt Blends. U.S. Patent 5,641,825. Chevron Chemical Company.

Bakal, G., and Diaz, A. (2005). The Lowdown on Lauric Arginate: Food Antimicrobial Hammers Away at Plasma Membrane, Disrupting a Pathogen's Metabolic Process. Food Qual. 12(1), 54-61.

Bastarrachea, L. J., Wong, D. E., Roman, M. J., Lin, Z., & Goddard, J. M. (2015). Active packaging coatings. Coatings, 5(4), 771–791.

Ball, M.J. 1995. Oxidation Studies of a Novel Barrier Polymer System. Ph.D. Thesis. Aston University, Birmingham, UK.

Barbaro, G., Galdi, M.R., Di Maio, L., Incarnato, L. (2015). Effect of BOPET film surface treatments on adhesion performance of biodegradable coatings for packaging applications. Eur. Polym. J. 68, 80-89.

Becerril, R., Nerín, C.,Silva, F. 2020. Encapsulation Systems for Antimicrobial Food Packaging Components: An Update. Molecules, 25(5), 1134.

Becerril, R., Manso, S., Nerin, C., Gómez-Lus, R. (2013). Antimicrobial activity of Lauroyl Arginate Ethyl (LAE), against selected food-borne bacteria. Food Control, 32(2), 404–408.

Behrendt, K., Dauzvardis, M.J., Hoch, R. 2013. Oxygen Scavenging Compositions, Articles Containing Same, and Methods of Their Use. U.S. Patent 2013/0285277.

Ben Salah, M., Abdelmelek, H. 2012. Study of Phenolic Composition and Biological Activities Assessment of Olive Leaves from different Varieties Grown in Tunisia. Medicinal Chemistry, 2(5), 107-111.

Bheda, J.H., Moore, I.V. 2007. Reactive Carriers For Polymer Melt Injection. U.S. Patent 7,294,671.

Blinka, T.A., Edwards, F.B., Miranda, N. R., Speer, D. V., Thomas, J.A. 1998. Oxygen scavenging metal-loaded ion-exchange compositions. U.S. Patent 5,834,079. Grace & Co.-Conn.

Byun, Y., Bae, H.J., Whiteside, S. 2012. Active warm-water fish gelatin film containing oxygen scavenging system. Food Hydrocol. 27, 250-255.

Byun, Y., Darby, D., Cooksey, K., Dawson, P., Whiteside, S. 2011. Development of oxygen scavenging system containing a natural free radical scavenger and a transition metal. Food. Chem. 124, 615-619.

Byun, Y., Kim. Y., Whiteside. S. 2010. Characterization of an antioxidant polylactic acid (PLA) film prepared with α-tocopherol, BHT and polyethylene glycol using film cast extruder. J. Food Eng. 100, 239–244.
Brody, A.L., Strupinsky, E.P. and Kline, L.R. (Eds.) 2001. Active Food Packaging for Food Applications. Boca Raton, FL: CRC Press.
Bugnicourt, E., Schmid, M., Nerney, O.M., Wildner, J., Smykala, L., Lazzeri, A., Cinelli, P. (2013). Processing and validation of whey-protein-coated films and laminates at semi-industrial scale as novel recyclable food packaging materials with excellent barrier properties, Adv. Mater. Sci. Eng. 2013, 1-10.
Bugatti, V., Brachi, P., Viscusi, G., & Gorrasi, G. 2019. Valorization of Tomato Processing Residues Through the Production of Active Bio-Composites for Packaging Applications. Front. Mat. 6.
Buonocore, G., Malinconico, M., Silvestre, C., 2016. Contenuti E Contenitori: Le Nuove Frontiere Del Packaging. http://www.cittadellascienza.it/centrostudi/2016/05/contenuti-e-contenitori-le-nuove-frontiere-del-packaging/.
Busolo, M.A., Lagaron, J.M. 2012. Oxygen scavenging polyolefin nanocomposite films containing an iron modified kaolinite of interest in active food packaging applications. Innov. Food Sci. Emerg. Technol. 16, 211–217.
Cahill, P.J., Chen, S.Y., 2000. U.S. Patent 6,083,585. BP Amoco Corp.
Cardona, E.D, Noriega, M.P, Sierra, J.D. 2011. Oxygen scavengers impregnated in porous activated carbon matrix for food and beverage packaging applications. J. Plast. Film Sheet. 28,63–78.
Carranza, S. 2010a. Modeling of oxygen scavenging polymers and composites. Ph.D. Thesis. University of Texas, Austin, Texas.
Carranza, S., Paul, D.R., Bonnecaze, R.T. 2010b. Design formulae for reactive barrier membranes. Chem. Eng. Sci. 65, 1151–1158.
Carranza, S., Paul, D.R., Bonnecaze, R.T. 2010c. Analytic formulae for the design of reactive polymer blend barrier materials. J. Membr. Sci. 360, 1-8.
Carranza, S., Paul, D.R., Bonnecaze, R.T. 2012. Multilayer reactive barrier materials, J. Membr. Sci. 399, 73-85.
Carrizo, D., Taborda, G., Nerín, C., Bosetti, O. 2016. Extension of shelf life of two fatty foods using a new antioxidant multilayer packaging containing green tea extract. Innov. Food Sci. Emerg. Technol. 33, 534–541.
Cichello, S. A. 2014. Oxygen absorbers in food preservation: a review. J. Food Sci. Tech. 52(4):1889–1895.
Cinelli, P., Schmid, M., Bugnicourt, E., Coltelli, M., & Lazzeri, A. 2016. Recyclability of PET/WPI/PE Multilayer Films by Removal of Whey Protein Isolate-Based Coatings with Enzymatic Detergents. Materials, 9(6), 473. doi:10.3390/ma9060473
Cinelli, P., Schmid, M., Bugnicourt, E., Wildner, J., Bazzichi, A., Anguillesi, I., Lazzeri, A. 2014. Whey protein layer applied on biodegradable

packaging film to improve barrier properties while maintaining biodegradability. Polym. Degrad. Stabil., 108, 151–157.
CIE. Colorimetry, 1986, CIE Publication No. 15.2, Central Bureau of the CIE, Wien, Austria.
Cha, D. ., Cooksey, K., Chinnan, M. ., Park, H. 2003. Release of nisin from various heat-pressed and cast films. LWT - Food Sci. Technol. 36(2), 209–213.
Charles, F., Sanchez, J., Gontard, N. 2006. Absorption kinetics of oxygen and carbon dioxide scavengers as part of active modified atmosphere packaging. J. Food Eng. 72, 1-7.
Chen, X., Chen, M., Xu, C., & Yam, K. L., 2019. Critical review of controlled release packaging to improve food safety and quality. Crit. Rev. Food Sci. Nutr., 59(15), 2386-2399.
Chen, X., Lee, D. S., Zhu, X., and Yam, K. L. 2012. Release Kinetics of Tocopherol and Quercetin from Binary Antioxidant Controlled-Release Packaging Films. J. Agric. Food Chem.. 60, 3492-3497.
Chi-Zhang, Y., Yam, K., Chikindas, M.L. (2004). Effective control of Listeria monocytogenes by combination of nisin formulated and slowly released into a broth system. Int. J. Food Microbiol. 90(1), 15–22.
Ching, T.Y., Goodrich, J.L., Leonard, J.P., Russell, K.W. 2006. Polymer with pendent cyclic olefinic functions for oxygen scavenging packaging. U.S. Patent 7,097,890. Chevron Phillips Chemical Co.
Ching, T.Y., Katsumoto, K., Current, S.P., Theard, L.P. 1997. U.S. Patent 5,627,239. Chevron Chemical
Company.
Ching, T.Y., Katsumoto, K., Current, S.P., Theard, L.P. 1999. U.S. Patent 5,859,145. Chevron Chemical
Company.
Cilliers, J. J. L., and Singleton, V. L. 1989. Nonenzymic autoxidative phenolic browning reactions in a caffeic acid model system. J. Agricult. Food Chem. 37, 890–896.
Cinar, A., Cansev, A., Sahan, Y., 2011. Phenolic Compounds of Olive by-products and Their Function in the Development of Cancer Cells. Biyoloji Bilimleri Araştırma Dergisi – Res. J. Biol. Sci. 4 (2): 55-58.
Cioffi, G., Pesca, M. S., De Caprariis, P., Braca, A., Severino, L., De Tommasi, N. 2010. Phenolic compounds in olive oil and olive pomace from Cilento (Campania, Italy) and their antioxidant activity. Food Chem. 121(1), 105–111.
Çoban, O., Bora, M. Ö., Kutluk, T., Özkoç, G. 2017. Mechanical and thermal properties of volcanic particle filled PLA/PBAT composites. Polym. Compos. 39(S3), E1500–E1511.
Cochran, M.A., Rickworth Folland, J.W.N., Melvin E.R. 1991. Packaging. U.S. Patent 5,021,515.

Collette, W.N. and Schmidt, S.L. 1998. Oxygen scavenging composition for multilayer preform and container. U.S. Patent 5,759,653. Continental PET Technologies, Inc.

Corcuff, R., Arul, J., Hamza, F., Castaigne, F., Makhlouf, J., 1996, Storage of broccoli florets in ethanol vapor enriched atmospheres., Postharvest Biol. Technol, 7(3), 219-229.

Coronel-León, J., López, A., Espuny, M. J., Beltran, M. T., Molinos-Gómez, A., Rocabayera, X., Manresa, A., 2016. Assessment of antimicrobial activity of Nα -lauroyl arginate ethylester (LAE®) against Yersinia enterocolitica and Lactobacillus plantarum by flow cytometry and transmission electron microscopy. Food Control, 63, 1–10.

Correa, J. P., Molina, V., Sanchez, M., Kainz, C., Eisenberg, P., & Massani, M. B. 2017. Improving ham shelf life with a polyhydroxybutyrate/polycaprolactone biodegradable film activated with nisin. Food Packag. Shelf Life, 11, 31–39.

Crank, J. 1975. The Mathematics of Diffusion, 2nd edn. Oxford, UK: Oxford University Press.

Cruz, R.S, Soares, N.F.F, Andrade, N.J. 2007. Efficiency of oxygen - absorbing sachets in different relative humidities and temperatures. Cienc. Agrotec. 31, 1800-1804.

Cruz, R.S., Camilloto, G.P., Dos Santos Pires, A.C. 2012. Oxygen scavengers: an approach on food preservation. In: Structure and Function of Food Engineering, Eissa, A.A. (Ed.) Wien, Austria: InTech, pp. 21-42.

Cussler, E.L. 1997. Diffusion. Cambridge, UK: Cambridge University Press.

Damaj, Z., Joly, C., Guillon, E. 2015. Toward new polymeric oxygen scavenging systems: Formation of poly(vinyl alcohol) oxygen scavenger film. Packag. Technol. Sci., 28, 293– 302.

Delgado-Adámez, J., Bote, E., Parra-Testal, V., Martín, M. J., Ramírez, R. 2016. Effect of the Olive Leaf ExtractsIn Vitroand in Active Packaging of Sliced Iberian Pork Loin. Packag. Tech. Sci. 29(12), 649–660.

De la Mata, P., Dominguez-Vidal, A., Bosque-Sendra, J. M., Ruiz-Medina, A., Cuadros-Rodríguez, L., & Ayora-Cañada, M. J. (2012). Olive oil assessment in edible oil blends by means of ATR-FTIR and chemometrics. Food Control, 23(2), 449–455.

De Marco, E., Savarese, M., Paduano, A., Sacchi, R. 2007. Characterization and fractionation of phenolic compounds extracted from olive oil mill wastewaters. Food Chemistry, 104(2), 858-867.

De Moraes Crizel T., de Oliveira Rios A., D. Alves V., Bandarra N., Moldão-Martins M., Hickmann Flôres S., 2018, Active food packaging prepared with chitosan and olive pomace. Food Hydrocolloids, 74, 139–150.

Demicheva, M. 2015. Novel oxygen scavenger systems for functional coatings (degree thesis). Arcada University of Applied Sciences, Helsinki, Finland.

DeRoover, B., Coppens, G., Devaux, J., Legras, R., Momtaz, A. 1996. Contribution to poly(m-xylylene adipamide) characterization: Hydrolysis,

condensation, and oxidation in the melt. J. Polym. Sci. A Polym. Chem. 34, 1039–1047.
Deshpande, G.N. 2014. Thermoplastic Polymers Comprising Oxygen Scavenging Molecules. U.S. Patent 2014/0228524.
Devlieghere, F., Vermeiren, L., Debevere, J. 2004. New preservation technologies: Possibilities and limitations. Int. Dairy J. 14, 273-285.
DeWit, J.N.; Klarenbeek, G., 1984. Effects of various treatments on structure and solubility of whey proteins. J. Dairy Sci., 67, 2701–2710.
Di Felice, R., Cazzola, D., Cobror, S., Oriani, L. 2008. Oxygen permeation in PET bottles with passive and active walls. Packag. Technol. Sci. 21, 405-415.
Di Maio, L., Marra, F., Bedane, T.F., Incarnato, L., Saguy, S. 2017. Oxygen transfer in co-extruded multilayer active films for food packaging. AIChE J. 63, 5215-5221.
Di Maio L., Scarfato, P., Galdi, M.R., Incarnato, L. 2015. Development and oxygen scavenging performance of three-layer active PET films for food packaging J. Appl. Polym. Sci. 132, 41465.
Dombre, C., Guillard, V., Chalier, P., 2015. Protection of methionol against oxidation by oxygen scavenger: An experimental and modelling approach in wine model solution. Food Packag. Shelf Life 3, 76–87.
Dombre, C., Marais, S., Chappey, C., Lixon-Bouquet, C., Chalier, P. 2014. The behavior of wine aroma compounds related to structure and barrier properties of virgin, recycled and active PET membranes, J. Membr. Sci. 463, 215-225.
European Commission. (2017). Commission Regulation (EU) 2017/752 of 28 April 2017 amending and correcting Regulation (EU) No 10/2011 on plastic materials and articles intended to come into contact with food. Official Journal of the European Union, L113/18, 18-23.
European Commission. (2011). Commission regulation (EC) No 10/2011 f 14 January 2011 on plastic materials and articles intended to come into contact with food. Official Journal of the European Union, L135, 3-11.
European Commission. (2009). Commission regulation (EC) No 450/2009 of 29 May 2009 on active and intelligent materials and articles intended to come into contact with food. Official Journal of the European Union, L12/1, 1-89.
Echeverría, I., López-Caballero, M. E., Gómez-Guillén, M. C., Mauri, A. N., Montero, M. P. (2018). Active nanocomposite films based on soy proteins-montmorillonite- clove essential oil for the preservation of refrigerated bluefin tuna (Thunnus thynnus) fillets. Int. J. Food Microbiol. 266, 142–149.
Ejaz, M., Arfat, Y. A., Mulla, M., & Ahmed, J. (2018). Zinc oxide nanorods/clove essential oil incorporated Type B gelatin composite films and its applicability for shrimp packaging. Food Packag. Shelf Life, 15, 113–121.

Ellen Mac Arthur Foundation, 2015. Delivering The Circular Economy A Toolkit For Policymakers. https://www.ellenmacarthurfoundation.org
Evans, R.H., Niederst, J., Share, P.E. 2010. Oxygen Scavenging Composition. U.S. Patent 2010/0247821. Valspar Sourcing, Inc.
Fakhouri, F. M., Martelli, S. M., Caon, T., Velasco, J. I., Mei, L. H. I. 2015. Edible films and coatings based on starch/gelatin: Film properties and effect of coatings on quality of refrigerated Red Crimson grapes. Postharvest Biol. Tec. 109, 57–64.
Fang, Y., Tung, M. A., Britt, I. J., Yada, S., Dalgleish, D. G. 2002. Tensile and Barrier Properties of Edible Films Made from Whey Proteins. J. Food Sci. 67(1), 188–193.
Farjami, T., Madadlou, A., Labbafi, M. 2015. Characteristics of the bulk hydrogels made of the citric acid cross-linked whey protein microgels. Food Hydrocoll., 50, 159–165.
Fava, F., Marson, A., Steffanut, P., Johann, L. 2014. Oxygen Scavenging Plastic Material. International Patent Application WO 2014/044366. Clariant International Ltd.
Ferrari, M.C., Carranza, S., Bonnecaze R.T., Tung K.K., Freeman B.D., Paul D.R. 2009. Modeling of oxygen scavenging for improved barrier behavior: blend films. J. Membr. Sci. 329, 183-192.
Floros, J.D., Dock, L.L., Han, J.H. 1997. Active packaging technologies and applications. Food Chem. Drug. Packag. 20, 10–17.
Fogler, H.S., 1999. Elements of Chemical Reaction Engineering, 3rd edn. Upper Saddle River, NJ: Prentice Hall.
Foltynowicz, Z. 2018. Nanoiron-Based Composite Oxygen Scavengers for Food Packaging. In: Composites Materials for Food Packaging, Cirillo, G., Kozlowski, M.A. and Spizzirri, U.G. (Eds.) 1st edn, Hoboken, NJ: John Wiley & Sons, pp. 209-234.
Foltynowicz, Z., Kozak, W., Stoinska, J., Urbanska, M., Muc, K., Dominiak, A., Kublicka, K. 2012. Nanoiron-based oxygen scavengers. International Patent Application WO 2012/091587 A1.
Fortunati, E. , Luzi, F., Dugo, L., Fanali, C., Tripodo, G., Santi, L., Kenny, J.M., Torre, L., Bernini, R. 2016. Effect of hydroxytyrosol methyl carbonate on the thermal, migration and antioxidant properties of PVA-based films for active food packaging. Polym. Int., 65, 872-882.
Gaikwad, K.K., Singh, S., Lee, Y.S. 2018. Oxygen scavenging films in food packaging. Environ. Chem. Lett. 16, 523–538.
Gaikwad, K.K., Lee, Y.S., 2017a. Effect of storage conditions on the absorption kinetics of non-metallic oxygen scavenger suitable for moist food packaging. J. Food Meas. Charact. 11, 965–971.
Gaikwad, K.K., Singh. S., Lee, Y.S., 2017b. A pyrogallol-coated modified LDPE film as an oxygen scavenging film for active packaging materials. Prog. Org. Coat. 111, 186–195.

Gaikwad, K. K., Lee, S. M., Lee, J. S., & Lee, Y. S., 2017c. Development of antimicrobial polyolefin films containing lauroyl arginate and their use in the packaging of strawberries. J. Food Meas. Charact., 11(4), 1706–1716.
Gaikwad, K.K, Lee, J.Y, Lee, Y.S. 2016. Development of polyvinyl alcohol and apple pomace bio-composite film with antioxidant properties for active food packaging application. J. Food. Sci. Technol. 53, 1608–1619.
Galdi, M.R. and Incarnato, L. 2011. Influence of composition on structure and barrier properties of active PET films for food packaging applications. Packag. Technol. Sci. 24, 89–102.
Galdi, M.R. and Incarnato, L. 2010. Production and Characterization of Active Transparent PET Films for Oxygen Sensitive Foods Packaging. Proceedings of 5th International Conference on Times of Polymers and Composites, 1255, pp. 199-201. College Park, USA: American Institute of Physics.
Galdi, M.R. 2010. Design and production of active films for food packaging application (doctoral dissertation). University of Salerno, Italy.
Galotto, M., Anfossi, S., Guarda, A. 2009. Oxygen absorption kinetics of sheets and films containing a commercial iron-based oxygen scavenger. Food Sci. Technol. Int. 15, 159-168.
Ganiari, S., Choulitoudi, E., & Oreopoulou, V. 2017. Edible and active films and coatings as carriers of natural antioxidants for lipid food. Trends Food Sci. Tech. 68, 70–82.
Gauthier, W. and Speer, D.V., 2001. Oxygen Scavenging Composition And Method Of Using The Same. U.S. Patent 6,214,254. Cryovac, Inc.
Gemili, S., Yemenicioğlu, A., and Altınkaya, S. A. 2009. Development of cellulose acetate based antimicrobial food packaging materials for controlled release of lysozyme. J. Food Eng. 90, 453-462.
Ghanbari, R., Anwar, F., Alkharfy, K. M., Gilani, A. H., Saari, N. 2012. Valuable nutrients and functional bioactives in different parts of olive (Olea europaea L.) - a review. Int. J. Mol. Sci. 13(3), 3291-3340.
Gherardi, R., Becerril, R., Nerin, C., Bosetti, O. (2016). Development of a multilayer antimicrobial packaging material for tomato puree using an innovative technology. LWT - Food Science and Technology, 72, 361–367.
Gillen K.T., Clough R.L., 1992. Rigorous experimental confirmation of a theoretical model for diffusion-limited oxidation, Polymer, 33, 4358-4365.
Goddard, J,M., Hotchkiss, J.H. 2007. Polymer surface modification for the attachment of bioactive compounds. Prog. Polym. Sci. 32, 698–725.
Gohil, R. M., Wysock, W. A. 2014. Designing efficient oxygen scavenging coating formulations for food packaging applications. Packag. Technol. Sci. 27, 609-623.
Gonçalves, C. M. B., Tomé, L. C., Garcia, H., Brandão, L., Mendes, A. M., Marrucho, I. M. 2013. Effect of natural and synthetic antioxidants

incorporation on the gas permeation properties of poly(lactic acid) films. J. Food Eng. 116(2), 562–571.
Graf, E. 1994. U.S. Patent No. 5,284,871. U.S. Patent and Trademark Office, Washington.
Guillard, V., Gaucel, S., Fornaciari, C., Angellier-Coussy, H., Buche, P., Gontard, N., 2018. The Next Generation of Sustainable Food Packaging to Preserve Our Environment in a Circular Economy Context. Front. Nutr. 5, 121.
Haile, D. M., De Smet, S., Claeys, E., Vossen, E. 2013. Effect of light, packaging condition and dark storage durations on colour and lipid oxidative stability of cooked ham. Int. J. Food Sci. Tech. 50, 239-247.
Hafsa, J., Smach, M. ali, Ben Khedher, M. R., Charfeddine, B., Limem, K., Majdoub, H., et al. 2016. Physical, antioxidant and antimicrobial properties of chitosan films containing Eucalyptus globulus essential oil. Lebensmittel-Wissenschaft und -Technologie- Food Sci. Technol. 68, 356–364.
Haghighi, H., De Leo, R., Bedin, E., Pfeifer, F., Siesler, H.W., Pulvirenti A. (2019) Comparative analysis of blend and bilayer films based on chitosan and gelatin enriched with LAE (lauroyl arginate ethyl) with antimicrobial activity for food packaging applications. Food Packag. Shelf Life. 19, 31-39.
Halász, K., Hosakun, Y., Csóka, L. 2015. Reducing Water Vapor Permeability of Poly(lactic acid) Film and Bottle through Layer-by-Layer Deposition of Green-Processed Cellulose Nanocrystals and Chitosan. Int. J. Polym. Sci. 2015, 954290.
Hauser, C., & Wunderlich, J. 2011. Antimicrobial packaging films with a sorbic acid based coating. Procedia Food Science, 1, 197–202.
Higueras, L., Lopez-Carballo, G., Hernandez-Munoz, P., Gavara, R., Rollini, M. (2013). Development of a novel antimicrobial film based on chitosan with LAE (ethyl-Nα-dodecanoyl-l-arginate) and its application to fresh chicken. Int. J. Food Microbiol. 165(3), 339-345.
Hong, S.-I., Krochta, J. M. 2004. Whey protein isolate coating on LDPE film as a novel oxygen barrier in the composite structure. Packag. Technol. Sci. 17(1), 13–21.
Hu, Y.S., Prattipati, V., Hiltner, A., Baer, E., Mehta, S. 2005a. Improving transparency of stretched PET/MXD6 blends by modifying PET with isophthalate. Polymer, 46, 5202–5210.
Hu, Y.S., Prattipati, V., Mehta, S., Schiraldi, D.A., Hiltner, A., Baer, E. 2005b. Improving gas barrier of PET by blending with aromatic polyamides. Polymer, 46, 2685–2698.
Hutter, S., Ruegg, N., Yildirim, S. 2016. Use of palladium based oxygen scavenger to prevent discoloration of ham. Food Packag. Shelf Life, 8, 52-62.

Infante, M., Pinazo, A., Seguer, J. (1997). Non-conventional surfactants from amino acids
and glycolipids: Structure, preparation and properties. Colloids Surf. A. 123–124, 49–70.
Inoue, Y., Komatsu, T. 1990a. US Patent 5,116,660. Mitsubishi Gas Chemical Co. Inc.
Inoue, Y., Komatsu, T., Moriya, T., 1990b. U.S. Patent 5,143,769 Mitsubishi Gas Chemical Co. Inc.
Izumi H., Watada A.E., Douglas W., 1996. Optimum O2 or CO2 atmosphere for storing broccoli florets at various temperatures, J. Amer. Soc. Hort. Sci., 121(1), 127–131.
Jamshidian, M., Tehrany, E.A., Cleymand, F., Leconte, S., Falher, T., Desobry, S. 2012. Effects of synthetic phenolic antioxidants on physical, structural, mechanical and barrier properties of poly lactic acid film. Carbohydr. Polym. 87, 1763–1773.
Jamshidian M., Arab Tehrany E., Desobry S., 2013, Antioxidants Release from Solvent-Cast PLA Film: Investigation of PLA Antioxidant-Active Packaging. Food and Bioprocess Technology, 6(6), 1450–1463.
Janjarasskul, T., Tananuwong, K., Krochta, J.M. 2011. Whey protein film with oxygen scavenging function by incorporation of ascorbic acid. J. Food Sci. 76, 561–568.
Javidi, Z., Hosseini, S. F., & Rezaei, M. (2016). Development of flexible bactericidal films based on poly(lactic acid) and essential oil and its effectiveness to reduce microbial growth of refrigerated rainbow trout. LWT - Food Sci. Technol. 72, 251–260.
Jerdee, G.D., Leonard, J.P., Ching, T.Y., Goodrich, J.L., Rodgers, B.D., Schmidt, R.P. 2003. US patent 6,569,506.
Jiang, S., Zhang, T., Song, Y., Qian, F., Tuo, Y., & Mu, G. 2019. Mechanical properties of whey protein concentrate based film improved by the coexistence of nanocrystalline cellulose and transglutaminase. Int. J. Biol. Macromol. 126, 1266-1272.
Johansson, K., Jönsson, L., Järnström, L. 2011. Oxygen scavenging enzymes in coatings – Effect of coating procedures on enzyme activity. Nord. Pulp. Pap. Res. J. 26, 197-204.
Johnson, D.R, Decker, E.A. 2015. The role of oxygen in lipid oxidation reactions: a review. Annu. Rev. Food Sci. Technol. 6, 171–190.
Joo, E., Chang, Y., Choi, I., Lee, S. B., Kim, D. H., Choi, Y. J., Han, J. (2018). Whey protein-coated high oxygen barrier multilayer films using surface pretreated PET substrate. Food Hydrocoll., 80, 1–7.
Kaiser, K., Schmid, M., Schlummer, M. 2017. Recycling of Polymer-Based Multilayer Packaging: A Review. Recycling, 3(1), 1.
Kashiri, M., Cerisuelo, J. P., Domínguez, I., López-Carballo, G., Hernández-Muñoz, P., and Gavara, R. 2016. Novel antimicrobial zein film for controlled release of lauroyl arginate (LAE). Food Hydrocoll.61, 547-554.

Kokoszka, S., Debeaufort, F., Lenart, A., Voilley, A. 2010. Liquid and vapour water transfer through whey protein/lipid emulsion films. J. Sci. Food Agric. 90(10), 1673–1680.

Kruijf, N., van Beest, M., Rijk, R., Sipiläinen-Malm, T., Paseiro Losada, P., De Meulenaer, B. 2002.

Active and intelligent packaging: applications and regulatory aspects. Food Addit. Contam. 19, 144-162.

Kumada, K. 1965. Studies on the colour of humic acids. Soil Sci. Plant Nutr. 11, 11–16.

Labuza, T., Breene, M.W. 2007. Applications of active packaging for improvement of shelf-life and nutritional quality of fresh and extended shelf-life foods. J. Food Process. Pres. 13, 1-69.

Lagaron, J.M. (2011). Multifunctional and nanoreinforced polymers for food packaging. Cambridge, Woodhead Publishing.

Langowski, H-C., and Wanner, T. 2005. Organic oxygen scavenger/indicator. EP1952140B1 (WO 2007/059901 A1).

Lee, J., Jeong, S., Lee, H., Cho, C. H., Yoo, S. 2018. Development of a sulfite-based oxygen scavenger and its application in kimchi packaging to prevent oxygen-mediated deterioration of kimchi quality. J. Food Sci. 83, 3009-3018.

Lehner, M., Schlemmer, D., Sängerlaub, S. 2015. Recycling of blends made of polypropylene and an iron-based oxygen scavenger – Influence of multiple extrusions on the polymer stability and the oxygen absorption capacity. Polym. Degrad. Stabil. 122, 122-132.

Li, W., Li, L., Cao, Y., Lan, T., Chen, H., & Qin, Y. 2017. Effects of PLA Film Incorporated with ZnO Nanoparticle on the Quality Attributes of Fresh-Cut Apple. Nanomaterials, 7(8), 207.

Li, H., Tung, K.K., Paul, D.R., Freeman, B.D., Stewart, M.E, Jenkins, J.C. 2012. Characterization of oxygen scavenging films based on 1,4-polybutadiene. Ind. Eng. Chem. Res. 51, 7138–7145.

Li, G., Shankar, S., Rhim, J.-W., Oh, B.-Y. 2015. Effects of preparation method on properties of poly(butylene adipate-co-terephthalate) films. Food Sci. Biotechnol. 24(5), 1679–1685.

Lindner, M., Rodler, N., Jesdinszki, M., Schmid, M., Sängerlaub, S. 2017. Surface energy of corona treated PP, PE and PET films, its alteration as function of storage time and the effect of various corona dosages on their bond strength after lamination. J. Appl. Polym. Sci. 135(11), 45842.

Liu, X., Wang, T., Chow, L. C., Yang, M., & Mitchell, J. W. 2014. Effects of Inorganic Fillers on the Thermal and Mechanical Properties of Poly(lactic acid). Int. J. Polym. Sci. 2014, 827028.

Luo, H., 2011. Extraction of Antioxidant Compounds from Olive (Olea europaea) Leaf. Master Thesis in Food Technology, Massey University, Albany, New Zealand.

Mabeck, J.T, Malliaras, G.G. 2006. Chemical and biological sensors based on organic thin-film transistors. Anal. Bioanal. Chem. 384, 343–353.

Mahajan, K., Lofgren, E.A., Jabarin, S.A. 2013. Development of active barrier systems for Poly(ethylene terephthalate). J. Appl. Polym. Sci., 129, 2196–2207

Mahieu, A., Terrié, C., Youssef, B. 2015. Thermoplastic starch films and thermoplastic starch/polycaprolactone blends with oxygen-scavenging properties: Influence of water content. Ind. Crop. Prod. 72, 192-199.

Maisanaba, S., Llana-Ruiz-Cabello, M., Gutiérrez-Praena, D., Pichardo, S., Puerto, M., Prieto, A. I., et al. 2017. New advances in active packaging incorporated with essential oils or their main components for food preservation. Food Rev. Int. 33(5), 447–515.

Manzanarez-López, F., Soto-Valdez, H., Auras, R., & Peralta, E. 2011. Release of α-Tocopherol from Poly(lactic acid) films, and its effect on the oxidative stability of soybean oil. J. Food Eng, 104(4), 508–517.

Marcos, B., Sárraga, C., Castellari, M., Kappen, F., Schennink, G., Arnau, J. 2014. Development of biodegradable films with antioxidant properties based on polyesters containing α-tocopherol and olive leaf extract for food packaging applications. Food Packag. Shelf Life, 1, 140–150.

Martelli S.M., Motta C., Alberton T.C.J., Casagrande Bellettini I., Pinheiro do Prado A.C., Manique Barreto P.L., Soldi V., 2017, Edible carboxymethyl cellulose films containing natural antioxidant and surfactants: α-tocopherol stability, in vitro release and film properties. LWT - Food Science and Technology, 77, 21-29.

Matche, R.S, Sreekumar, R.K, Raj, B. 2011. Modification of linear low density polyethylene film using oxygen scavengers for its application in storage of bun and bread. J. Appl. Polym. Sci. 122, 55–63.

McHugh, T.H., AUJARD, J.F., KROCHTA, J.M., 1994. Plasticized Whey Protein Edible Films: Water Vapor Permeability Properties. J. Food Sci. 59(2), 416–419.

Messin, T., Follain, N., Guinault, A., Miquelard-Garnier, G., Sollogoub, C., Delpouve, N., Gaucher, V., Marais, S. 2017. Confinement effect in PC/MXD6 multilayer films: Impact of the microlayered structure on water and gas barrier properties J. Membr. Sci., 525, 135-145.

Michiels, Y., Van Puyvelde, P., Sels, B. 2017. Barriers and chemistry in a bottle: Mechanisms in today's oxygen barriers for tomorrow's materials. Appl. Sci. 7, 665.

Mills, A., Doyle, G., Peiro, A.M., Durrant, J. 2006. Demonstration of a novel, flexible, photocatalytic oxygen-scavenging polymer film. J. Photochem. Photobiol. A. 177, 328–331.

Miltz, J., Perry, M. 2005. Evaluation of the performance of iron-based oxygen scavengers, with comments on their optimal applications. Packag. Technol. Sci. 18, 21–27.

Mirabella, N., Castellani, V., Sala, S. 2014. Current options for the valorization of food manufacturing waste: a review. J. Clean. Prod. 65(0), 28-41.
Miranda, N.R. and Speer, D.V. 2005. Poly(lactic acid) in Oxygen Scavenging Article. U.S. Patent 6,908,652.
Møller, J.K.S., Jakobsen, M., Weber, C.J., Martinussen, T., Skibsted, L.H., Bertelsen, G. 2003. Optimisation of colour stability of cured ham during packaging and retail display by a multifactorial design. Meat Science, 63, 169-175.
Molling, J., Seezink, J., Teunissen, B., Muijrers-Chen, I., Borm, P. 2014. Comparative Performance of a panel of commercially available antimicrobial nanocoatings in Europe. Nanotechnol. Sci. Appl. 97.
Moreno, O., Gil, À., Atarés, L., Chiralt, A. (2017). Active starch-gelatin films for shelf life extension of marinated salmon. LWT - Food Sci. Technol. 84, 189–195.
Moudache, M., Colon, M., Nerín, C., Zaidi, F. 2017. Antioxidant effect of an innovative active plastic film containing olive leaves extract on fresh pork meat and its evaluation by Raman Spectroscopy. Food Chem. 229, 98-103.
Moudache, M., Colon, M., Nerín, C., Zaidi, F. 2016. Phenolic content and antioxidant activity of olive by-products and antioxidant film containing olive leaf extract. Food Chem. 212, 521-527.
Mu, H., Gao, H., Chen, H., Tao, F., Fang, X., Ge, L. 2013. A nanosised oxygen scavenger: Preparation and antioxidant application to roasted sunflower seeds and walnuts. Food Chem. 136, 245-50.
Muriel-Galet V., López-Carballo, G., Gavara, R., Hernández-Muñoz, P. 2012. Antimicrobial food packaging film based on the release of LAE from EVOH. Int. J. Food Microbiol. 157(2), 239-244.
Muriel-Galet, V., López-Carballo, G., Hernández-Muñoz, P., & Gavara, R. 2014. Characterization of ethylene-vinyl alcohol copolymer containing lauril arginate (LAE) as material for active antimicrobial food packaging. Food Packag. and Shelf Life. 1(1), 10–18.
Nakae, K., Kawakita, T., Kume, T., Sugiyama, M. 1990. U.S. Patent 5,089,323. Sumitomo Chemical Co.
Nerin C., Becerril R., Manso S., Silva F. 2016. “Ethyl Lauroyl Arginate (LAE): Antimicrobial Activity and Applications in Food Systems” In: Antimicrobial Food Packaging, ed. J. Barros-Velázquez (London, Elsevier Science), pp. 305-312.
Nerin, C., Silva, F., Manso, S., and Becerril, R. 2016. “The downside of antimicrobial packaging: Migration of packaging elements into food”. In: Antimicrobial Food Packaging, ed. J. Barros-Velázquez (London, Elsevier Science), pp. 81-90.
Nerín, C. 2010. Antioxidant active food packaging and antioxidant edible films. In: Oxidation in foods and beverages and antioxidant applications. Volume 2: Management in different industry sectors, Decker, E.A., Elias,

R.J., McClements, D.J. (Eds.) Cambridge, UK: Woodhead Publishing Ltd, pp. 496-515.
Nestorson, A., Neoh, K.G., Kang, E.T., Järnström, L., Leufvén, A. 2008. Enzyme immobilization in latex dispersion coatings for active food packaging. Packag. Technol. Sci., 21, 193-205.
Nunes, M. A., Pimentel, F. B., Costa, A. S. G., Alves, R. C., & Oliveira, M. B. P. P., 2016. Olive by-products for functional and food applications: Challenging opportunities to face environmental constraints. Innov. Food Sci. Emerg. Technol., 35, 139–148.
Nuxoll, E.E., Cussler, E.L. 2005. The third parameter in reactive barrier films. AIChE J. 51, 456–463.
Otero, V., Becerril, R., Santos, J.A., Rodríguez-Calleja, J.M., Cristina Nerín, García-López, M.L. (2014). Evaluation of two antimicrobial packaging films against Escherichia coli O157:H7 strains in vitro and during storage of a Spanish ripened sheep cheese (Zamorano). Food Control. 42, 296-302.
Oliveira, C.M.; Ferreira, A.C.S.; De Freitas, V.; Silva, A.M.S. 2011. Oxidation mechanisms occurring in wines.Food Res. Int., 44, 1115–1126.
Otles S., Semih I., 2012, Treatment of Olive Mill Wastewater and the Use of Polyphenols Obtained After Treatment. Italian Journal of Food Safety, 1, 85-100.
Oudjedi, K., Manso, S., Nerin, C., Hassissen, N., Zaidi, F. 2019. New active antioxidant multilayer food packaging films containing Algerian Sage and Bay leaves extracts and their application for oxidative stability of fried potatoes. Food Control. 98, 216-226.
Owens, D. K. and Wendt, R. C. (1969), Estimation of the surface free energy of polymers. J. Appl. Polym. Sci., 13: 1741-1747.
Pagno, C. H., de Farias, Y. B., Costa, T. M. H., de Oliveira Rios, A., and Flôres, S. H. 2016. Synthesis of biodegradable films with antioxidant properties based on cassava starch containing bixin nanocapsules. J. Food Sci. Tech. 53, 3197-3205.
Pant, A.F., Özkasikci, D., Fürtauer, S. Reinelt, M., 2019. The Effect of Deprotonation on the Reaction Kinetics of an Oxygen Scavenger Based on Gallic Acid. Front. Chem. 7:680.
Pant, A.F., Dorn, J., Reinelt, M., 2018. Effect of temperature and relative humidity on the reaction kinetics of an oxygen scavenger based on gallic acid. Front. Chem. 6, 587.
Pant, A.F., Sangerlaub, S., Muller, K. 2017. Gallic acid as an oxygen scavenger in bio-based multilayer packaging films, Materials 10, 489.
Paul, D.R., Kemp, D.R. 1973. The diffusion time lag in polymer membranes containing adsorptive fillers. J. Polym. Sci. C. 41, 79-93.
Paul, D.R., Koros, W.J. 1976. Effect of partially immobilizing sorption on permeability and the diffusion time lag. J. Polym. Sci. B. 14, 675-685.
Peirsman, D., Valles, V. 2016. Oxygen-Scavenging Polymers. U.S. Patent 20,160,346,760.

Pezo, D., Navascués, B., Salafranca, J., Nerín, C. 2012. Analytical procedure for the determination of Ethyl Lauroyl Arginate (LAE) to assess the kinetics and specific migration from a new antimicrobial active food packaging. Anal. Chim. Acta. 745, 92–98.

Pezo, D., Salafranca, J., Nerín, C. 2008. Determination of the antioxidant capacity of active food packagings by in situ gas-phase hydroxyl radical generation and high-performance liquid chromatography–fluorescence detection. J. Chromatogr. A, 1178(1-2), 126–133.

Ravindran, R., & Jaiswal, A. K. Exploitation of Food Industry Waste for High-Value Products. Trends in Biotechnology, 34(1), 58-69.

Ravishankar Rai, V., Jamuna Bai, A., 2017. Food Safety and Protection, 1st edn. Milton Park, UK: Taylor & Francis Inc.

Restuccia, D., Spizzirri, U. G., Parisi, O. I., Cirillo, G., Curcio, M., Iemma, F., et al. 2010. New EU regulation aspects and global market of active and intelligent packaging for food industry applications. Food Control, 21(11), 1425–1435.

Ribeiro-Santos, R., Andrade, M., Melo, N. R. de, & Sanches-Silva, A. 2017. Use of essential oils in active food packaging: Recent advances and future trends. Trends Food Sci. Tech. 61, 132–140.

Rigane, G., Bouaziz, M., Baccar, N., Abidi, S., Sayadi, S., Salem, R. B. 2012. Recovery of hydroxytyrosol rich extract from two-phase Chemlali olive pomace by chemical treatment. J. Food Sci. 77(10), 1077-1083.

Robertson, G.L. 2013. Food Packaging: Principles and Practice, 3rd edn. Boca Raton, FL: CRC Press.

Rohini, M. 2008. Development of controlled release antimicrobial films from low methyoxyl pectin.

Rutgers University.

Ros-Chumillas, M., Belissario, Y., Iguaz, A., López, A. 2007. Quality and shelf life of orange juice aseptically packaged in PET bottles. J. Food Eng. 79, 234–242.

Roselló-Soto, E., Koubaa, M., Moubarik, A., Lopes, R. P., Saraiva, J. A., Boussetta, N., Grimi, N., & Barba, F. J. 2015. Emerging opportunities for the effective valorization of wastes and by-products generated during olive oil production process: Non-conventional methods for the recovery of high-added value compounds. Trends Food Sci. Tech. 45(2), 296-310.

Rubilar, J.F., Candia, D., Cobos, A., Díaz, O., Pedreschi, F. 2016. Effect of nanoclay and ethyl-Nα-dodecanoyl-L-arginate hydrochloride (LAE) on physico-mechanical properties of chitosan films. LWT - Food Sci. Technol. 72, 206-214

Rubio-Senent, F., Rodríguez-Gutiérrez, G., Lama-Muñoz, A., García, A., Fernández-Bolaños, J. 2015. Novel pectin present in new olive mill wastewater with similar emulsifying and better biological properties than citrus pectin. Food Hydrocoll. 50, 237-246.

Sabatini, N. 2010). Recent Patents in Olive Oil Industry: New Technologies for the Recovery of Phenols Compounds from Olive Oil, Olive Oil Industrial by-Products and Waste Waters. Recent Pat. Food Nutr. Agric. 2(2), 154-159.

Sanches-Silva, A., Costa, D., Albuquerque, T. G., Buonocore, G. G., Ramos, F., Castilho, M. C., et al. 2014. Trends in the use of natural antioxidants in active food packaging: A review. Food Addit. Contam. Part A, 31(3), 374–395

Sängerlaub, S. and Müller, K. 2017. Long-time performance of bottles made of PET blended with various concentrations of oxygen scavenger additive stored at different temperatures. Packag. Technol. Sci. 30, 45–58.

Scarfato P., Di Maio L., Milana M.R., Giamberardini S., Denaro M., Incarnato L. (2017). Performance properties, lactic acid specific migration and swelling by simulant of biodegradable poly(lactic acid)/nanoclay multilayer films for food packaging. Food Addit. Contam. Part A. 34(10), 1730–1742.

Scarfato, P., Avallone, E., Galdi, M. R., Di Maio, L., Incarnato, L. 2015a. Preparation, characterization, and oxygen scavenging capacity of biodegradable α-tocopherol/PLA microparticles for active food packaging applications. Polym. Compos. 38, 981–986.

Scarfato, P., Di Maio, L., & Incarnato, L. 2015b. Recent advances and migration issues in biodegradable polymers from renewable sources for food packaging. J. Appl. Polym. Sci. 132(48), 42597.

Schmid, M., Sängerlaub, S., Wege, L., Stäbler, A. 2014. Properties of Transglutaminase Crosslinked Whey Protein Isolate Coatings and Cast Films. Packag. Technol. Sci., 27(10), 799–817.

Schmid, M., Dallmann, K., Bugnicourt, E., Cordoni, D., Wild, F., Lazzeri, A., Noller, K. 2012. Properties of Whey-Protein-Coated Films and Laminates as Novel Recyclable Food Packaging Materials with Excellent Barrier Properties. Int. J. Polym. Sci. 2012, 1–7.

Severino, R., Ferrari, G., Vu, K. D., Donsì, F., Salmieri, S., & Lacroix, M. 2015. Antimicrobial effects of modified chitosan based coating containing nanoemulsion of essential oils, modified atmosphere packaging and gamma irradiation against Escherichia coli O157:H7 and Salmonella Typhimurium on green beans. Food Control, 50, 215–222.

Shahidi, F.; Naczk, M. 2003. Phenolics in Food and Nutraceuticals; CRC Press: Boca Raton, FL, USA.

Share, P.E., Pillage, K.R., Skillman, C.I., Fuchs, P.E. 2012. Oxygen Scavenging Polymers. U.S. Patent 8,182,888. Valspar Sourcing, Inc.

Shin, Y., Shin, J., Lee, Y.S. 2011. Preparation and characterization of multilayer film incorporating oxygen scavenger. Macromol. Res. 19, 869–875.

Shouten R., Zhang X., Verschoor J., van Kooten O., 2009. Development of colour of broccoli heads as affected by controlled atmosphere storage and temperature, Postharvest Biol. Technol., 51(1), 27-35.
Sillero L., Prado R., Labidi J., 2018, Optimization of Different Extraction Methods to Obtaining Bioactive Compounds from Larix Decidua Bark . Chemical Engineering Transactions, 70, 1369-1374.
Silva, N. H. C. S., Vilela, C., Almeida, A., Marrucho, I. M., Freire, C. S. R. 2018. Pullulan-based nanocomposite films for functional food packaging: Exploiting lysozyme nanofibers as antibacterial and antioxidant reinforcing additives. Food Hydrocoll. 77, 921–930.
Silva, F., Gracia, N., McDonagh, B. H., Domingues, F. C., Nerín, C., Chinga-Carrasco, G. 2019a. Antimicrobial activity of biocomposite films containing cellulose nanofibrils and ethyl lauroyl arginate. J. Mater. Sci. 54:12159–12170.
Silva, F., Caldera, F., Trotta, F., Nerín, C., Domingues, F. C. 2019b. Encapsulation of coriander essential oil in cyclodextrin nanosponges: A new strategy to promote its use in controlled-release active packaging. Innov. Food Sci. Emerg. Technol., 102177.
Simionato, I., Domingues, F. C., Nerín, C., Silva, F. 2019. Encapsulation of cinnamon oil in cyclodextrin nanosponges and their potential use for antimicrobial food packaging. Food Chem. Toxicol. 132, 110647.
Solovyov, S.E. 2014. Oxygen Scavengers. In: Kirk-Othmer Encyclopedia of Chemical Technology. Hoboken, NJ: John Wiley & Sons.
Solovyov S.E. and Goldman A.Y. 2007. Mass Transport and Reactive Barriers in Packaging: Theory, Applications, and Design. Lancaster, PA: DEStech Publications.
Solovyov, S.E. and Goldman, A.Y. 2006. Optimized design of multilayer barrier films incorporating a reactive layer. III. Case analysis and generalized multilayer solutions, J. Appl. Polym. Sci. 100, 1966-1977.
Solovyov, S.E., Goldman, A.Y. 2005a. Theory of transient permeation through reactive barrier films I. Steady state theory for homogeneous passive and reactive media. Int. J. Polym. Mater. 54, 71-91.
Solovyov, S.E., Goldman, A.Y. 2005b. Theory of transient permeation through reactive barrier films II. Two layer reactive-passive structures with dynamic interface. Int. J. Polym. Mater. 54, 93-115.
Solovyov, S.E., Goldman, A.Y. 2005c. Theory of transient permeation through reactive barrier films III. Solute ingress dynamics and model lag times. Int. J. Polym. Mater. 54, 117-139.
Sothornvit, R., Krochta, J.M., 2000. Oxygen permeability and mechanical properties of films from hydrolyzed whey protein. J. Agric. Food Chem. 48(9), 3913–3916.
Souza, M. P., Vaz, A. F. M., Silva, H. D., Cerqueira, M. A., Vicente, A. A., & Carneiro-da-Cunha, M. G. 2015. Development and characterization of an

active chitosan-based film containing quercetin. Food Bioprocess Tech. 8(11), 2183–2191.
Speer, D.V., Roberts, W.P., Morgan, C.R. 1993. Method and compositions for oxygen scavenging. U.S. Patent, 5,211,875.
Sun, D.W., 2016. Computer Vision Technology for Food Quality Evaluation, 2nd edn. London, UK: Academic Press.
Suppakul, P., Miltz, J., Sonneveld, K., Bigger, S.W. 2003. Active packaging technologies with an emphasis on antimicrobial concise reviews in food science. J. Food Sci. 68, 408–420.
Tercan S., Seker M., 2012, Comparison of polyphenol extractions from olive pomace and solid fraction of olive mill waste water. Natural Product Research, 26(19), 1837–1841.
Tian, F., Decker, E. A., & Goddard, J. M. 2013. Controlling lipid oxidation of food by active packaging technologies. Food & Function, 4, 669–680.
Tibbitt, J.M., Cahill, P.J., Rotter, G.E., Sinclair, D.P., Brooks, G.T., Behrends, R.T. 2007. Oxygen Scavenging Monolayer Bottles. U.S. Patent 7,214,415. BP Corporation North America Inc.
Tiimob, B. J., Rangari, V. K., Mwinyelle, G., Abdela, W., Evans, P. G., Abbott, N., … Jeelani, S. (2018). Tough aliphatic-aromatic copolyester and chicken egg white flexible biopolymer blend with bacteriostatic effects. Food Packag. Shelf Life. 15, 9–16.
Tulsyan, G., Richter, C., Diaz, C.A. 2017. Oxygen scavengers based on titanium oxide nanotubes for packaging applications: Oxygen scavengers based on titanium oxide nanotubes. Packag. Technol. Sci. 20, 251-256.
Tung, D., Sisson, E. A., Leckonby, R. A. 2004. Oxygen-scavenging resin compositions having low haze. U.S. Patent 6,780,916.
u Nisa, I., Ashwar, B. A., Shah, A., Gani, A., Gani, A., and Masoodi, F. A. (2015). Development of potato starch based active packaging films loaded with antioxidants and its effect on shelf life of beef. Int. J. Food Sci. Tech. 52, 7245-7253
Uribe, E., Lemus-Mondaca, R., Vega-Gálvez, A., López, L., Pereira, K., López, J., Ah-Hen, K., & Di Scala, K. 2013. Quality characterization of waste olive cake during hot air drying: Nutritional Aspects and Antioxidant Activity. Food Bioprocess. Tech. 6(5), 1207-1217.
Van Krevelen, D.W., Nijenhuis, K. 1997. Properties of Polymers, third completely revised edition, Elsevier Science B.V., Amsterdam, The Netherlands.
Venkateshwaran, L.N., Chokshi, D.J., Chiang, W.L. 1999. Efficiency Oxygen-Scavenging Compositions and Articles. U.S. Patent 5,885,481. Amoco Corporation.
Venkateshwaran, L.N., Chokshi, D.J., Chiang, W.L., Tsai, B.C. 1998. Oxygen-Scavenging Compositions and Articles. U.S. Patent 5,744,056. Amoco Corporation.

Vera, P., Canellas, E., Nerín, C. 2018. New Antioxidant Multilayer Packaging with Nanoselenium to Enhance the Shelf-Life of Market Food Products. Nanomaterials, 8(10), 837.
Vera, P., Echegoyen, Y., Canellas, E., Nerín, C., Palomo, M., Madrid, Y., Cámara, C. 2016. Nano selenium as antioxidant agent in a multilayer food packaging material. Anal. Bioanal. Chem. 408(24), 6659–6670.
Vermeiren, L., Heirlings, L., Devlieghere, F. and Debevere, J. 2003. Oxygen, ethylene and other scavengers. In: Novel Food Packaging Techniques, Ahvenainen, R. (Ed.). Boca Raton, FL: CRC Press.
Vermeiren, L., Devlieghere, F., van Beest, M., de Kruijf, N., Debevere, J. 1999. Developments in the active packaging of foods, Trends Food Sci. Technol. 10, 77-86.
Vidović, E., Faraguna, F., Jukić, A. 2016. Influence of inorganic fillers on PLA crystallinity and thermal properties. J. Therm. Anal. Calorim. 127(1), 371–380.
Vilela, C., Kurek, M., Hayouka, Z., Röcker, B., Yildirim, S., Antunes, M. D. C., Nilsen-Nygaardf, J.,
Kvalvåg Pettersen, M., Freire, C. S. R., 2018. A concise guide to active agents for active food packaging. Trends Food Sci. Technology, 80, 212-222.
Vilela, C., Pinto, R. J. B., Coelho, J., Domingues, M. R. M., Daina, S., Sadocco, P., et al. (2017). Bioactive chitosan/ellagic acid films with UV-light protection for active food packaging. Food Hydrocoll., 73, 120–128.
Vissers, M. N., Zock, P. L., Katan, M. B. 2004. Bioavailability and antioxidant effects of olive oil phenols in humans: a review. Eur. J. Clin. Nutr. 58(6), 955–965.
Volf, I., Ignat, I., Neamtu, M., Popa, V. 2014. Thermal stability, antioxidant activity, and photo-oxidation of natural polyphenols. Chemical Papers, 68(1).
Wang, H., Qian, J., & Ding, F. 2018. Emerging chitosan-based films for food packaging applications. J. Agric. Food Chem. 66(2), 395–413.
Wang, L.-F., Rhim, J.-W., Hong, S.-I. 2016. Preparation of poly(lactide)/poly(butylene adipate-co-terephthalate) blend films using a solvent casting method and their food packaging application. LWT - Food Sci. Technol. 68, 454–461.
Wessling, C., Nielsen, T., Leufven, A., Jagerstad, M.,1998. Mobility of tocopherol and BHT in LDPE in contact with fatty food simulants. Food Addit Contam. 15, 709–715.
Wicochea-Rodríguez, J. D., Chalier, P., Ruiz, T., Gastaldi, E., 2019. Active Food Packaging Based on Biopolymers and Aroma Compounds: How to Design and Control the Release. Front. Chem. 7.
Winestrand, S., Johansson, K., Järnström, L., Jönsson, L. 2013. Co-immobilization of oxalate oxidase and catalase in films for scavenging of oxygen or oxalic acid. Biochem. Eng. J. 72, 96–101.

Witzel, R.F., Burnham, R.W., Onley J.W. 1973. Threshold and suprathreshold perceptual color differences. J. Optical Society of America, 63, 615-625.

Wrona, M., Blasco, S., Becerril, R., Nerin, C., Sales, E., Asensio, E., 2019. Antioxidant and antimicrobial markers by UPLC ®–ESI-Q-TOF-MS E of a new multilayer active packaging based on *Arctostaphylos uva-ursi*. Talanta, 196, 498-509.

Wrona, M., Nerín, C., Alfonso, M. J., Caballero, M.Á. 2017a. Antioxidant packaging with encapsulated green tea for fresh minced meat. Innov. Food Sci. Emerg. Technol. 41, 307–313.

Wrona, M., Cran, M. J., Nerín, C., Bigger, S. W. 2017b. Development and characterisation of HPMC films containing PLA nanoparticles loaded with green tea extract for food packaging applications. Carbohydr. Polym. 156, 108–117.

Wrona, M., Bentayeb, K., Nerín, C. 2015. A novel active packaging for extending the shelf-life of fresh mushrooms (*Agaricus bisporus*). Food Control, 54, 200–207.

Wu, Y., Qin, Y., Yuan, M., Li, L., Chen, H., Cao, J., and Yang, J. 2014. Characterization of an antimicrobial poly (lactic acid) film prepared with poly (ε-caprolactone) and thymol for active packaging. Polym. Advan. Technol. 25, 948-954.

Yang, C., Nuxoll, E.E., Cussler, E.L. 2001. Reactive Barrier Films. AIChE J. 47, 295-302.

Yee, Y. Y., Ching, Y. C., Rozali, S., Awanis Hashim, N., Singh, R. 2016. Preparation and Characterization of Poly(lactic Acid)-based Composite Reinforced with Oil Palm Empty Fruit Bunch Fiber and Nanosilica. BioResources, 11(1), 2269-2286.

Yildirim, S., Röcker, B., Rüegg, N., Lohwasser, W. 2015. Development of palladium-based oxygen scavenger: Optimization of substrate and palladium layer thickness. Packag. Technol. Sci. 28, 710-718.

Yildirim, S., Röcker, B., Pettersen, M. K., Nilsen-Nygaard, J., Ayhan, Z., Rutkaite, R., et al. (2018). Active packaging applications for food. Compr. Rev. Food Sci. F., 17, 165–199.

Yu, W. X., Hu, C. Y., and Wang, Z. W. (2017). Release of Potassium Sorbate from Pectin-Carboxymethyl Cellulose Films into Food Simulant. J. Food Process. Pres. 41.

Yuan, G., Chen, X., Li, D. 2016. Chitosan films and coatings containing essential oils: The antioxidant and antimicrobial activity, and application in food systems. Food Res. Int. 89, 117–128.

Zainab,W.A. and Dong, Y. (2019). Biodegradable and Water Resistant Poly(vinyl) Alcohol (PVA)/Starch (ST)/Glycerol (GL)/Halloysite Nanotube (HNT) Nanocomposite Films for Sustainable Food Packaging. Front. Mat. 6. h

Zonder, L., Mccarthy, S., Rios, F., Ophir, A., Kenig, S. (2014). Viscosity Ratio and Interfacial Tension as Carbon Nanotubes Distributing Factors in

Melt-Mixed Blends of Polyamide 12 and High-Density Polyethylene. Adv. Polym. Technol., 33, 21427.